Uniform and Non-Uniform EBGS Assisted Microstrip Transmission Line as Microwave Filter

S. M. Anayetullah

Md. Abu-Al Shufian

Md. Mahfuz Ahmed

Md. Golam Rasul

Department of Electrical & Electronic Engineering

A thesis submitted to the Eastern University

in partial fulfillment of the requirement for the degree of

Bachelor of Science

2012

Statement of Originality

We hereby certify that the content of this thesis is the result of work done by us and has not been submitted for a higher degree to any other University or Institution.

……..	…….
S.M. Anayetullah	**Md.Mahfuz Ahmed**
I.D. 082800051	I.D. 082800080
…….	…….
Md. Abu Al Shufian	**Md. Golam Rasul**
I.D. 082800056	I.D. 082800102

External:

……

S. M. Shakil Hassan

Lecturer,
Department of Electrical
& Electronic Engineering,
Eastern University,
Bangladesh .

Supervisor:

……

Prof. Dr. Md. Nurunnabi Mollah

Dean,
Faculty of Engineering
& Technology,
Eastern University,
Bangladesh.

Acknowledgements

It gives us a lot pleasure to convey our heartfelt gratitude to Professor Dr. Md. Nurunnabi Mollah for his continuous and constant guidance throughout our thesis work. We received continuous motivation and suggestions from him and in our academic life, we are proud of having such a dynamic and punctual supervisor. His contributions and encouragements we cannot repay. We wish him sound and healthy and longer life.

We are very much thanked full to S. M. Shakil Hassan (Lecturer, Faculty of Engineering & Technology, Eastern University) for his kind help on providing us “Zealand ie3D” and “PCAAD” software and trained us to use that software too. All the designs that are made during our thesis are simulated by “Zealand ie3D” software and “PCAAD” is used to calculate some important values. He also helped us to understand some important terminologies and provided us soft copy of several books. However, we will remember his support during our whole life span.

Our faculty members always heard from us about our progress whenever we met and they encouraged us to complete the research work with successful approach and they motivate us to give our best effort throughout the research work. We cannot ever repay to their encouragement and inspiration.

Our senior brother S. M. Arman Ullah (M.Sc student of University of South West Fellia, Germany) helped us by providing some valuable research papers and motivated us throughout the thesis. Another person from our computer Lab executive member named Dilip Kumar who helped us by providing Microsoft Visio software, which is used for drawing the designs for this paper. We are very thankful to all of them.

Eastern University

Department of Electrical and Electronic Engineering,

B. Sc. Dissertation

Uniform and Non-Uniform EBGS Assisted Microstrip Transmission Line as Microwave Filter

Students:

S. M. Anayetullah

Md. Abu-Al Shufian

Md. Mahfuz Ahmed

Md. Golam Rasul

Supervisor:

Prof. Dr. Md. Nurunnabi Mollah.

June, 2012

Summary

Using Electromagnetic Bandgap Structures (EBGS) is a new technology to improve the performances of existing RF and microwave active and passive devices. Due to the realization of growing demand for larger bandwidth, high capacity RF and microwave devices as well as better efficiency in the field of wireless technologies new technologies of designing such devices are being reported all over the world. On the consequence of such latest technologies realizing microwave filters and antennas with Electromagnetic Bandgap Structures are one of the best of them. The technological design is very simple than any other devices – it is just made upon a dielectric substrate with copper coating on both sides. By etching these copper coating: microstrip transmission line (T-line) on the upper side and EBGS on the ground plan are made (a typical design is shown in figure 1); which shows the performance like stopband, passband and LPF filters (figure 2 is a result of a typical design).

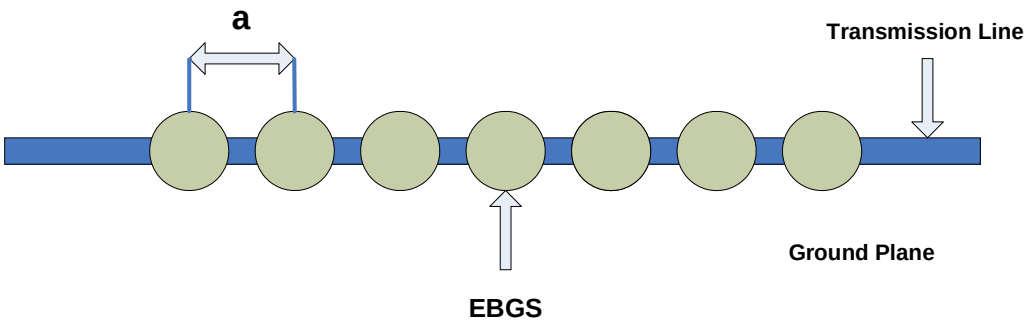

Figure 0.1 : Geometry of a circular EBGS assisted microstrip Transmission line.

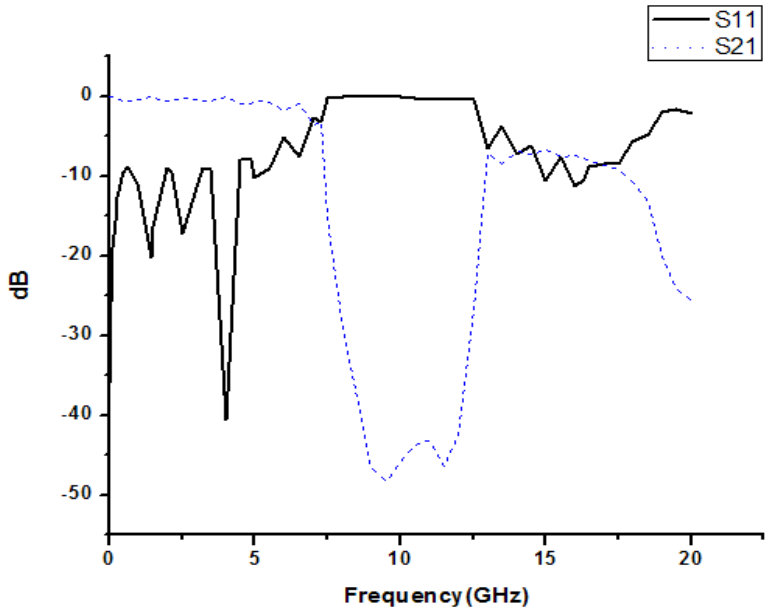

Figure 0.2: S-Parameter performance of Circular EBGS assisted Transmission line

Throughout the whole thesis work some parametric studies and several new designs of EBGS are introduced and described. The thesis concerns the planar EBG structures in the forms of conventional circular, square, triangular, hexagonal and rectangular EBGSs and various patterned dumbbell shaped EBGS as well as some hybrid designs of EBGS. Ripple free passband and wider stopband properties and low pass properties of filters are observed. Use of binomially distributed regular and dumbbell shaped designs are studied and ripple free low pass performance is achieved. Electromagnetic field is confined at the beneath of the T-line is proved and classified filter performances are realized for various designs in this paper. EBGSs, in recent years, have become most popular due to their low profile, ease of fabrication and integration with monolithic microwave integrated circuits (MMICs).

Contents

List of Figures

List of Tables

List of Abbreviations

EBGS	**Electromagnetic Bandgap Structures**
T-line	**Transmission Line**
MMICs	**Monolithic Microwave Integrated Circuits**
FF	**Filling Factor**
VLF	**Very Low Frequency**
LF	**Low Frequency**
MF	**Medium Frequency**
HF	**High Frequency**
VHF	**Very High Frequency**
UHF	**Ultra High Frequency**
SHF	**Super High Frequency**
EHF	**Extreme High Frequency**
AR	**Aspect Ratio**
VSWR	**Voltage Standing Wave Ratio**
RL	**Return Loss**
IL	**Insertion Loss**
EBG	**Electromagnetic bandgap**
LPF	**Low pass filter**
MMIC	**Microwave monolithic integrated circuit**
EM	**Electromagnetic**
1-D, 2-D, 3-D	**One dimensional, two dimensional, three dimensional**
RF	**Radio frequency**
BW	**Bandwidth**
dB	**Decibel**
VNA	**Vector network analyzer**
3-G	**Third generation**

List of Major Symbols

ε	Dielectric constant
γ	Propagation constant
β	Phase Constant
π	Pi = 3.1415927
ω	Angular frequency
k	Wave number (/m)
Γv	Voltage Reflection Co-efficient
Γp	Power Reflection Co-efficient
Γ or T	Transmission Co-efficient

Chapter 1 : Introduction to Microwave Engineering

1.1 Introduction:

The microwave refers to an alternating current signals with frequencies between 300 MHz and 300 GHz with corresponding electrical wavelength between $\lambda = c/f$ = 1m and λ = 1mm respectively. It is quite impossible to solve microwave network problem using standard circuit theory directly but standard circuit theory is an approximation of the broader theory of electromagnetism as described by Maxwell's equations. The lumped circuit element approximations of circuit theory are not valid at microwave frequencies significantly over the physical extent of the device, because the device dimensions are on the o. Microwave components are often distributed elements, where the phase of a voltage or current changes significantly over the physical extend of the device.

Microwaves are electromagnetic waves whose wavelengths are ranging from one meter to one millimeter. Equivalently we can say that the frequencies of microwaves are ranging from 300 MHz (0.3 GHz) to 300 GHz are known as microwaves. Very Low Frequency (VLF), Low Frequency (LF), Medium Frequency (MF), High Frequency (HF), Very High Frequency (VHF), Ultra High Frequency (UHF), Super High Frequency (SHF) & Extreme High Frequency (EHF) all are treated as microwaves as their frequency range is in between the frequency range of microwave frequency range. The frequency band with their designation & typical service are given below as a form of table.

Table 1.1: Frequency Band Designation.

Frequency Band	Designation	Typical Service
3 – 30 kHz	Very Low Frequency (VLF)	Navigation, Sonar
30 – 300 kHz	Low Frequency (LF)	Radio beacons, Navigational aids
300 – 3000 kHz	Medium Frequency (MF)	AM Broadcasting, Maritime radio, Coast Guard Communication, Direction finding
3 – 30 MHz	High Frequency (HF)	Telephone, Telegraph, Facsimile, Shortwave international broadcasting, amateur radio, Citizen's band, Ship-to-coast and ship-to-aircraft communication
30 – 300 MHz	Very High Frequency (VHF)	Television, FM broadcasting, Air-traffic control, Police, Taxicab mobile radio, Navigational aids
300 – 3000 MHz	Ultra High Frequency (UHF)	Television, Satellite communication, Radiosonde, Surveillance radar, Navigational aids,
3 – 30 GHz	Super High Frequency (SHF)	Air borne radar, Microwave links, Common-carrier land, Mobile communication, Satellite communication
30 – 300 GHz	Extreme High Frequency (EHF)	Radar

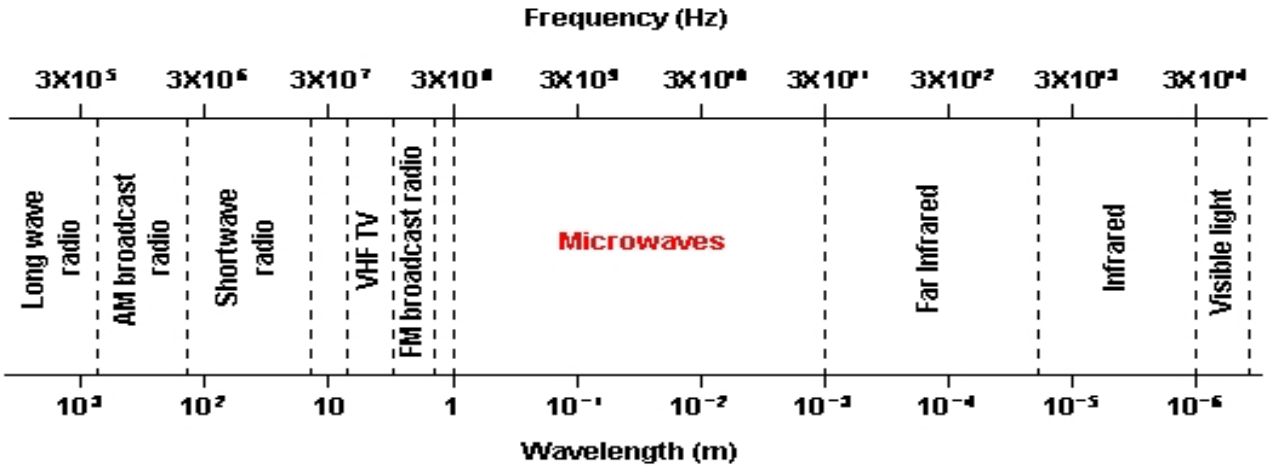

Figure 1.1: Frequency range of waves.

In the UHF band, up to around a frequency of 1 GHz, most communication circuits are constructed using lumped-parameter circuit components. But in the frequency range from 1 up to 100 GHz or higher, lumped circuit elements are usually replaced by transmission line and waveguide components, generally known as distributed components because at high frequency typical inductor becomes short circuit and capacitor becomes open circuited; therefore, some new suitable realizations and technologies are badly needed for wireless system in case higher frequency operation.

1.2 Applications of Microwave Engineering:

Just as the high frequencies and short wave lengths of microwave energy make for difficulties in analysis and design of microwave components and systems, these same factors provide unique opportunities for the application of microwave system. This is because of following considerations:

- Antenna gain is proportional to the electrical size of the antenna. At higher frequencies, more antenna gain is therefore possible for a given physical antenna size, which has important consequences for implementing miniaturized microwave systems.

- More bandwidth can be realized at higher frequencies. Bandwidth is critically important because available frequency bands in the electromagnetic spectrum are being rapidly depleted.
- Microwave signals travel by line of sight are not bent by the ionosphere as are lower frequency signals and thus satellite and terrestrial communication links with very high capacities are possible.
- Effective reflection area (radar cross section) of a radar target is proportional to the target's electrical size. Thus generally microwave frequencies are preferred for radar systems.
- Various molecular, atomic, and nuclear resonances occur at microwave frequencies, creating a variety of unique applications in the areas of basic science, remote sensing, medical diagnostics and treatment, and heating methods.
- Various molecular, atomic, and nuclear resonances occur at microwave frequencies, creating a variety of unique applications in the areas of basic science, remote sensing, medical diagnostics and treatment, and heating methods.

Today, the majority of applications of microwaves are related to radar and communication systems. Radar systems are used for detecting and locating targets and for air traffic control systems, missile tracking radars, automobile collision avoidance systems, weather prediction, motion detectors, and a wide variety of remote sensing systems.
Microwave communication systems handle a large fraction of the world's international and other long haul telephone, data and television transmissions.

Most of the currently developing wireless telecommunications systems, such as direct broadcast satellite (DBS) television, personal communication systems (PCSs), wireless local area networks (WLANS), cellular video (CV) systems, and global positioning satellite (GPS) systems rely heavily on microwave technology

Radar systems find application in military, commercial and scientific systems. Rader is used for detecting and locating air, ground and seagoing targets as well as for missile guidance and fire

control. In commercial sector radar technology is used for air traffic control, motion detector, vehicle collision avoidance and distance measurement. Scientific applications of radar include weather prediction, remote sensing of the atmosphere, the oceans, the ground and medical diagnostics and therapy. Microwave radiometry which is the passive sensing of microwave energy emitted from object is used for remote sensing of the atmosphere and the earth as well as medical diagnostics and imaging for security applications.

1.3 Microwave Transmission lines:

Transmission lines that are use to convey microwave frequency signals called microwave transmission lines.

In an electronic system, the delivery of power requires the connection of two wires between the source and the load. At low frequencies, power is considered to be delivered to the load through the wire.

In the microwave frequency region, power is considered to be in electric and magnetic fields that are guided from lace to place by some physical structure. Any physical structure that will guide an electromagnetic wave place to place is called a Transmission Line.

1.4 Microwave filters:

Microwave filters represent a class of electronic filter design to operate on signals in the MHz to GHz frequency ranges. This frequency range is the range used by most broadcast radio, television, wireless communications like Cell phone, Wi-Fi, Wi-Max and the most radio frequency and microwave devices will include some kinds of filtering on the signals transmitted or received. Such filters are commonly used as buildings blocks to duplexers and diplexers to combine or separate multiple frequency bands.

There are mainly four types of filters with respect to functions,

- Low-pass filter
- High-pass filter
- Band-pass filter
- Band-stop filter

1.5 Different type of filtering devices:

A large variety of passive microwave circuit components or devices have been developed for use in both laboratory and in microwave communication & radar systems. The most commonly used microwave devices including transmission line, waveguides, attenuators, phase shifters, directional couplers, power dividers, hybrid junctions, isolators or gyrators and circulators.

The amount of active microwave devices is not very few. A lot of active microwave devices been developed for use in both laboratory and in microwave communication & radar systems. The most commonly used active microwave devices including oscillators, power amplifier, mixers etc.

It is known to everybody that the electronic filters are circuits that remove unwanted frequency components from incoming signal and thus enhance the range of frequency we want. An electronic filter that operates within the range of frequency from 0.3 to 300 GHz is basically defined as microwave filters. On the other hand, a microwave filter is a frequency selective two-port network with low levels of attenuation or insertion loss in its pass-band and specified high levels of attenuation in its stop-band. Typical frequency responses include low-pass (allows only frequencies below a cutoff frequency to pass), high-pass (allow only frequencies above a cutoff frequency to pass), band-pass (select only a desired band of frequencies) and band-reject or band-stop (eliminate an undesired band of frequencies) characteristics. Applications can be found in virtually any type of microwave communication, radar, or test and measurement system.

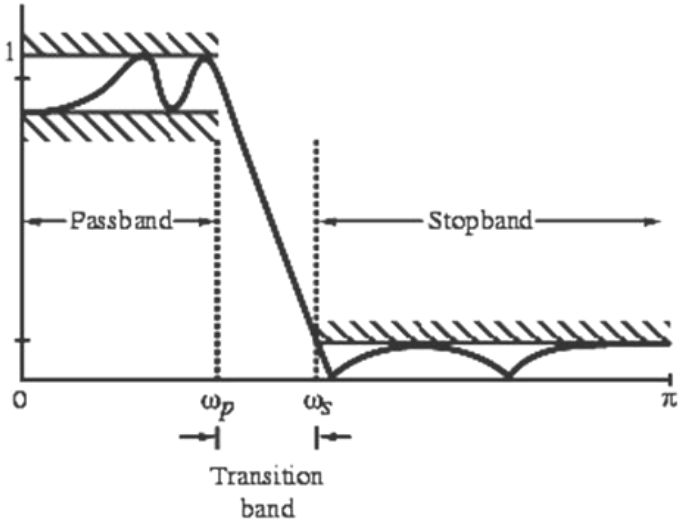

Figure 1.2: Basic filter prototype showing pass-band-stop-band performance.

An example specification for a microwave low pass filter response is shown in Fig. 1.2. In this example, the pass-band insertion loss must be less than 1 dB from D.C. to 4 GHz. The stop-band attenuation must be greater than 50 dB from 8 GHz to 18 GHz. In addition there is a specification on the input return loss return loss of greater than 20 dB in the pass-band. This means that any signal incident on the filter in the frequency range of its pass-band must be 99% transmitted or absorbed; only 1% of incident power can be reflected. A high level of return loss, typically 20 dB or greater, implies a flat low ripple insertion loss characteristics, which is very desirable from the point of view of signal distortion.

In general, microwave filters are most often made up of one or more coupled resonators and thus any technology that can be used to make resonators can also be used to make filters. The unloaded quality factor of the resonators being used will generally set the selectivity the filter can achieve.

1.5.1 Lumped - element LC filters:

An LC tank circuit consisting of parallel or series inductors and capacitors is a best example of a simplest resonator structure. These LC tank circuits have the advantage of being very compact & small in size, but having the low quality factor of the resonators which leads to relatively poor performance.

Figure 1.3 : Commercial photograph of Lumped-element LC filters.

Lumped-Element LC filters have both an upper and lower frequency range. When the frequency gets very low such as kHz to Hz range, then the size of the inductors used in the tank circuit becomes prohibitively large. Very low frequency filters are often designed with crystals to

overcome this problem. As the frequency gets higher, into the 600 MHz and higher range, the inductors in the tank circuit become too small to be practical.

1.5.2 Planar filters:

Micro-strip transmission lines (as well as CPW or strip-line) can also make good resonators and filters which offer a better compromise in terms of size and performance with respect to lumped element filters. The process used to manufacture micro-strip circuits is very similar to the processes used to manufacture PCB and these filters have the advantage of largely being planar. Precision planar filters are manufactured using a thin-film process. Higher *Q* factors can be obtained by using low dielectric materials for the substrate such as quartz or sapphire and lower resistance metals such as gold.

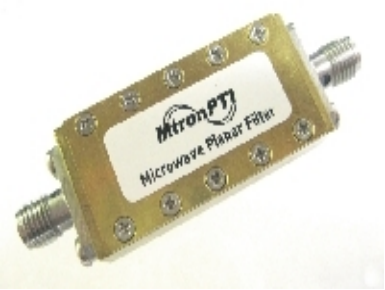

Figure 1.4: Commercial photograph of Planer filters

1.5.3 Coaxial filters:

Coaxial transmission lines provide higher quality factor than planar transmission lines and are thus used when higher performance is required. The coaxial resonators may make use of high-dielectric constant materials to reduce their overall size.

Figure 1.5: Commercial photograph of Coaxial filters

1.5.4 Cavity filters:

Still widely used in the 40 MHz to 960 MHz frequency range, well constructed cavity filters are capable of high selectivity even under power loads of at least a megawatt. Higher *Q* as well as increased performance stability at closely spaced (down to 75 kHz) frequencies can be achieved by increasing the internal volume of the filter cavities.

Physical length of conventional cavity filters can vary from over 82" in the 40 MHz range, down to under 11" in the 900 MHz range.

Figure 1.6: Commercial photograph of Cavity filters.

In the microwave range (1000 MHz (or 1 GHz) and higher), cavity filters become more practical in terms of size and a significantly higher quality factor than lumped element resonators and filters, though power handling capability may diminish.

1.5.5 Dielectric filters:

Pucks made of various dielectric materials can also be used to make resonators. As with the coaxial resonators, high-dielectric constant materials may be used to reduce the overall size of the filter. With low-loss dielectric materials, these can offer significantly higher performance than the other technologies previously discussed.

Figure 1.7: Commercial photograph of Dielectric filters.

1.5.6 Electro acoustic filters:

Electro acoustic resonators based on piezoelectric materials can be used for filters. Since acoustic wavelength at a given frequency is several orders of magnitude shorter than the electrical wavelength, electro acoustic resonators are generally smaller than electromagnetic counterparts such as cavity resonators.

A common example of an electro acoustic resonator is the quartz resonator which essentially is a cut of a piezoelectric quartz crystal clamped by a pair of electrodes. This technology is limited to some tens of megahertz. For microwave frequencies, thin film technologies such as surface acoustic wave (SAW) and bulk acoustic wave (BAW) have been used for filters.

1.6 Microwave Filter design:

There is a vast amount of published literature on the design of microwave filters from which some are highly mathematical. Fortunately there are some relatively straight forward procedures which enable us to design certain useful classes of microwave filters.

Filter designing using the image parameter method consist of a cascade of simpler two-port filter sections to provide the desired cutoff frequencies and attenuation characteristics but do not allow the specification of a frequency response over the complete operating range. Thus, although the procedure is relatively simple, the design of filters by the image parameter method often must be iterated many times to achieve the desired results.

A more modern procedure, called the insertion loss method, uses network synthesis techniques to design filter with a completely specified frequency response. The design is simplified by beginning with low-pass filter prototypes that are normalized in terms of impedance and frequency. Transformations are then applied to convert the prototype designs to the desired frequency range and impedance level.

Both the image parameter and the insertion loss method of filter design provide lumped element circuits. For microwave applications such designs usually must be modified to use distributed elements consisting of transmission line sections.

1.6.1 PBGS and EBGS:

Photonic Band Gap (PBG) materials, also known as photonic crystals, are materials which have a band gap due to a periodicity in the materials dielectric properties. The band gap in photonic crystals represents the forbidden energy range where wave behaving photons can not be transmitted through the material. This behavior is equivalent to electrons in crystalline semiconductors and in the same manner PBG materials can be used to affect and control the movement of electromagnetic waves.

Recently researchers decided that PBGS is not the appropriate name. The name should be EBGS because the structures actually affect electromagnetic waves not photonic waves. So previously called PBGS are now called EBGS.

1.6.2 EBG Structures:

EBG structures are periodic in nature, which may be realized by drilling, cutting and etching on the metal or substrates. They may be formed in the ground plane or over the substrate. The transmission line can also be modified to form EBG characteristics without having any perturbation in the ground plane. This new idea can be extended to filter, antenna and other microwave component and devices where the complexity of packaging is minimized. The EBG configuration is categorized as shown in figure 2.1. On the basis of dimension, EBG structures may be divided into 1-D, 2-D and 3-D EBGSs. Following are the descriptions of different EBG structures.

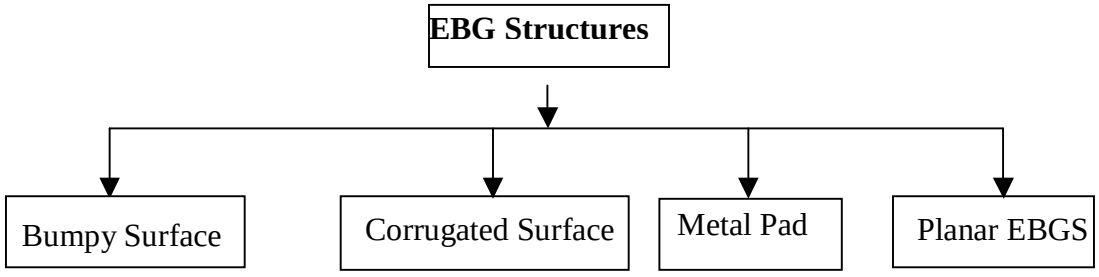

Figure 1.8: Different EBG structures

1.6.3 Applications of EBG Structure:

Due to the unique properties of EBG engineered structures, they find many applications in microwave circuit components and devices. To realize microwave filters, mixers, antennas, power amplifiers, phased arrays etc. the stopband and passband created by the EBG structures to enhance performances of devices. Here the beneficial effects of EBGSs in different devices are discussed.

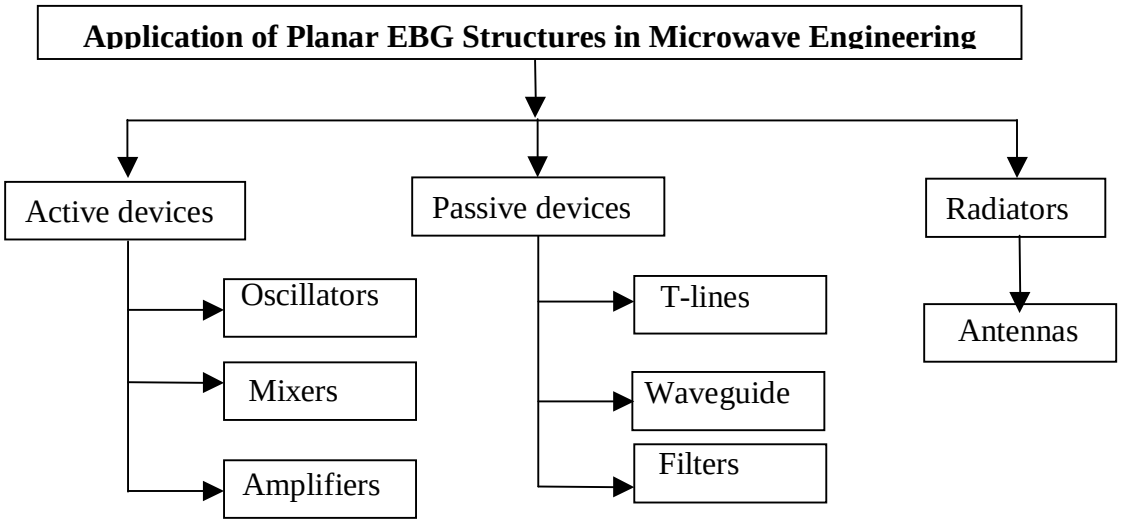

Figure 1.9: Tree- structure of applications of planar EBGSs.

1.7 Objective of the Thesis:

The goal of this thesis is to find out the effect of uniform and non-uniform EBGS on micro-strip transmission line regarding band-stop and low pass filtering operation as well as to observe the performance of various designs. The use of proper EBG structure is very important for filtering operation. Hence, some parametric studies are done and several designs are tested and their results are described. Some investigations are focused on the improvement of the performances and transforming the pattern of the results. Some characteristic changing patterns are studied to find out the relation between some parameter and filtering performance.

- **The project has the following objectives:**

- Design of novel EBG elements on the ground plate of micro-strip transmission line that will provide broadband and distinct pass-band and stop-band characteristics.

- Circular and square shaped EBGS design for different filling factor with also investigated to achieve better performance.
- Effects of etching area on the performances of filtering operation for circular, square, triangular and hexagonal shaped EBGS will be investigated.
- Effect of thickness on the performance of filtering operation will also be investigated.
- Effect of one line and three line EBGS will be studied.
- Performance of non-uniform binomially distributed EBGS will also be studied.
- Performance of some modified non-uniform EBGS will also be analyzed.
- Different patterned Dumbbell shape EBGS also be investigated to achieve more compactness.
- Binomially distributed dumbbell shaped designs will be investigated to achieve ripple free low pass performance.

1.8 Original Contributions:

The following items are the original contributions stemmed from the thesis.

- Effect of filling factor is closely inspected and the filtering performance is described.
- EBGS of circular, square, triangular and hexagonal shape of same etching shows almost same results.
- Analysis of one line and three line EBGS shows same performance.
- Non-uniform binomially distributed EBGS shows low pass characteristics.
- Some modified designs shows good low pass characteristics.
- Dumbbell shaped EBGS assisted designs are more compact and shows low pass performance
- Binomially distributed dumbbell shaped designs shows ripple free low pass performance.

1.9 Thesis outlines:

Followings are the outline of the thesis.

- In chapter 1, the introduction of the research work is reported.
- In chapter 2, the basic theory of periodic structures and design equations are presented. To get the idea about the pass-band-stop-band phenomena of the EBGS, numerical result for dispersion diagram has been reported.
- In chapter 3, study of different parameters of uniform EBGS and microstrip transmission line are presented and simulated data are analyzed.
- In chapter 4, binomially distributed even and odd numbered EBGS assisted microstrip transmission line are studied and several designs are analyzed. Some modified non-uniform designs are also investigated.
- In chapter 5, uniform and binomially distributed non-uniform dumbbell shaped designs are studied and some parametric studies are made.
- In chapter 6, conclusions and recommendation for future work have been presented.

Chapter 2 : Theoretical Background

2.1 Introduction:

Recently EBGSs have occupied significant portions of microwave engineering literature to enhance the performance of many microwave devices and components. The nomenclature EBG is actually used in the optical communication. Recently they are scaled down to RF engineering. They are very old concepts in terms of periodic structures. EBG structures are periodic in nature. They originate from stopband and passband like periodic structures. To understand the stopband and passband phenomena in EBG structures, it is better to study the conventional periodic structure.

Waveguides and transmission lines loaded at periodic intervals with identical reactive elements are referred to as periodic structures. This type of period structures yield two distinct properties, namely Passband – stopband characteristics; and Stemming waves with phase velocity lower than the velocity of light in free space.

In the passband the EM wave is unattenuated along the structure. There may be some incidental conductor loss only. On the other hand, in the stopband the EM wave is totally attenuated so that it cannot propagate throughout the structure. This stopband – passband characteristics are very important to suppress the surface waves, a crucial issue in microwave engineering.

EM wave having the velocity lower than the velocity of light in free-space is called slow wave. Periodic perturbation in the ground plane provides periodic discontinuity. Thus the slow wave property of the EM wave is achieved. Slow wave structures (SWSs) are promising candidates for compact design.

2.2. Microwave Transmission lines Theories:

What is Microwave Transmission Line?

Transmission lines that are use to convey microwave frequency signals called microwave transmission lines.

In an electronic system, the delivery of power requires the connection of two wires between the source and the load. At low frequencies, power is considered to be delivered to the load through the wire.

In the microwave frequency region, power is considered to be in electric and magnetic fields that are guided from lace to place by some physical structure. Any physical structure that will guide an electromagnetic wave place to place is called a Transmission Line.

The basic difference between conventional circuit theory and transmission line theory is the electrical size. Circuit analysis assumes that the physical dimensions of a network are much smaller than the electrical wavelength, while transmission lines may be a considerable fraction of a wavelength or many wavelengths, in size. Thus a transmission line is a distributed-parameter network, where voltage and currents can vary in magnitude and phase over its length.

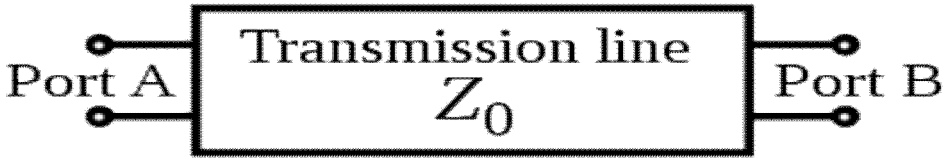

(a)

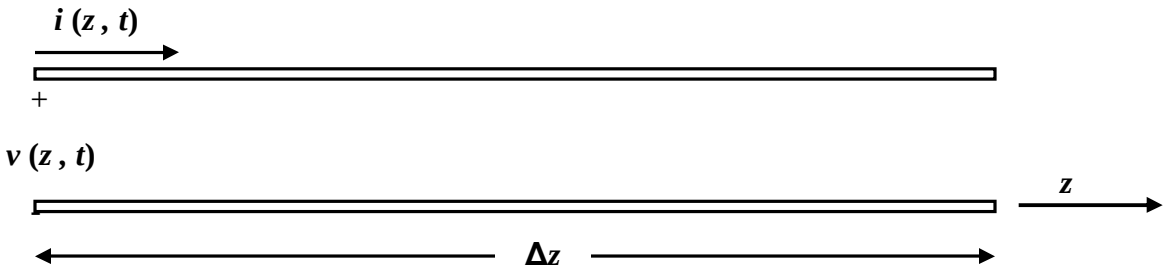

(b)

Figure 2.1: **(a) Two ports T-line, (b) Voltage and current definitions**

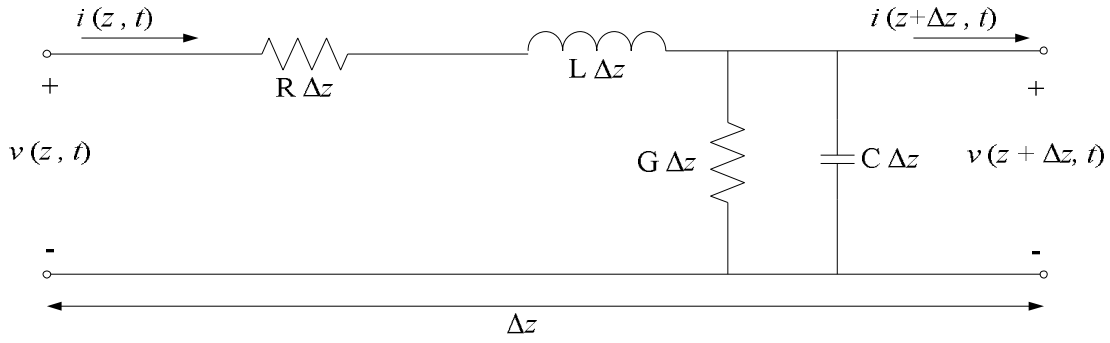

(c)

Figure 2.2:(c) Lumped-element equivalent circuit.

As shown in figure 2.1(a), a transmission line is often schematically represented as a two-wire line, since transmission lines (for TEM wave propagation) always have at least two conductors. The piece of line of infinitesimal length Δz of figure 2.1(a) can be modeled as a lumped-element circuit, as shown in figure 2.1(b), where R, L, G, C are per unit length quantities defined as follows:

R = series resistance per unit length, for both conductors (Ω/m)

L = series inductance per unit length, for both conductors (H/m)

G = shunt conductance per unit length (S/m)

C = shunt capacitance per unit length (F/m)

The series inductance L represents the total self-inductance of the two conductors and the shunt capacitance C is due to the close proximity of the two conductors. The series resistance R represents the resistance due to the finite conductivity of the conductors and the shunt conductance G is due to dielectric loss in the material between the conductors. A finite length of transmission line can be viewed as a cascade of sections of the form shown in figure 2.1(b).

From the circuit of figure 2.1(b), Kirchhoff's voltage and current law can be applied to give

$$v(z,t) - R\Delta z\, i(z,t) - L\Delta z \frac{\partial i(z,t)}{\partial t} - v(z+\Delta z,t) = 0 \qquad (2.1)$$

$$i(z,t) - G\Delta z v(z+\Delta z,t) - C\Delta z \frac{\partial v(z+\Delta z,t)}{\partial t} - i(z+\Delta z,t) = 0 \quad (2.2)$$

Dividing 2.1 and 2.2 by Δz and taking the limit as $\Delta z \to 0$ gives the following differential equations:

$$\frac{\partial v(z,t)}{\partial z} = -Ri(z,t) - L\frac{\partial i(z,t)}{\partial t} \quad (2.3)$$

$$\frac{\partial i(z,t)}{\partial z} = -Gv(z,t) - C\frac{\partial v(z,t)}{\partial t} \quad (2.4)$$

These equations are known as telegrapher's equations. For the sinusoidal steady-state condition with cosine-based phasors simplify to

$$\frac{dv(z)}{dz} = -(R + j\omega L)I(z) \quad (2.5)$$

$$\frac{dI(z)}{dz} = -(G + j\omega C)V(z) \quad (2.6)$$

These two equations can be solved simultaneously to give wave equation for V (z) and I (z):

$$\frac{d^2V(z)}{dz^2} - \gamma^2 V(z) = 0 \quad (2.7)$$

$$\frac{d^2I(z)}{dz^2} - \gamma^2 I(z) = 0 \quad (2.8)$$

Where $\gamma = \alpha + j\beta = \sqrt{(R + j\omega L)(G + j\omega C)}$ (2.9)

The complex propagation constant which is the function of frequency. Traveling wave solution can be found as

$$V(z) = V_0^+ e^{-\gamma z} + V_0^- e^{\gamma z} \quad (2.10)$$

$$I(z) = I_0^+ e^{-\gamma z} + I_0^- e^{\gamma z} \quad (2.11)$$

Where the $e^{-\gamma z}$ term represents wave propagation in the +z direction and the $e^{\gamma z}$ term represents wave propagation in the –z direction. So the current on the line is

$$I(z) = \frac{\gamma}{R + j\omega L}\left[V_0^+ e^{-\gamma z} - V_0^- e^{\gamma z}\right] \tag{2.12}$$

And the characteristic impedance Zo is

$$Z_0 = \frac{R + j\beta L}{\gamma} = \sqrt{\frac{R + j\omega L}{G + j\omega C}} \tag{2.13}$$

The above solution was for a general transmission line, including loss effects and it was seen that the propagation constant and characteristic impedance were complex. In many practical cases the loss of the line is very small to be neglected. Setting R = G = 0 in equation (2.9) gives the propagating constant.

$$\gamma = \alpha + j\beta = j\omega\sqrt{LC} \tag{2.14}$$

$$\beta = j\omega\sqrt{LC} \tag{2.15}$$

$$\alpha = 0 \tag{2.16}$$

As expected for the lossless case, the attenuation constant α is zero. The characteristic impedance of equation (2.13) is reduce to

$$Z_0 = \sqrt{\frac{L}{C}} \tag{2.17}$$

That is now a real number. The general solutions for voltage and current on the lossless transmission line can be written as

$$V(z) = V_0^+ e^{-j\beta z} + V_0^- e^{j\beta z} \tag{2.18}$$

$$I(z) = I_0^+ e^{-j\beta z} + I_0^- e^{j\beta z} \tag{2.19}$$

Where the wave length and the phase velocity are

Wave length, $$\lambda = \frac{2\pi}{\beta} = \frac{2\pi}{\omega\sqrt{LC}} \quad (2.20)$$

Phase velocity, $$v_p = \frac{\omega}{\beta} = \frac{1}{\sqrt{LC}} \quad (2.21)$$

2.2.1 Some Terminologies of Loaded T-Line facts:

First of all, A T-line is said to be loaded when transmitter or receiver will be connected with it. There can be several ports on T-line; but for the ease of depiction a standard T-line of two ports will be considered.

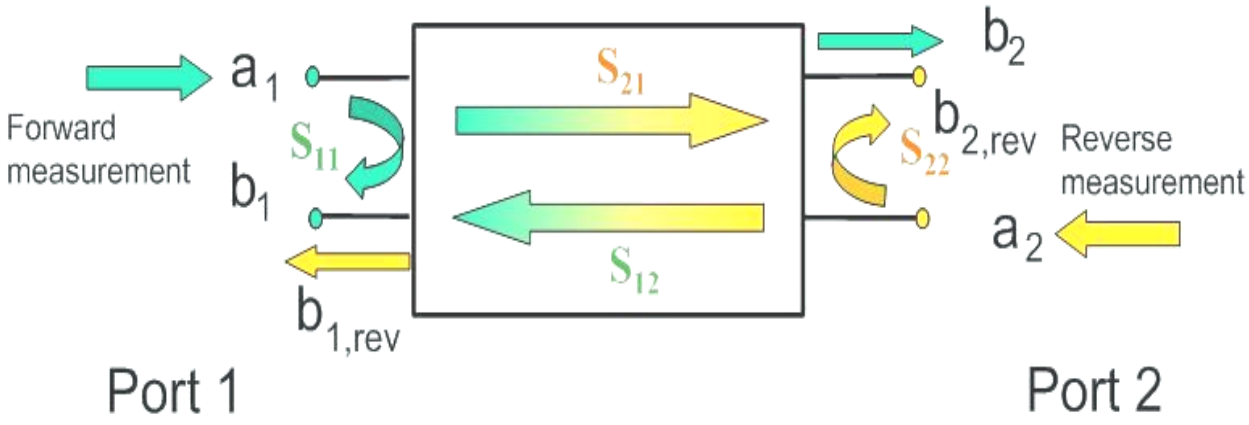

Figure 2.3: **A two ports T-line showing S – parameter matrix.**

Here,

S11 = input port voltage reflection co-efficient.
S12 = reverse voltage gain.
S21 = forward voltage gain.
S22 = output port voltage reflection co-efficient.

However, on the basis of these parameters some important ratios and factors as well as terminologies are defined, they are –

Reflection Co-efficient (Γr or Γ): The ratio of the reflected Power or voltage to the incident Power or voltage is known as reflection co-efficient.

$$\Gamma_r = \frac{\text{Reflected Power or voltage}}{\text{Incident Power or Voltage}}$$

Transmission Co-efficient (Γ_T or T): The ratio of the transmitted power or voltage to the incident power or voltage is known as transmission co-efficient.

$$\Gamma_T = \frac{\text{Transmitte d Power or voltage}}{\text{Incident Power or Voltage}}$$

Return Loss (R_L): Calculation of reflection co-efficient in deci-bell (dB) unit is called Return loss. Therefore, return loss (RL) is defined as:

$R_L = -20 \log |\Gamma r|$ dB. (For voltage)

$R_L = -10 \log |\Gamma r|$ dB. (For power)

Insertion Loss (I_L): Calculation of transmission co-efficient in deci-bell (dB) unit is known as Return loss. Therefore, Insertion loss (I_L) is defined as:

$I_L = -20 \log |\Gamma_T|$ dB (For voltage)

$I_L = -10 \log |\Gamma_T|$ dB (For power)

Voltage Standing Wave Ratio (VSWR): Standing wave ratio (SWR) is the ratio of the voltage of a partial standing wave at antinodes (maximum) to the voltage at an adjacent node (minimum) is known as VSWR.

$$VSWR = \frac{V_{max}}{V_{min}} = \frac{1 + \rho}{1 - \rho}$$

2.2.2 The Terminated Lossless Transmission Line:

Assume that a lossless transmission line is terminated in an arbitrary load impedance Z_L as shown is figure 2.3.

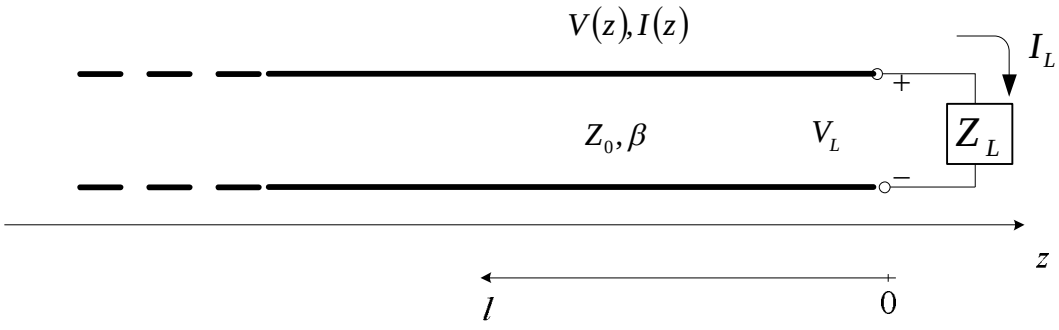

Figure 2.4: **A transmission line terminated in a load impedance Z_L.**

An incident wave of the form $V_0^+ e^{-j\beta z}$ is generated from a source at z < 0. It has been seen that the ratio of voltage to current for such traveling wave is the characteristic impedance, Zo. But when the line is terminated in an arbitrary load $Z_L \neq$ Zo, the ratio of voltage to current at the load must be Z_L. Thus, a reflected wave must be excited with the appropriate amplitude to satisfy this condition. The total voltage on the line can be written as the sum of incident and reflected waves:

$$V(z) = V_0^+ e^{-j\beta z} + V_0^- e^{j\beta z} \tag{2.22}$$

Similarly, the load current on the line is described by

$$I(z) = \frac{V_0^+}{Z_0} e^{-j\beta z} - \frac{V_0^-}{Z_0} e^{j\beta z} \tag{2.23}$$

The total voltage and current at the load are related by the load impedance, so at z = 0 we must have

$$Z_L = \frac{V(0)}{I(0)} = \frac{V_0^+ + V_0^-}{V_0^+ - V_0^-} Z_0 \tag{2.24}$$

Solving for V_0^- gives

$$V_0^- = \frac{Z_L - Z_0}{Z_L + Z_0} V_0^+ \qquad (2.25)$$

The amplitude of the reflected voltage wave normalized to the amplitude of the incident voltage wave is defined as voltage reflection co-efficient, Γr:

$$\Gamma r = \frac{V_0^-}{V_0^+} = \frac{Z_L - Z_0}{Z_L + Z_0} \qquad (2.26)$$

The total voltage and current waves on the line can be then written as

$$V(z) = V_0^+ \left[e^{-j\beta z} + \Gamma e^{j\beta z} \right] \qquad (2.27)$$

$$I(z) = \frac{V_0^+}{Z_0} \left[e^{-j\beta z} - \Gamma e^{j\beta z} \right] \qquad (2.28)$$

From these equations it is seen that the voltage and current on the line consist of a superposition of an incident and reflected wave; such waves are called standing waves. Only when $\Gamma r = 0$ there is no reflected wave. To obtain $\Gamma = 0$, the load impedance Z_L must be equal to the characteristic impedance Zo of the transmission line which can be easily understood from equation 2.23. Such a load is then said to be matched to the line, since there is no reflection of the incident wave.

When the load is mismatched, not all of the available power from the generator is delivered to the load. This "loss" is called return loss (RL) and is defined as

$$RL = -20\log | \Gamma r | \text{ dB} \qquad (2.29)$$

So that a matched load ($\Gamma = 0$) has a return loss of ∞ dB (no reflected power) whereas total reflection ($| \Gamma | = 1$) has a return loss of 0 dB(all incident power is reflected).

If the load is matched to the line, $\Gamma = 0$ and the magnitude of the voltage on the line is $|V(z)| = |V_0^+|$, which is a constant. Such a line is sometimes said to be "Flat". When the load is mismatched, however, the presence of a reflected wave leads to standing waves where the magnitude of the voltage on the line is not constant. Thus we get

$$|V(z)| = |V_0^+ \| 1 + \Gamma e^{2j\beta z}| = |V_0^+ \| 1 + \Gamma e^{-2j\beta l}| = |V_0^+ \| 1 + |\Gamma| e^{j(\theta - 2\beta l)}| \qquad (2.30)$$

Where l = - z is positive distance measured from the load at z = 0 and θ is the phase of the reflection co-efficient ($\Gamma = |\Gamma| e^{j\theta}$). This result shows that the voltage magnitude oscillates with position z along the line. The maximum value occurs when the phase term $e^{j(\theta - 2\beta l)} = 1$ and is given by

$$V_{\max} = |V_0^+|(1 + |\Gamma|) \tag{2.31}$$

The minimum value occurs when the phase term $e^{j(\theta - 2\beta l)} = -1$ and is given by

$$V_{\min} = |V_0^+|(1 - |\Gamma|) \tag{2.32}$$

As $|\Gamma|$ increases, the ratio of V_{max} to V_{min} increases, so a measure of mismatch of a line, called the standing wave ratio (SWR), can be defined as

$$\text{SWR} = \frac{V_{\max}}{V_{\min}} = \frac{1 + |\Gamma|}{1 - |\Gamma|} \tag{2.33}$$

This quantity is also known as the voltage standing wave ratio (VSWR). From the equation it is seen that SWR is a real number such that $1 \le \text{SWR} \le \infty$, where SWR = 1 implies that a matched load.

Now consider a transmission line of characteristic impedance Zo feeding a line of different characteristic impedance Z1. If the load is infinitely long or if it is terminated in its own characteristic impedance as a result there are no reflections from its end then the input impedance seen by the feed line is Z1. Thus the reflection co-efficient, Γ is

$$\Gamma r = \frac{Z_1 - Z_0}{Z_1 + Z_0} \tag{2.34}$$

Not the entire incident wave is reflected; some of it is transmitted onto the second line with voltage amplitude given by a transmission co-efficient, T. Now the voltage for z < 0 is

$$V(z) = V_0^+ \left[e^{-j\beta z} + \Gamma r e^{j\beta z} \right] \quad \text{for } z < 0 \tag{2.35}$$

Where V_0^+ is the amplitude of the incident voltage wave on the feed line. The voltage wave for $z > 0$, in the absence of reflections, is outgoing only and can be written as

$$V(z) = V_0^+ T e^{-j\beta z} \qquad \text{for } z > 0 \qquad (2.36)$$

Equating these voltages at z = 0 gives the transmission co-efficient, T as

$$T = 1 + \Gamma = 1 + \frac{Z_1 - Z_0}{Z_1 + Z_0} = \frac{2Z_1}{Z_1 + Z_0} \qquad (2.37)$$

The transmission co-efficient between two points in a circuit is often expressed in dB as the insertion loss, I_L

I_L = -20 log | T | dB

2.3 Types of transmission lines:

- Two wire line
- Coaxial cable
- Waveguide
  - Rectangular
  - Circular
- Planar Transmission Lines
  - Coplanar Waveguide
  - Strip line
  - Microstrip line
  - Slot line
  - Fin line
  - Coplanar slot line

2.3.1 Co-planner waveguide:

A coplanar waveguide (CPW) fabricated on a substrate was first demonstrated by C. P. Wen in 1969. Since that time, tremendous progress has been made in CPW based microwave integrated circuits (MICs). A conventional CPW on a dielectric substrate consists of a center strip conductor with semi-infinite ground planes on either side as shown in fig 3.4. This structure supports a quasi-TEM mode of propagation as microstrip line.

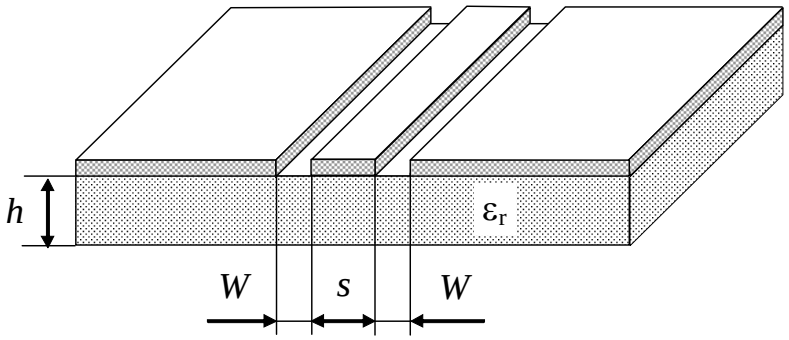

Figure 2.5: Conventional CPW

For CPW, the dimension of the center strip, the gap, the thickness and permittivity of the dielectric substrate determine the effective dielectric constant ε_{eff}, characteristic impedance Zo and the attenuation constant α of the line. Using conformal mapping, it can be shown that Zo and ε_{eff} for a CPW on an infinitely thick dielectric substrate are given as below:

$$\varepsilon_{eff} = \frac{1 + \varepsilon_r}{2} \tag{2.38}$$

$$Z_0 = \frac{30\pi}{\sqrt{(\varepsilon_r + 1)/2}} \frac{K(k_0')}{K(k_0)} \tag{2.39}$$

Where,

$$k_0 = \frac{W}{W + 2G}$$

$$k_0' = \sqrt{1 - k_0^2}$$

And K(x) is the complete elliptic integral. More complicated expressions are available for the CPW with substrate of finite thickness.

2.3.2 Strip-line:

The basic strip transmission line consists of a thin conducting strip of width W centered between two wide conducting ground planes of separation H and the entire region between the ground planes is filled with a dielectric of relative permittivity εr.

Stripline is usually constructed by etching the center conductor on a grounded substrate of thickness H/2 and then covering it with another grounded substrate of the same thickness as shown in figure 2.5

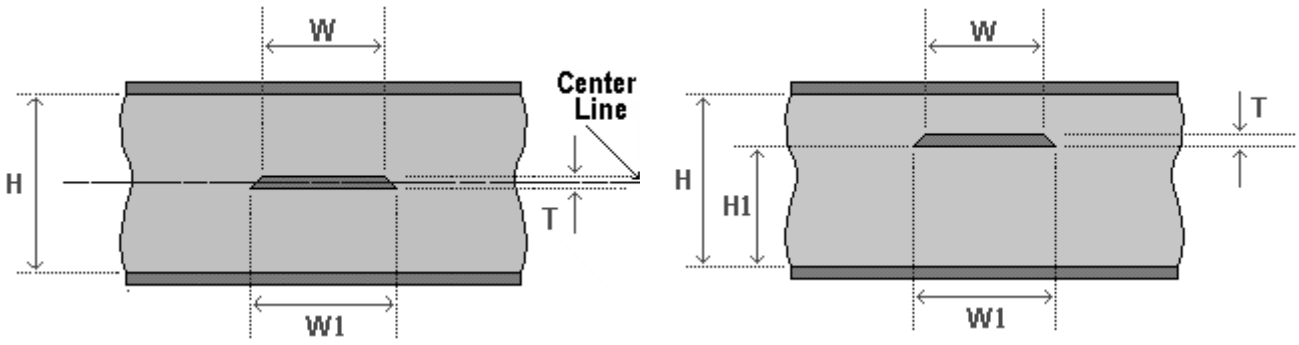

(a) (b)

Figure 2.6: **Geometry of stripline (a) symmetric stripline & (b) offset stripline**

Because they consists of two conductors and a homogeneous dielectric, striplines support TEM waves which is the desired mode of operation. This is because of the simpler electrostatic analysis that may be used when considering TEM mode of operation.

It also supports higher TM and TE modes which may be avoided by using shorting screws between ground planes and by restricting the plane spacing to less than λ/4.

The phase velocity (v_P), propagation constant (β) and characteristic impedance (Zo) of a stripline at TEM mode is given by:

$$v_P = \frac{1}{\sqrt{\mu_0 \varepsilon_0 \varepsilon_r}}$$

$$\beta = \frac{\omega}{v_P} = \omega\sqrt{\mu_0 \varepsilon_0 \varepsilon_r} = k_0\sqrt{\varepsilon_r}$$

$$Z_0 = \sqrt{\frac{L}{C}} = \frac{\sqrt{LC}}{C} = \frac{1}{v_P C} \qquad (2.40)$$

Where, L and C are the inductance and capacitance per unit length of the line. Therefore, Zo can be found by knowing the value of C.

Using an approximate electrostatic solution, it can be shown that the capacitance per unit length is given by:

$$C = \frac{W}{\sum_{\substack{n=1 \\ odd}}^{\infty} \frac{2a\sin(n\pi W/2a)\sinh(n\pi b/2a)}{(n\pi)^2 \varepsilon_0 \varepsilon_r \cosh(n\pi b/2a)}} \quad \text{F/m} \qquad (2.41)$$

Where, 'a' is the width of the substrate.

2.3.3 Micro-strip:

The microstrip line consists of conductor of width W printed on a thin, grounded dielectric substrate of thickness 'd' and relative permittivity εr. In a microstrip transmission line the dielectric does not completely surround the conducting strip and consequently the fundamental mode of propagation is not a pure TEM mode. As it can be seen from the figure 3.6, most of the field lines are contained in the dielectric region and some fraction in the air region above the substrate (h region).

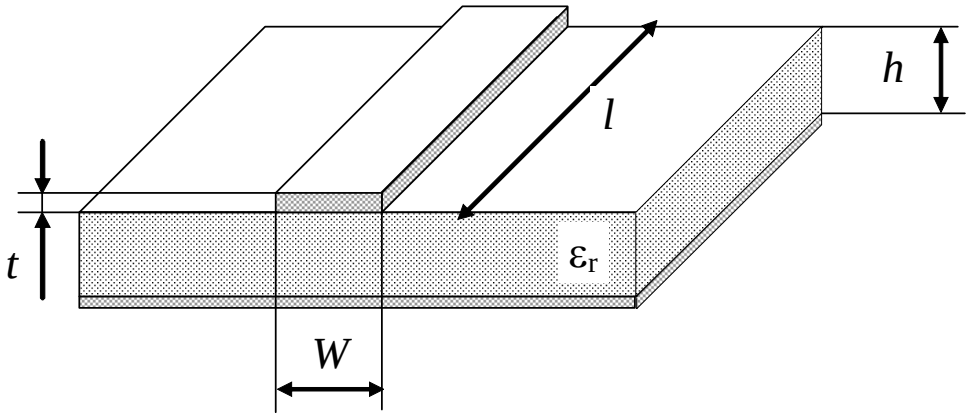

Figure 2.7: **Geometry of basic microstrip transmission line**

The phase velocity equals c in the air region and $\frac{c}{\sqrt{\varepsilon_r}}$ inside the dielectric. Thus, a phase match at the dielectric-air interface would be impossible to attain for a TEM type wave.

In fact, the field decays exponentially away from the dielectric surface, with most of the field contained in or near the dielectric (a fact concerning surface waves). At high frequencies, typically more than few gigahertz and with an electrically very thin dielectric substrate ($d << \lambda$), the field generally become more tightly bound to the dielectric, making the fields essentially the same as those of static case and so the fields are quasi-TEM.

Good approximations for the phase velocity and propagation constant can be obtained from static and quasi-static solutions.

The phase velocity (v_P) and propagation constant (β) of a TEM mode is given by:

$$v_P = \frac{c}{\sqrt{\varepsilon_{eff}}} \tag{2.42}$$

$$\beta = k_0\sqrt{\varepsilon_{eff}} \tag{2.43}$$

Where, ε_{eff} is the effective dielectric constant of the microstrip line. Fig 3.7 shows the geometry of a quasi-TEM microstrip line where ε_r has been replaced with a homogeneous medium of effective relative permittivity, ε_{eff}.

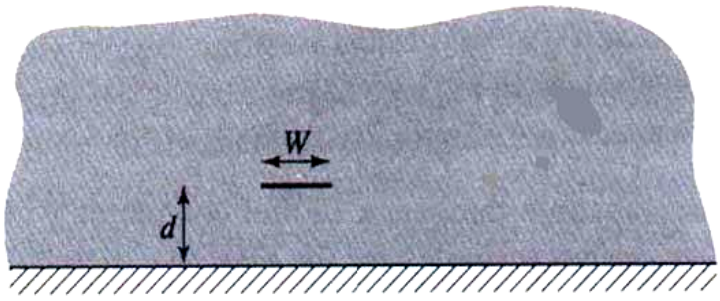

Figure 2.8: **Equivalent geometry of quasi-TEM microstrip line.**

This effective dielectric constant is given by:

$$\varepsilon_{eff} = \frac{\varepsilon_r + 1}{2} + \frac{\varepsilon_r - 1}{2}\frac{1}{\sqrt{1+12d/W}} \tag{2.44}$$

Where

$$1 < \varepsilon_{eff} < \varepsilon_r$$

Using an approximate electrostatic solution, it can be shown that the capacitance per unit length is given by:

$$C = \frac{W}{\sum_{\substack{n=1 \\ odd}}^{\infty} \frac{4a\sin(n\pi W/2a)\sinh(n\pi d/a)}{(n\pi)^2 W\varepsilon_0\left[\sinh(n\pi d/a)+\varepsilon_r\cosh(n\pi d/a)\right]}} \quad \text{F/m} \qquad (2.45)$$

Where 'a' is the width of the substrate.

The characteristic impedance can be calculated by the equations given below:

$$Z_0 = \begin{cases} \dfrac{60}{\sqrt{\varepsilon_{eff}}}\ln\left(\dfrac{8d}{W}+\dfrac{W}{4d}\right) & \text{for W/d} < 1 \\ \dfrac{120\pi}{\sqrt{\varepsilon_{eff}}\left[W/d+1.393+0.667\ln(W/d+1.444)\right]} & \text{for W/d} > 1 \end{cases} \qquad (2.46)$$

2.4 Microwave Network analysis:

Circuits operating at low frequencies, for which the circuit dimensions are small relative to the wavelength, can be treated as an interconnection of lumped passive or active components with unique voltages and currents defined at any point in the circuit. In this situation the circuit dimensions are small enough so that there is negligible phase change from one point in the circuit to another. The fields can be considered as TEM fields supported by two or more conductors. This leads to a quasi-static type of solution of Maxwell's equations and to the well-known Kirchhoff voltage and current laws and impedance concepts of circuit theory. The solution to Maxwell's equation gives the electrical and magnetic fields at all points in space. But usually we are interested in only the voltage or current at a set of terminals, the power flow through a device or some other type of "global" quantity.

Earlier in this chapter we derived the propagation constant and characteristic impedance of the line. This allowed the transmission line to be treated as a distributed component characterized by its length, propagation constant and characteristic impedance. We can interconnect various component and use network or transmission line theory to analyze the behavior of the entire system of components including effects such as multiple reflection loss, impedance transformation and transition from one type of transmission medium to another (i.e. coaxial to microstrip). A transition between different transmission lines generally can't be treated as a simple junction

between two transmission lines, but must be argumented with some type of equivalent circuit to account for reactances associated with the transition.

At this point some terms obviously come in front of use that really needs to be discussed are impedance matching and various parameters (i.e. Z, Y, S & ABCD parameters).

2.4.1 Impedance Matching:

When a given load is to be connected to generator by means of a transmission line many wavelength long, it's preferable to match the load and generator to the transmission line at each end of the line.

Now if we use various type of transmission lines in between generator to load then each joining part of the different component must be matched, otherwise maximum power will not be transferred from one part to another which will reduce frequency sensitivity. A small change in operating frequency will change the electrical length βl of a long line by an appreciable fraction of π rad.

2.4.2 Network Parameters:

At microwave frequencies the measurement of voltage or current is difficult unless a clearly terminal pair which is named as port is available. Such a terminal pair may be present in the case of TEM type line (such as coaxial cable, microstrip or stripline), but doesn't strictly exist for non-TEM lines (such as rectangular, circular or surface waveguides).

So for measuring voltage, current and transmission of power from one port to another through microwave networks some parameters are needed such as impedance parameter or Z parameters – useful for measuring series connected networks and Admittance parameters or Y parameters – useful for measuring parallel connected networks. But whenever dealing with high frequency, greater than 3 GHz, is needed then the measurement of voltage and current using Z and Y parameter for both TEM and non-TEM mode becomes impractical cause the value of voltage and current at that network change with respect to time.

In this situation another parameter is introduced named Scattering parameter or S parameter. S parameters are measured from incident, reflected and transmitted wave rather than voltage and

current wave. Thus the limitation of Z and Y parameter has been overcome though network analysis can be done by S parameter easily for both TEM and non-TEM type of transmission lines.

The network parameters that have been discussed earlier can be used to characterize a microwave network with an arbitrary number of ports. But in practice many microwave networks consists of a cascade connection of two or more two-port networks. Thus a new parameter has been introduced named ABCD parameters. When a microwave network consists of different components cascade together then it's a bit difficult to analyze that network using S parameter, here the ABCD parameter got the significance.

2.5 Realization of EBGS for different filtering Operations:

Each type of filters has different type of applications in the field of microwave communication system. Depending on the criterion of filter performance, their applications and realizations are given bellow.

2.5.1 Realization of stopband filter:

Conventional EBGS are always forms single stopband performance at the designed frequency. There is a well defined formula deduced from the Bragg's condition for circular shaped EBGS. However, square and triangular shaped EBGS of same etching area of the circular shaped EBGS show the same results as conventional circular EBGS shows.

2.5.2 Realization of multi stopbands filter:

Attempt will be taken to design a multi (dual, triple and even more stopbands) stopband filter by EBGSs and dumbbell shaped EBGSs. The multi stopband filter will be realized by a typical type of modified dumbbell shaped EBGS and dual bands are formed too for both the as usual dumbbell shaped EBGS and modified dumbbell shaped EBGS.

2.5.3 Realization of LPF:

All the available works on LPF are seen to use EBGSs/dumbbell shaped EBGSs in the ground plane to improve the performance of conventional LPF. Such designs need to take care both in ground plane and in conductor plane. In the present research the non-uniform distribution of EBGSs and dumbbell shaped EBGSs are considered to realize improved LPF performance without having any attention into conductor layer. Taking care of slots etched in the ground plane is only needed.

2.6 Periodic Structures:

An infinite transmission line or waveguide periodically loaded reactive elements is referred to as a periodic structure. As shown in Figure 2.8, periodic structure can take various forms, depending on the transmission line media being used.

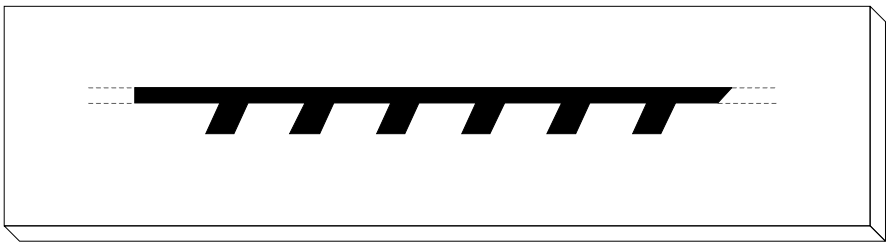

(a)

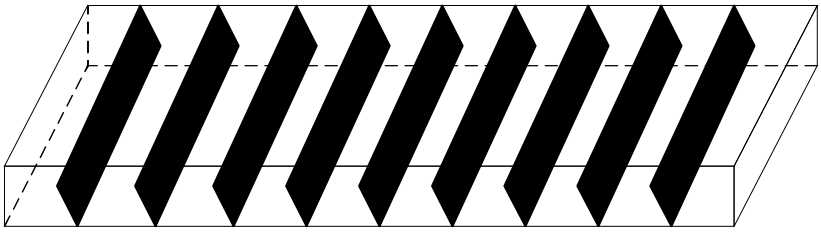

(b)

Figure 2.9: **Examples of periodic structures. (a) Periodic stubs on a micro strip line. (b) Periodic diagrams in a wave guide.**

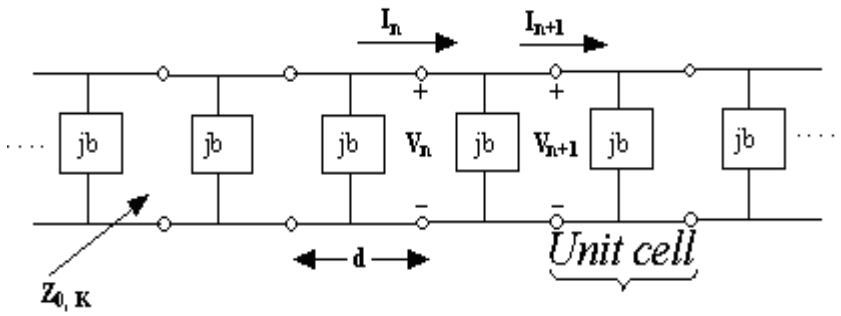

Figure 2.10: **Equivalent circuit of a periodically loaded transmission line. The unloaded line has characteristics impedance Zo and propagation constant k.**

Often loading elements are formed as discontinuities in the line, but in any case they can be modeled as lumped reactances across a transmission line as shown in Figure 3.9. Periodic structures supports slow-wave propagation (slower than the phase velocity of the unloaded line), and have passband and stopband characteristics similar to those of filters; they find application in traveling-wave tubes, masers, phase shifters, and antennas.

2.6.1 Circuit Analysis of a Periodic Structure:

A transmission line can be considered as the combination of finite unit cell of the structure. Figure 3.10(a) is the equivalent circuit of a basic unit cell of a capacitively loaded coaxial line and figure 3.10(b) is the complete transmission line composed of basic unit cell.

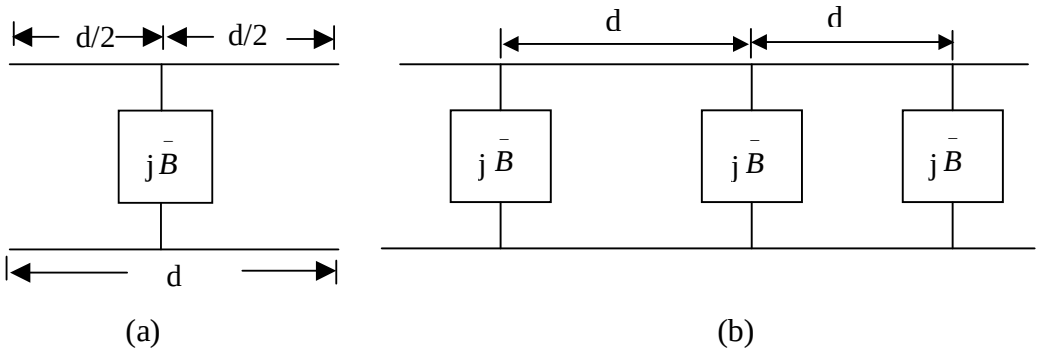

Figure 2.11: **(a) Equivalent circuit model of a unit cell, (b) a transmission line cascaded by unit cells. The unit cell may be divided into three parts as a transmission line of length d/2 on either side of normalized succeptance B.**

Relationship between input and output variables

Let,

V_n and I_n are the input voltage and current variables respectively.

V_{n+1} and I_{n+1} are the output voltage and current variables respectively.

The relationship can be found by using ABCD transmission matrix. Overall ABCD parameters of a unit cell

$$\begin{bmatrix} A & B \\ C & D \end{bmatrix} = \begin{bmatrix} \cos\theta/2 & j\sin\theta/2 \\ j\sin\theta/2 & \cos\theta/2 \end{bmatrix} \begin{bmatrix} 1 & 0 \\ j\bar{B} & 1 \end{bmatrix} \begin{bmatrix} \cos\theta/2 & j\sin\theta/2 \\ j\sin\theta/2 & \cos\theta/2 \end{bmatrix} \quad (2.47)$$

Where θ = k0 and Unit cell is symmetrical where A = D.

When EM wave propagates through periodic structures, the voltage and current at (n+1)th terminal are equal to the value of voltage and current of the nth terminal except the phase delay. It is noted that voltage and current is valid only for lossless lines.

The relation of V and I are assumed as follows.

$V_{n+1} = e^{-\gamma d} V_n$ (2.48)

$I_{n+1} = e^{-\gamma d} I_n$ (2.49)

It can be written as -

$$\begin{bmatrix} V_n \\ I_n \end{bmatrix} = \begin{bmatrix} A & B \\ C & D \end{bmatrix} \begin{bmatrix} V_{n+1} \\ I_{n+1} \end{bmatrix} = e^{\gamma d} \begin{bmatrix} V_{n+1} \\ I_{n+1} \end{bmatrix}. \quad (2.50)$$

Using equation (2.48) and (2.49), equation (2.50) generates a matrix Eigen value equation for the solution of V_{n+1} and I_{n+1}. The determinant is put to be zero.

$$\begin{bmatrix} A - e^{\gamma d} & B \\ C & D - e^{\gamma d} \end{bmatrix} = 0 \quad (2.51)$$

$AD - BC - e^{\gamma d}(A+D) + e^{2\gamma d} = 0$ (2.52)

Assuming reciprocal circuit, letting AD-BC = 1 we have

$1 + e^{2\gamma d} - e^{\gamma d}(A+D) = 0$ (2.53)

$$\cosh \gamma d = \frac{A+D}{2} \quad (2.54)$$

Expansion of (2.50) shows A = D = $\cos\theta$ - $\frac{\bar{B}}{2}\sin\theta$. Putting these values in equation (2.54), we have

$\cosh\gamma d = \cos\theta - \frac{\bar{B}}{2}\sin\theta$ (2.55)

Equation (2.55) is very vital equation to understand passband and stopband phenomena created by periodic structure.

Explanation:

The phenomena can be explained by the following cases:

Case 1: $\alpha = 0, \beta \neq 0$. This case corresponds to non-attenuating propagating wave on the periodic structure. This case defines the passband of the structure. Then equation (2.55) reduces to

$\cos\beta d = \cos\theta - \frac{\bar{B}}{2}\sin\theta$ (2.56),

Which can be solved for β, if the magnitude of the right hand side is less than or equal to unity. Case 1 is limited to <1 AND >-1.

Case 2: $\alpha \neq 0, \beta = 0$. In this case the wave does not propagate, but is attenuated along the line. This case defines the stopband of the structure. As the line is assumed to be lossless, power is not dissipated, rather is reflected back to the input of the line. Under this condition the equation (2.56) reduces to

$\cosh\alpha d = \cos\theta - \frac{\bar{B}}{2}\sin\theta$ (2.57)

The magnitude of equation (3.57) reduces to

$\cosh\alpha d = \left|\cos\theta - \frac{\bar{B}}{2}\sin\theta\right| \geq 1,$ (2.58)

Equations (2.56)-(2.57) are very important to understand the propagation of EM waves through periodic structures. It is apparent that there will be frequency bands for which unattenuated wave propagation is possible separated by frequency bands in which the wave is attenuated. Fully attenuated wave stems stopband and unattenuated wave generates passband. Thus these equations help understand of stopband and passband phenomena of PBGS.

Let us consider $d \leq \lambda 0$ in a case. So the electrical length $\theta = k^{0} d$ will be small and βd is also small. Under this condition

$$\cos\theta = 1 - \theta 2/2 \tag{2.59}$$

$$\cos\beta d = 1 - \frac{\beta^2 d^2}{2} \tag{2.60}$$

Equation (2.56) comes into the following form

$$\Rightarrow 1 - \frac{\beta^2 d^2}{2} = 1 - \frac{k_0^2 d^2}{2} - \frac{B k_0 d}{2} \tag{2.61}$$

We have the relations

$$k_0^2 = \omega^2 \mu^0 \varepsilon^0 = \omega^2 LC \tag{2.62}$$

$$\bar{B} = \frac{B}{Y_c} = \omega C^0 \sqrt{L/C} \qquad [Z_c = \sqrt{L/C}] \tag{2.63}$$

So,

$$1 - \frac{B^2 d^2}{2} = 1 - \frac{k_0^2 d^2}{2} - \frac{\bar{B} k_0 d}{2}$$

$$\Rightarrow \beta^2 d^2 = k_0^2 d^2 + \bar{B} k_0 d$$

$$\Rightarrow \beta^2 = k_0^2 + \frac{\bar{B} k_0}{d}$$

Substituting k0 and $\bar{B}$ from (2.62) and (2.63) in the above equation we have

$$\beta^2 = \omega^2 LC + \omega^2 \frac{LC_0}{d}$$

$$\Rightarrow \beta = \omega \sqrt{L(C + C_0/d)} \tag{2.64}$$

Equation (2.64) is very important to understand the slow-wave effect of periodic structures. The new value of capacitance $C + C_0/d$ is observed. So capacitance has been increased by C_0/d. Therefore it is found that at low frequencies where

$d << \lambda^0$, the load line behaves as a shunt capacitance $C + C_0/d$ per unit length. The increase in β reduces of the phase velocity.

For periodic structure the characteristic impedance (CI) becomes,

$$Z_B = \sqrt{\frac{\mathrm{L}}{C + \frac{C_0}{d}}}$$

It is seen that capacitance has increased by $\frac{C_0}{d}$.

The characteristic impedance of a periodic structure depends on the terminal plane. Lets say if the normalized characteristic impedance in the reference plane is $\overline{Z_B}$ and if the terminal planes are shifted a distance l in the –z direction, the new normalized CI becomes

$$\overline{Z}'_{B'} = \frac{\overline{Z_B} + j\tan k_0 l}{1 + j\overline{Z_B}\tan k_0 l} \qquad (2.65)$$

2.6.2 Significance of EBGS as periodic structures:

Electromagnetic Bandgap or EBG engineered structures may have different forms such as bumpy surface, corrugated surface, metal pad or high-impedance surface and planar EBG structures. Normally the ground plane is perturbed by EBGSs with different shape and different lattice structures. The shape may be uniform and non-uniform circular, square, rectangular, triangular patterned and the structures are named on the basis of the grid arrangement such as square, rectangular, triangular and honeycomb etc. Different shapes and sizes of EBGSs provide different S-parameter performances. The location of the EBG elements under the microstrip transmission line greatly influences the performance of the transmission line.

However one of their main significances is their ability to generate stopband performance periodically. Stopband is very useful to improve the performance of the microwave devices and components. For an example, to suppress of any unwanted transmission of signal the center of the stopband is chosen to be equal to the center of the unwanted signal. This concept is highly preferred for harmonic suppression of filter. For the beam steering purpose the frequency of operation is chosen so that it remains within the passband of transmission line.

Another significance of EBGSs is their ability to provide slow-wave properties. For the compact design this property is used. Practically EBGSs can be used in amplifiers, mixers, filters, waveguides, antennas and many other devices to improve their performances.

2.7 Some useful Theorems:

2.7.1 Slow wave:

Slow wave structures act to reduce the group velocity of a transmission line, or increase its group delay compared to a normal "fast-wave" structure.

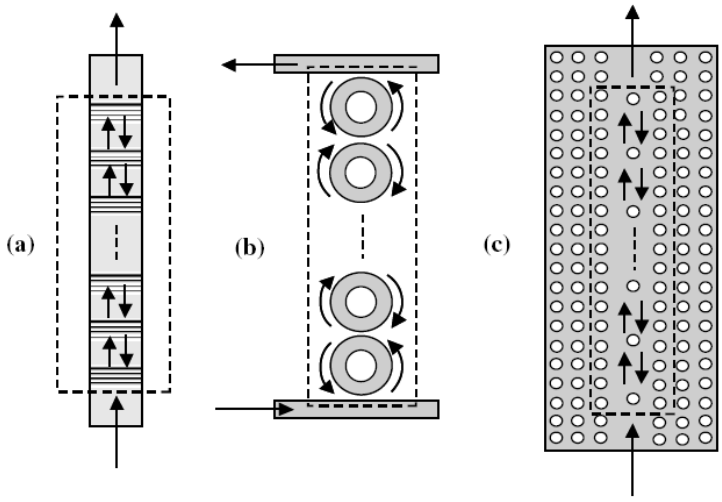

Figure 2.12: **Slow-wave optical structure (SWS)**

Slow-wave structures are useful in shrinking distributed elements. In microwave engineering, cost is a linear function of circuit area, so any tricks we can employ to shrink designs are worth knowing about.

Let's start the topic by providing the following definition:

✧ **Slow-wave factor:**

The ratio of the wave velocity of a "native" transmission line to a slow-wave structure. The higher the slow-wave factor, the more the transmission line's wavelength is reduced compared to its "normal" wavelength in the chosen dielectric medium. By "normal" we are comparing it to CPW or microstrip or stripline.

✧ **Metal-insulator-semiconductor structures (MIS)**

Silicon is usually a very poor insulator. By creating a microstrip line on top of silicon, with a dielectric layer such as silicon dioxide in between, a strange thing can happen. The electric field

does not penetrate into the silicon (which tries to shorts it out) but the magnetic field does. The separation of electrical and magnetic energy slows the wave propagation. Substantial reduction in wavelength is possible.

Ga As can also be used to create a MIS slow-wave structure. In this case an epitaxial layer is grown on top of the wafer, because Ga As is such a good semi-insulating substrate. A layer of low-loss dielectric is added on top

✧ **Cross-tie slow-wave circuits**

These classes of circuits are sometimes called "artificial" transmission lines. Note that there are other implementations of slow-wave that are similar, all that is requires is a periodic structure of electrically short high-impedance and low-impedance lines.

The cross-tie slow-wave structure replaces a continuous transmission line with an artificial transmission line made up of many electrically-small segments. The segment impedance alternates from Z1 to Z2 along the chain. One impedance is lower than Zo, the other is higher than Zo. The high impedance section can be created using a CPW structure with very wide gaps, the low impedance section is enabled by the cross-tie capacitance shunting from the center conductor to the dual grounds.

2.7.2 Bragg's Law:

Bragg's law gives the angles for coherent and incoherent scattering from a crystal lattice. When X-rays are incident on an atom, they make the electronic cloud move as does any electromagnetic wave. The movement of these charges re-radiates waves with the same frequency (blurred slightly due to a variety of effects); this phenomenon is known as Rayleigh scattering (or elastic scattering). The scattered waves can themselves be scattered but this secondary scattering is assumed to be negligible.

A similar process occurs upon scattering neutron waves from the nuclei or by a coherent spin interaction with an unpaired electron. These re-emitted wave fields interfere with each other either constructively or destructively (overlapping waves either add together to produce stronger peaks or subtract from each other to some degree), producing a diffraction pattern on a

detector or film. The resulting wave interference pattern is the basis of diffraction analysis. This analysis is called Bragg diffraction.

Bragg diffraction (also referred to as the Bragg formulation of X-ray diffraction) was first proposed by William Lawrence Bragg and William Henry Bragg in 1913 in response to their discovery that crystalline solids produced surprising patterns of reflected X-rays (in contrast to that of, say, a liquid). They found that these crystals, at certain specific wavelengths and incident angles, produced intense peaks of reflected radiation (known as Bragg peaks). The concept of Bragg diffraction applies equally to neutron diffraction and electron diffraction processes. Both neutron and X-ray wavelengths are comparable with inter-atomic distances (~150 pm) and thus are an excellent probe for this length scale.

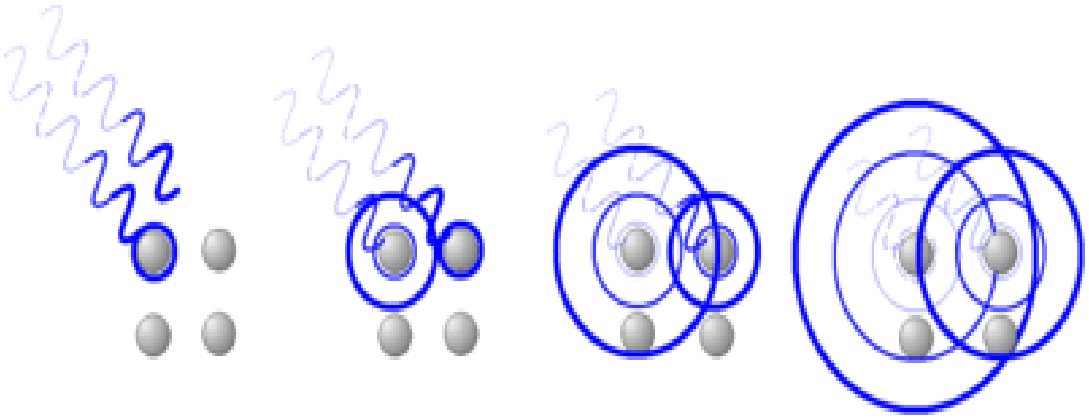

Figure 2.13: **X-rays interact with the atoms in a crystal.**

W. L. Bragg explained this result by modeling the crystal as a set of discrete parallel planes separated by a constant parameter d. It was proposed that the incident X-ray radiation would produce a Bragg peak if their reflections off the various planes interfered constructively. The interference is constructive when the phase shift is a multiple of 2π; this condition can be expressed by Bragg's law,

$$n\lambda = 2d\sin\theta \qquad (2.66)$$

Where n is an integer, λ is the wavelength of incident wave, d is the spacing between the planes in the atomic lattice, and θ is the angle between the incident ray and the scattering planes. Note that moving particles, including electrons, protons and neutrons, have an associated De Broglie wavelength.

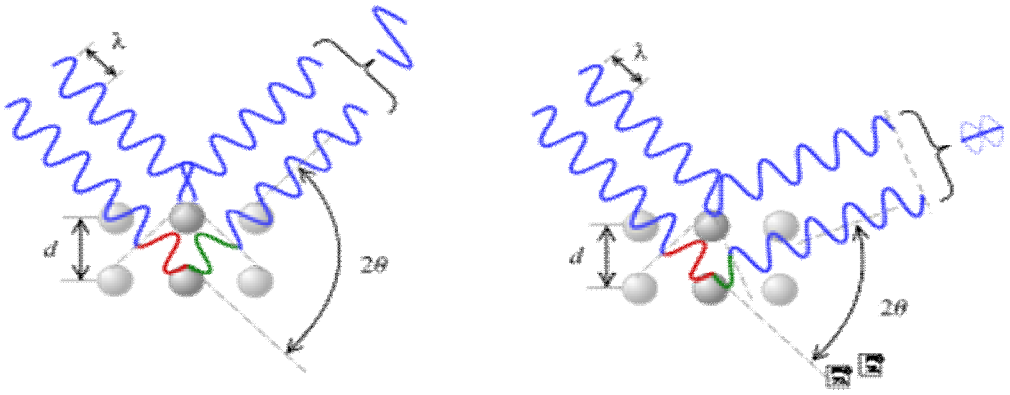

Figure 2.14: **According to the 2θ deviation, the phase shift causes constructive (left figure) or destructive (right figure) interferences.**

2.7.3 Permittivity:

In electromagnetism, absolute permittivity is the measure of the resistance that is encountered when forming an electric field in a medium. In other words, permittivity is a measure of how an electric field affects, and is affected by, a dielectric medium. The permittivity of a medium describes how much electric field (more correctly, flux) is 'generated' per unit charge. Less electric flux exists in a medium with a high permittivity (per unit charge) due to polarization effects. Permittivity is directly related to electric susceptibility, which is a measure of how easily a dielectric polarizes in response to an electric field. Thus, permittivity relates to a material's ability to transmit (or "permit") an electric field.

In SI units, permittivity ε is measured in farads per meter (F/m); electric susceptibility χ is dimensionless. They are related to each other through

$$\varepsilon = \varepsilon_r \varepsilon_o = (1 + \chi)\varepsilon_o$$

where ε_r is the relative permittivity of the material

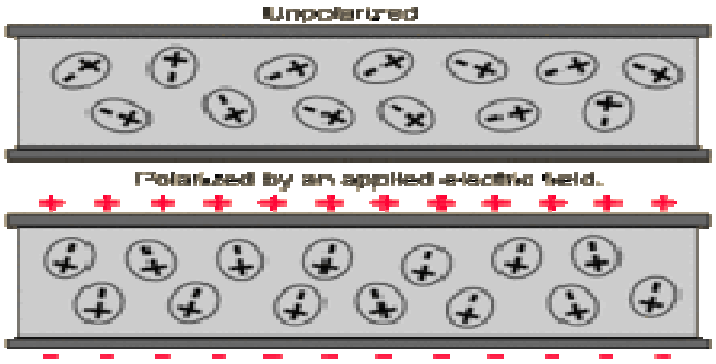

Figure 2.15: **A dielectric medium showing orientation of charged particles creating polarization effects. Such a medium can have a higher ratio of electric flux to charge (permittivity) than empty space**

✧ Permittivity of free space

The permittivity in vacuum (free space) is denoted as ε_o. Its value is $8.85418782 \times 10^{-12}$ Farads per meter (see our page on physical constants). No material has a permittivity lower than that of a vacuum.

2.7.4 Effective and relative Permittivity:

✧ Relative permittivity

Materials other than vacuum have permittivity higher than ε_o, often they are referred to by their relative permittivity, denoted ε_r:

$\varepsilon_{material} = \varepsilon_o \times \varepsilon_r$

In microwaves, we often refer to relative permittivity as the "dielectric constant". These terms are interchangeable.

An alert professor points out the relative permittivity is not always a constant for a given material, it can change with frequency, temperature, date of manufacture or supplier, or even direction of propagation.

Most microwave materials have dielectric constant between 2.2 (PTFE) and 9.9 (alumina), because so many materials are engineered by mixing these two materials. If particle size is kept small compared to a wavelength, and the ratio of materials is well maintained from batch to batch,

the mixture will be well behaved. See our pages on soft and hard substrate materials for data on a wide variety of materials.

✧ **Effective permittivity**

In non-TEM transmission lines such as those realized in microstrip media, most of the electric fields are constrained within the substrate, but a fraction of the total energy exists within the air above the board. The effective permittivity (a.k.a. effective dielectric constant) takes this into account. The effective dielectric constant of a fifty-ohm transmission line on ten mil alumina is a number somewhere around 7, which is less than the dielectric constant of the substrate bulk material (9.8), but more than that of air (which is 1).

Another example of an effective dielectric constant is if you were to create a stripline circuit using two sheets of substrates with different dielectric constants. To a first order, the effective dielectric constant would be the average of the two materials' dielectric constants.
A third example is coplanar waveguide transmission lines with air above the substrate. Here the effective dielectric constant is very nearly the average of the substrate dielectric constant and one (the relative dielectric constant of air). Thus the effective dielectric constant of CPW circuits on GaAs (ER=12.9) is approximately 6.5.

2.7.5 Power in dB:

The term dB or decibel is a relative unit of measurement used frequently in electronic communications to describe power gain or loss. Decibels are used to specify measured and calculated values in audio systems, microwave system gain calculations, satellite system link-budget analysis, antenna power gain, light-budget calculations and in many other communication system measurements. In each case the dB value is calculated with respect to a standard or specified reference.

The dB value is calculated by taking the log of the ratio of the measured or calculated power (P2) with respect to a reference power (P1). This result is then multiplied by 10 to obtain the value in dB. The formula for calculating the dB value of two ratios is shown in equation 2.66. Equation 2.66 is commonly referred to as the power ratio form for dB.

$$dB = 10 \log_{10} \frac{P_2}{P_1}$$

(2.67)

Equation 2.66 can be modified to provide a dB value based on the ratio of two voltages. By using the power relationship $P = V^2/R$, the relationship shown in equation 2.67 is obtained.

$$db = 10 \log_{10} \frac{V_2^2 / R_2}{V_1^2 / R_1}; \quad (let\ R_1 = R_2)$$

$$\therefore \quad dB = 10 \log_{10} \frac{V_2^2}{V_1^2}$$

(2.68)

By simplifying the equation, a dB relationship based on voltage ratios instead of power is obtained. The voltage gain calculation is shown below in equation 2.68.

$$dB = 20 \log_{10} \frac{V_2}{V_1}$$

(2.69)

The dB unit is often used in specifying input and output signal level requirements for different communication systems. An example of specified audio levels can be found in microwave transmitters. It is common for a +8dBm input level to be specified. Notice that a lower case m has been attached to the dB value. This indicates that the specified dB level is relative to a 1 milli watt reference. In standard audio systems 0dBm is defined as .001 watt measured with respect to a load termination of 600 ohms. A 600 ohm balanced audio line is the standard for professional audio and telecommunications.

0 dBm is defined as 1 mW measured with respect to a 600 ohm termination

The voltage measured across a 600 ohm load for an 0dBm level is .775 volts. This value is derived below using equation 2.67.

$$dB = 10 \log_{10} \frac{P_2}{P_1}$$

$$where\ P_2 = \frac{V_2^2}{600}\ and\ P_1 = .001\ watts$$

Since 1mW is the specified reference for 0dBm, the voltage reference can be derived as shown in equation 2.70.

$$0dBm = 10 \log \frac{V_2^2/600}{.001}$$

$$0dBm = \log \frac{V_2^2/600}{.001}$$

$$\log^{-1} 0\,dBm = \frac{V_2^2/600}{.001}$$

$$\frac{V_2^2/600}{.001}$$

$$.6 = V_2^2$$

$$\therefore\ .77459 = V_2$$

$$dB = 20 \log_{10} \frac{V_2}{V_1}$$

(2.70)

This is the voltage reference for 0dB with respect to a 600 ohm load. To determine the voltage required at the input of the microwave transmitter to provide a +8dBm level, use the voltage gain equation 2.68 letting V1 equal the 0.775 reference in the equation

$$dBm = 20 \log_{10} \frac{V_2}{.775}$$

To solve for V2 for a +8dBm level;

$$+8dBm = 20\log_{10}\frac{V_2}{.775}$$

$$.4 = \log\frac{V_2}{.775}$$

$$\log^{-1}(.4) = \frac{V_2}{.775}$$

$$\therefore \quad 1.946712 = V_2$$

Thus for a +8 dBm level to be present at the input of the microwave transmitter, approximately 1.95 volts must be present across the 600 ohm input.

The term dBm also applies to communication systems which have standard termination impedance other than 600 ohms. For example, video and some RF systems are terminated with 75 ohms. The 0dBm value is still defined as 1mW but measured with respect to a 75 ohm termination instead of 600 ohms. Therefore the voltage reference for an 0dBm system with respect to 75 ohms is;

$$v = \sqrt{P * R} = \sqrt{(.001) * (75)} = .27386\ volts$$

To calculate the voltage gain or loss with respect to a 75 ohm load use equation 5 if a voltage is specified and the dB value is needed.

$$dBm(75) = 20\log_{10}\frac{V}{.27386}$$

More commonly encountered in communications are 50 ohm systems. The dBm voltage reference for a 50 ohm system is:

$$V = \sqrt{P \bullet R} = \sqrt{.001 \bullet 50} = .2236\ volts$$

To calculate the voltage gain or loss, expressed in dB for a 50 ohm system, use equation 3 with the value for V2=.2236. This relationship is shown in equation 2.70.

$$dBm(\mathbf{50}) = \mathbf{20} log_{10} \frac{V}{.2236}$$

(2.71)

It is common for power to be expressed in watts instead of milliwatts. In this case the dB unit is obtained with respect to 1 watt and the dB values are expressed as dBW.

0 dBW is defined as 1 watt measured with respect to 50 ohms.

Remember, dB is a relative measurement. As shown by equations 2.66 and 2.68, both power and voltage gains can be expressed,in dB, relative to a reference value. In the case of dBW the reference is 1 watt, therefore equation 3.66 is written with 1 watt replacing the reference P1. This gives equation 2.71.

$$dBW = 10 \log_{10} \frac{P_2}{1W}$$

(2.72)

It is common in communication receivers to express voltage measurements in terms of dBuV, dB-microvolts. For voltage gain calculations involving dBuV use equation 2.68 and specify 1uV as the reference (V1) in the calculations as shown in equation 2.72.

$$dB\mu V = 20 \log \frac{V_2}{1\mu V}$$

(2.73)

There are a multitude of applications involving the use of dB for calculations involving relative values. The important thing to remember is that a relative reference is typically specified or understood when calculating or measuring a dB value.

dBm 1 milliwatt (.001W), Typical measurement for audio input/output specifications. Also used in low power optical transmitter specifications.

dBm(600) The standard audio reference power level defined by 1 milliwatt measured with respect to a 600 ohm load. This measurement is commonly used in broadcasting, professional audio applications and is a common telephone communications standard.

dBm(50) This standard is defined by 1 milliwatt measured with respect to a 50 ohm load. This measurement is commonly used in RF transmissions/receiving systems.

dBm(75) This standard is defined by 1 milliwatt measured with respect to a 75 ohm load. This standard is common in some RF systems particularly cable TV systems.

dBmW This is the generic form for a 1 milliwatt reference, also written as dBm. This term usually has an inferred load reference, depending on the application.

dBW This is a common form for power amplification relative to a 1 watt reference (usually 50 ohms). Typical applications are found in RF Power Amplifiers and High Power Audio Amplifiers specifications.

dBuV This is a common form for specifying input RF levels to a communications receiver. This is called dB microvolt where 1 microvolt = 1*10E-6V.

dBV While this dB term is defined, it is rarely used in defining communication systems. The dB value is obtained with respect to 1 Volt.

dB/bit This is a common term used for specifying the dynamic range or resolution for a Pulse Coded Modulation (PCM) system such as a CD player. This reference is defined by 20 Log (2)/bit = 6.02dB/bit.

dBi This is dB isotropic . It is used as the reference when defining Antenna Gain.

dB/Hz This is relative noise power in 1-Hz bandwidth. This term is used often in digital communications and in defining a laser's Relative Intensity Noise (RIN). For a laser system, this is an electrical not an optical measurement. A typical1 RIN for a semiconductor laser is -150 dB/Hz.

dBW/K-Hz This is a common term used when analyzing carrier-to-noise (C/N) in a communications link such as a satellite link budget. This value is based on the Boltzmann's constant expressed in dB as 10 Log (1.38*10E-23) = -228.6 dBW/K-Hz.

2.8 Conclusion:

In this chapter some basic parameters and facts of T-line and microwave filter designing are discussed. Theoretical and also mathematical expressions are studied in this chapter. These will be used in the later chapters for designing microwave filters and describing their performacnces. Basically, this chapter expresses the theoretical back ground of microwave filter designing. Considering these facts in to account further implementation and filter realization will be made in the bellow chapters.

Chapter 3 : Study and Analysis of EBGS Assisted micro-strip line as Band-stop filter

3.1 Introduction:

In the field of microwave filter designing and obtaining better filtering performances of microwave devices use of EBG structures are the most powerful tactics. The stopband characteristic causes the dramatic improvement in the performance by suppressing surface waves, leakage and spurious transmission. FF is one of the important controlling factors to yield wider and distinct stopband that should be optimized to maintain a smoother transmission in the passband. In the literature for circular patterned EBGS, the optimized FF of 0.25 [1] is considered. Thickness of transmission lines, dielectric constant of used material, different shape of EBGS, Etching area of EBGS and number of EBGS used are also important factors that control filtering performance.

Periodic EBG structures are etched at the ground plane or over the substrate. The transmission line can also be modified to form EBG characteristics without having any perturbation in the ground plane[2]-[4]. This new idea can be extended to filter, antenna and other microwave component and devices where the complexity of packaging is minimized.

3.2 Simple Microstrip Transmission line and its performance:

T-line is just a line with a defined length and width on the upper surface of the substrate which is created by removing copper coating from the surface except the desired region. The figure is shown below where the blue region is a typical T-line whose length is 100 mm and width is 2.2642 mm (calculated by PCAAD for 50Ω microstrip T-line where dielectric constant of the substrate is 2.45 and thickness is 31 mils).

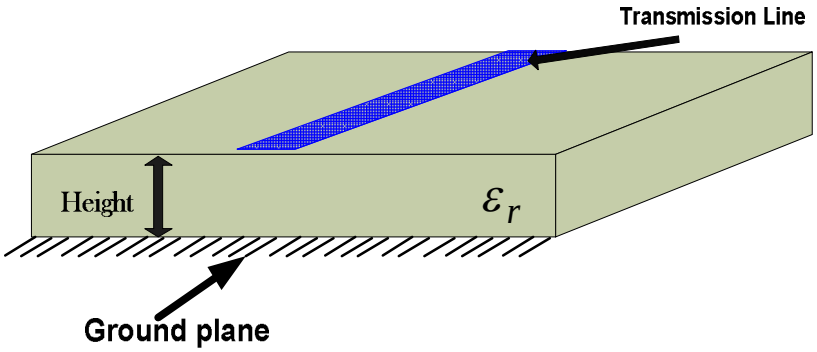

Figure 3.1: **Geometry of a standard 50-ohm microstrip transmission line on a substrate whose dielectric constant is 2.45 and thickness is 31 mils.**

✧ **S-Parameter Performance of a microstrip T-line:**

S-Parameter performances are inspected from the plotted curves of the simulation by Zeland ie3d where the curves of S_{11} (return loss) and S_{21} (insertion loss) are only shown here. Stopband and passband yield the frequency band width of insertion loss and return loss at -20 dB and -10 dB respectively. The following graph is plotted by Grapher software by taking simulated data from the Zeland ie3d.

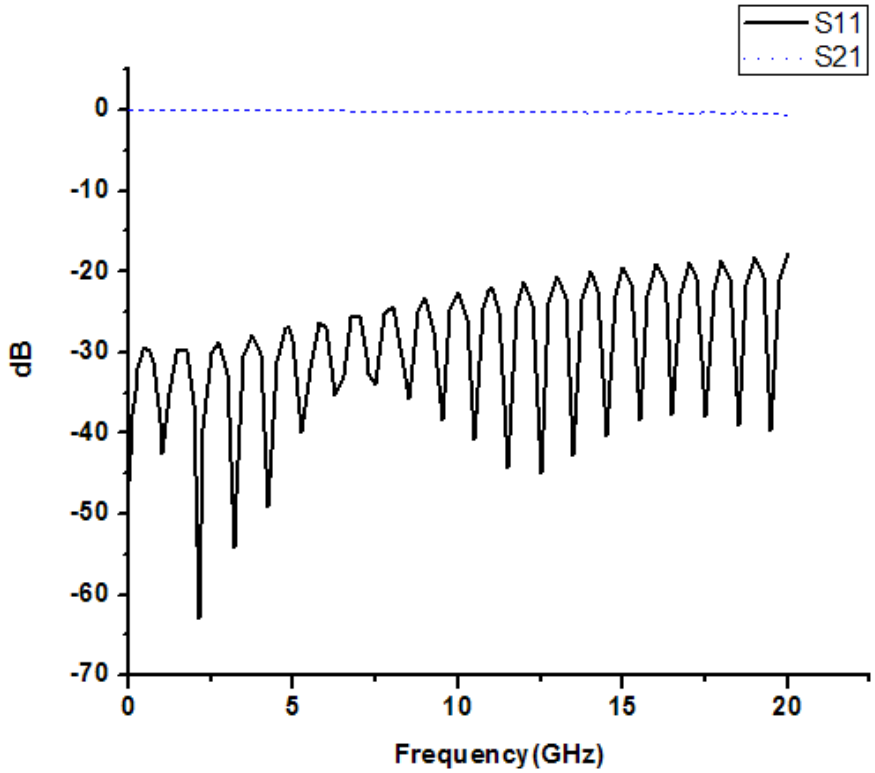

Figure 3.2: S-parameter performance of 50 Ω T-line, length is 100 mm and width is 2.2642 mm.

Within the range of 0-20GHz the signal has transmitted between two ports with negligible loss and there is no stopband formed. The return loss performance of the ideal microstrip line over the whole frequency range is also excellent and < - 10 dB. Since, there is no appreciable insertion loss observed at the s-parameter performance of the T-line, therefore it characterizes an ideal transmission line.

3.3 Microstrip Transmission Line over Uniform circular EBGS:

With the inclusion of EBGSs the dispersion characteristics of a transmission line change. At first a microstrip transmission line with unperturbed ground plane is designed that does not provide any stopband characteristics as shown in 3.2. Then the effect is observed on the dispersion characteristics in the form of scattering parameters matrices versus frequency by perturbing the ground plane with circular EBGSs. EBG structures are created by picking up copper by etching process. A constant distance is maintained between the centers of consecutive EBGS which is determined by Bragg's law.

3.4 Necessary Designing equations:

In the EBG engineering it is a conventional rule to use Bragg's condition to calculate the central stopband frequency provided by EBGSs. Under this condition, inter-cell separation (known as period) is approximately equal to half wavelength of the stopband central frequency. From the inter-cell separation, the size of the EBG element is calculated on the basis of FF.

The center frequency of the stopband is calculated approximately with the following expression:

$f_0 = c/ \lambda o$ (3.1)

Where,

fo = the center frequency of the stopband

λo= Wave length of electro magnetic wave in air.

c = the speed of light in free space

As explained by the theory of slow wave structure, the wave length of slow wave is less than the wave length λo. Relation between them are explained as

$\lambda g = \lambda o/\sqrt{\varepsilon}eff$

Where,

λg= Wave length of slow wave.

εeff= Effective dielectric constant.

Inner element spacing is also an important factor that determines the space between the EBGS is generally denoted by 'a'.

From Bragg's law we know,

$a = \lambda g/2$

And the Filling factor (FF) is determined by

$FF = r/a$

Where,

r= radius of circular EBGS.

For square shape EBGS

$FF = b/a$

Where,

b= side of square.

3.5 Optimum Filling Factor (FF) Analysis:

Filling Factor (FF) is a fractional quantity that is used to determine the size of the conventional EBG structures for a particular unit cell to keep the center frequency at particular point. As the center frequency is 10 GHz, calculated unit cell length is 10.43 mm which is also denoted by 'a'.

The radius of the circular shaped EBG is determined by the formula FF=r/a.

From the above equation if FF is assumed to be 0.25 then calculated r=2.6075 mm.

3.5.1 FF Analysis for Circular shape EBGS:

Optimum value of FF for uniform circular shape EBGS is 0.25 reported by Itoh[ref]. For verifying this statement S-parameter performances are observed for designs having seven EBGSs for FF between 0.10 and 0.39. A typical designing diagram of the transmission line is shown below,

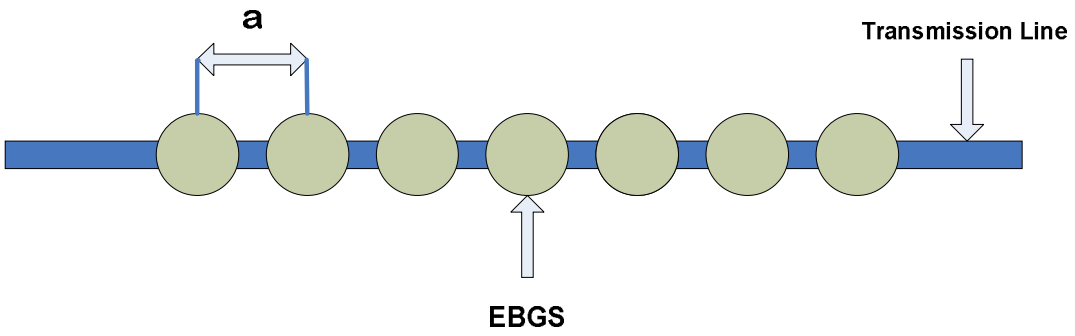

Figure 3.3: **Typical design of a seven circular shape EBGS.**

✧ **S-Parameter Performances analysis:**

S-parameter performance for FF of 0.10, 0.13, 0.16, 0.19, 0.22, 0.25, 0.28, 0.31, 0.32, 0.34, 0.36 and 0.39 were studied. Substrate used was Taconic having dielectric constant of 2.45, height of 31 mils and the inner-element spacing (period) a = 10.4308 mm, which was calculated for the centre frequency of 10GHz. They show following performances as the table describes

Table 3.1: Data table taken from above S-Parameters observed for Variation of Filling Factor.

Filling Factor	Pass band (GHz)	Stop band width (GHz)	Depth of Stop band (at center frequency, 10 GHz)	Maximum Ripple Height (dB)	-3 dB Cut-off frequency (GHz)
0.10	8.9596	0	-1.9485	-0.2582	0
0.13	8.628	0	-6.9935	-0.4567	8.910395
0.16	8.97	0	-14.547	-1.0248	8.386008
0.19	7.04788	1.75065	-23.2454	-1.84914	8.06509
0.22	6.71332	3.23692	-31.7999	-0.912682	7.594288
0.25	6.84165	4.23386	-39.611	-1.476634	7.382862
0.28	5.07743	5.00741	-45.7696	-3.62662	6.881204
0.31	6.44955	5.61271	-47.6024	-4.97170	7.046781
0.32	7.193777	5.75909	-47.5164	-5.22859	7.046843
0.34	6.325917	6.01	-46.5875	-5.493526	7.007255
0.36	6.221654	6.14656	-45.220	-3.288139	5.807917
0.39	6.31773	6.17564	-43.0942	-3.849579	6.374698

Following two curves are formed by using the data from the table which is necessary to find out the optimum FF for getting better performances.

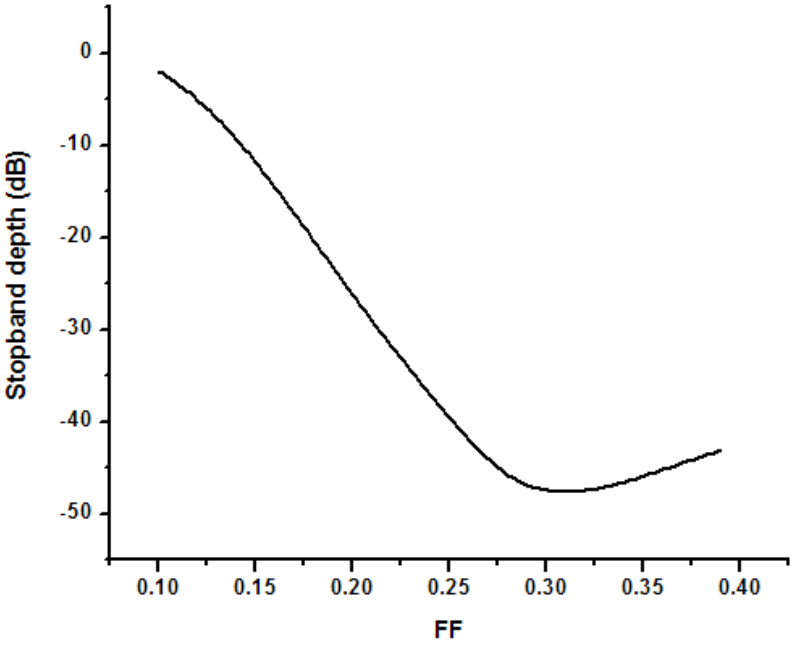

(a)

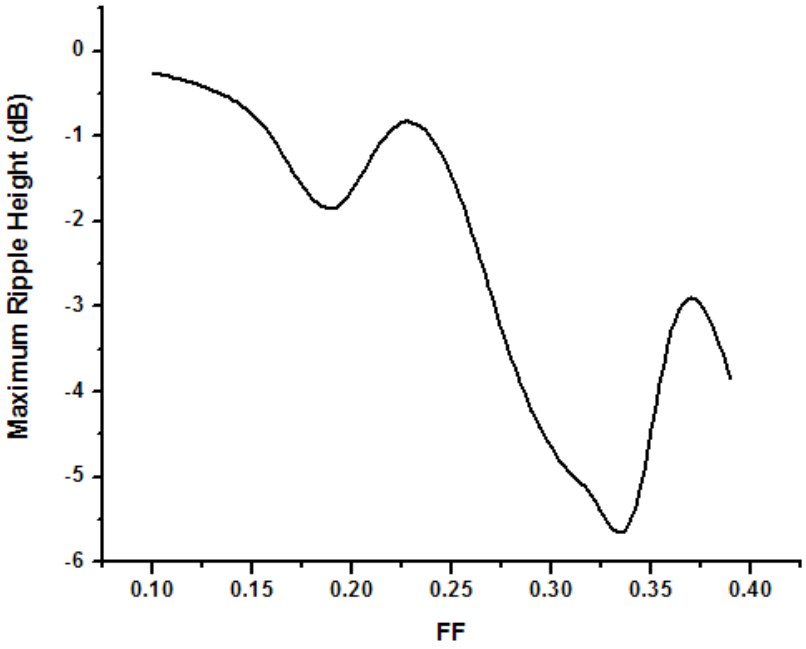

(b)

Figure 3.4: (a) Stopband depth (at center frequency, 10 GHz) Vs Filling factor (b) Maximum ripple height Vs Filling factor curve for circular EBGS.

In graph (a) Stopband depth is maximum for FF=0.31 which is -47.6024 dB. On the other hand for FF= 0.25 stopband depth is. -39.611 dB which is also a very good depth. In graph (b) Maximum ripple height for FF=0.31 is -4.9717 dB. It is comparatively very high can create noise on the system. But from the graph we see for FF=0.25 the maximum ripple height is -1.4766 dB. This ripple height is very good for smooth filtering.

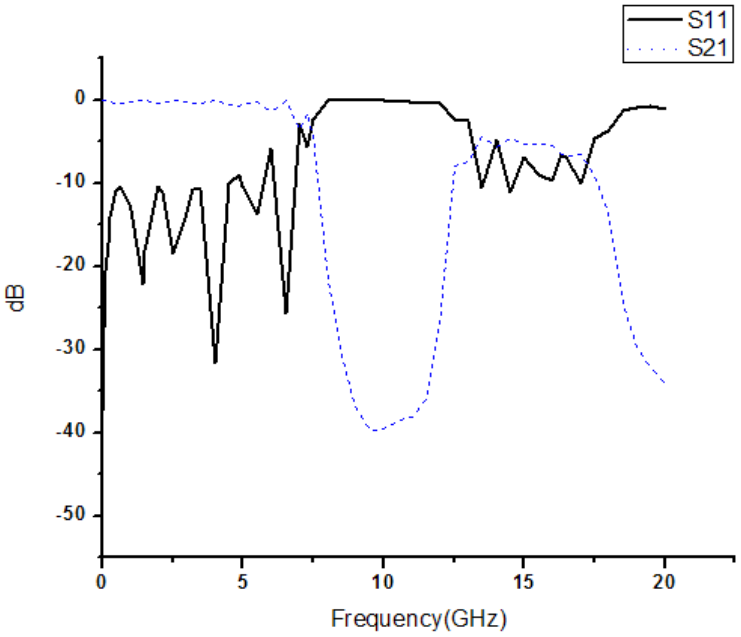

(a)

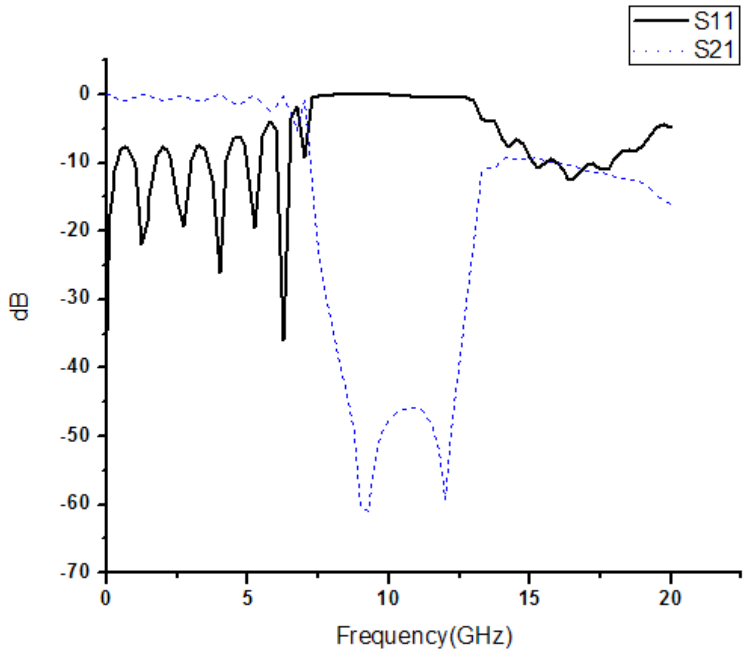

(b)

Figure 3.5: Return loss and Insertion loss Vs FF curve for (a) FF=0.25 (b) FF=0.31.

From the graphs of 3.5 (a) & (b) it is observed that for FF=0.25 in passband the curve contains fewer ripples than for FF=0.31.

So FF=0.25 gives better performance hence it is chosen as optimum value of FF by Prof. T. Itoh [1].

3.5.2 FF Analysis for Square shape EBGS:

Square shapes are designed on the same substrate plate as it has been used earlier for circular EBGS. For finding optimum value of FF for square shaped EBGS S-parameter performances are observed for designs having seven EBGSs for FF between 0.25 and 0.54. The sides of square

EBGS is determined by equation b= FF*a.

A typical designing diagram of the transmission line is shown below,

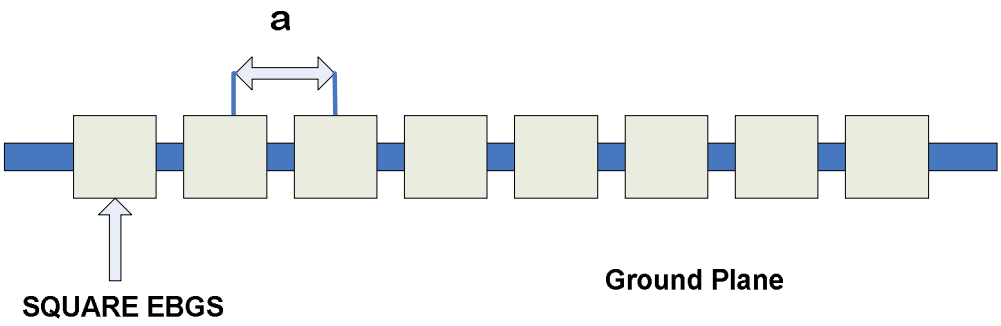

Figure 3.6: **Typical design using seven square shape EBGS**.

✧ S-Parameter Performances analysis:

S-parameter performance for FF of 0.25, 0.28, 0.29, 0.30, 0.33, 0.36, 0.39, 0.42, 0.45, 0.48 and 0.54 were studied. Substrate used was Taconic having dielectric constant of 2.45, height of 31 mils and the inner-element spacing (period) a = 10.4308 mm, which was calculated for the centre frequency of 10GHz. They show following performances as the table describes

Table 3.2: Data table taken from above S-Parameters observed for Variation of Filling Factor of square shape.

Filling Factor	Pass band (GHz)	Stop bandwidth (GHz)	Depth of Stopband (at center frequency, 10 GHz)	Maximum Ripple Height (dB)
0.25	8.44481	0	-9.62524	-0.7473
0.29	8.20581	0	-16.0657	-1.26665
0.30	8.17642	0	-17.1761	-1.7238
0.33	7.9013	1.69054	-22.9836	-1.7586
0.36	7.5925	2.61875	-28.578	-1.69233
0.39	6.68489	3.46405	-33.1782	-0.98855
0.42	6.57842	4.0203	-37.3743	-0.65505
0.45	6.43231	4.42666	-41.9837	-1.47571
0.48	7.1909	4.84999	-45.1873	-4.12936
0.54	6.13752	5.52569	-48.7598	-4.777023

Again we got the following curve by using the data from the table which is necessary to find out the optimum FF for getting better performances.

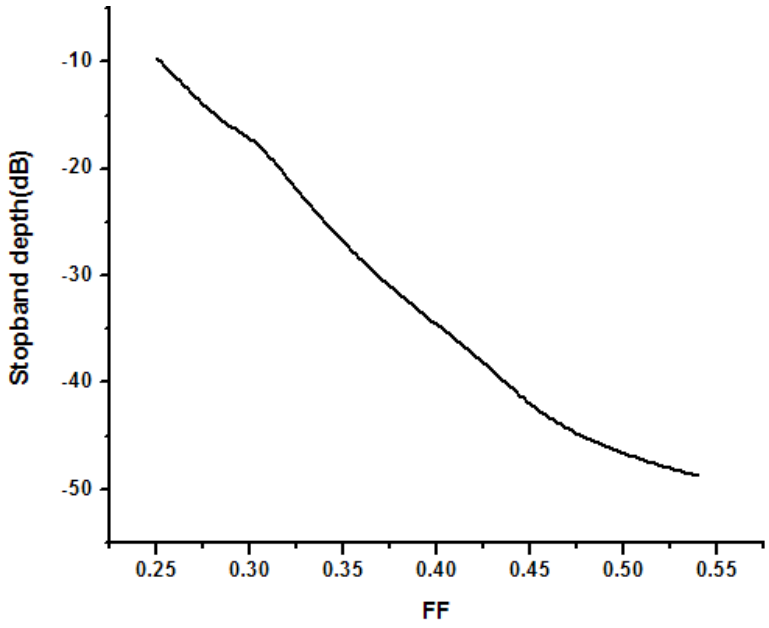

(a)

Figure 3.7: (a) Stopband's depth (at center frequency, 10 GHz) Vs Filling factor.

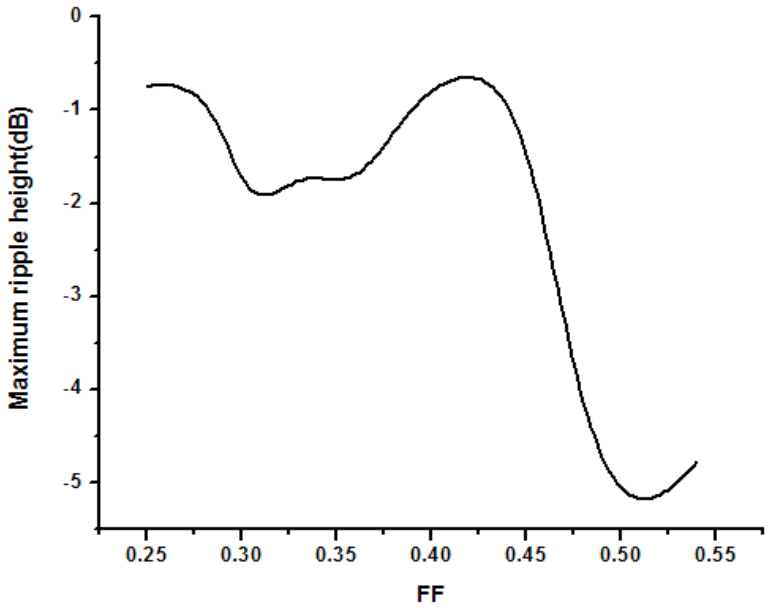

(b)

Figure 3.8: **(b) Maximum ripple height Vs Filling factor curve for square shape EBGS.**

From graph (a) it is observe that stopband depth rises approximately linearly with the rise of FF. From graph (b) we find that FF=0.45 has a very suitable maximum ripple height compare to 0.48 & 0.54 that can give smooth filtering operation. Also from graph (a) it is seen that for FF= 0.45 the stopband depth is -41.9837 dB which is also a suitable depth.

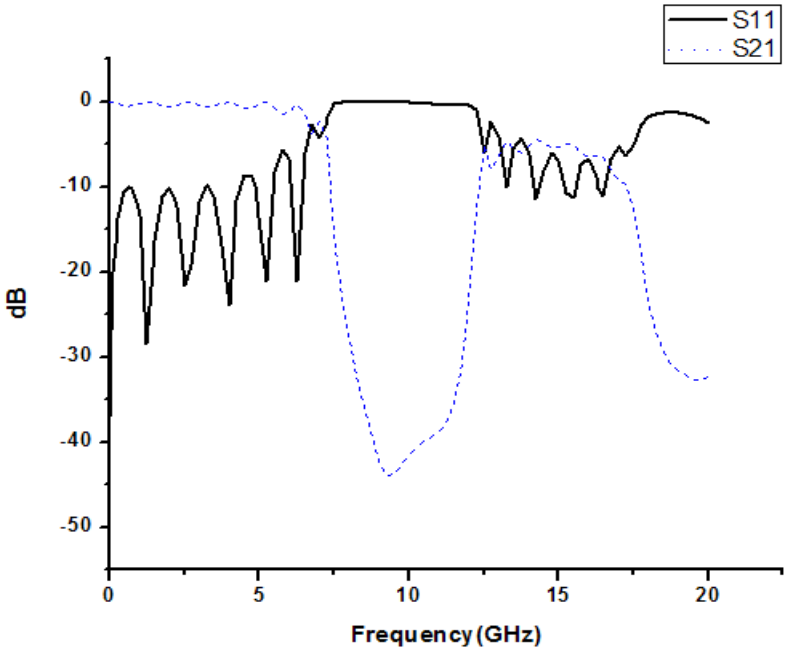

(a)

Figure 3.9: **Return loss and Insertion loss Vs FF curve for (a) FF=0.45**

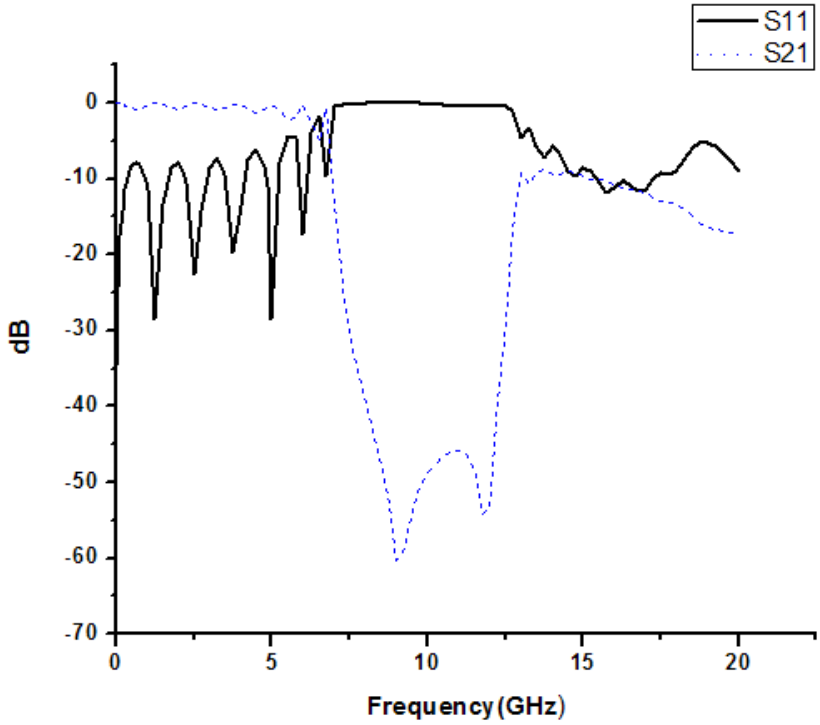

(b)

Figure 3.10: **Return loss and Insertion loss Vs FF curve for (b) FF=0.54.**

From the graphs of 3.9 (a) & 3.10 (b) it is observed that for FF=0.45, passband the curve contains fewer ripples than for FF=0.54.

Here, for square shape EBGS FF=0.45 gives best performance. So 0.45 is the optimum value of FF for square shape.

3.6 Comparison of 1-D and 2-D EBGS for Different Shape:

1D (one dimensional) EBG Patterns are those in which EBGS are only exist at the beneath of the T-line in a single row. 2D (two dimensional) EBG structures are those in which two additional parallel rows of same parameters will be etched at the ground plan along with the EBGS row that is exactly bellow to the T-line. Now 2-D structures will be studied for comprising the performance between them.

3.6.1 Circular Shape:

Both 1D and 2D designs are made from the calculation of FF=0.25 for centre frequency 10 GHz. Seven EBGS are used for one line and three lines also. The area of each circular EBGS is $\pi r^2 = 21.36314$. Here substrate thickness is 31 mils and dielectric constant is 2.45 and T-line is standard 50 Ω microstrip line. Inner element spacing and inner row spacing is 10.3408 mm.

✧ 1D circular Design:

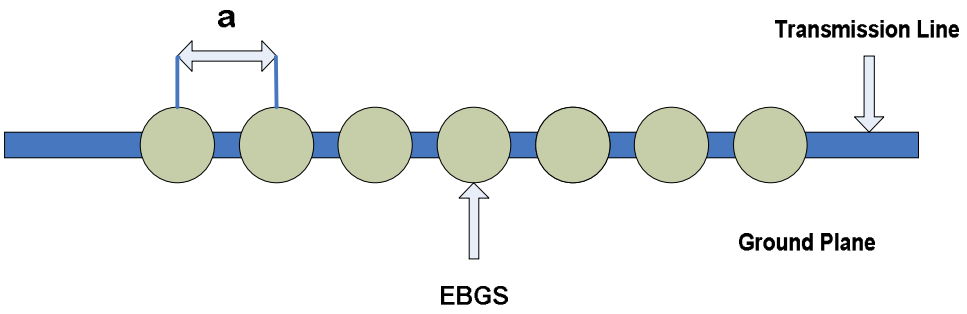

Figure 3.11: **1D circular pattered EBGS etched beneath the T-line.**

✧ 2D circular Design:

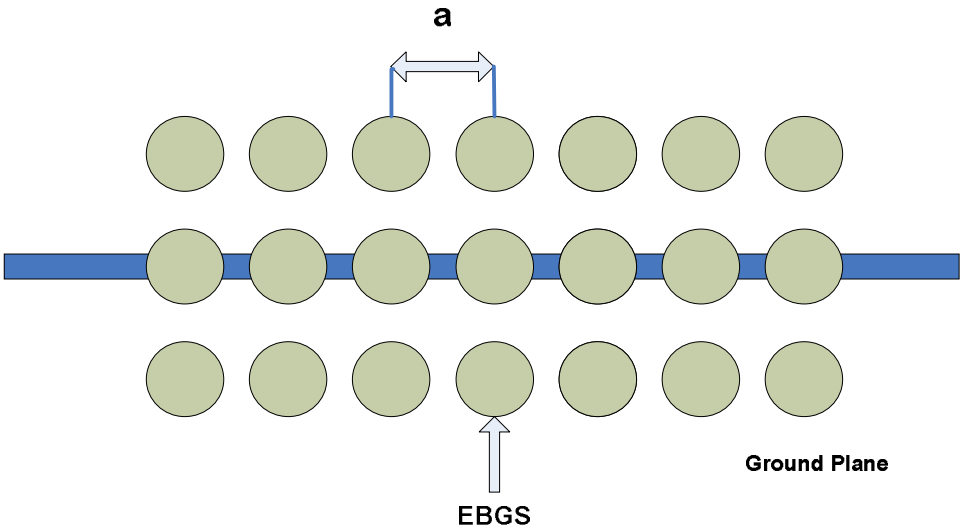

Figure 3.12: 2D circular pattered EBGS.

✧**S-Parameter Performances:**

S-Parameter performance graphs for both 1-D and 2-D EBG structures are shown below.

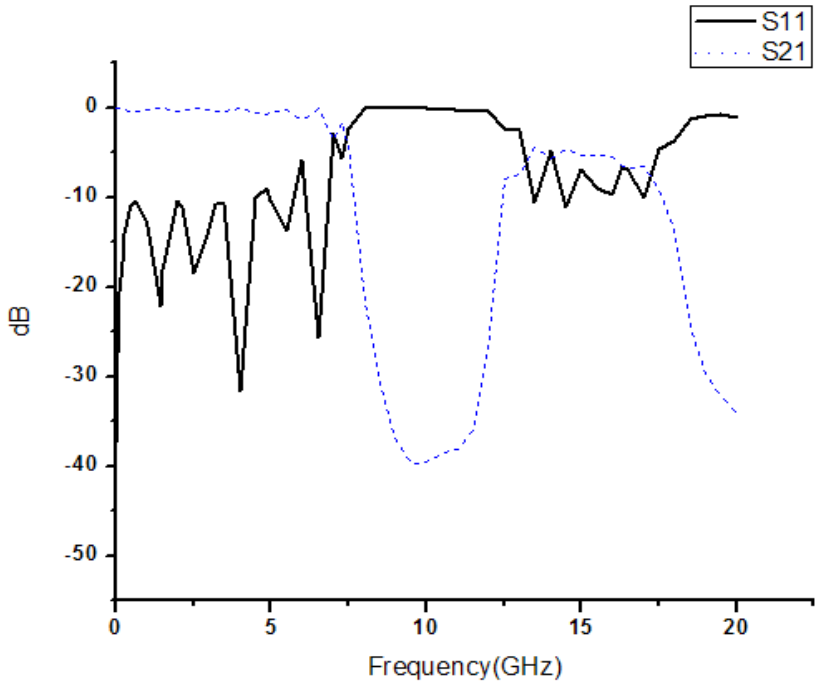

(a)

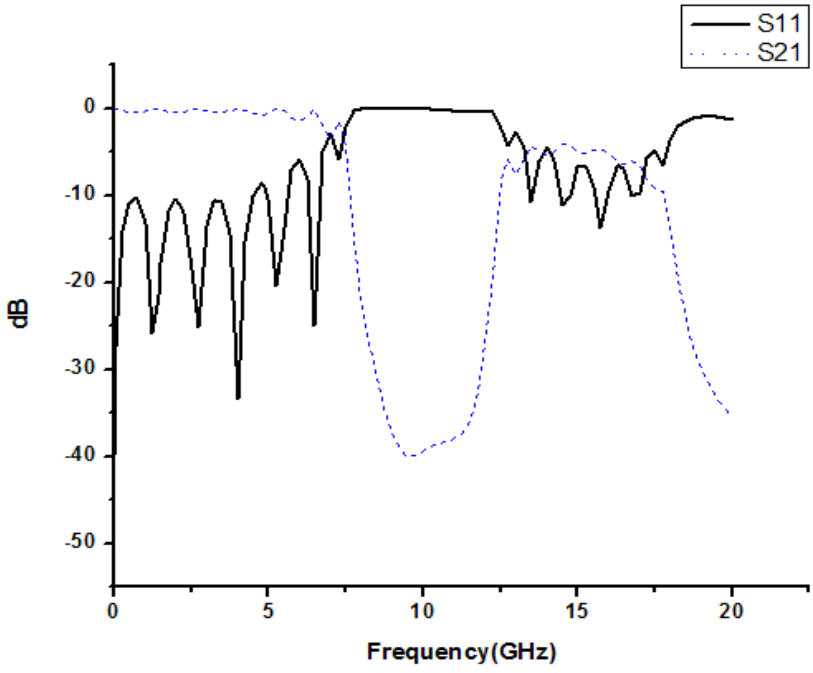

(b)

Figure 3.13: **S-Parameter performance graph for (a) 1D and (b) 2D circular shaped EBGS**

Table 3.3: Table shows comparison between 1D and 2D square shaped EBGS

Dimension	FF	10 dB Return Loss - Bandwidth Passband (GHz)	20 dB Insertion Loss - Stopband Starting (GHz)	20 dB Insertion Loss - Stopband Ending (GHz)	20 dB Insertion Loss - Stop bandwidth (GHz)	Stopband depth at centre frequency of 10 GHz (dB)	Maximum Ripple Height (dB)	-3 dB Cut-off frequency (GHz)
1 D	0.25	6.84165	7.95014	12.1840	4.23386	-39.6110	-1.47663	7.3828
2 D	0.25	6.68696	7.93332	12.2268	4.29352	-39.3687	-1.47815	7.3797

From the observation of the S-Parameter performances table, all the parameters - stopband depth, 10 dB pass band width, 20 dB stop band width, maximum ripple height and cut off frequency at -3 dB are almost same for both 1D & 2D structure. So it can be said that 1-D and 2-D structures shows same performance.

Therefore the decision can be made that only the EBGS that are etched just beneath of the ground plane of microstrip transmission line have effect on travelling waves through it. So there is no necessity to use 3 line EBGS.

3.6.2 Square shape:

Both 1D and 2D designs are made for square shape EBGS also. The value of FF used is 0.45 which is the optimum value for square shape EBGS as determined earlier. The centre frequency is set to 10 GHz and seven EBGS is used for both one line and three lines. Here substrate thickness is 31 mils and dielectric constant is 2.45 and T-line is standard 50 Ω microstrip line. Inner element spacing and inner row spacing is 10.3408 mm. The side of square is b=FF*a= 4.6935mm. Hence the area of each square EBGS is b^2= 22.0289 mm^2.

✧**1D square Design:**

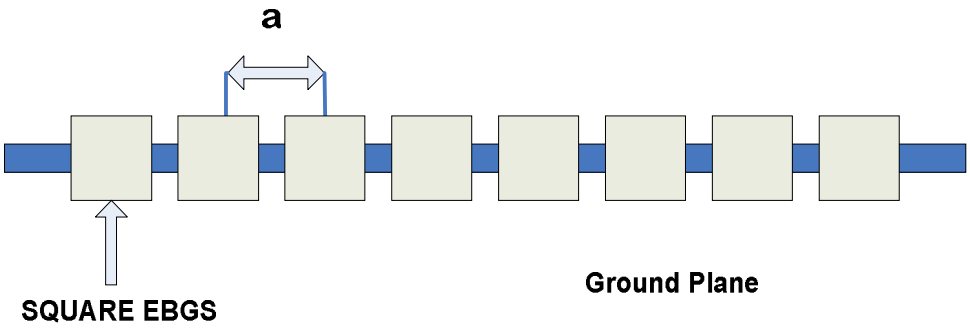

Figure 3.14: **1D square pattered EBGS etched beneath the T-line.**

✧**2D square Design:**

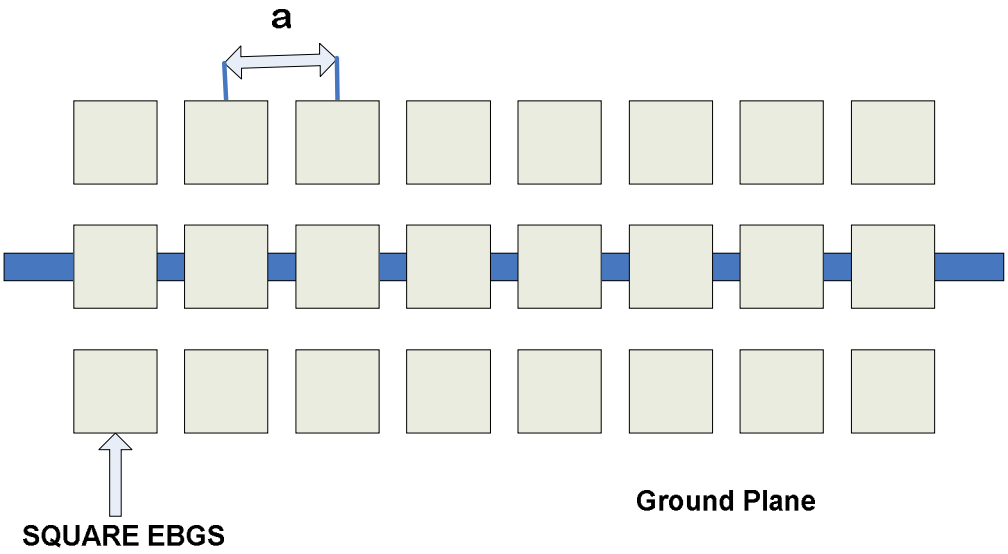

Figure 3.15: **2D square pattered EBGS.**

✧**S-Parameter Performances:**

S-Parameter performance graphs for both 1-D and 2-D EBG structures are shown below.

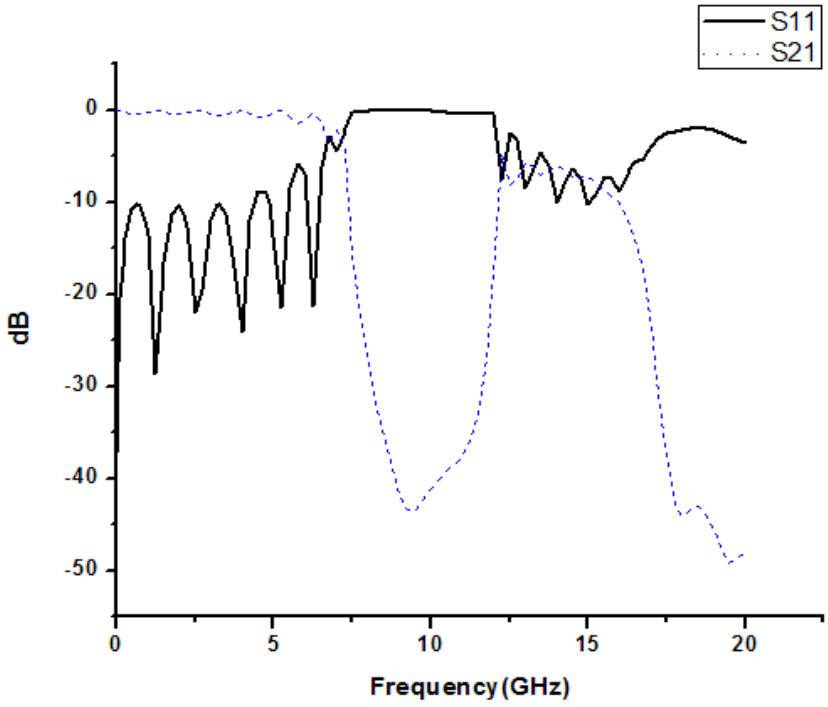

(a)

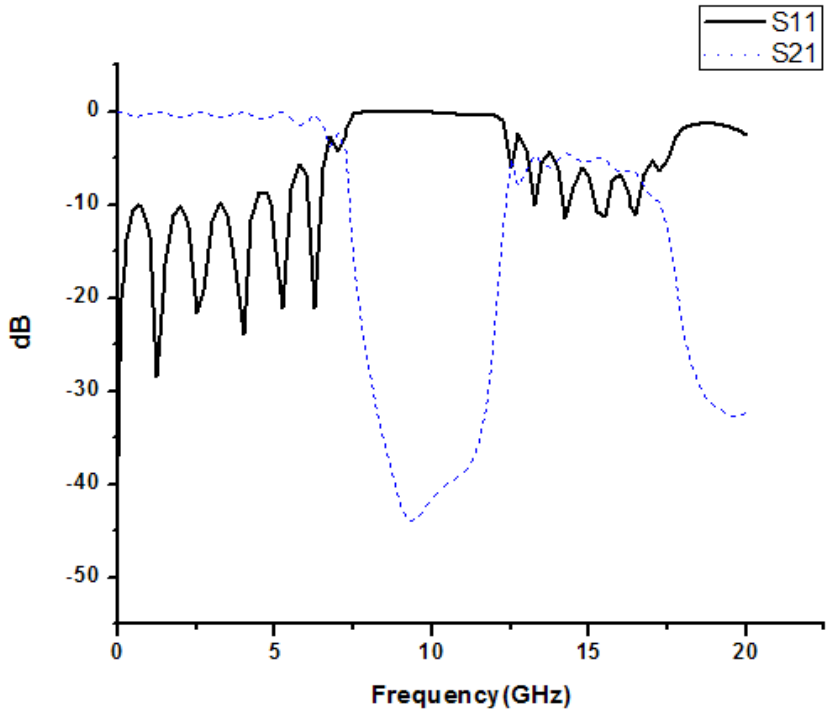

(b)

Figure 3.16: **S-Parameter performance graph for (a) 1D and (b) 2D square shaped EBGS**

Table 3.4: Table shows comparison between 1D and 2D square shaped EBGS

Dimension	FF	10 dB Return Loss - Bandwidth Passband (GHz)	20 dB Insertion Loss - Stopband Starting (GHz)	20 dB Insertion Loss - Stopband Ending (GHz)	20 dB Insertion Loss - Stop bandwidth (GHz)	Stopband depth at centre frequency of 10 GHz (dB)	Maximum Ripple Height (dB)	-3 dB Cut-off frequency (GHz)
1 D	0.45	6.43231	7.65061	12.0773	4.42666	-41.9837	-1.47571	7.08901
2 D	0.45	6.43358	7.64749	12.07918	4.43169	-41.5388	-1.49559	7.08594

From the observation of the S-Parameter performances table here also seen that all the parameters are approximately same for 1-D and 2-D structures. Hence, it can be claim that there are no effects of EBGS which are away from microstrip transmission line and disconnected from the EBGS that lies beneath T-line that is electromagnetic field is only confined at the beneath of the T-line.

3.7 Effects of numbers of EBGS on S-parameter performance:

Number of EBGS is very important factor to design a desired filter. Depending on the number of EBGS Stop band depth increases and corresponding Pass band ripples height increases. Therefore to get better performance trade off is to be done between Stop band depth and Pass band ripple height. Here, all performances are observed for circular EBGS and FF=0.25, where substrate thickness is 31 mil and ε_r=2.45.

Typical designs for different numbers of EBGS that are simulated shown below:

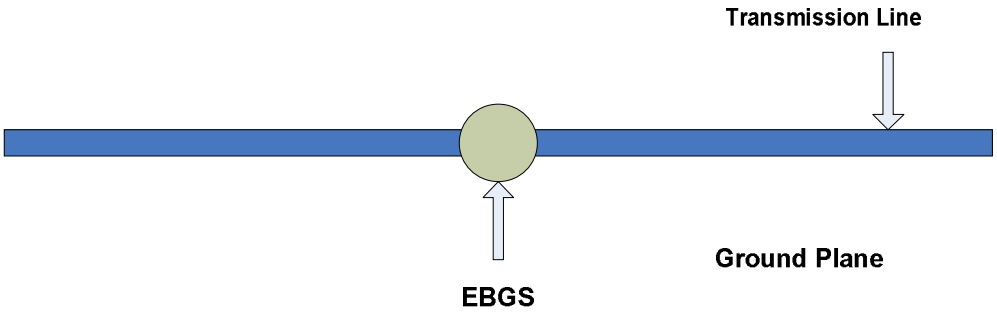

(a)

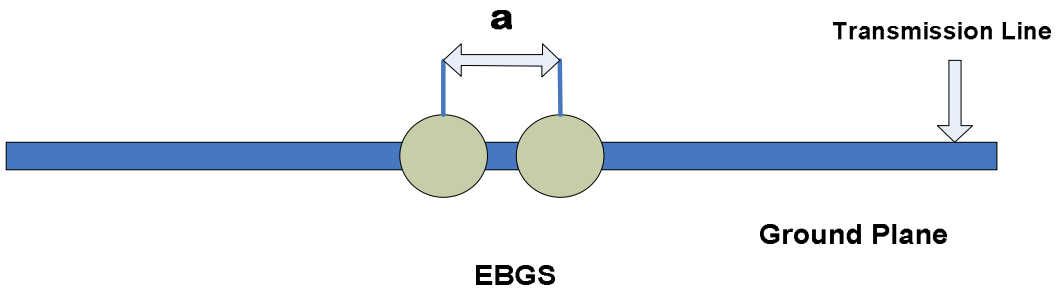

(b)

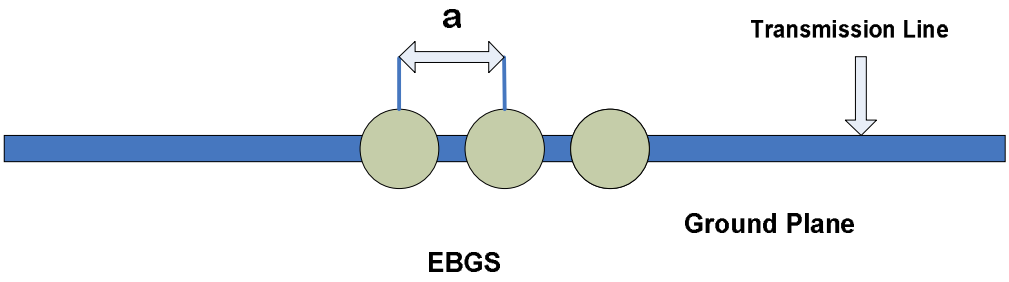

(c)

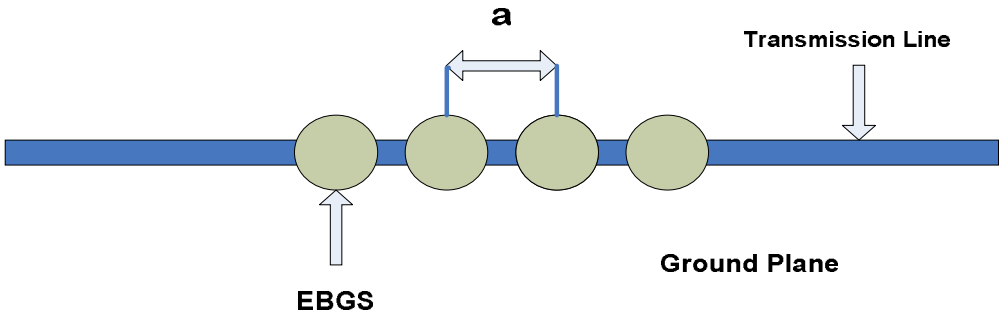

(d)

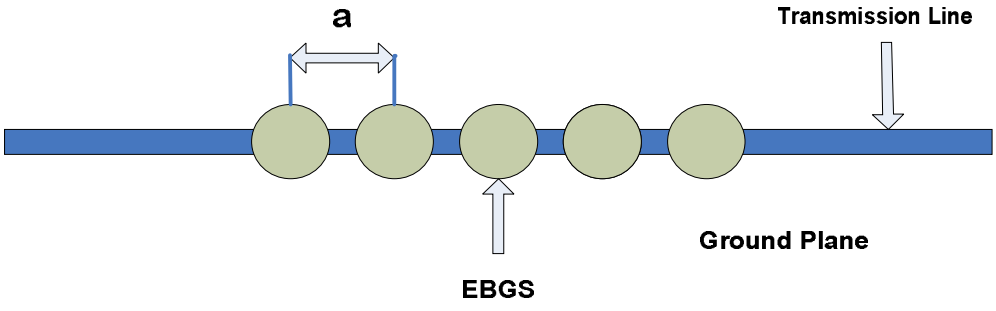

(e)

Figure 3.17: **Microstrip Transmission line design using (a) One EBGS (b) Two EBGS (c) Three EBGS (d) Four EBGS (e) Five EBGS**

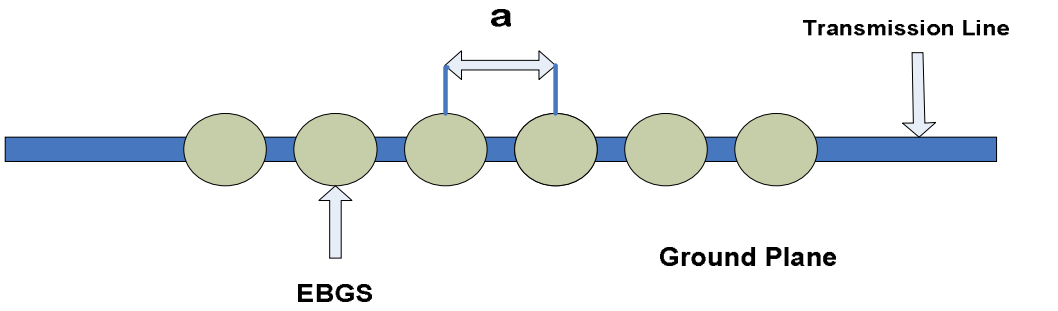

(f)

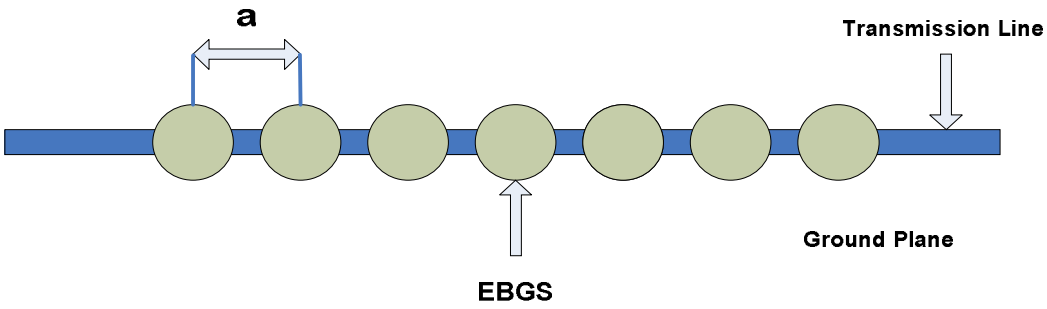

(g)

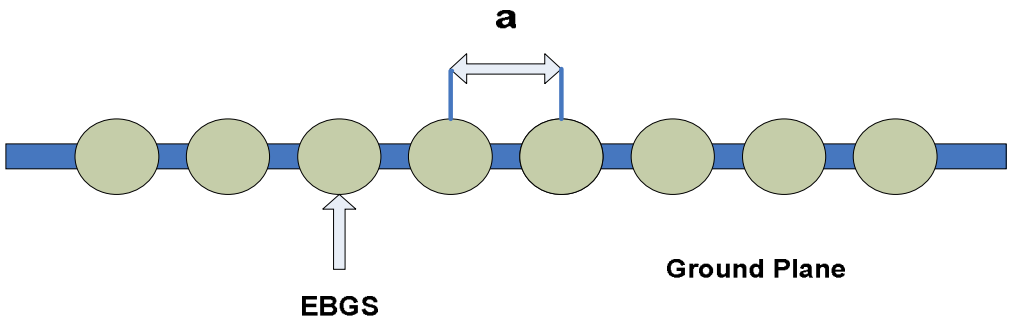

(h)

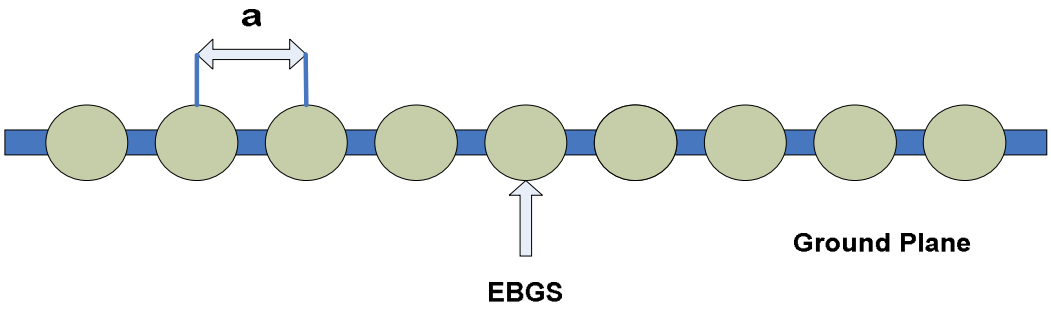

(i)

Figure 3.18: **Microstrip Transmission line design using (f) Six EBGS (g) Seven EBGS (h) Eight EBGS (i) Nine EBGS.**

Following tables shows the results of those simulations.

Table 3.5: Table shows variation of S-parameter for various numbers of EBGS.

No. of EBGS	10 dB Return Loss Bandwidth - Pass band (GHz)	20 dB Insertion Loss Bandwidth – Stop band (GHz)	Stopband's Depth (at center frequency, 10 GHz)	Ripple Height (dB)	-3 dB Cut-off frequency (GHz)
1	3.9318921	0	-2.0555316	-2.57137874	0
2	5.495276	0	-8.4636297	-0.57800855	7.011121
3	6.4441152	0	-13.548199	-0.76480614	6.982943
4	6.9690977	1.46536	-21.785695	-1.26168437	7.142215
5	7.1619719	3.53278	-26.516837	-1.62698574	7.322794
6	7.3524829	3.92476	-34.981609	-2.64165017	7.377427
7	6.84165	4.23386	-39.611	-1.47663457	7.382862
8	6.8979294	4.34689	-50.321469	-3.1556716	7.529114
9	6.1842466	4.44687	-89.302437	-3.95911325	7.54224

In the above table an increase on depth is seen due to increase of number of EBGS. Stop bandwidth, maximum ripple height at passband and no of ripples in passband is also increases with the increase of no of EBGS. Ripples in passband create noise signals. So trade off should be made between stopband depth and ripple heights.

We got the following curve by using the data from the table which is necessary to find out the optimum no of EBGS for getting better performances.

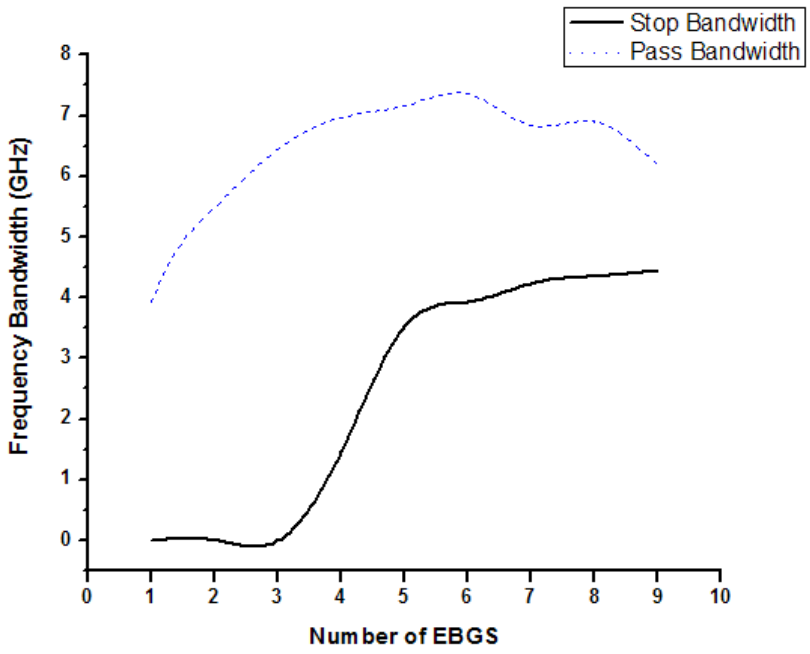

(a)

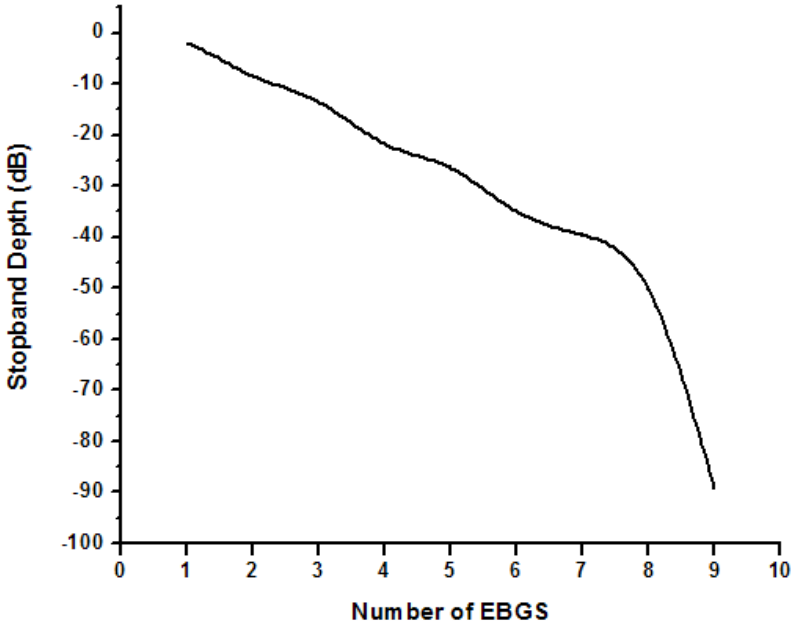

(b)

Figure 3.19: **(a) Effect on Pass band and Stop band width due to variation of number of EBGS, (b) Stopband depth (at center frequency, 10 GHz) Vs number of EBGS.**

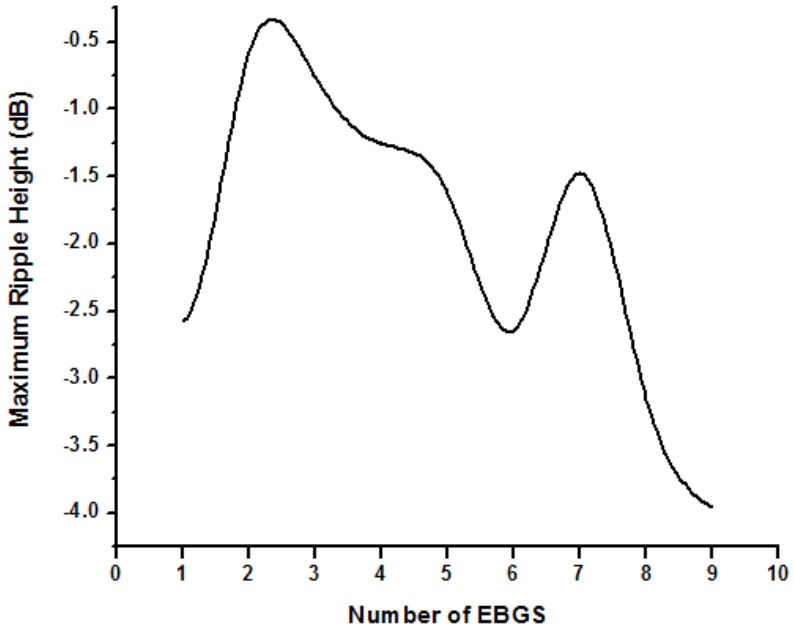

(c)

Figure 3.20: **(c) Maximum ripple height Vs number of EBGS.**

These curves express that no desired stop band is formed bellow four EBGS for this particular type of design, however the most important message of these curves is that insertion loss always increases with the increase of the number of EBGS and it reaches to the deepest position for nine EBGS (figure (b)). With respect to ripple height design using seven EBGS is the most efficient design.(figure (c)) and also for seven EBGS we got a good depth of -39.611 dB. But the highest depth is -89.3024 dB which is found for nine EBGS.

✧S-Parameter Performances of designs having seven and nine EBGS:

S-Parameter performance graphs for designs using seven and nine EBGS are shown below.

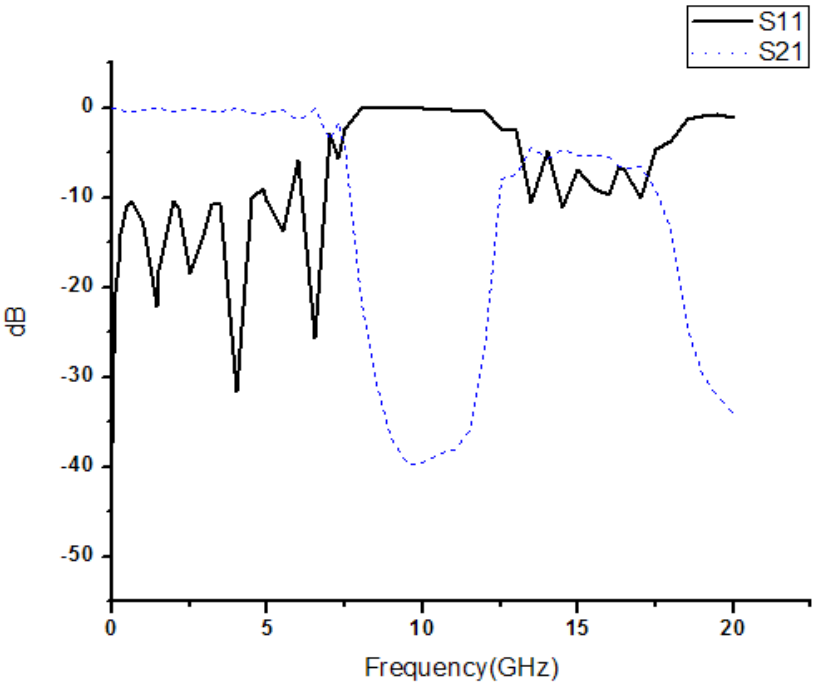

(a)

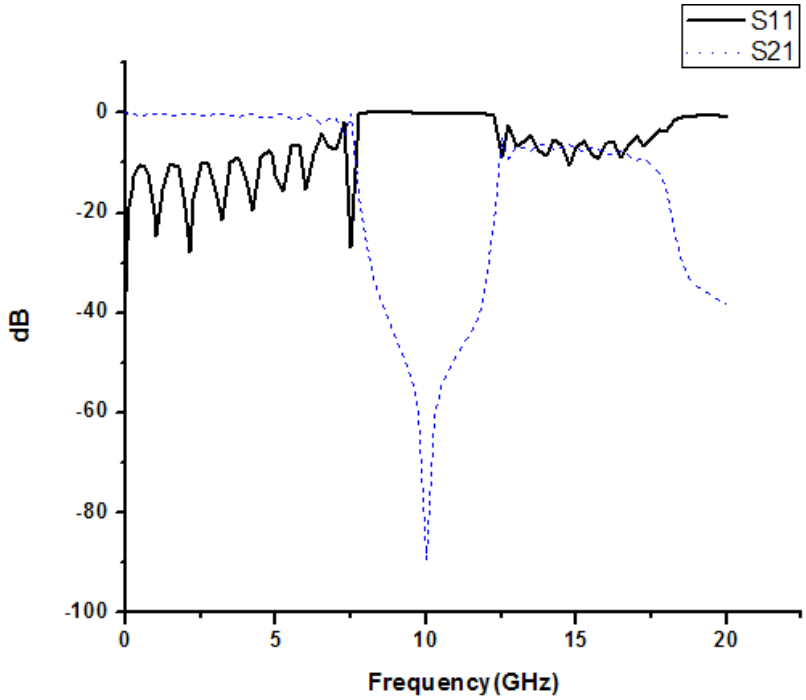

(b)

Figure 3.21: **S-Parameter performance graph for designs using (a) Seven (b) Nine EBGS.**

From the following S-Parameter performance graphs and data tables we can conclude that both seven and nine could be the optimum number of EBGS for such type of designs.

3.8 Analysis of same Etching area of different shaped EBGS:

To observe the effects of s-parameter performances of different shapes of EBGS the following designs of uniform 1D EBGS are simulated on Zeland ie3d.All the designs are made on the substrate whose thickness is 31 mils and dielectric constant is 2.45 as well as at the beneath of 50Ω microstrip T-line. All of them are of same etching area and the area is calculated from the circular shaped EBGS whose FF is 0.25 and that is 21.36314 mm^2. Number of EBGS used for all the shapes were seven.

3.8.1 Designs:

✧**Circular**

Circular EBGS of this design are made from the equation FF = r/a, here FF = 0.25, a = 10.4308 mm (inner element spacing) and r is the radius of the circular EBGS (r= 2.6077 mm) for center frequency 10 GHz.

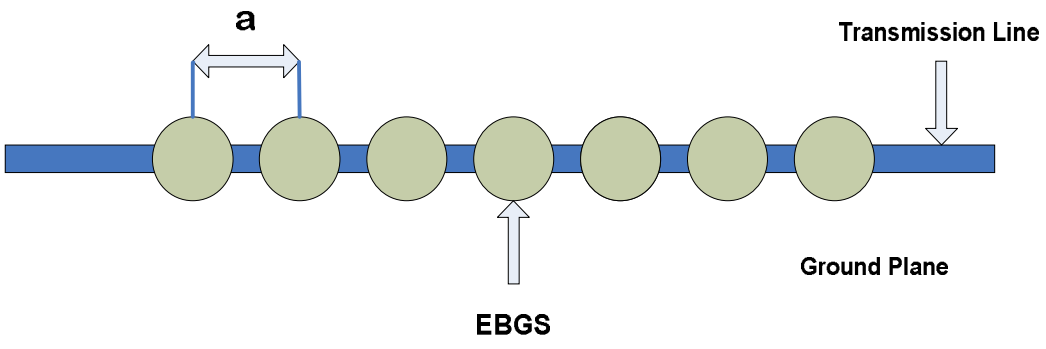

Figure 3.22: **Circular shaped EBGS designed on 50 Ω microstrip T-line on the substrate of dielectric constant 2.45 and thickness 31 mils.**

✧**Square**

The area of the square shaped EBGS is maintained 21.36314 mm^2 as area the circular shape EBGS. The arm of the square b is calculated from b^2=21.36314 mm^2 which is 4.622 mm.

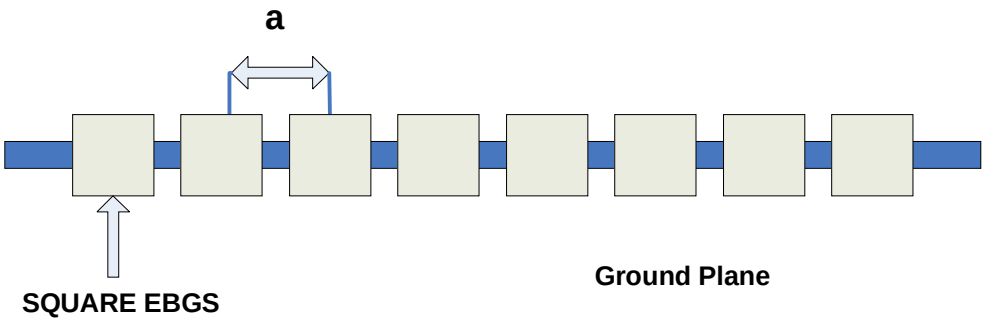

Figure 3.23: **Square shaped EBGS designed on 50 Ω microstrip T-line on the substrate of dielectric constant 2.45 and thickness 31mils.**

✧**Triangular**

Equilateral Triangle is another shape of EBGS that is inspected to observe the performance whose arm (e = 7.024mm) is calculated from the equation, $\frac{\sqrt{3}}{4}e^2 = \pi r^2 = 21.36314$ mm2 to keep the area as same as circular EBGS. Since, there is no defined option to draw triangle, hence the option of drawing circular shape entity is used by choosing "Number of segments for circle" as 3; however, for this we calculated the radius of the circle from $r = \frac{e}{\sqrt{3}} = 4.0553\ mm$.

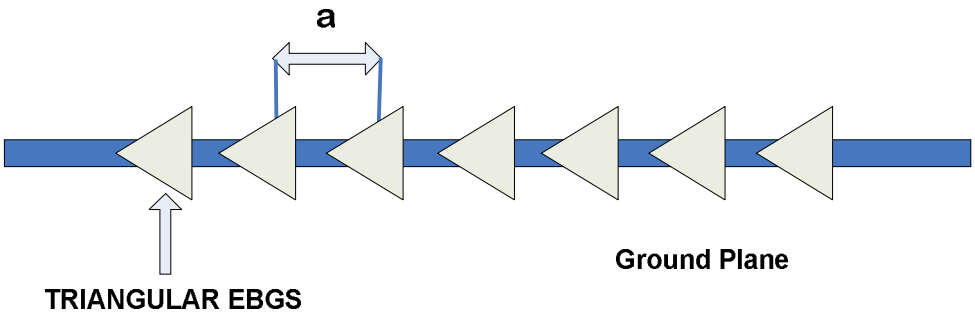

Figure 3.24: **Equilateral triangular shaped EBGS designed on 50 Ω microstrip T-line on the substrate of dielectric constant 2.45 and thickness 31mils.**

✧**Hexagonal**

Hexagon is another type of EBGS that is also inspected to observe the performance to find out the effect of same etching area for different shaped EBGS. Here, hexagon's arm (t=4.967mm) is calculated from the equation $\frac{3\sqrt{3}}{2}t^2 = \pi r^2 = 21.36314$ mm2 to keep the area as same as circular EBGS. Like drawing equilateral triangle, this time "Number of segments for circle" is chosen as 6 and the radius of the required circle is found by r = t.

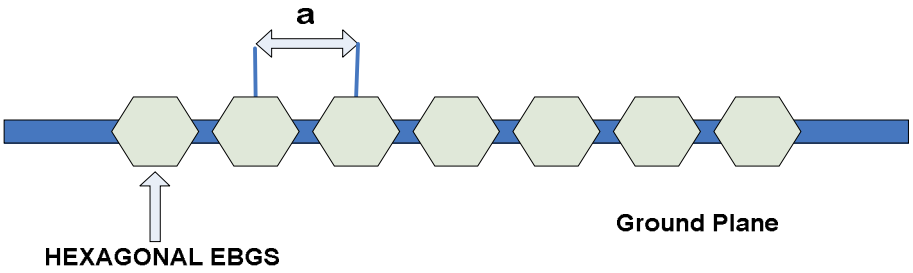

Figure 3.25: **Hexagonal EBGS designed on 50 Ω microstrip T-line on the substrate of dielectric constant 2.45 and thickness 31 mils.**

3.8.2 Results:

S-parameters of above different shapes of EBGS are shown in this section. All the results here are drawn by OriginPro 7.5 software with the data found by the simulation of the designs by Zeland ie3d. Following results are to be closely observed to take a definite decision about the fact.

✧**Circular**

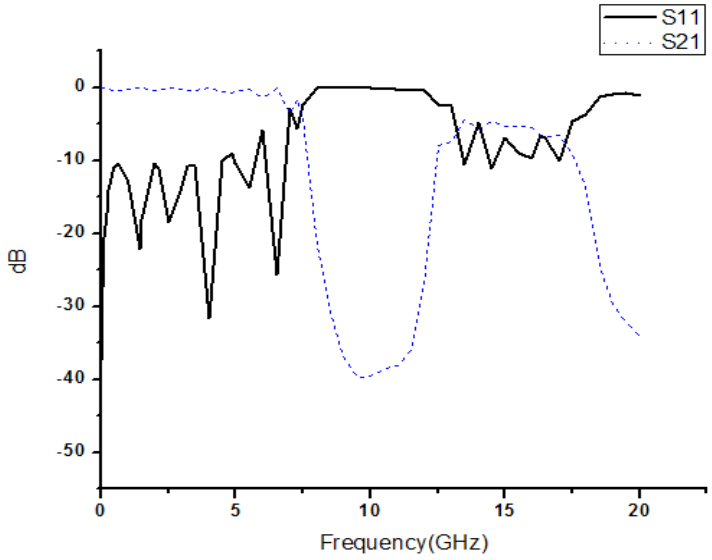

Figure 3.26: **Simulated S-parameters performances of conventional circular shape EBGS.**

From the above S-parameter performance curve we inspect 20dB Insertion Loss band width is 4.23386 GHz and pass band at 10dB Return loss is 6.84165 GHz. The depth is found at center frequency 10 GHz which is -39.611 dB and maximum ripple height is found -1.47663 dB.

✧ **Square**

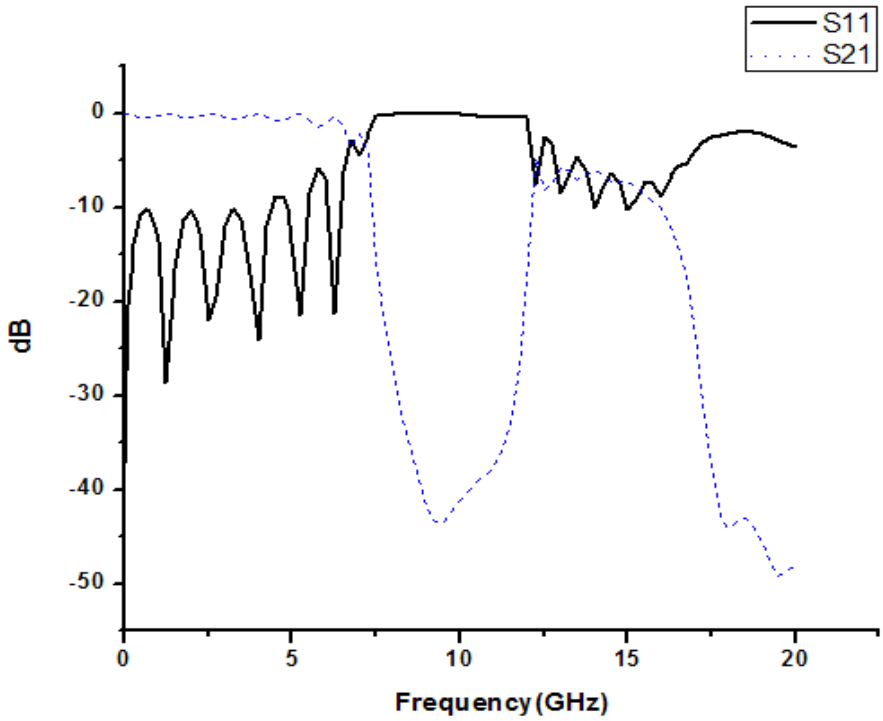

Figure 3.27: **Simulated S-parameters performances of square shape EBGS.**

In this figure, center frequency of Stopband is also occurred at 10 GHz. 10 dB Return Loss Bandwidth is 6.425939 GHz , 20 dB Insertion Loss Bandwidth is 4.33309 GHz, stop band depth is -40.7876 dB and maximum ripple height is found -1.41315 dB. The result is said to be similar to the circular shape EBGS.

✧**Triangular**

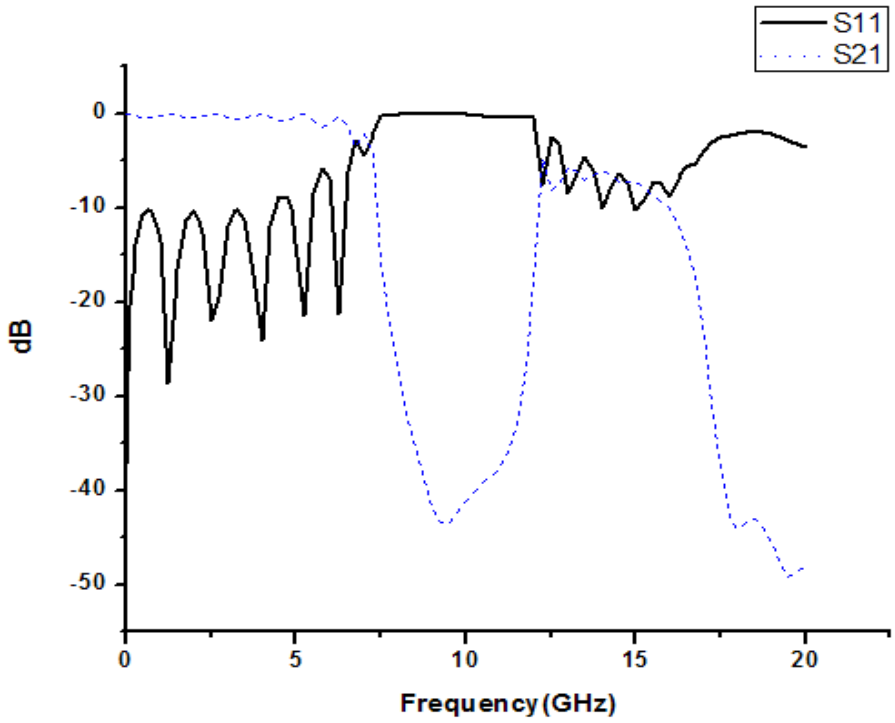

Figure 3.28: **Simulated S-parameters performances of equilateral Triangular shaped EBGS.**

Here almost the same results are also observed for the new equilateral triangular shaped EBGS. The centre frequency is very much close to 10 GHz .The 10 dB Return Loss pass bandwidth and 20 dB Insertion Loss stop bandwidth are 6.43631 dB and 4.28072 dB respectively. Maximum ripple height is found -1.4402 dB and the stop band depth is -41.1549 dB which is also very close to circular and square shape EBGS.

✧**Hexagonal**

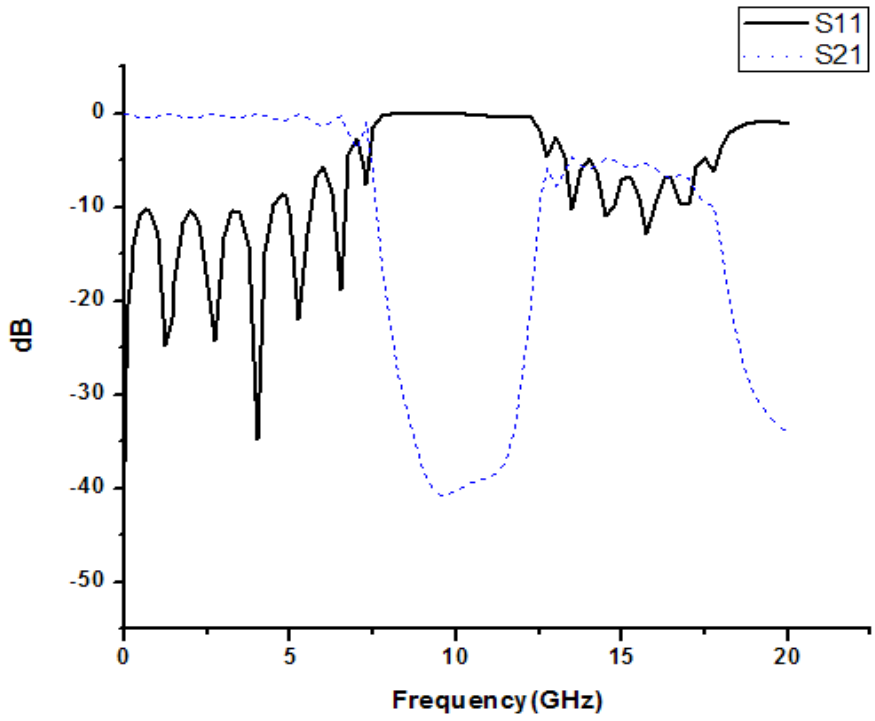

Figure 3.29: **Simulated S-parameters performances of Hexagonal shaped EBGS.**

This performamce of regular Hexagonal EBGS once again shows almost same criteria of that for Circular, Square and Equilateral Triangular shaped EBGS. Here, center frequency of Stopband is also occurred at 10 GHz and the depth is almost similar to all other. 10 dB Return Loss Bandwidth is 6.65378 GHz and 20 dB Insertion Loss Bandwidth is 4.36847 GHz. Maximum ripple height is found -1.44958 dB and the stop band depth is -40.19687 dB The result is said to be similar to the circular shape EBGS.

The following table has accumulated all necessary data for observing the results closely.

Table 3.6: Data table of S-parameter performances of different shaped of EBGS.

Shape of Design	10 dB Return Loss Bandwidth - Pass band (GHz)	20 dB Insertion Loss Bandwidth - Stop band (GHz)	Depth of Stopband (at center frequency, 10 GHz)	Ripple Height (dB)	-3 dB Cut-off frequency (GHz)
Circular	6.84165	4.23386	-39.611	-1.4766345	7.382862
Square	6.4259393	4.33309	-40.7876446	-1.4131549	7.261042
Triangular	6.4363101	4.28072	-41.1549298	-1.4402475	7.097884
Hexagonal	6.6537819	4.36847	-40.1968729	-1.4495797	7.352437

The above table is clearly showing that the performances of various type (or shaped) of EBGS, where Passand and Stopband width as well as depth of Stopband are very similar to each other. Therefore, it can be said that irrespective shapes and designs the performances are remain almost similar.

3.9 Analysis varying dielectric constant:

To realize the dependency of S-Parameter performance due to variation of dielectric constant this study has been taken for dielectric constants of 1.5, 2.0, 2.45, 3.0, 3.5, 4.0, 5.0, 7.5, 10.0 and 12 for circular shaped EBGS. It is observed that Effective dielectric constant primarily depends on the relative dielectric constant (Effective dielectric constant is calculated from PCAAD) and various parameters of T-line and EBGS (i.e. width of the T-line, Spacing and radius of the circular shape EBGS) for a particular specification (such as particular center frequency) are directly related to the Effective dielectric constant. For each simulation the substrate thickness and center frequency has been fixed to 31 mills and 10 GHz respectively.

✧S-Parameter Performances analysis:

Bellow Table is showing results of s-parameter performances for various dielectric constants where designs are implemented to keep the center frequency at 10 GHz and seven EBGSs are used in all designs.

Table 3.7: Data table of S-Parameter performance of designs of various dielectric Constants.

Dielectric Constant	10 dB Return Loss Bandwidth – Pass band (GHz)	20 dB Insertion Loss Bandwidth –Stop band (GHz)	Ripple Height (dB)	Band Depth at center frequency (10 GHz) (dB)
1.5	6.14077	4.58774	-3.2455	-43.3585
2	5.8996	4.28422	-3.6193	-41.9603
2.45	6.84165	4.23386	-1.476634	-39.611
3	7.66065	3.8999	-2.7082	-37.1729
3.5	6.85032	3.80979	-2.412090	-35.97537
4	7.83990	3.55062	-2.399014	-33.63798
5	7.72268	3.13029	-2.2684	-31.8534
7.5	8.16561	2.1252	-1.9122	-23.9605
10	8.17493	0.43492	-1.620649	-19.60810
12	8.38664	0	-1.063998	-17.39067

As the dielectric constant increases the radius of the circular EBGS decreases hence from the Bragg's condition inter-element spacing decreases to keep FF at 0.25mm.

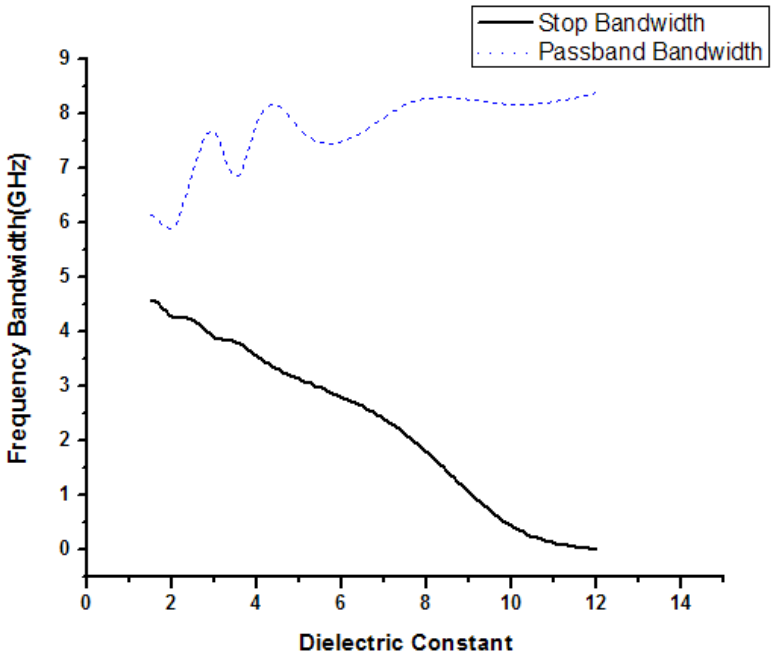

(a)

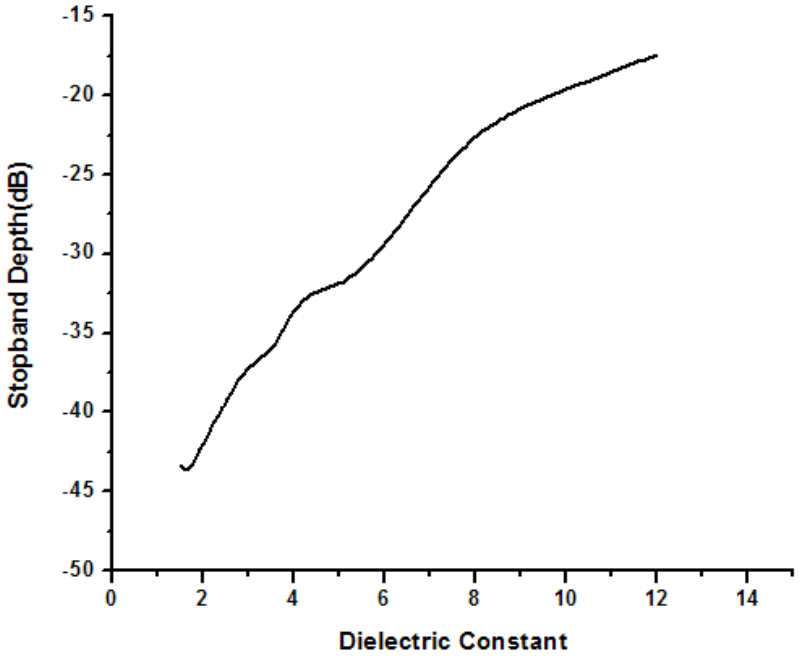

(b)

Figure 3.30: **(a) Return loss and insertion loss curves due to variation of dielectric constants of the substrate, (b) Stopband depth Vs Dielectric constant curve.**

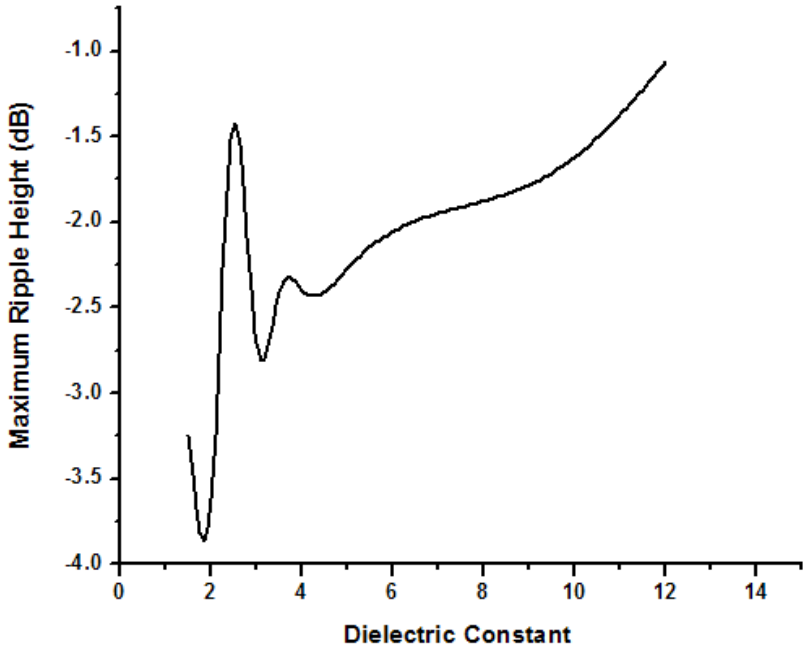

(c)

Figure 3.31: **(c) Maximum ripple height Vs dielectric constant curve.**

The graph (b) of above figure which is drawn from the data above of table, it is observed that depth increases with the increase of dielectric constant. Also stop bandwidth decreases with the increase of dielectric constant. From figure (c) the maximum ripple height is very suitable for dielectric constant 2.45 which is -1.47663 and from figure (b) the stop band depth for 2.45 is -39.611. If a trade off is made between maximum ripple height and stop band depth, 2.45 is the most suitable dielectric constant. The choice of dielectric constant, verily, depends on the preference of the designer and the availability of the substrate on the market.

3.10 Analysis varying thickness of Transmission line:

Variation of thickness analysis of the substrate is important as due to this variation, variation on the width of the T-line is experienced if the dielectric constant is same. Using PCAAD we calculated the width due to 50Ω T-line, are given bellow –

Table 3.8: Table showing the relative widths for different thickness calculated by PCAAD.

Thickness (mil)	Width (mm)
13	0.94892
15	1.09557
17	1.24164
19	1.38772
21	1.5338
23	1.67987
25	1.82595
27	1.97202
29	2.1181
31	2.26418
33	2.39242
35	2.55633

✧**S-Parameter Performances analysis:**

The S-parameters are closely inspected and the data of corresponding performances of the various T-lines designed using the thickness mentioned on the above table are added in the bellow table.

Table 3.9: Data taken from S-Parameters of circular EBGS based designs that have variety of Substrate thickness.

Substrate thickness (mils)	10 dB Return Loss Bandwidth – Pass band (GHz)	20 dB Insertion Loss Bandwidth –Stop band (GHz)	Band Depth	Maximum Ripple Height (dB)
13	5.120367	6.86322	-54.98592	-2.825234
15	6.156025	6.53194	-54.71630	-2.617693
17	6.112868	6.1989	-53.41525	-2.294595
19	5.283870	5.9066	-51.97928	-2.234661
21	7.05036	5.61313	-49.7645	-4.26739
23	6.44289	5.33213	-47.8864	-4.43464
25	6.39289	5.04483	-45.8199	-3.95255
27	7.18643	4.80	-43.6443	-3.66652
29	7.31188	4.52918	-41.5067	-3.79666
31	6.84165	4.23388	-39.6111	-1.47663
33	6.70626	4.03192	-37.3685	-3.09348
35	7.68223	3.78714	-35.3985	-2.88092

From the above table we got the following graph that expresses the effect of change of substrate thickness.

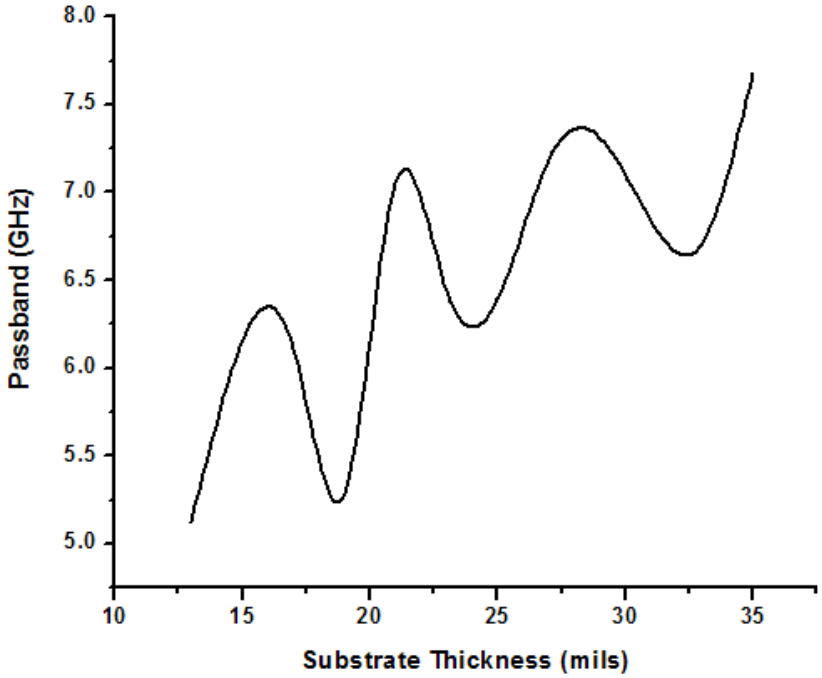

(a)

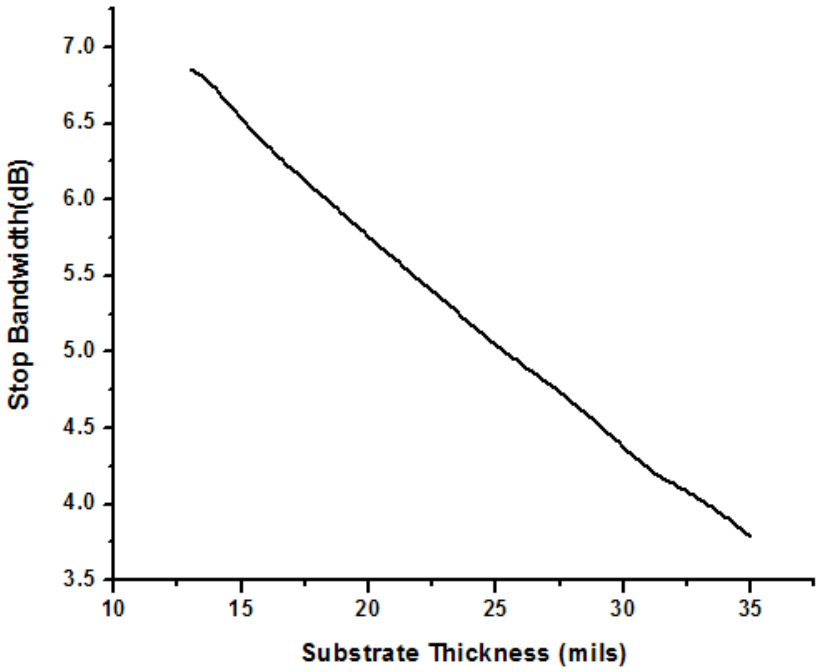

(b)

Figure 3.32: **(a) Pass band Vs Substrate thickness (b) Stop bandwidth Vs Substrate thickness**

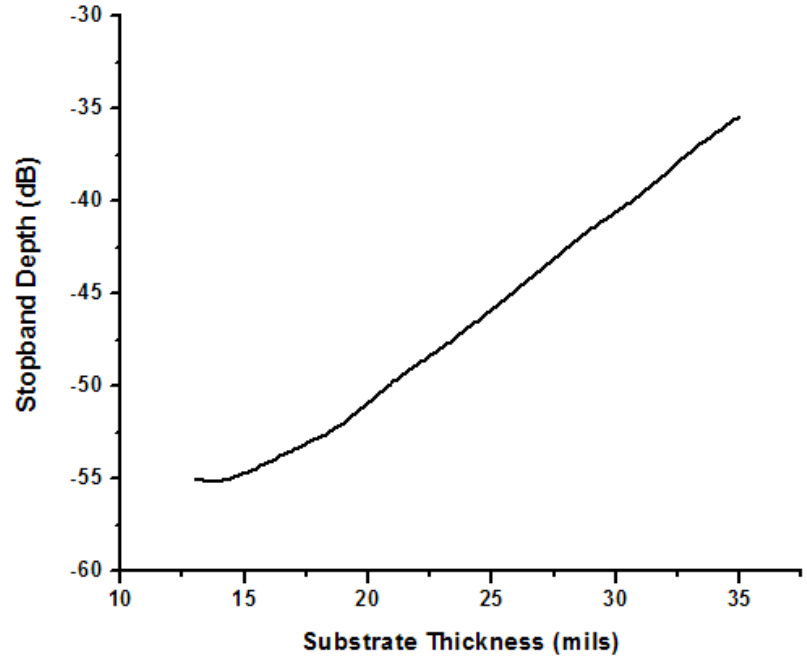

(c)

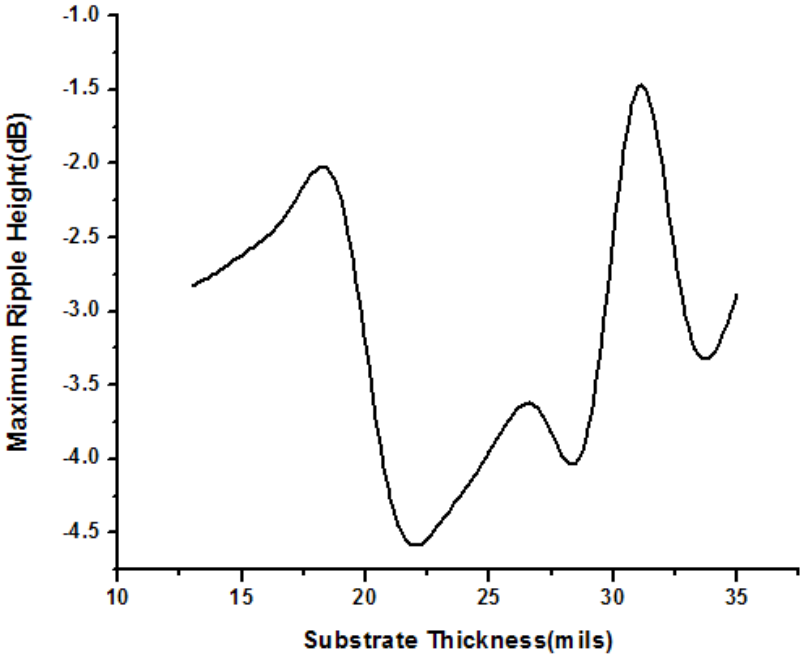

(d)

Figure 3.33: **(c) Stopband depth Vs substrate thickness (d) Maximum ripple height curve Vs Substrate thickness.**

From figure (b) it is seen that stop bandwidth decreases linearly with the increase of substrate thickness. Also stopband depth decreases with the increase of substrate thickness (figure (c)). Observing figure (d) we find that ripple height is minimum for 31 mils. So31 mils gives better performance.

Chapter 4 : Study and Analysis of binomially distributed non-uniform EBGS

4.1 Introduction:

EBG structures are realized by defecting the ground plane by etching or by drilling the substrate. The dispersion characteristics are found to be sensitive on the shape of the EBG elements, the lattice structures, the height and the value of the dielectric constant of the substrate, the number of EBG elements, the stopband frequency and the filling factor (FF) that is defined to be the volumetric ratio of one EBG element to one unit cell. V.Radisic et proposed a 2-D uniform circular patterned PBG to yield wider and distinct stopband under the constrained of optimized value of FF = 0.25[1]. Beyond this value ripples height in the passband is significant. Very recently the non-uniform distribution of EBGs[5] have been proposed to yield better performances where they have used FF beyond the value of optimized FF reported in the literature. Y.Qian et al investigated the role of shape of the PBG elements and the grid structures on the performances [6]. In this chapter we *are* investigating the s-parameter performances of a microstrip transmission line where the ground plane has been perturbed by Binomially distributed EBGs at transmission band. At transmission band we have investigated the microstrip line at frequency of 10 GHz to see the performance.

4.2 Binomial distribution:

In probability theory and statistics, the binomial distribution is the discrete probability distribution of the number of successes in a sequence of independent yes/no experiments, each of which yields success with probability. Such a success/failure experiment is also called a Bernoulli experiment or Bernoulli trial; when $n = 1$, the binomial distribution is a Bernoulli distribution. The binomial distribution is the basis for the popular binomial test of statistical significance.

The binomial distribution is frequently used to model the number of successes in a sample of size n drawn with replacement from a population of size N. If the sampling is carried out without replacement, the draws are not independent and so the resulting distribution is a hyper geometric distribution, not a binomial one. However, for N much larger than n, the binomial distribution is a good approximation, and widely used.

4.3 Pascal's triangle:

In mathematics, Pascal's triangle is a triangular array of the binomial coefficients in triangle. It is named after the French mathematician, Blaise Pascal in much of the Western world, although other mathematicians studied it centuries before him in India, Greece, Iran, China, Germany, and Italy.

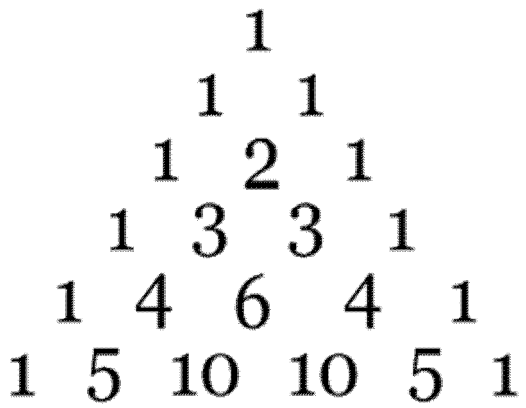

Figure 4.1: Pascal's triangle.

The rows of Pascal's triangle are conventionally enumerated starting with row $n = 0$ at the top. The entries in each row are numbered from the left beginning with $k = 0$ and are usually staggered relative to the numbers in the adjacent rows. A simple construction of the triangle proceeds in the following manner. On row 0, write only the number 1. Then, to construct the elements of following rows, add the number directly above and to the left with the number directly above and to the right to find the new value. If either the number to the right or left is not present, substitute a zero in its place. For example, the first number in the first row is 0 + 1 = 1, whereas the numbers 1 and 3 in the third row are added to produce the number 4 in the fourth row.

This construction is related to the binomial coefficients by Pascal's rule, which says that if

$$(x+y)^n = \sum_{k=0}^{n} \binom{n}{k} x^{n-k} y^k \qquad 4.1$$

Then,

$$\binom{n}{k} = \binom{n-1}{k-1} + \binom{n-1}{k}$$

For any nonnegative integer n and any integer k between 0 and n.

Pascal's triangle has higher dimensional generalizations. The three-dimensional version is called Pascal's pyramid or Pascal's tetrahedron, while the general versions are called Pascal's simplices.

4.4 Coefficients calculation for radius of EBGS

Coefficient calculation for radius of un-uniform EBGS is done by use of Pascal's triangle.

Pascal's rule also gives rise to Pascal's triangle:

```
0:                    1
1:                  1   1
2:                1   2   1
3:              1   3   3   1
4:            1   4   6   4   1
5:          1   5   10  10  5   1
6:        1   6   15  20  15  6   1
7:      1   7   21  35  35  21  7   1
8:    1   8   28  56  70  56  28  8   1
```

Following two steps are followed in coefficient calculation,

Step 1:

Here if N no of EBGS is used in designing the filter, level N-1 is taken as reference. For example, if there is five EBGS in the design, level 4 is taken as reference as it contains five numbers.

Level 4 contains numbers, 1, 4, 6, 4, and 1 respectively.

Step 2:

Then the numbers are divided by the central number. For even number of EBGS there will be two same numbers in the center. In this case the central number is 6.

So by dividing by 6 we got: 0.16667, 0.6667, 1, 0.6667, and 0.16667 respectively.

These are the desired coefficient. Observing these coefficients we find that the EBGS at center is the largest. As EBGS moves away from the center, their radius decreases.

4.5 Analysis for Odd Number of EBGS

To observe the effect of binomially distributed odd number of EBGS we studied seven and nine EBGS assisted transmission line. We simulated designs for various FF and found different results. Results shows that binomially distributed odd numbered EBGS assisted transmission lines are good for low pass filter.

4.5.1 Seven EBGS

S-parameters of FF of 0.3, 0.35, 0.4, 0.45 and 0.5 where the substrate is Taconic having dielectric constant of 2.45, height of 31 mils and the inner-element spacing (period) a = 10.4308 mm were simulated. We calculated the coefficients as described in section **4.4**. The coefficients for seven EBGS are 0.05, 0.30, 0.75, 1.00, 0.75, 0.30 and 0.05 respectively. A typical geometry of design is shown bellow,

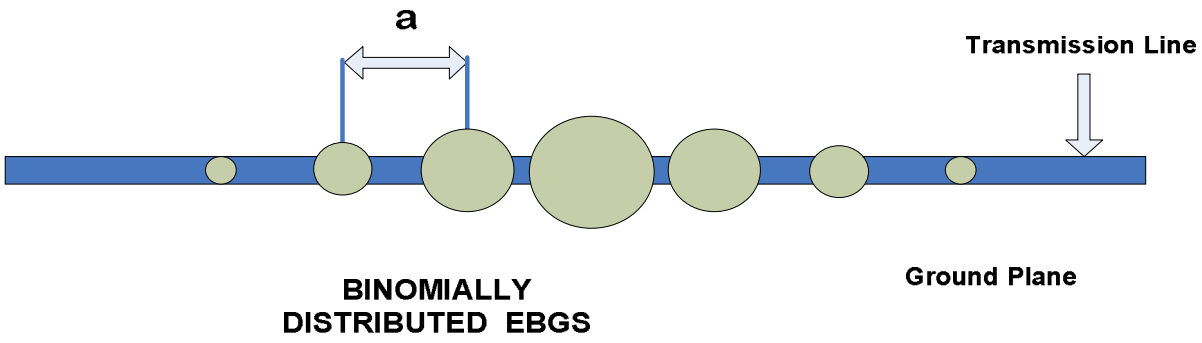

Figure 4.2: **Geometry of binomially distributed seven EBGS assisted transmission line.**

By inspecting the S-parameter performances table 4.1 is made.

Table 4.1: Variation of performances due to the variation of filling factor for seven EBGS.

Filling Factor	Pass band (GHz)	Stop band width (GHz)	Depth of Stop band (at center frequency,10 GHz)	Maximum Ripple Height (dB)	-3 dB Cut-off frequency (GHz)
0.30	6.21874	0	-14.5358	-0.44303	6.9490
0.35	6.08948	0.3803	-19.0919	-0.63533	6.6250
0.40	6.02933	3.1049	-22.5774	-0.93847	6.49624
0.45	6.08781	3.6335	-25.1491	-1.26988	6.49217
0.50	6.25220	3.6788	-26.3126	-1.72019	6.64671

From the above data table it is seen that for seven EBGS depth increases with the increase of FF and bellow FF=0.35 there is no -20 dB stopband. In this case FF=0.50 gives best result.

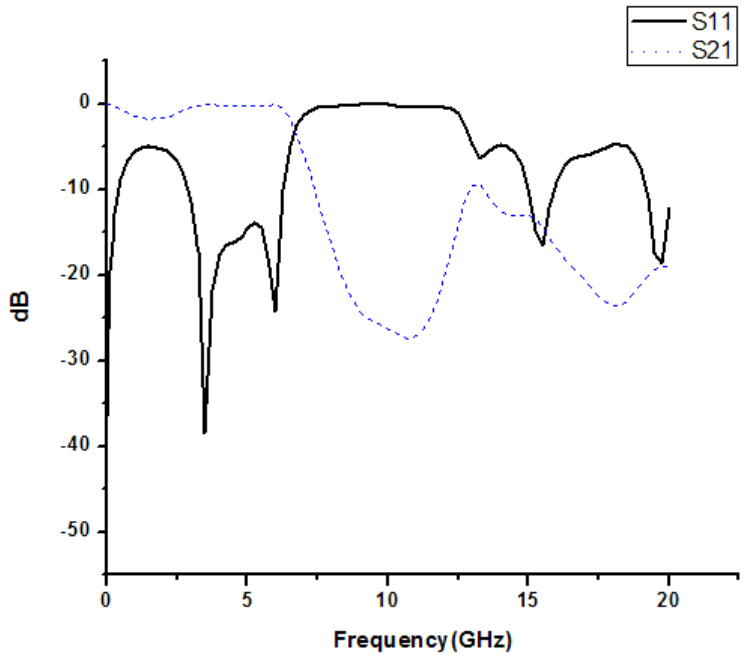

Figure 4.3: **S-Parameter performance graph for FF=0.50**

Here it is observed that the s-parameter characteristics curve shows low pass characteristics instead of band stop characteristics.

4.5.2 Nine EBGS

S-parameter characteristics for FF=0.5 where the substrate was Taconic having dielectric constant of 2.45, height of 31 mils and the inner-element spacing (period) a = 10.4308 mm were simulated. We calculated the coefficients as described in section **4.4**. The coefficients for nine EBGS are 0.0143, 0.1143, 0.40, 0.80, 1.00, 0.80, 0.40, 0.1143 and 0.0143 respectively. A typical geometry of design is shown bellow,

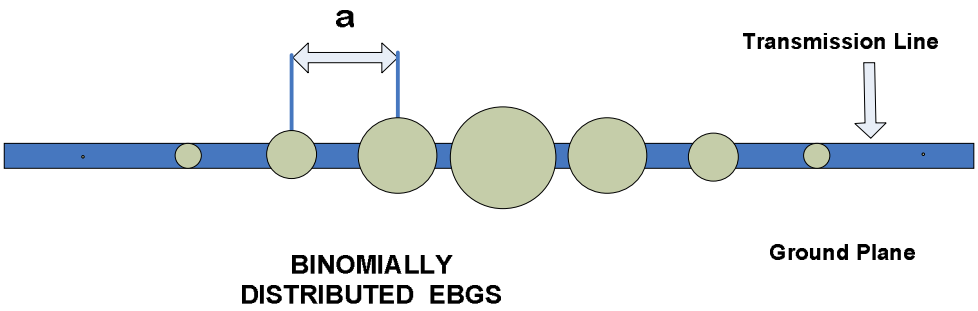

Figure 4.4: **Geometry of binomially distributed nine EBGS assisted transmission line.**

✧S-Parameter performance:

The graph bellow shows the s-parameter of the above design.

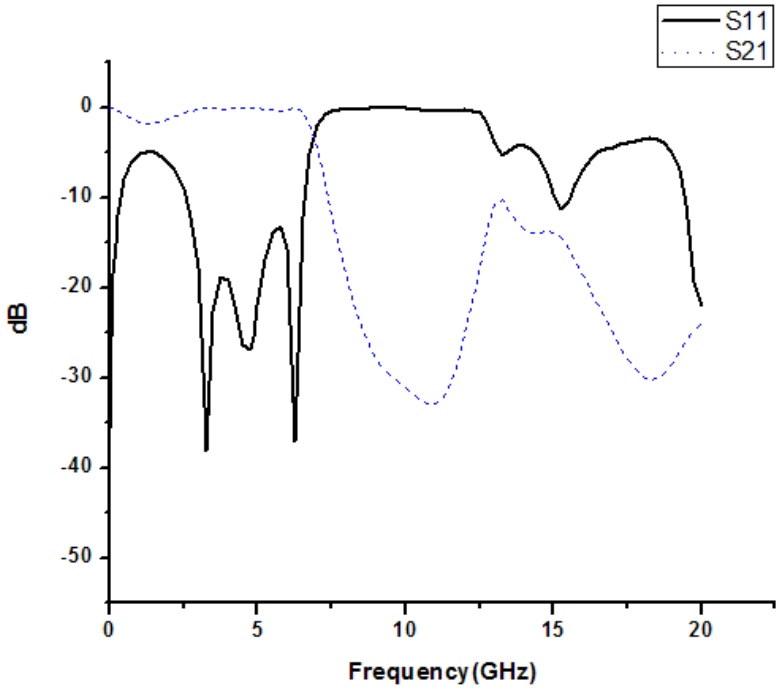

Figure 4.5: **S-Parameter performance graph for FF=0.50**

From the above S-parameter performance we inspect 20dB Insertion Loss stop band width is 4.2670 GHz and passband is 6.5757 GHz. The depth at the center frequency of 10 GHz is -31.049 dB. This curve also shows low pass characteristics.

4.6 Analysis for Even Number of EBGS:

To observe the effect of binomially distributed even number of EBGS we studied eight and ten EBGS assisted transmission line. We simulated designs for various FF and found different results. Results shows that binomially distributed even numbered EBGS assisted transmission lines are also good for low pass filter.

4.6.1 Eight EBGS:

S-parameters of FF of 0.35, 0.4 and 0.5 where the substrate was Taconic having dielectric constant of 2.45, height of 31 mils and the inner-element spacing (period) a = 10.4308 mm were simulated. We calculated the coefficients as described in section **4.4**. The coefficients for eight

EBGS are 0.0286, 0.20, 0.60, 1.00, 1.00, 0.60, 0.20 and 0.0286 respectively. A typical geometry of design is shown bellow,

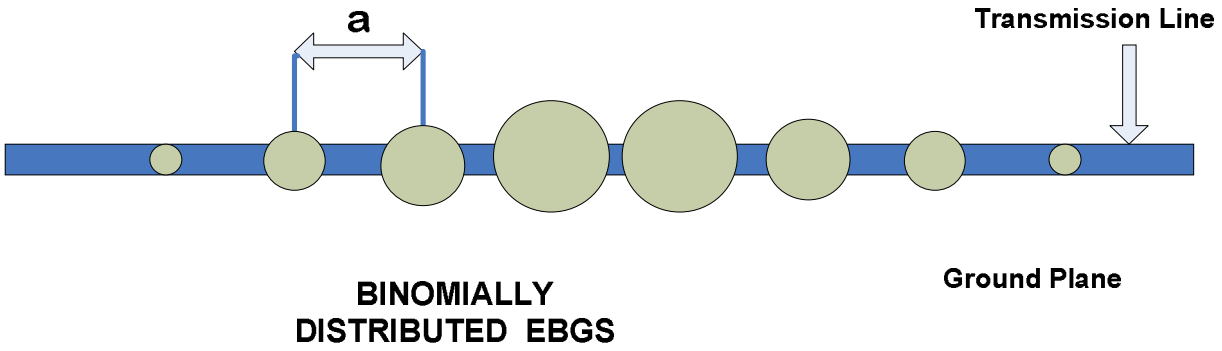

Figure 4.6: **Geometry of binomially distributed eight EBGS assisted transmission line.**

By inspecting the S-parameter performances of simulated designs table 4.2 is made.

Table 4.2: Variation of performances due to the variation of filling factor for eight EBGS.

Filling Factor	Pass band (GHz)	Stop band width (GHz)	Depth of Stop band (at center frequency, 10 GHz)	Maximum Ripple Height (dB)	-3 dB Cut-off frequency (GHz)
0.35	6.23065	2.82419	-24.52928	-0.760321	6.710493
0.40	6.27455	3.8211	-28.4266	-1.121310	6.639394
0.50	6.79710	3.66898	-30.44479	-2.05165	6.991505

From the above data table it is seen that for eight EBGS, FF=0.50 gives best result.

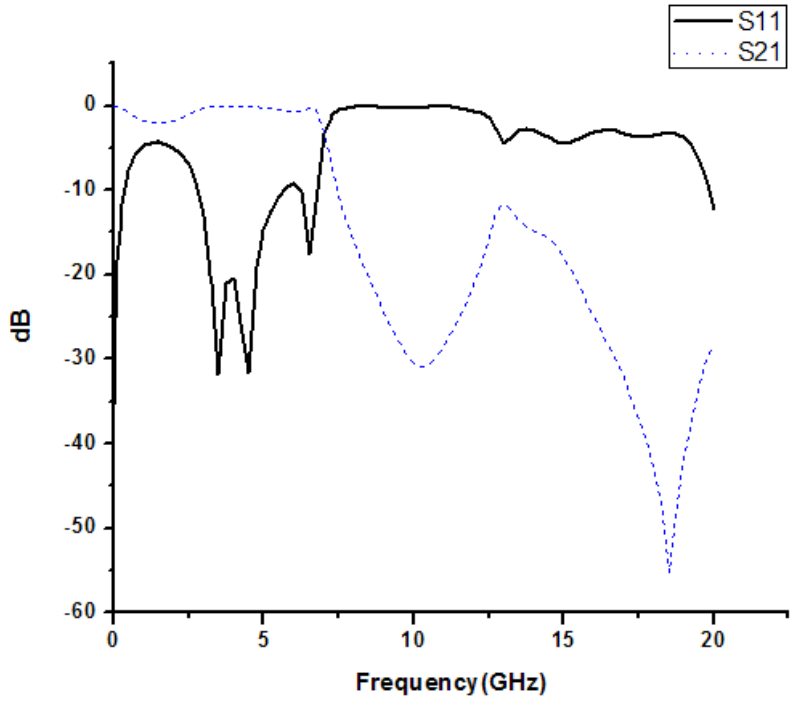

Figure 4.7: **S-Parameter performance graph for FF=0.50**

Here the curve shows the shape of low pass filter but the depth and other parameters are not sufficient enough to be a good low pass filter.

4.6.2 Ten EBGS:

S-parameters of FF of 0.4, 0.45 and 0.5 where the substrate was Taconic having dielectric constant of 2.45, height of 31 mils and the inner-element spacing (period) a = 10.4308 mm were simulated. We calculated the coefficients as described in section **4.4**. The coefficients for ten EBGS are 0.00794, 0.07, 0.286, 0.67, 1.00, 1.00, 0.67, 0.286, 0.07 and 0.00794 respectively. A typical geometry of design is shown bellow,

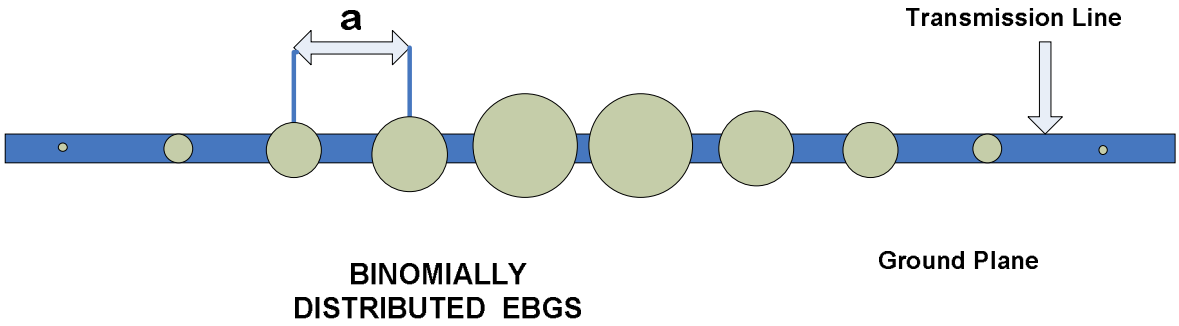

Figure 4.8: **Geometry of binomially distributed ten EBGS assisted transmission line.**

By inspecting the S-parameter performances of simulated designs table 4.3 is made.

Table 4.3: Variation of performances due to the variation of filling factor for ten EBGS.

Filling Factor	Pass band (GHz)	Stop band width (GHz)	Depth of Stop band (at center frequency, 10 GHz)	Maximum Ripple Height (dB)	-3 dB Cut-off frequency (GHz)
0.40	6.99151	4.51627	-35.3894	-1.55583	6.78188
0.45	6.56243	4.50892	-35.1383	-1.53842	6.77759
0.50	6.95403	4.17373	-35.0487	-2.04603	7.07460

From the above data table it is seen that for ten EBGS, FF=0.45 gives best result.

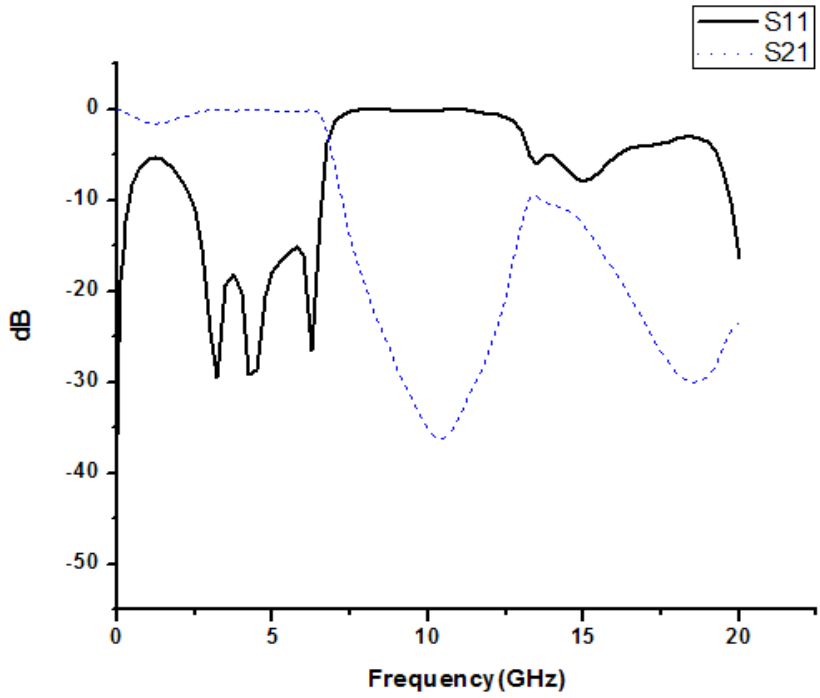

Figure 4.9: **S-Parameter performance graph for FF=0.45**

Here the depth is -35.1383 dB and stopband width is 4.50892 GHz. From the curve it is seen that after passing the center frequency of 10GHz the insertion loss curve rises to -10 dB but again falls down. Here passband is 6.5624295 GHz. So we can say this will block all the frequencies that exceed the passband. Though it passes some frequencies over 12.5 GHz, we can consider those negligible.

4.7 Some modified Designs and Their Performances:

We also simulated and studied some other modified non-uniform designs. Previously we calculated the coefficients using binomial distribution. In this case we used some random and modified coefficients and studied s-parameter performance. We found some good low pass filtering performance for some modified non-uniform design.

4.7.1 Designs:

Following designs contains non-uniform EBGS. Standard 50Ω microstrip T-line and the substrate of 31 mils thick and dielectric constant of 2.45 are used for all the designs in this section. Inner element spacing is a=10.43 mm and circular shape EBGS are used in designs where radius are calculated by some random pattern.

✧Design 1:

In the following design eight EBGS is used and the Filling factor is 0.45. Coefficients of radius are chosen 0.25, 0.50, 0.75, 1, 1, 0.75, 0.50 and 0.25 respectively.

For FF=0.45,

Radius is r=FF*a = 0.45*10.43 = 4.6935 mm

So after multiplying by our coefficients the radius of our non-uniform modified design becomes 1.1734, 2.3468, 3.5201, 4.6935, 4.6935, 3.5201, 2.3468 and 1.1734 mm respectively. Typical geometry of the design is given bellow,

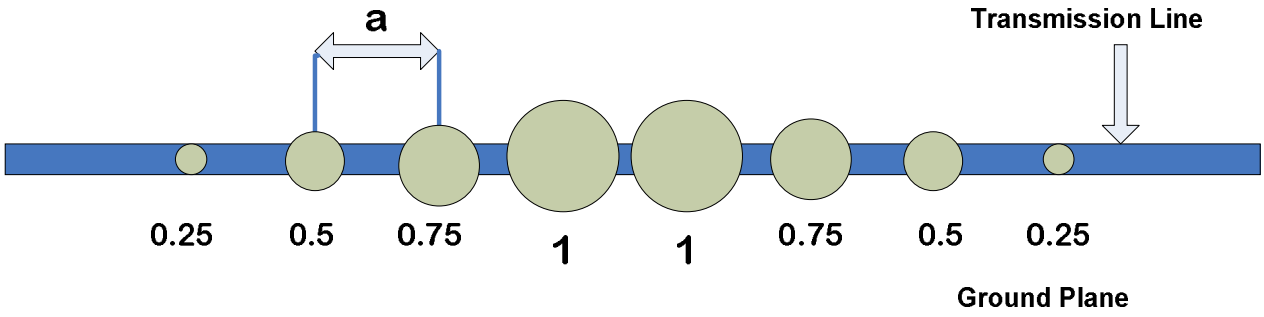

Figure 4.10: **Non-Uniform design using eight EBGS having coefficients of radius 0.25, 0.50, 0.75, 1, 1, 0.75, 0.50 and 0.25 respectively for FF=0**

✧Design 2:

In the following design eight EBGS is used and the Filling factor is 0.50. Coefficients of radius are chosen 0.25, 0.50, 0.75, 1, 1, 0.75, 0.50 and 0.25 respectively.

For FF=0.50,

Radius is r=FF*a = 0.50*10.43 = 5.215 mm

So after multiplying by our coefficients the radius of our non-uniform modified design becomes 1.3038, 2.6075, 3.9911, 5.215, 5.215, 3.9911, 2.6075 and 1.3038 mm respectively. Typical geometry of the design is given bellow,

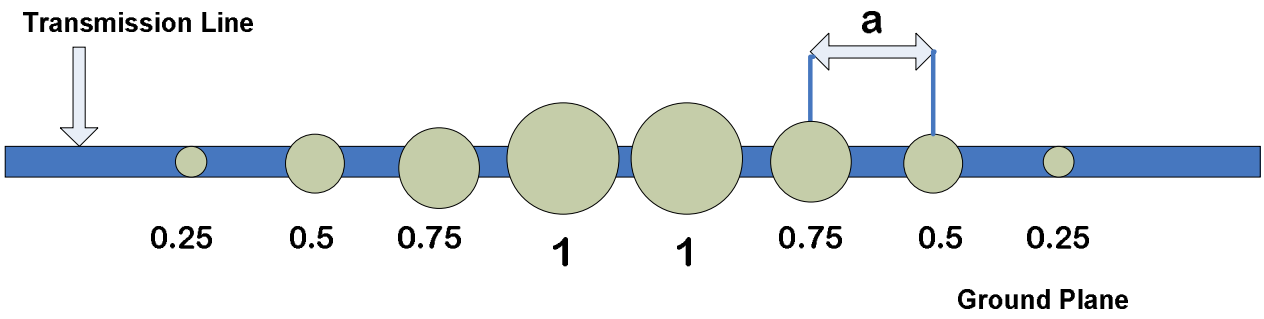

Figure 4.11: **Non-Uniform design using eight EBGS having coefficients of radius 0.25, 0.50, 0.75, 1, 1, 0.75, 0.50 and 0.25 respectively for FF=0.50.**

✧Design 3:

In the following design ten EBGS is used and the Filling factor is 0.50. Coefficients of radius are chosen 0.20, 0.40, 0.60, 0.80, 1, 1, 0.80, 0.60, 0.40 and 0.20 respectively.

For FF=0.50,

Radius is r=FF*a = 0.50*10.43 = 5.215 mm

So after multiplying by our coefficients the radius of our non-uniform modified design becomes 1.043, 2.086, 3.129, 4.172, 5.215, 5.215, 4.172, 3.129, 2.086 and 1.043 mm respectively. Typical geometry of the design is given bellow,

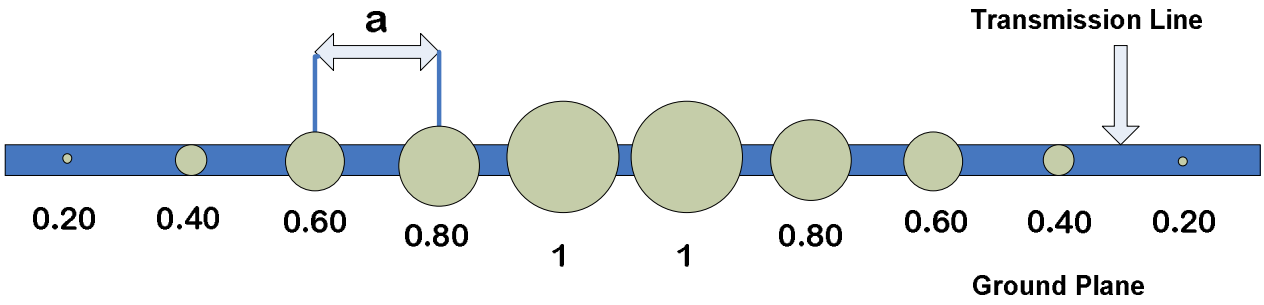

Figure 4.12: **Non-Uniform design using ten EBGS having coefficients of radius 0.20, 0.40, 0.60, 0.80, 1, 1, 0.80, 0.60, 0.40 and 0.20 respectively for FF=0.50.**

✧Design 4:

In the following design ten EBGS is used and the Filling factor is 0.45. Coefficients of radius are chosen 0.20, 0.40, 0.60, 0.80, 1, 1, 0.80, 0.60, 0.40 and 0.20 respectively.

For FF=0.45,

Radius is r=FF*a = 0.50*10.43 = 4.6935 mm

So after multiplying by our coefficients the radius of our non-uniform modified design becomes 0.9387, 1.8774, 2.8161, 3.7548, 4.6935, 4.6935, 3.7548, 2.8161, 1.8774 and 0.9387 mm respectively. Typical geometry of the design is given bellow,

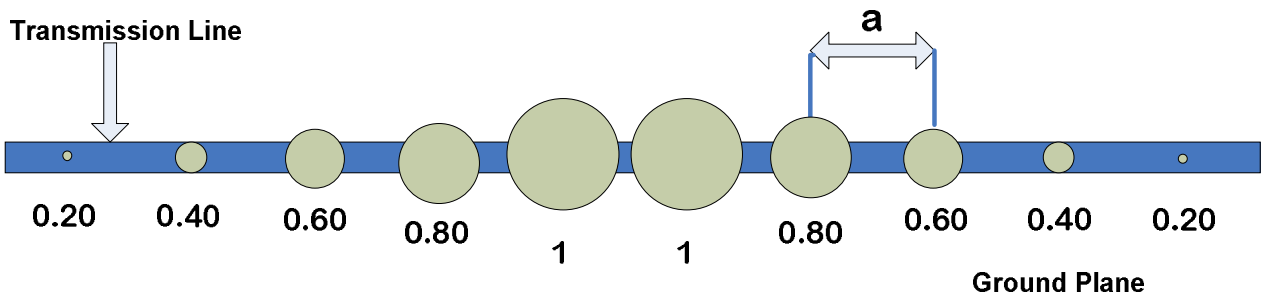

Figure 4.13: **Non-Uniform design using ten EBGS having coefficients of radius 0.20, 0.40, 0.60, 0.80, 1, 1, 0.80, 0.60, 0.40 and 0.20 respectively for FF=0.45.**

✧**Design 5:**

The following design is made by modifying the design of binomially distributed ten EBGS assisted transmission line where the coefficients were 0.00793, 0.0724, 0.286, 0.67, 1, 1, 0.67, 0.286, 0.0724 and 0.00793 respectively. But for our design we used coefficients 0.0724, 0.286, 0.67,1, 1, 1, 1, 0.67, 0.286 and 0.0724 respectively.

For FF=0.45,

Radius is r=FF*a = 0.50*10.43 = 4.6935 mm

So after multiplying by our coefficients the radius of our non-uniform modified design becomes 0.3353, 1.341, 3.129, 4.6935, 4.6935, 4.6935, 4.6935, 3.129, 1.341 and 0.3353 mm respectively. Typical geometry of the design is given bellow,

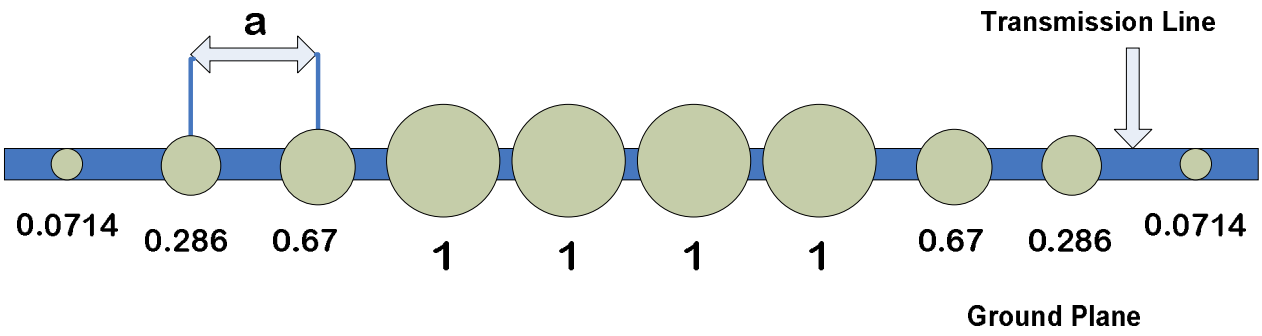

Figure 4.14: **Non-Uniform design using ten EBGS having coefficients of radius 0.0724, 0.286, 0.67,1, 1, 1, 1, 0.67, 0.286 and 0.0724 respectively for FF=0.45.**

4.7.2 Results:

S-parameter performance curves for above designs are shown bellow.

✧Design 1:

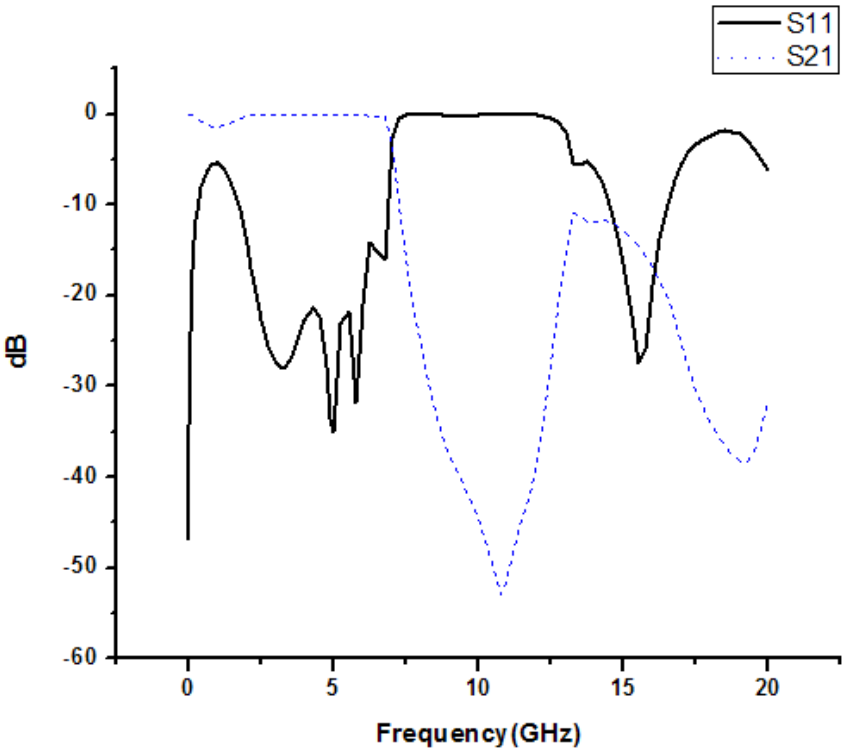

Figure 4.15: **S-parameter performance of modified design 1.**

From the above performance it is clearly seen that the depth at center frequency (10 GHz) is -44.5717 dB, passband width is 6.8645 GHz. The ripple height -1.4672 dB and -3dB cut off frequency is 6.9654 GHz. This gives very sharp cut off. It is also seen that there are only one ripple in the passband that is very good for smooth filtering operation.

✧**Design 2:**

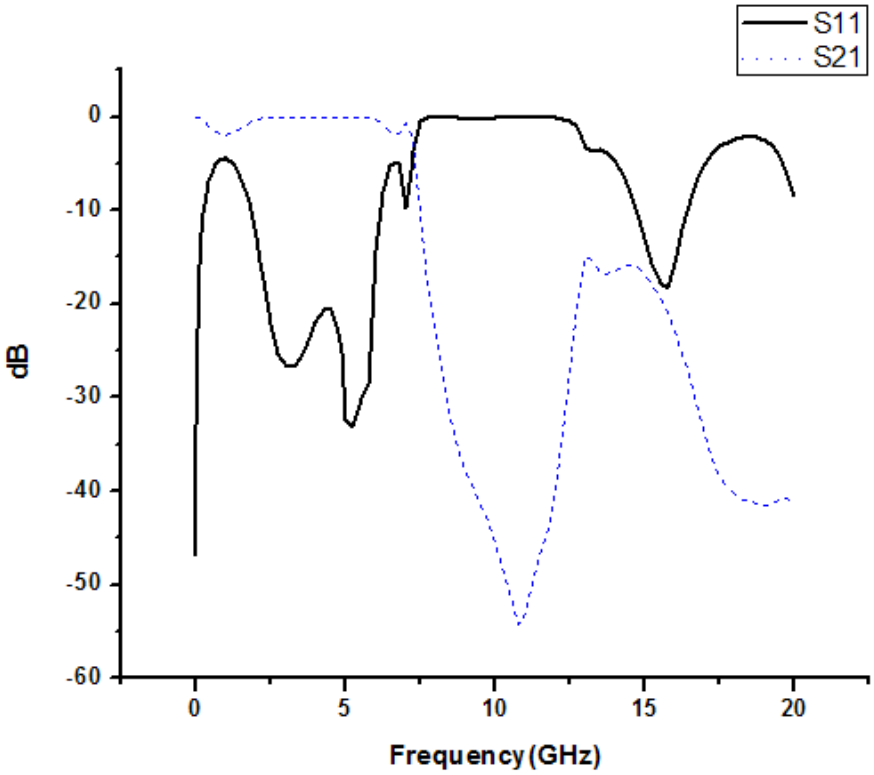

Figure 4.16: **S-parameter performance of modified design 2.**

Analyzing the above performance graph we found that the depth at center frequency (10 GHz) is -45.4627dB, passband width is 6.1730143 GHz. Maximum ripple height is -2.0085 dB which is reasonably good. -3dB cut off frequency is 7.275095 GHz which gives very sharp cut off also. So we can conclude that the design is suitable for low pass filtering.

✧**Design 3:**

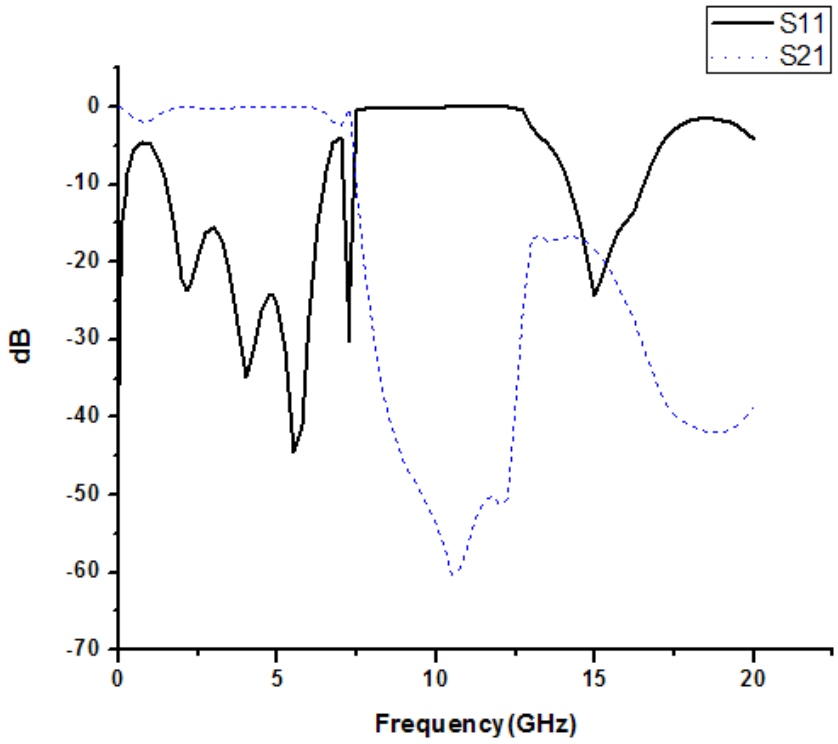

Figure 4.17: **S-parameter performance of modified design 3.**

The s-parameter performance of design 3 shows similar characteristics as design 2. Both have 2 ripples in similar positions .The ripple heights values are not same but very close which are -2.00848848 dB and -2.29658849 dB for design 2 and design 3 respectively. The depth at center frequency is -54.0309 dB and -3dB cut off frequency is 7.326287 GHz. The passband width is 7.4002 GHz. The shape shows low pass characteristics.

✧**Design 4:**

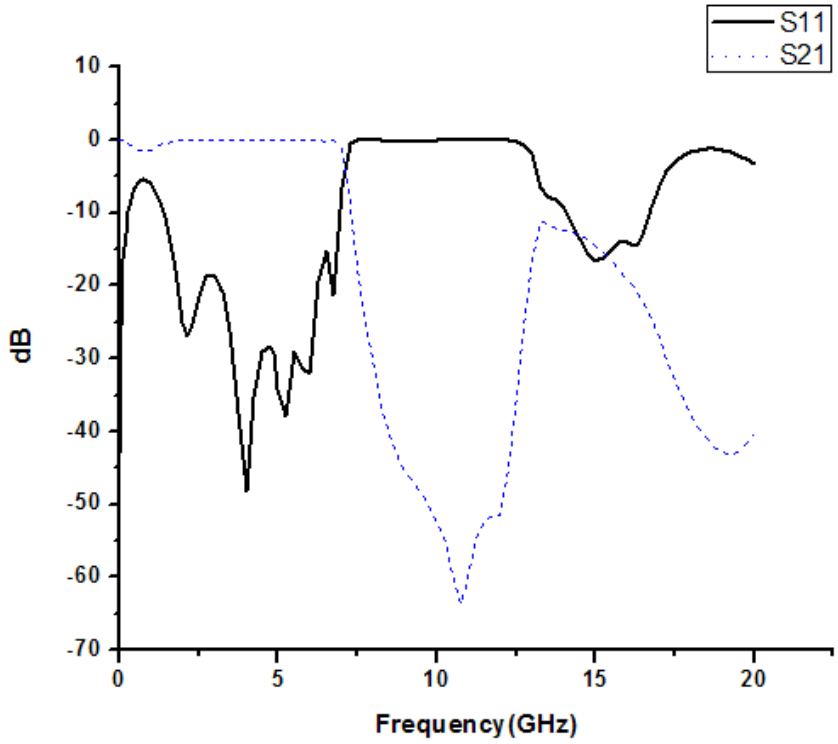

Figure 4.18: **S-parameter performance of modified design 4.**

Analyzing the s-parameter performance of design 4 we found that it shows similar characteristics to that of design 1. It also has only one ripple in the passband and ripple height is numerically very close. The depth at center frequency is greater than that which we got for design 1 is -52.3349 dB and passband width is 6.9405 GHz. -3 dB cut off frequency is 7.0588 GHz. So design 4 gives better performance than design 1.

✧**Design 5:**

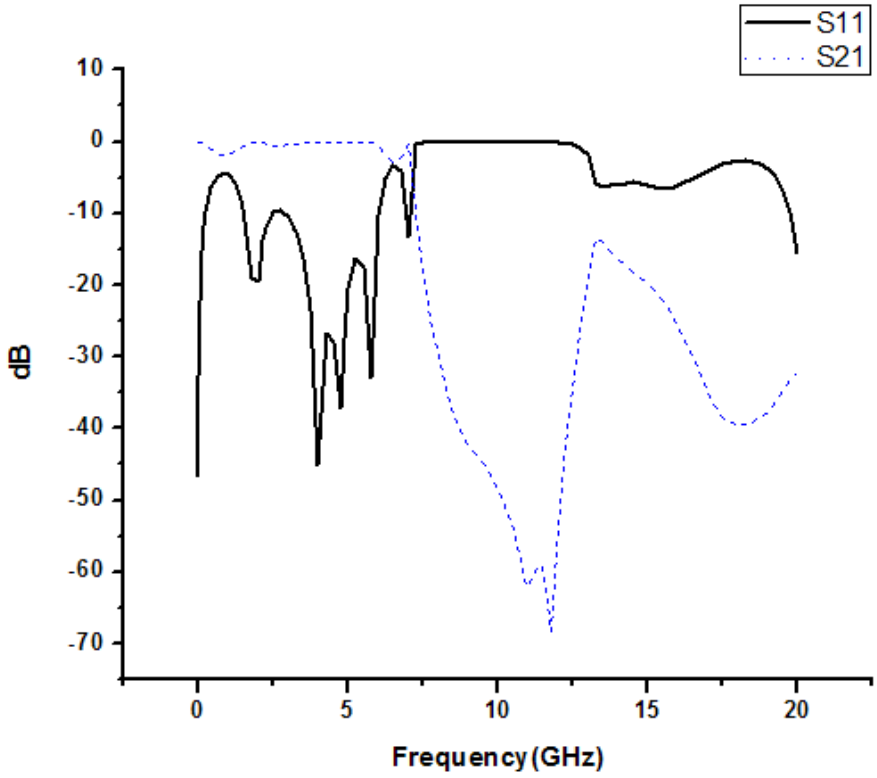

Figure 4.19: **S-parameter performance of modified design 5.**

From the above performance it is clearly seen that the depth at center frequency (10 GHz) is -48.3778 dB, passband width is 7.0642887 GHz. The ripple height -2.8097 dB and -3dB cut off frequency is 7.071737 GHz. Hence we can say that the performance curve reflects a very good low pass filtering performance.

4.8 Conclusions:

Microstrip transmission lines over binomially distributed EBGs have been designed and investigated theoretically. We investigated the s-parameter performances in terms of 10 dB RLBW, 20 dB rejection bandwidth and ripple height in the passband. We found wider stopband for even numbered EBGs that we can compare with LPF. Also simulating our modified designs we found relatively ripple free passband and sharp cut off. A modified design tends to show low pass filtering performance more than band stop performance.

Chapter 5 : Study of Dumbbell shape EBGS

5.1 Introduction:

The uniplanar compact EBG (UC-EBG) structure has been used for few applications [8]. UC-PBG structure has been applied to conventional LPF that improves the filter performance [1]. Low and high impedance transmission line sections have realized the LPF. The UC-EBG structure has been used in the ground plane of the filter. This structure is complex in nature. Next the researcher appeared with dumbbell shaped EBGS [8] where regular EBGS are connected with narrower slots in the ground plane. The frequency of operation can be changed with the dumbbell shaped EBGS dimensions. The dumbbell shaped EBGS can also be used to realize LPF [8]. Two designs for LPF having T-junction stub as well as cross-junction opened stub in conjunction with dumbbell shaped EGS is used in the ground plane. Dumbbell shaped EGS has been modeled with the lumped parameters. L. Garde *et al* [9] proposed non-uniform ring patterned dumbbell shaped dumbbell shaped EGS to design LPF as EBGS with non-uniform distribution is proposed [12]. They have used dumbbell shaped EBGS in the ground plane of a conventional LPF. The conventional LPF is implemented with transmission line obtained by the Richard's transformation that yields different transmission with different impedances (High-Low impedance sections). H-W Liu *et al*. [10] Proposed a LPF with multilayer fractal EBGS. A two-level fractal EBG plane has replaced the ground plane. In the intermediate plate EBGS have different shapes as the top layer is made of 3rd-order Sierpinski gaskets and the bottom layer is made of 1st-order Sierpinski carpets. Significant ripples appear in the passband. Although the LPF performance reported in [13] and [10] produces wide stopband yet the designs need to take care of both the bottom and top layouts that may be contrast to high-level applications.

The new model of dumbbell shaped EBGS provides a perturbed surface as ground plane of standard 50-ohm transmission line that yields the performance of LPF. It provides smoother passband and wider stopband. Only the perturbed ground plane needs to be taken care of.

In this chapter the evolution of dumbbell shaped EBGS of square, circular and triangular patterned reported. Various designs are also depicted on the basis of parametric studies i.e. narrow area effect, total area effect, effect for change in shape. Non-uniform binomially distributed dumbbell shaped EBGS is also studied. At the last part, some designs are made that gives good low pass filtering performance.

5.2 Theory of Dumbbell shape EBGS:

In the previous chapter, for conventional EBGS the center frequency of the stopband is approximately calculated by well-known formula of Bragg's condition. Using this formula, the period for any stopband frequency can be determined. The theory of dumbbell shaped EBGS is different from that. Here the dimensions of the dumbbell shaped slot (unit cell) control the current paths on the ground plane hence the equivalent inductance and capacitance of the ground. Fig. 5.1 shows the unit cell of a dumbbell shaped EBGS. It is composed of two larger slots connected by a narrow vertical slot. The larger slot is a square patterned EBG element. On the other hand narrower vertical slot is a rectangular patterned EBG element.

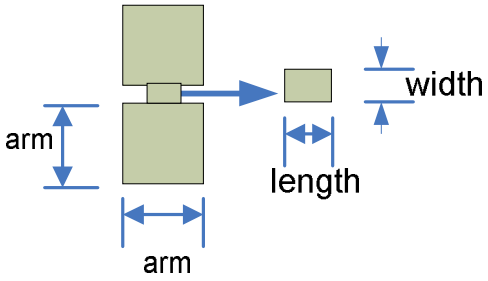

Figure 5.1: **Geometry of a unit cell of a dumbbell shape EBGS. The arm length of a larger square patterned slot is 'b'. The vertical slot is a rectangular patterned slot with w×g dimension; w is known as width and g is known as gap in the open literature.**

The unit cell is etched in the ground plane of a standard 50-ohm transmission line. In order to investigate the frequency characteristics of the unit EBGS cell, few structures having different 'b' and 'g' are simulated and not only square patterned larger slot but also rectangular, circular and triangular patterned dumbbell shaped EBGS are also simulated.

The lumped LC equivalent model can be expressed as [9]:

$$C = \frac{\omega_c}{Z_0 g_1}\left[\frac{1}{\omega_0^2 - \omega_c^2}\right] \tag{5.1}$$

$$L = \frac{1}{4\pi^2 f_0 C} \tag{5.2}$$

Where f_0 is the frequency of the attenuation pole, ω_C is the angular cutoff frequency, Z_0 is the characteristic impedance of the line, and g_1 is the admittance value of the Butterworth low pass filter response.

The equivalent circuit of dumbbell shaped EBGS unit cell is shown in Fig. 5.2.

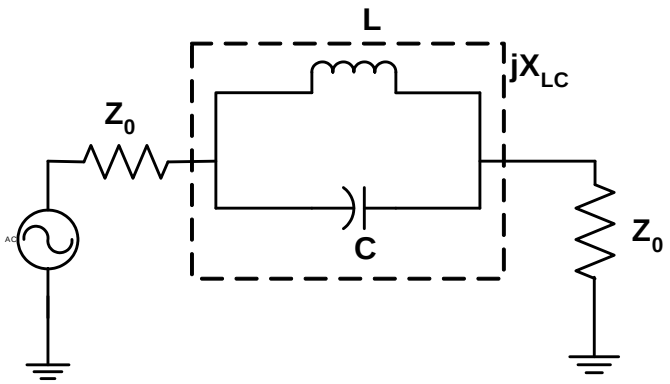

Figure 5.2: **The equivalent circuit of dumbbell shaped DGS unit.**

5.3 Performance comparison of Dumbbell shaped and regular shaped EBGS for same area:

In chapter 3 it is seen that same etching area plays a vital rule of designing EBGS of various design. Also different regular shapes like square, circular, triangular and hexagonal having same etching area shows same characteristics. Therefore, in this chapter the effect of same etching area is also studied for dumbbell shape EBGS as well as regular shapes EBGS to compare the difference of characteristics.

5.3.1 Designs. Type (A)

All designs are made with reference to the area of circular EBGS having FF=0.30. The area is 30.7582 mm^2.

✧ Designs. A (i) Regular Circular

This design has circular EBGS of radius 3.129 and inner element spacing is 10.43mm. The T-line is standard 50Ω microstrip line. The design is made on the substrate of 31 mils thick whose dielectric constant is 2.45. Seven numbers of EBGS was used.

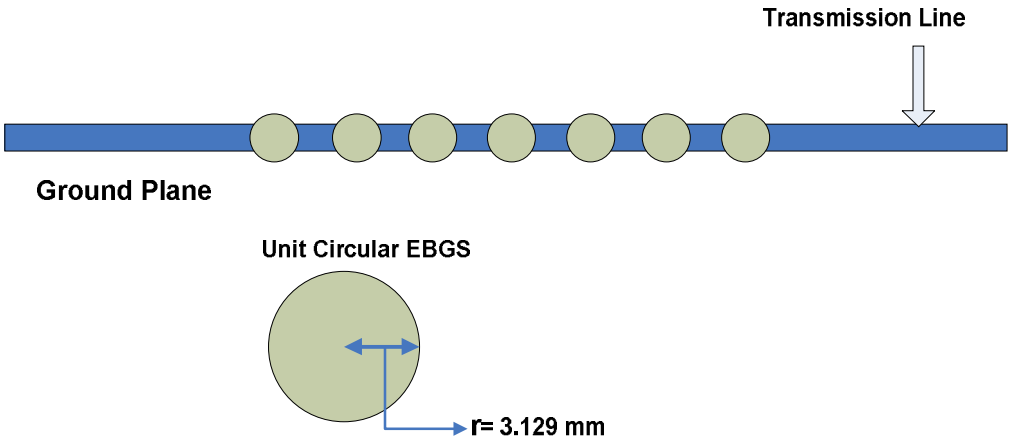

Figure 5.3: **Geometry of regular circular shape EBGS assisted microstrip t-line and a unit cell.**

✧Designs. A(ii) Regular Square

This design has square EBGS of arm 5.546 mm and inner element spacing is 10.43mm. The T-line is standard 50Ω microstrip line. The design is made on the substrate of 31 mils thick whose dielectric constant is 2.45. Seven numbers of EBGS was used.

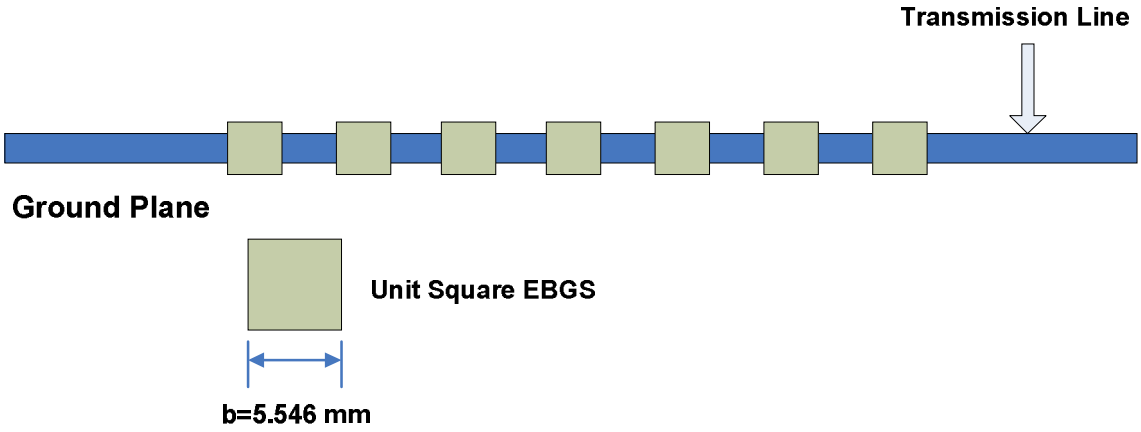

Figure 5.4: **Geometry of regular square shape EBGS assisted microstrip t-line and a unit cell.**

✧Designs. A(iii) Circular dumbbell shape

This design has two equal circular shaped bigger slots of radius 2.2089 mm and the rectangular narrow slots of dimensions 0.5mm*0.2mm (length * width) thus the total area becomes 30.7582mm^2 and inner element spacing is 10.4308mm. The T-line is standard 50Ω microstrip line. The design is made on the substrate of 31 mils thick whose dielectric constant is 2.45.

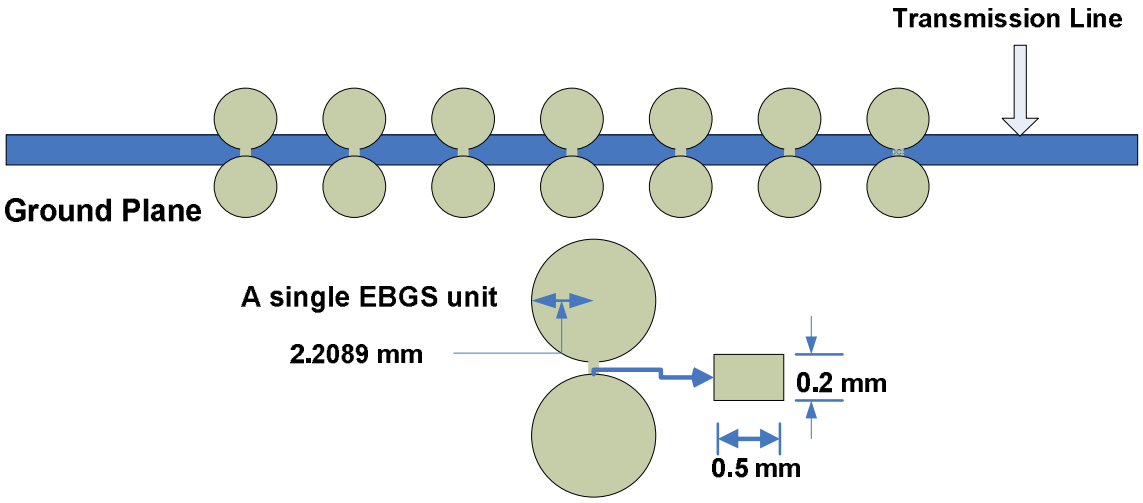

Figure 5.5: **Typical design of circular patterned dumbbell shaped EBGS with two circular shaped bigger slots (radius= 2.2089 mm) and narrow slots of 0.5 mm* 0.2mm (length*width).**

✧Designs. A(iv) Square dumbbell shape

This design has two equal square shaped bigger slots of arm 3.9152 mm and the rectangular narrow slots of dimensions 0.5mm*0.2mm (length * width) thus the total area becomes 30.7582mm^2 and inner element spacing is 10.4308mm. The T-line is standard 50Ω microstrip line. The design is made on the substrate of 31 mils thick whose dielectric constant is 2.45.

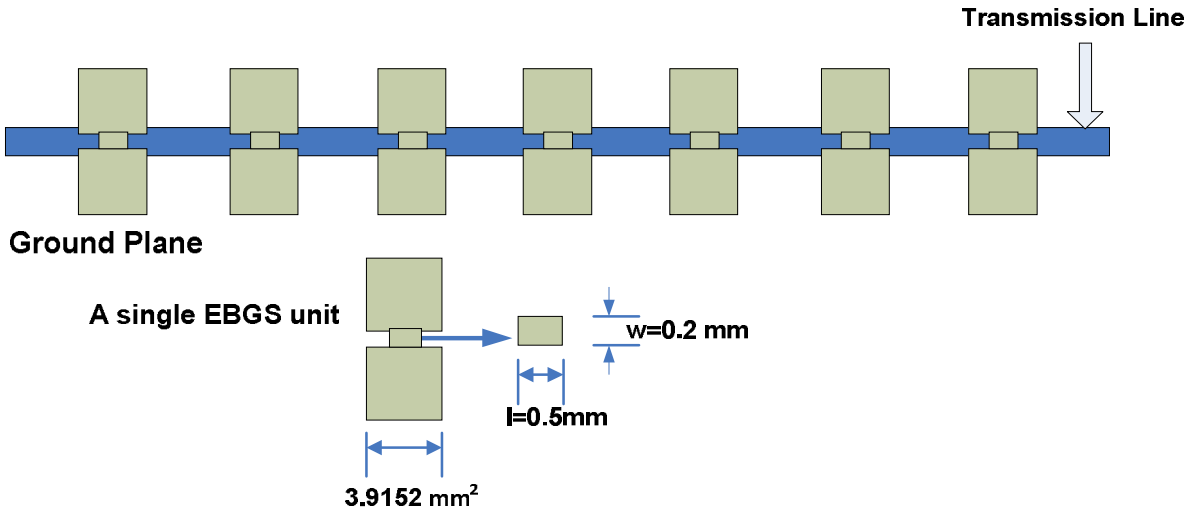

Figure 5.6: **Typical design of square patterned dumbbell shaped EBGS with two square shaped bigger slots (Arm= 3.9152 mm) and narrow slots of 0.5 mm* 0.2mm (length*width).**

5.3.2 Results Type (A)

All results of the Designs Type A are shown bellow.

✧Results. A(i) Regular Circular

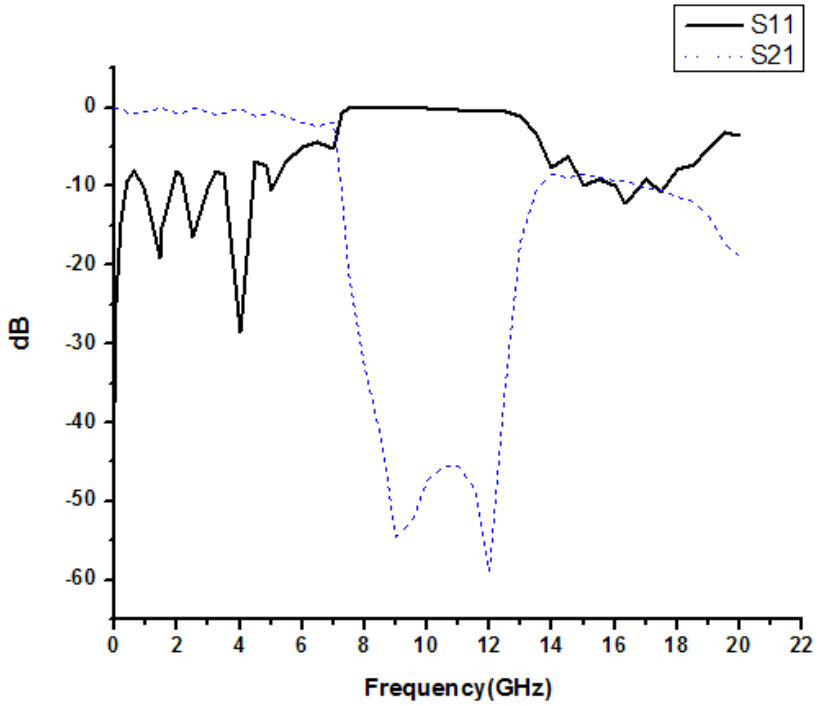

Figure 5.7: **S-parameter performance of regular circular shaped EBGS of total area 30.7582mm^2.**

From the above s-parameter performance graph it is found that the stopband starts from 7.4797 GHz and ends at 12.9182 GHz forming a stopband width of 5.43856 GHz. -3dB cut off frequency is observed as 7.035 GHz. Few ripples are seen on the graph and maximum ripple height is measured as -1.0742 dB, passband width of 4.9789 GHz is observed at -10 dB.

✧**Results. A(ii) Regular square**

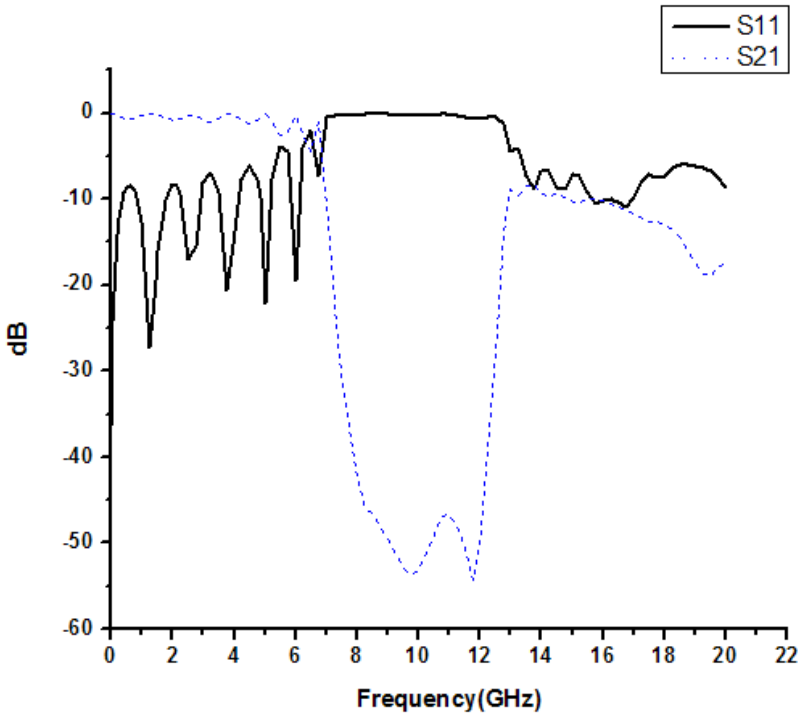

Figure 5.8: **S-parameter performance of regular square shaped EBGS of total area 30.7582mm^2.**

This performance also shows similar kind performance as Design. A(i). The performance parameters are observed as follows - stopband starts from 12.6408 GHz forming stopband width of 5.4391 GHz, 3 dB cut off frequency = 6.8 GHz, passband width = 6.154 GHz and ripple height = -2.395 dB which is similar to the above performance.

✧**Results. A(iii) Circular dumbbell shape**

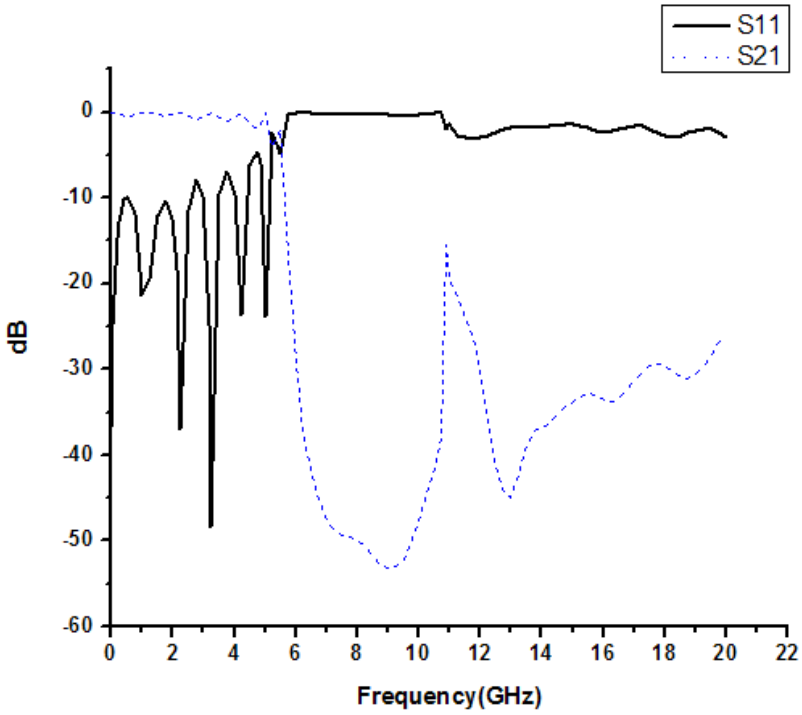

Figure 5.9: **S-parameter performance of circular dumbbell shaped EBGS of total area 30.7582mm^2.**

From the above s-parameter performance of circular dumbbell shape design it is observed that the stopband starts at 5.8164 GHz and ends at 10.8654 GHz forming a stopband width of 5.04902 GHz. -3 dB cut off frequency = 5.1849 GHz, passband width = 5.162 GHz and ripple height = --1.92878 dB. Comparing with previous two designs here a shift in the starting and ending of stopband is observed but the stopband width was nearly the same. The shift in central depth is also seen for this design. At 20 GHz the insertion loss curve just cross a 20dB and after reaching -16.4448 dB again it decreases and goes bellow 20 dB.

✧**Results. A(iv) Square dumbbell shape**

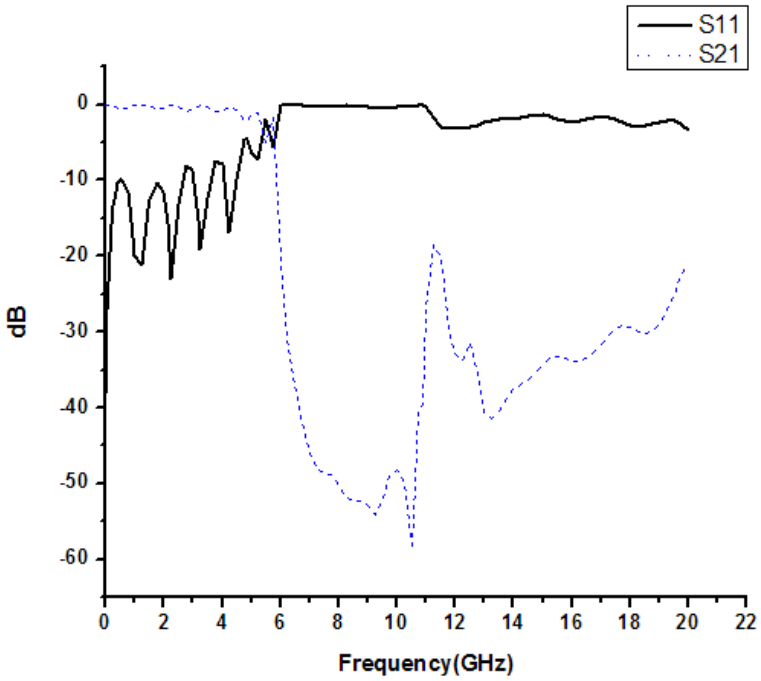

Figure 5.10: **S-parameter performance of square dumbbell shaped EBGS of total area 30.7582mm^2**

This performance also shows similar kind performance as Design. A(iii). Stopband starts at 5.9912GHz and ends at 11.2062 GHz forming a stopband width of 5.215 GHz where stopband is measured with the reference of -20 dB insertion loss. -3 dB cut off frequency = 5.3734 GHz, passband width = 4.4953 GHz and ripple height = -2.0309 dB. At 20 GHz the insertion loss curve just cross a little the 20dB line and again it decreases.

It can be said that regular circular and square shape designs shows similar result. On the hand, both dumbbell shape designs show same type of performance.

5.3.3 Designs. Type (B)

All designs are made with reference to the area of circular EBGS having FF=0.35. The area is 41.8653 mm^2.

✧ **Designs. B (i) Regular Circular**

This design has circular EBGS of radius 3.6505 and inner element spacing is 10.43mm. The T-line is standard 50Ω microstrip line. The design is made on the substrate of 31 mils thick whose dielectric constant is 2.45. Seven numbers of EBGS was used.

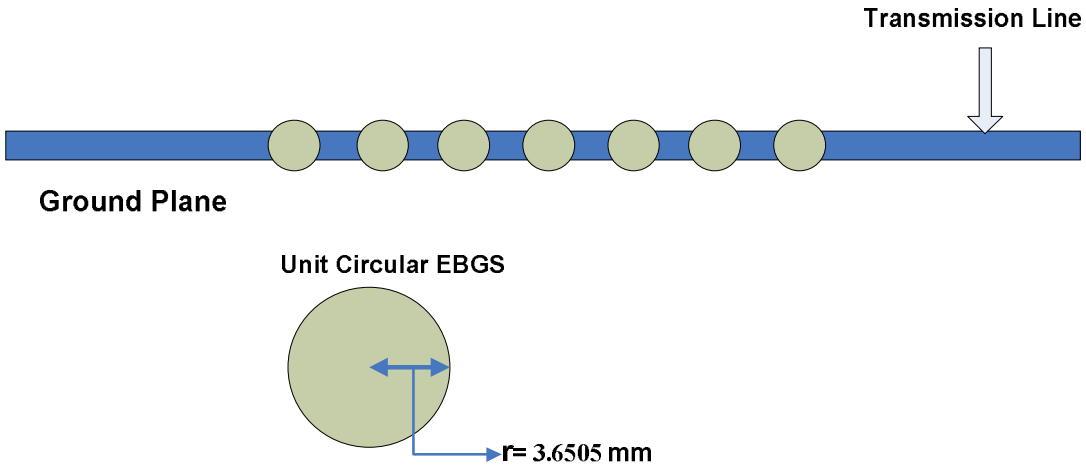

Figure 5.11: **A typical geometry of regular circular shape EBGS assisted microstrip t-line and a unit cell.**

✧Designs. B(ii) Regular Square

This design has square EBGS of arm 6.4703 mm and inner element spacing is 10.43mm. The T-line is standard 50Ω microstrip line. The design is made on the substrate of 31 mils thick whose dielectric constant is 2.45. Seven numbers of EBGS was used.

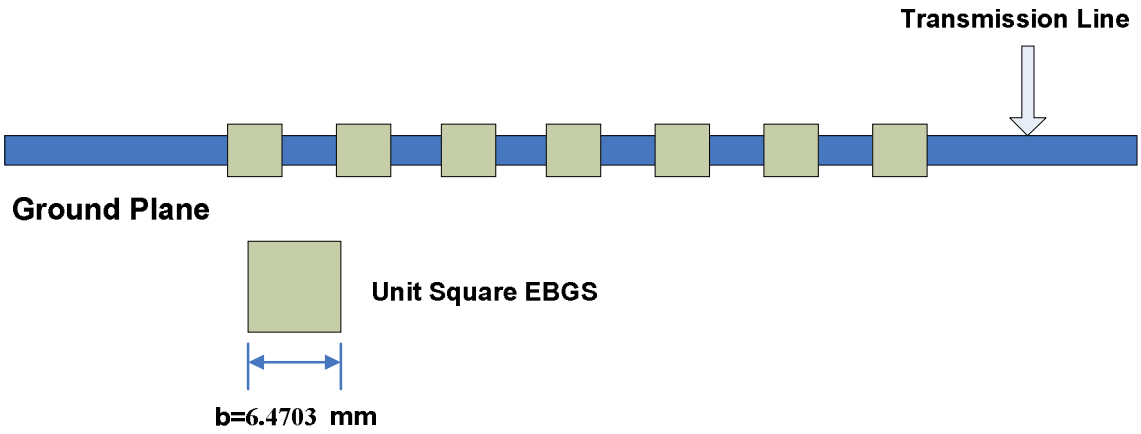

Figure 5.12: **A typical geometry of regular square shape EBGS assisted microstrip t-line and a unit cell.**

✧Designs. B(iii) Circular dumbbell shape

This design has two equal circular shaped bigger slots of radius 2.5782mm and the rectangular narrow slots of dimensions 0.5mm*0.2mm (length * width) thus the total area becomes 41.7653mm^2 and inner element spacing is 10.4308mm. The T-line is standard 50Ω microstrip line. The design is made on the substrate of 31 mils thick whose dielectric constant is 2.45.

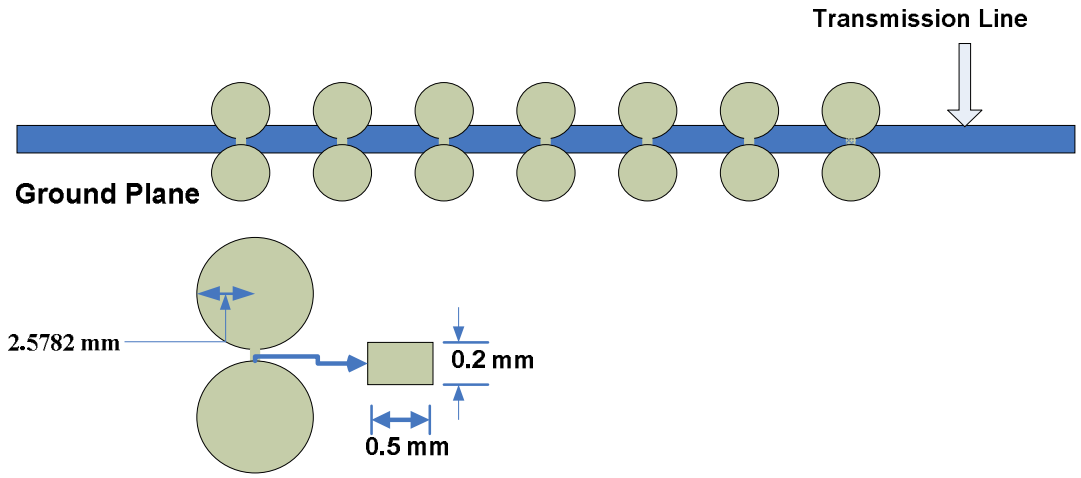

Figure 5.13: **Typical design of circular patterned dumbbell shaped EBGS with two circular shaped bigger slots (radius= 2.5782 mm) and narrow slots of 0.5 mm* 0.2mm (length*width).**

✧Designs. B(iv) Regular dumbbell shape

This design has two equal square shaped bigger slots of arm 4.5698 mm and the rectangular narrow slots of dimensions 0.5mm*0.2mm (length * width) thus the total area becomes 41.8653mm^2 and inner element spacing is 10.4308mm. The T-line is standard 50Ω microstrip line. The design is made on the substrate of 31 mils thick whose dielectric constant is 2.45.

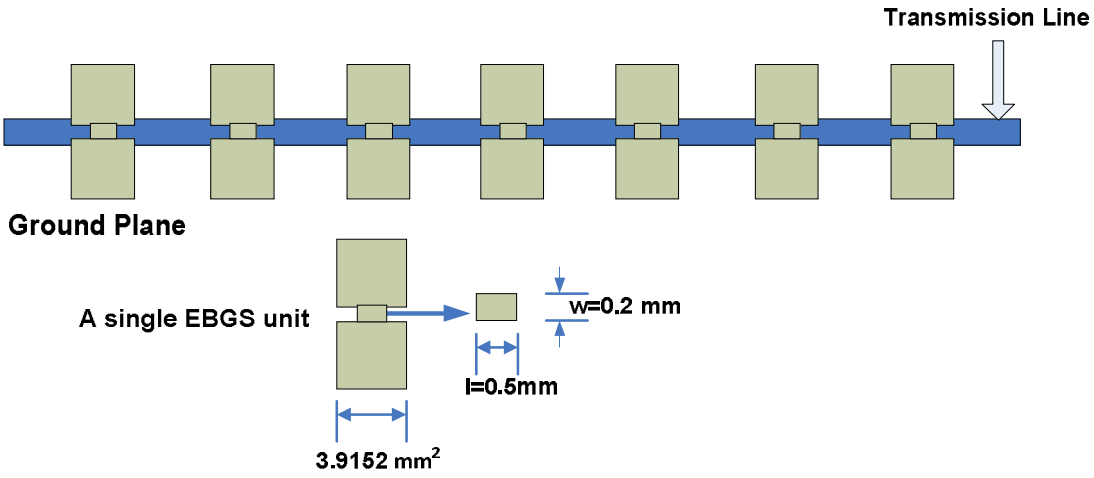

Figure 5.14: **Typical design of square patterned dumbbell shaped EBGS with two square shaped bigger slots (Arm = 4.5698 mm) and narrow slots of 0.5 mm* 0.2mm (length*width).**

5.3.4 Results Type (B)

All results of the Designs Type B are shown bellow.

✧Results. B(i) Regular circular

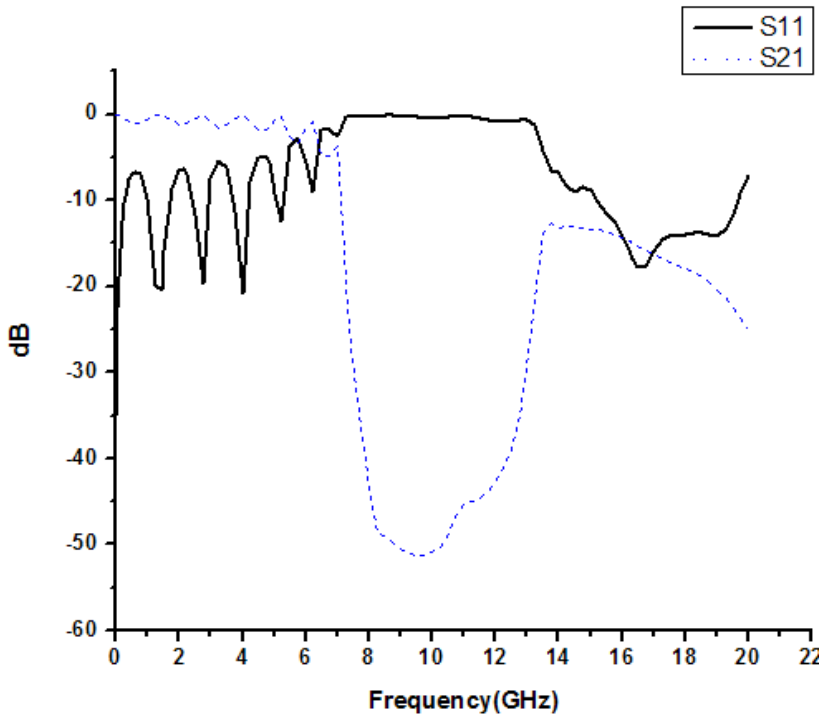

Figure 5.15: **S-parameter performance of regular circular shaped EBGS of total area 41.8653mm^2.**

From the above graph stopband starts from 7.2648 GHz ends at 13.2984 GHz giving a stopband width of 6.0337 GHz. 3dB cut off frequency is observed as 6.391 GHz. Few ripples are seen on the graph and ripple height is measured as -3.3952 dB, passband width of 5.3213 GHz is observed at 10 dB. Depth at 10 GHz is -50.941 dB.

✧**Results. B(ii) Regular square**

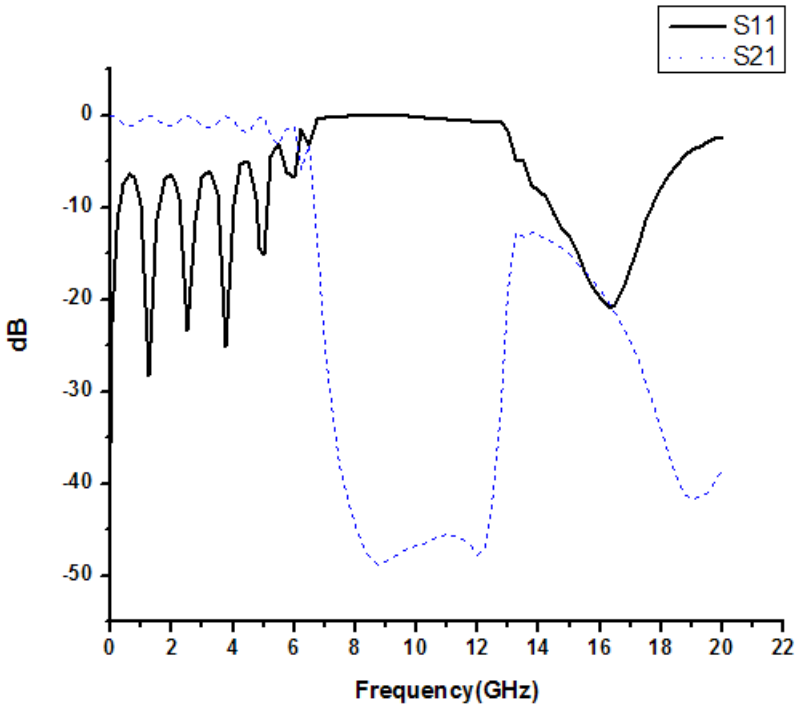

Figure 5.16: **S-parameter performance of regular square shaped EBGS of total area 41.8653mm^2.**

In this figure, the performance looks like similar to the above performance. However, performance parameters are observed as follows - stopband starts from 6.8874 GHz and ends at 12.98 GHz giving a bandwidth of 6.0925 GHz.- 3dB cut off frequency = 6.095 GHz, passband width = 5.112 GHz and ripple height is observed as -2.886 dB. Depth at 10 GHz was -46.812 dB.

✧**Results. B(iii) Circular dumbbell shape**

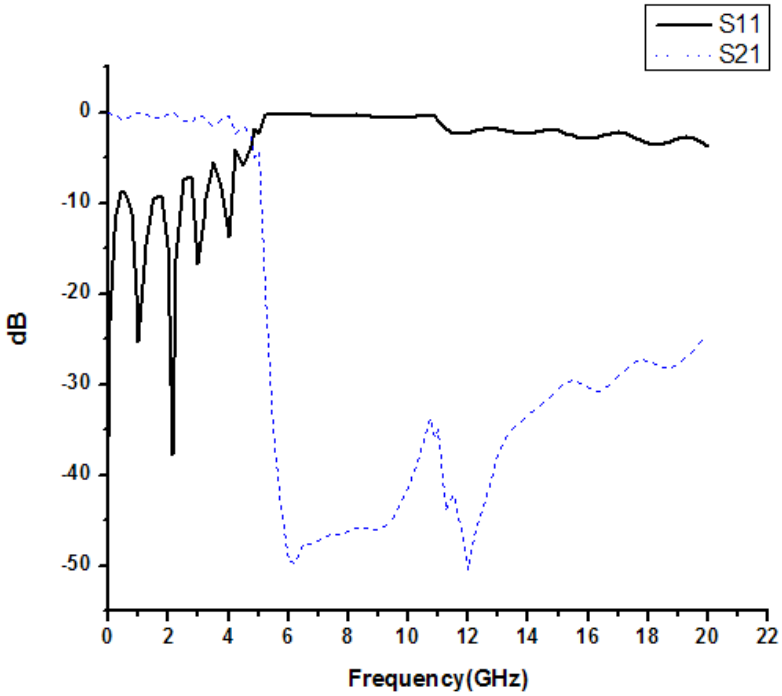

Figure 5.17: **S-parameter performance of circular dumbbell shaped EBGS of total area 41.8653mm^2.**

S-parameter performance of circular patterned dumbbell shaped EBGS has shown performance like low pass filter (LPF) and here performance parameters are observed as follows - stopband starts from 5.251 GHz, 3dB cut off frequency = 4.766 GHz, passband width = 4.096 GHz and ripple height is observed as - 1.5 dB. Depth at 10 GHz is observed -41.333 dB. However, at the stopband region too much ups and downs of Insertion Loss curve are present; but it remains bellow 20dB. On the other hand Return Loss curve at that region shows quite good performance – remains above -5dB all the time.

✧**Results. B(iv) Square dumbbell shape**

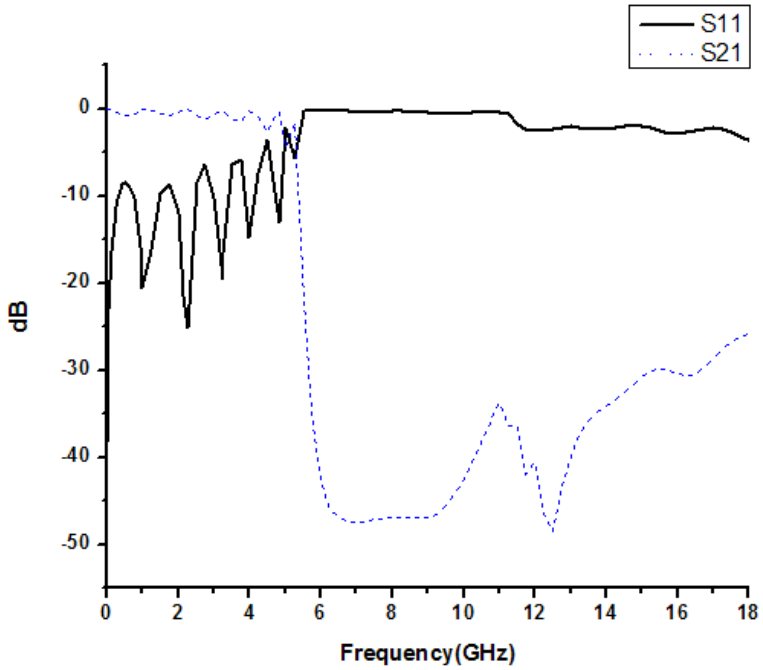

Figure 5.18: **S-parameter performance of square dumbbell shaped EBGS of total area 41.8653mm^2.**

In this figure, the performance looks like similar to the above performance. In this case too graph shows low pass filtering (LPF) performance. Also, in the stopband region Return Loss curve shows better performance. However, performance data are as follows - stopband starts from 5.475 GHz, 3dB cut off frequency = 5.267 GHz, passband width = 4.887 GHz and ripple height is -2.556 dB. Depth at 10 GHz is observed -42.45190 dB. Studying the results of Designs type (B) it is found that both circular and square pattern dumbbell shape shows similar performance and for dumbbell shape designs there is a shift in the starting of stopband formation. It is also observed that dumbbell shape designs shows low pass filtering performance.

5.4 Designs with different dimensions of narrow slot:

In this section, circular and square pattern dumbbell shape designs are made and simulated where the dimension of narrow slot varied but the bigger (circular or square) slot kept constant. Standard 50Ω microstrip T-line and the substrate of 31 mils thick and dielectric constant of 2.45 are used for all the designs in this section.

5.4.1 Circular dumbbell shape designs :

All circular pattern dumbbell shape designs made in this section have two bigger slots and a narrow slot in between them. Etch bigger slot has area of 21.3599 mm^2 which is the area for a regular circular shape EBGS having FF=0.25. Centre frequency is 10 GHz which gives the inner element spacing 10.43 and radius of etch bigger slot is 2.6075 mm. Seven numbers of EBGS units is used in all those designs.

✧Design 1

The following design has two circular shaped bigger slots of radius 2.6075 mm and the length and width of the rectangular narrow slots are 0.5 mm and 0.7mm respectively, thus the total area becomes 43.0698mm^2 and inner element spacing is 10.43mm. The T-line is standard 50Ω microstrip line. The design is made on the substrate of 31 mils thick whose dielectric constant is 2.45.

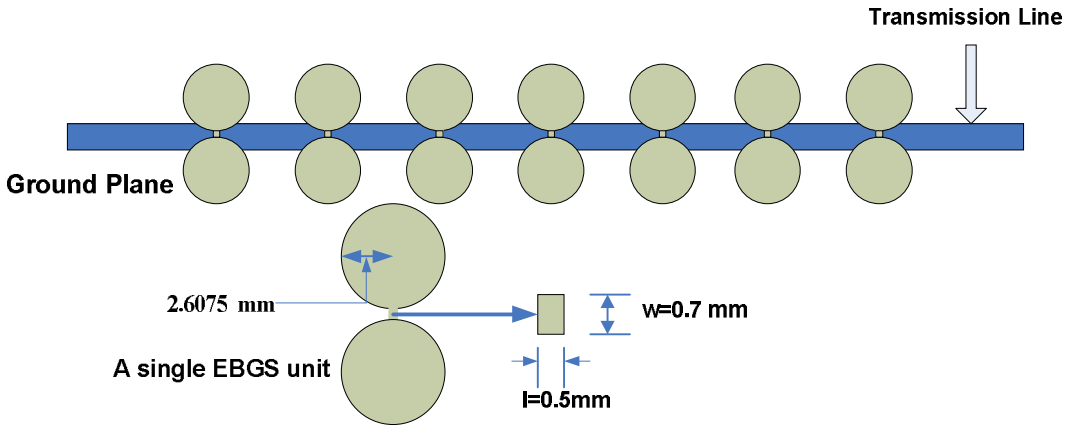

Figure 5.19: **Typical design of circular patterned dumbbell shaped EBGS with two circular shaped bigger slots (radius=2.6075 mm) and narrow slots of 0.5 mm* 0.7 mm (length*width).**

✧Design 2

The following design also has two circular shaped bigger slots of radius 2.6075 mm but in this design the length and width of the rectangular narrow slots are 0.5 mm and 0.2 mm respectively. The total area thus becomes 41.8198 mm^2. The inner element spacing is 10.43mm and the T-line is standard 50Ω microstrip line. The design is made on the substrate of 31 mils thick whose dielectric constant is 2.45.

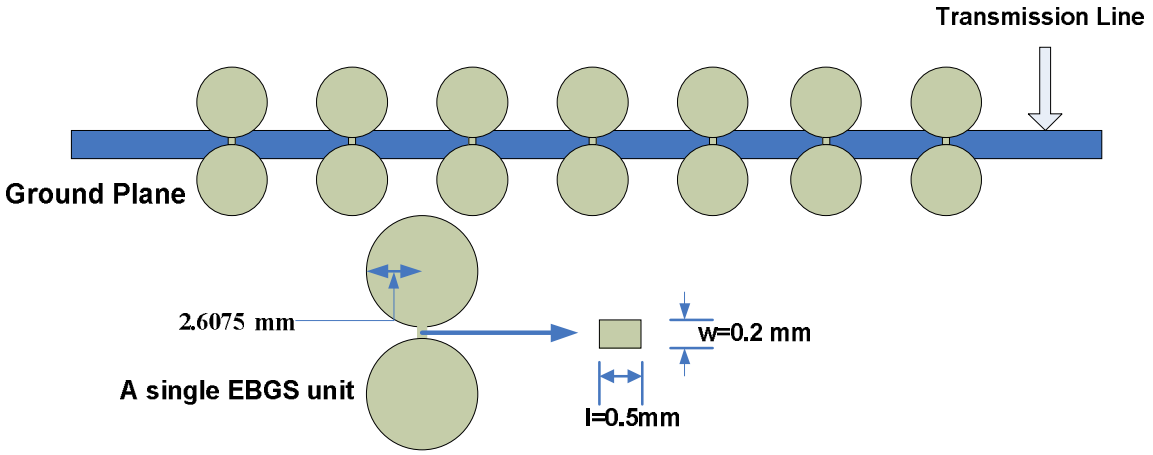

Figure 5.20: **Typical design of circular patterned dumbbell shaped EBGS with two circular shaped bigger slots (radius=2.6075 mm) and narrow slots of 0.5 mm* 0.2 mm (length*width).**

✧Design 3

In this design, the two circular shaped bigger slots has radius of 2.6075 mm. Its narrow slot is square shape having sides of 1 mm. In this case, the total area is 43.7198mm^2 and inner element spacing is 10.43mm. The T-line is standard 50Ω microstrip line. The design is made on the substrate of 31 mils thick whose dielectric constant is 2.45.

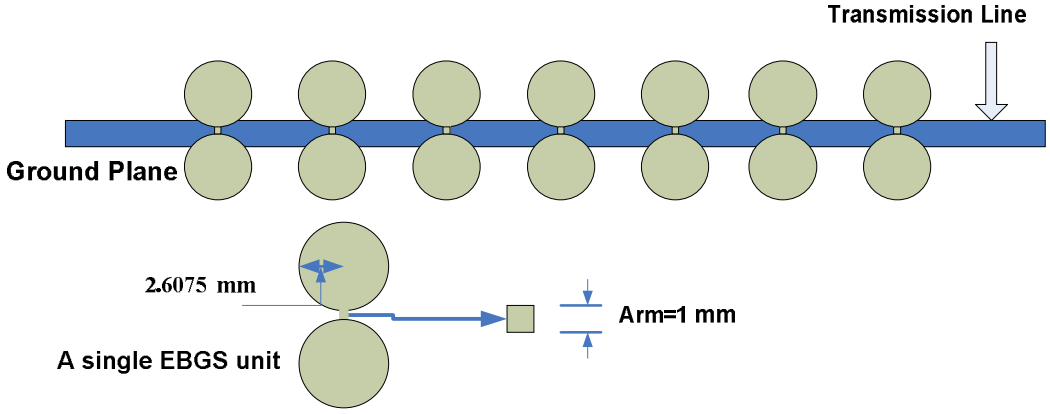

Figure 5.21: **Typical design of circular patterned dumbbell shaped EBGS with two circular shaped bigger slots (radius=2.6075 mm) and narrow slots of 1 mm* 1 mm (length*width).**

5.4.2 Circular dumbbell shape results:

The results of the designs made in section 5.4.1 are presented below:

✧Design 1

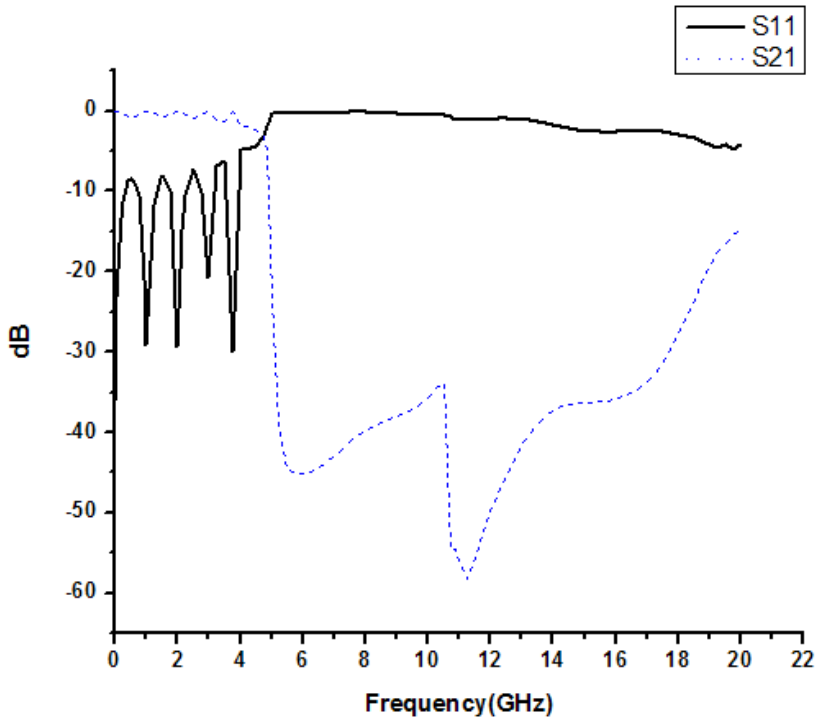

Figure 5.22: **S-parameter performance of circular pattern dumbbell shaped EBGS with narrow slot's dimension of 0.5 mm*0.7 mm(length* width).**

From the above graph it is seen that the stopband starts from 4.9706 GHz and ends at 18.9195 GHz, thus it gives a wide stopband of width 13.9489 GHz. 3dB cut off frequency is observed as 4.7067 GHz. Few ripples are seen on the graph and ripple height is measured as -1.2582 dB, passband width of 3.9476 GHz is observed at 10 dB return loss line.

✧**Design 2**

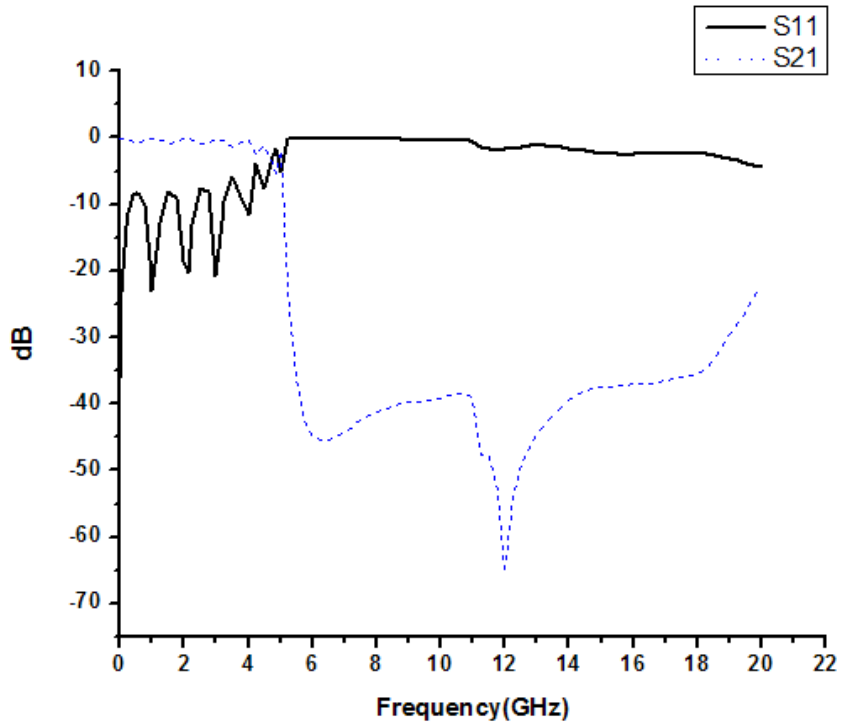

Figure 5.23: **S-parameter performance of circular pattern dumbbell shaped EBGS with narrow slot's dimension of 0.5 mm*0.2 mm (length* width).**

S-parameter performance of circular patterned dumbbell shaped EBGS has shown performance like low pass filter (LPF) and here performance parameters are observed as follows - stopband starts from 5.217 GHz, 3dB cut off frequency = 5.014 GHz, passband width = 4.0515 GHz and ripple height is observed as - -2.4375. However, at the stopband region remains bellow 20dB which is necessary to have low pass filtering performance. On the other hand Return Loss curve at that region shows quite good performance – remains above -5dB all the time.

✧**Design 3:**

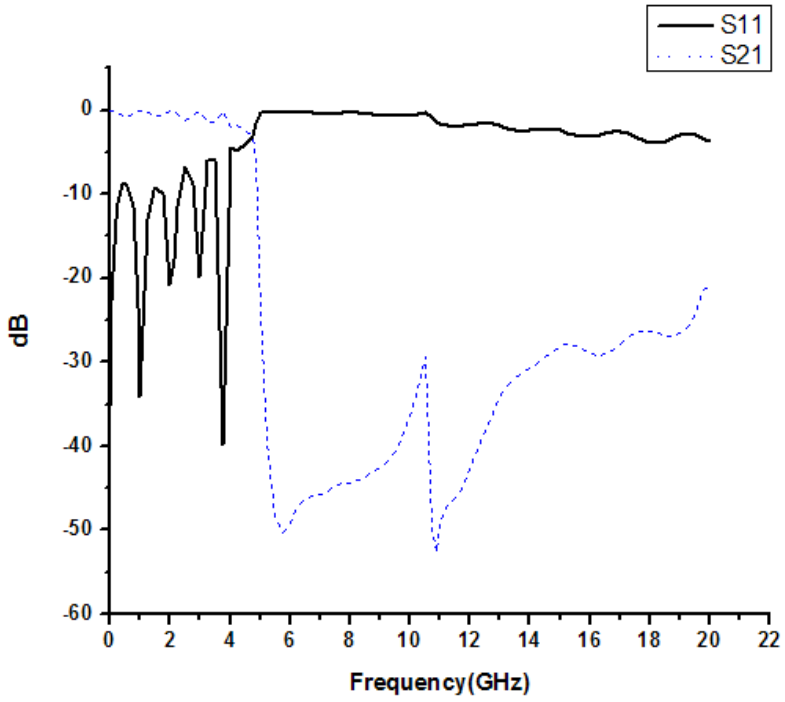

Figure 5.24: **S-parameter performance of circular pattern dumbbell shaped EBGS with narrow slot's dimension of 1 mm*1 mm(length* width).**

In this figure, the performance looks like similar to the above performance and at stopband region Insertion Loss curve shows better performance than that. However, performance parameters are observed as follows - stopband starts from 4.965 GHz, 3dB cut off frequency = 4.691 GHz, passband width = 3.961 GHz and ripple height is observed as -1.3827 dB.

Studying the above circular pattern dumbell shape designs it can be said that the designs with smaller dimensions of narrow slots gives better low pass filtering performance.

5.4.3 Square dumbbell shape designs

All square pattern dumbbell shape designs made in this section have two bigger slots and a narrow slot in between them. Etch bigger slot has area of 22.0289 mm^2 which is the area for a regular circular shape EBGS having FF=0.45. Centre frequency is 10 GHz which gives the inner element spacing 10.43 and arm of etch bigger slot is 4.6935 mm. Seven numbers of EBGS units is used in all those designs.

✧Design 1

The following design has two square shaped bigger slots of arm 4.6935 mm and the length and width of the rectangular narrow slots are 0.5 mm and 0.7mm respectively, thus the total area becomes 44.4078 mm^2 and inner element spacing is 10.43mm. The T-line is standard 50Ω microstrip line. The design is made on the substrate of 31 mils thick whose dielectric constant is 2.45.

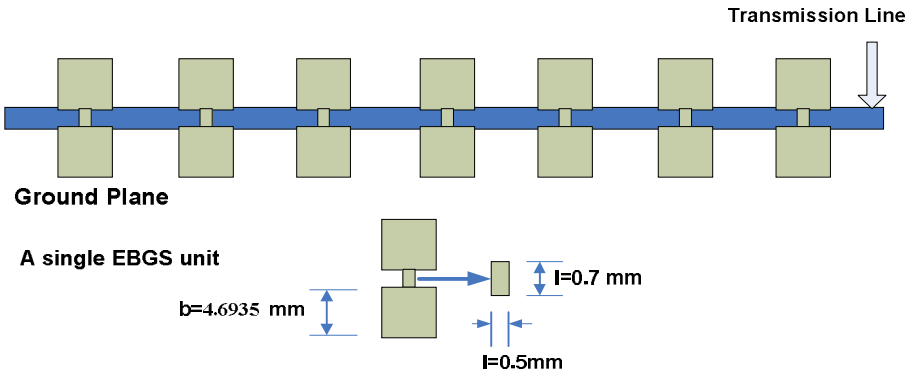

Figure 5.25: **Typical design of square patterned dumbbell shaped EBGS with two square shaped bigger slots (Arm = 4.6935 mm) and narrow slots of 0.5 mm* 0.7 mm (length*width).**

✧Design 2

The following design also has two square shaped bigger slots of arm 4.6935 mm but in this design the length and width of the rectangular narrow slots are 0.5 mm and 0.2 mm respectively. The total area thus becomes 44.1578 mm^2. The inner element spacing is 10.43mm and the T-line is standard 50Ω microstrip line. The design is made on the substrate of 31 mils thick whose dielectric constant is 2.45.

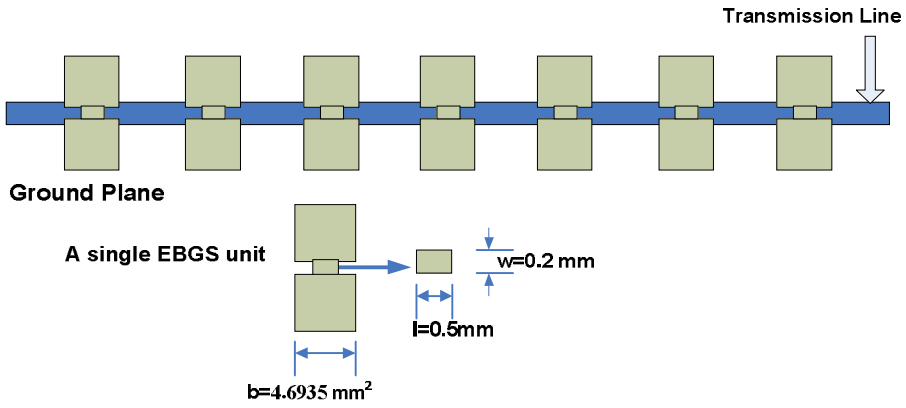

Figure 5.26: **Typical design of square patterned dumbbell shaped EBGS with two square shaped bigger slots (Arm = 4.6935 mm) and narrow slots of 0.5 mm* 0.2 mm (length*width).**

✧Design 3

In this design, the two circular shaped bigger slots has arm of 4.6935 mm. Its narrow slot is square shape having sides of 1 mm. In this case, the total area is 45.0578 mm^2 and inner element spacing is 10.43mm. The T-line is standard 50Ω microstrip line. The design is made on the substrate of 31 mils thick whose dielectric constant is 2.45.

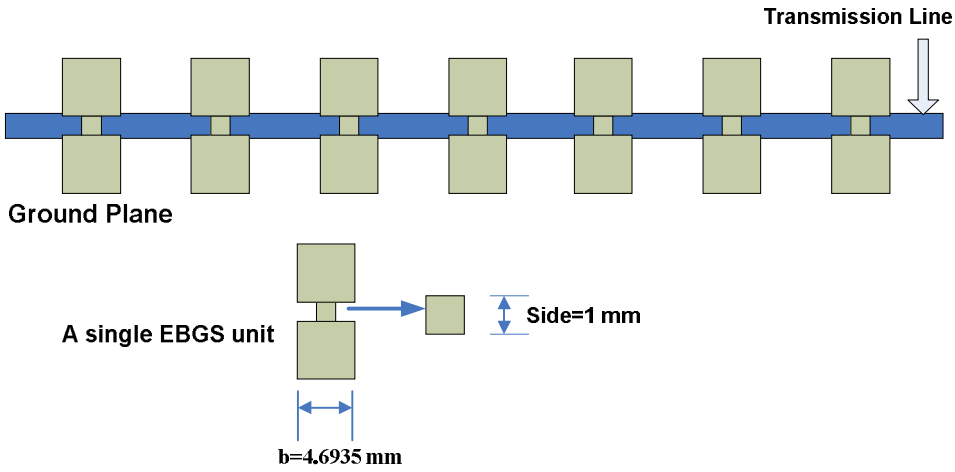

Figure 5.27: **Typical design of square patterned dumbbell shaped EBGS with two square shaped bigger slots (Arm = 4.6935 mm) and narrow slots of 1 mm* 1 mm (length*width).**

5.4.4 Square dumbbell shape results:

The results of the designs made in section 5.4.3 are presented below:

✧Design 1

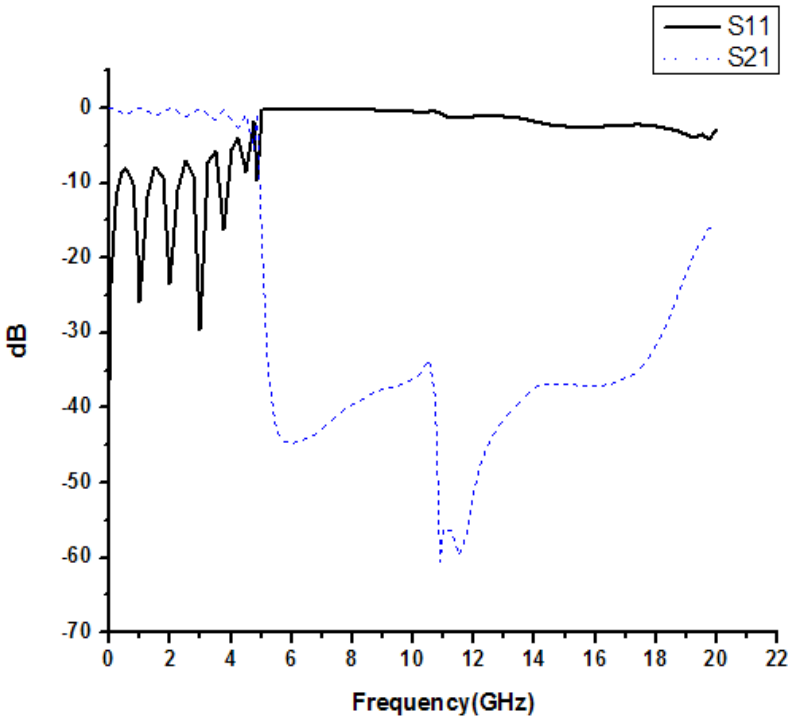

Figure 5.28: **S-parameter performance of square pattern dumbbell shaped EBGS with narrow slot's dimension of 0.5 mm*0.7 mm(length* width).**

From the above graph it is seen that the stopband starts from 5.0247 GHz and ends at 19.178 GHz, thus it gives a wide stopband of width 14.1533 GHz. 3dB cut off frequency is observed as 4.7971 GHz. Few ripples are seen on the graph and ripple height is measured as -2.5187 dB, passband width of 3.8957 GHz is observed at 10 dB return loss line. Depth at 10 GHz is -36.1848 dB.

✧**Design 2**

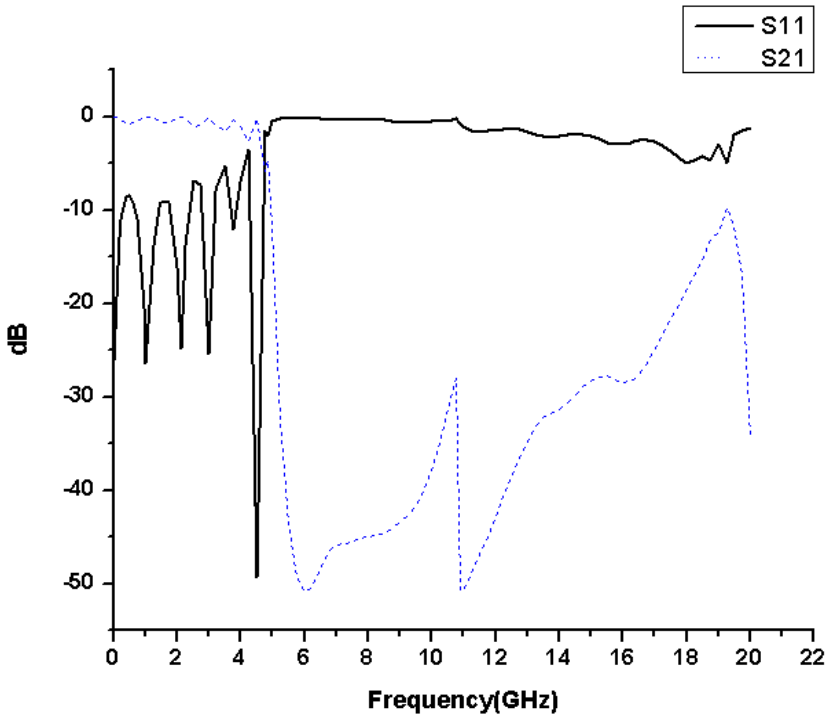

Figure 5.29: S-parameter performance of square pattern dumbbell shaped EBGS with narrow slot's dimension of 0.5 mm*0.2 mm(length* width).

Analyzing the above s-parameter performance graph it is found that, stopband starts from 5.0986 GHz and stop bandwidth is 12.676 GHz. 3dB cut off frequency is observed as 4.6244 GHz. Few ripples are seen on the graph and ripple height is measured -2.67dB, passband width of 4.7055 GHz is observed at 10 dB. At 17.77 GHz the insertion loss curve just cross a little the 20dB line and again it decreases.

✧**Design 3:**

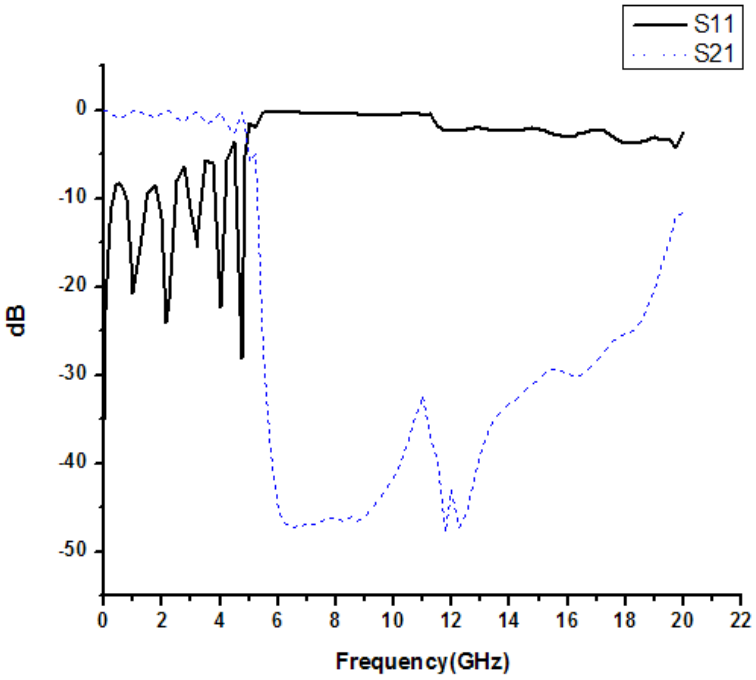

Figure 5.30: **S-parameter performance of square pattern dumbbell shaped EBGS with narrow slot's dimension of 1 mm*1 mm(length* width).**

This performance also shown similar kind performance like Design 1 and here the performance parameters are observed as follows - stopband starts from 5.4154 GHz, 3 dB cut off frequency = 4.888 GHz, passband width = 4.822340657 GHz and ripple height = -2.51 dB (almost similar to the performance of design 1.

Studying the above square pattern dumbell shape designs it can be said that the designs with same length but smaller width of narrow slots gives better low pass filtering performance.

5.5 Performance analysis of same total area but different narrow slots

Circular and square pattern dumbbell shape designs are made and are described in two different sections- 5.5.1 and 5.5.3 respectively. All the designs contain seven numbers of dumbbell shaped EBGS unit. Inner element spacing is considered 10.43 mm.

5.5.1 Circular dumbbell shape designs

In this section, all designs have same area but the dimensions of bigger circular shapes as well as the narrow slots are different. The total area of all unit EBGS is 21.3599 mm^2. In this section the dimensions of narrow slots are assumed and the radius of the bigger circular slots is calculated accordingly to make the area same. Standard 50Ω microstrip T-line and the substrate of 31 mils thick and dielectric constant of 2.45 are used for all the designs in this section.

✧Design 1

The design has total area of 21.3599 mm^2. The length and width of narrow slots are 1.5 mm and 1.2 mm respectively. Thus the area of narrow slot is 1.8 mm^2. Remaining area for bigger circular slots is 19.5599 mm^2. A single slot has area of 9.77995 mm^2. The radius of bigger slot is 1.764 mm.

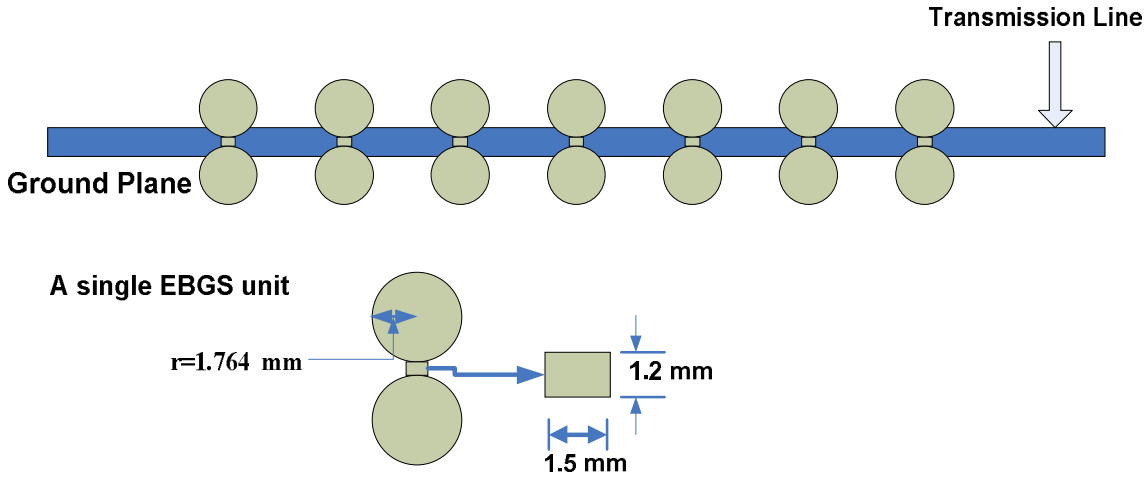

Figure 5.31: **Typical design of circular patterned dumbbell shaped EBGS with two circular shaped bigger slots (radius=1.764 mm) and narrow slots of 1.5 mm* 1.2 mm (length*width).**

✧Design 2

In this design, total area is also 21.3599 mm^2. The length and width of narrow slots are 1 mm and 0.7 mm respectively. Thus the area of narrow slot is .7 mm^2. Remaining area for bigger circular slots is 20.6599 mm^2. A single slot has area of 10.32995 mm^2. The radius of bigger slot is 1.81 mm.

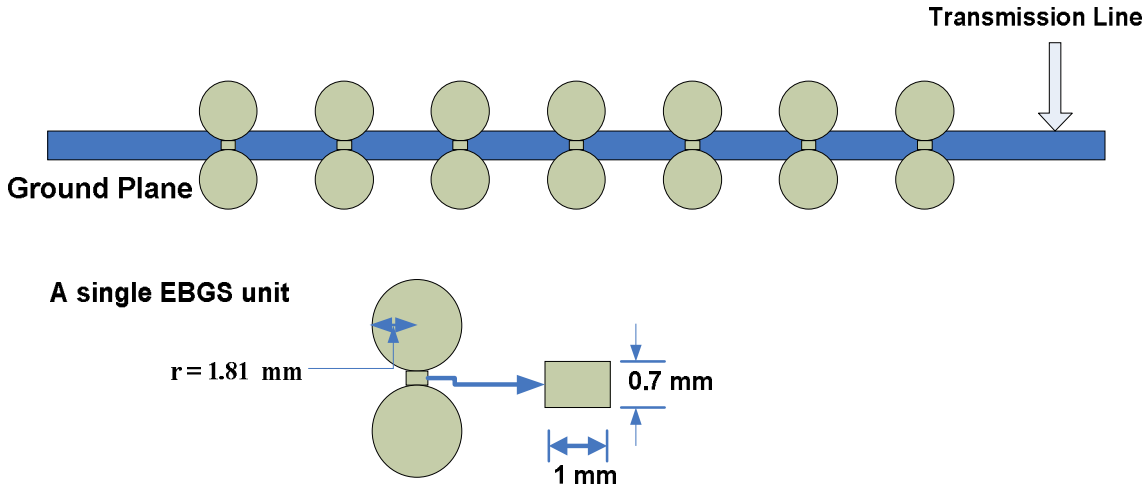

Figure 5.32: **Typical design of circular patterned dumbbell shaped EBGS with two circular shaped bigger slots (radius=1.81 mm) and narrow slots of 1 mm* .7 mm (length*width).**

✧Design 3

The length and width of narrow slots are assumed .5 mm and 0.2 mm respectively thus the area of a narrow slot is 0.1 mm^2. Considering the area 21.3599 mm^2 the radius of the bigger slots is calculated. The remaining area for bigger slots is 21.2599 mm^2. A single slot has area of 10.62995 mm^2. The radius of bigger slot is 1.84 mm.

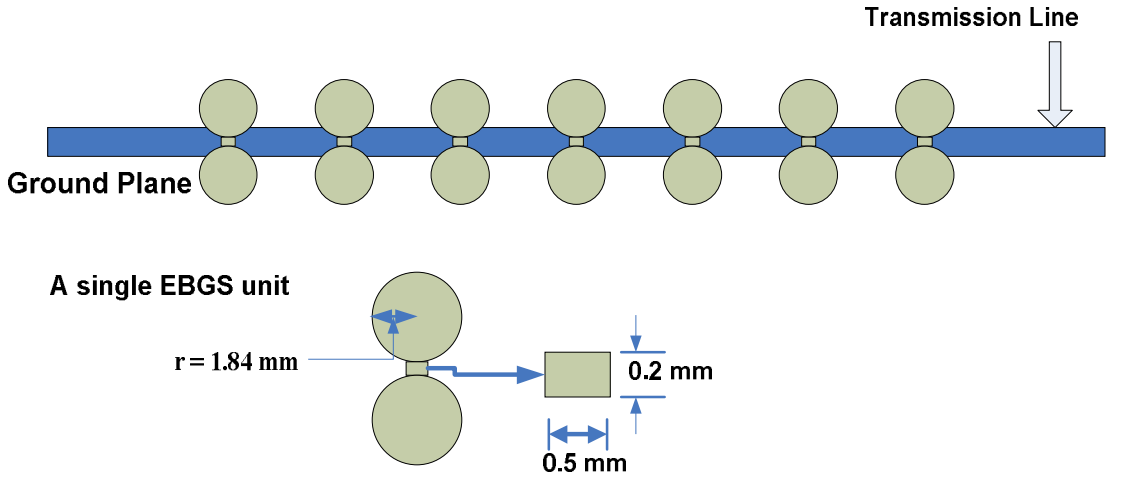

Figure 5.33: **Typical design of circular patterned dumbbell shaped EBGS with two circular shaped bigger slots (radius=2.6075 mm) and narrow slots of .5 mm* .2 mm (length*width).**

5.5.2 Circular dumbbell shape results

The results of the designs made in section 5.5.1 are presented below:

✧**Design 1**

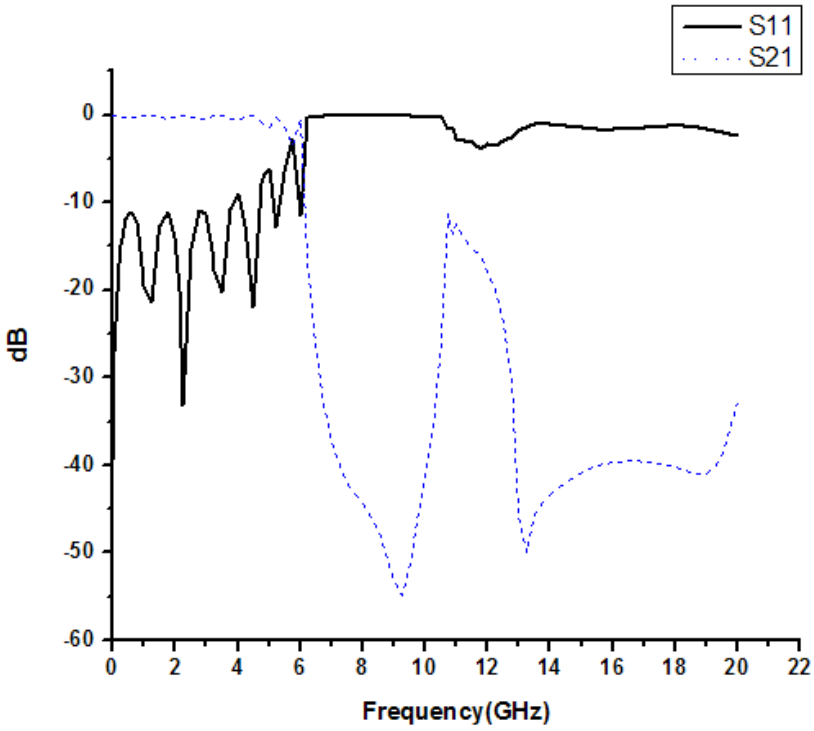

Figure 5.34: **S-parameter performance of circular pattern dumbbell shaped EBGS with narrow slot's dimension of 1.5 mm*1.2 mm(length* width).**

In the above S-parameter performance a quite small but well defined stopband performance is seen. Stopband started at 6.34 GHz and ended at 10.597 GHz; therefore, the stop band width became 4.257 GHz and passband width is 6.0314 GHz as well as 3dB cut off frequency is observed at 6.039 GHz. However, stopband ripple height is very small too in this result and it is only -1.357 dB; but some passband ripples are present above 10dB.

✧**Design 2**

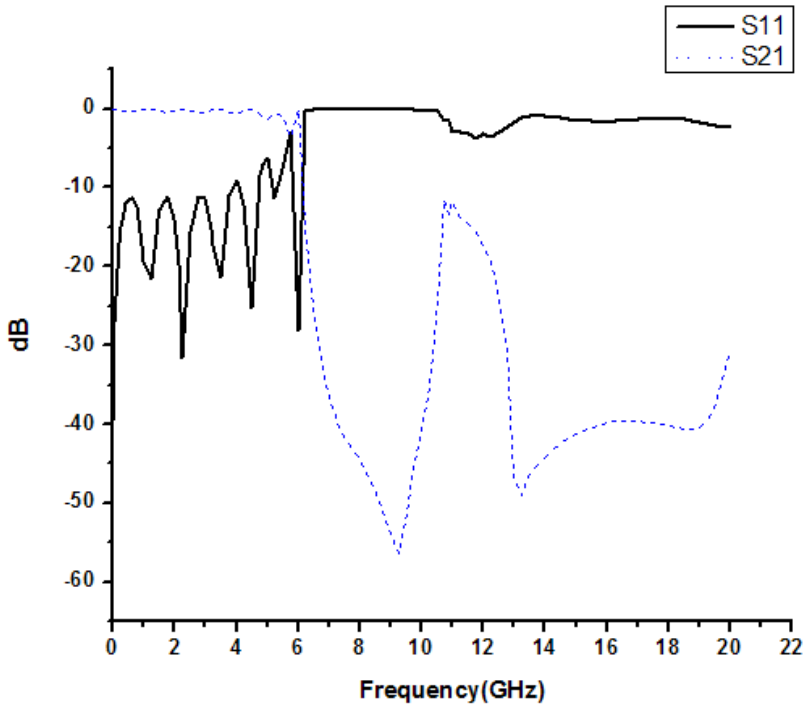

Figure 5.35: **S-parameter performance of circular pattern dumbbell shaped EBGS with narrow slot's dimension of 1 mm*0.7 mm(length* width).**

The s-parameter performance is very much similar to the previous one. In this case stopband started at 6.3738 GHz and ended at 10.5863 GHz; therefore, the stop band width became 4.2124 GHz (nearly same compared to the above performance) and passband width is 6.1629 GHz as well as 3dB cut off frequency is observed at 6.048 GHz. Therefore, smaller stopband and larger passband are found as well as cut off frequency is large and -3.1847 dB ripple height is observed.

✧**Design 3:**

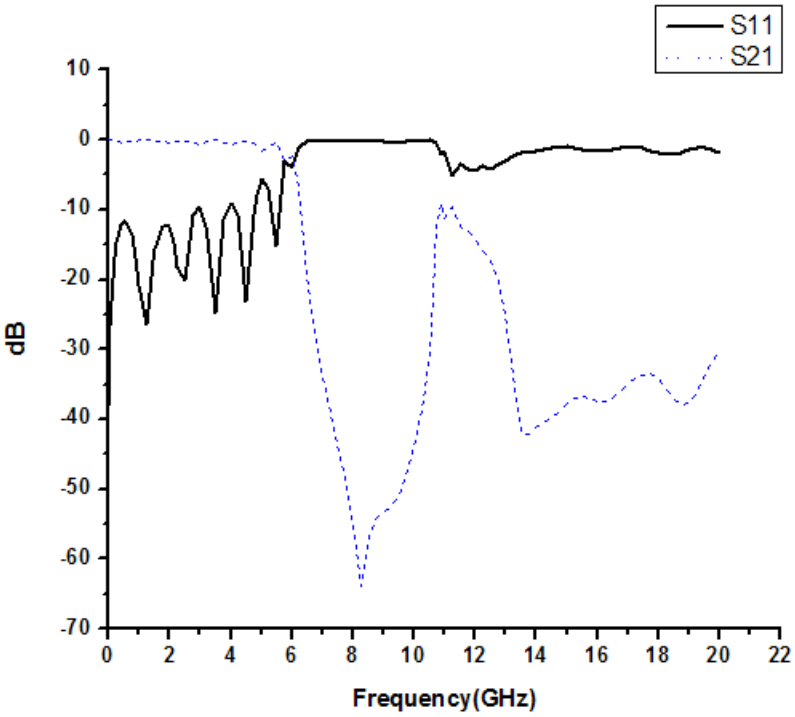

Figure 5.36: **S-parameter performance of circular pattern dumbbell shaped EBGS with narrow slot's dimension of 0.5 mm*0.2 mm(length* width).**

This is also like the above performance. However, the stopband width is : 10.6495 - 6.5178 = 4.1316 *GHz* and passband width is 5.6076 GHz . 3dB cut off frequency is 6.035 GHz. However, though passband ripples are present; stopband ripple height is small which is -1.5134 dB.

Therefore analyzing all the above s-parameter performance of this section it can be said that for equal total area, change in dimension of narrow slot cause little difference in performance.

5.5.3 Square dumbbell shape designs

In this section, all designs have same area but the dimensions of bigger circular shapes as well as the narrow slots are different. The total area of all unit EBGS is 21.3599 mm^2. In this section the dimensions of narrow slots are assumed and the arm of the bigger square slots is calculated accordingly to make the area same. Standard 50Ω microstrip T-line and the substrate of 31 mils thick and dielectric constant of 2.45 are used for all the designs in this section.

✧Design 1

The design has total area of 21.3599 mm^2. The side of the square narrow slot is 1.5 mm. Thus the area of narrow slot is 2.25 mm^2. Remaining area for bigger circular slots is 19.1099 mm^2. A single slot has area of 9.55495 mm^2. The arm of bigger slot is 3.091 mm.

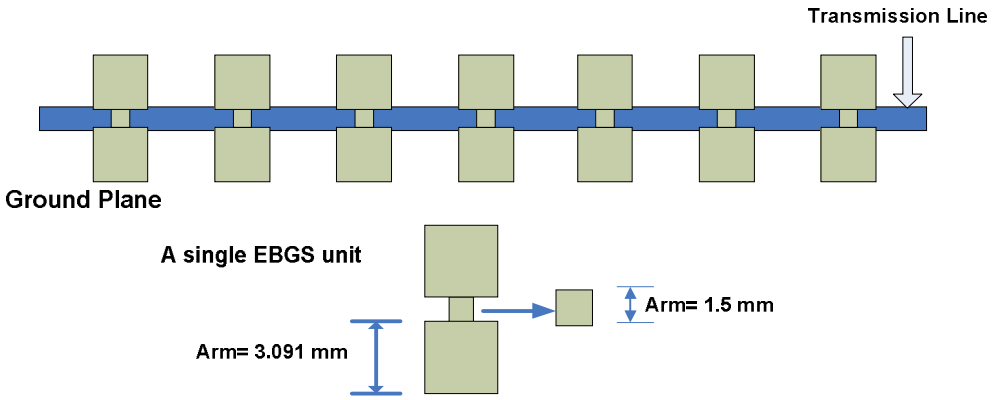

Figure 5.37: **Typical design of square patterned dumbbell shaped EBGS with two square shaped bigger slots (Arm = 3.091 mm) and narrow slots of 1.5 mm* 1.5 mm (length*width).**

✧Design 2

In this design, total area is also 21.3599 mm^2. The side of the square narrow slot is 1 mm. Thus the area of narrow slot is 1 mm^2. Remaining area for bigger circular slots is 20.3599 mm^2. A single slot has area of 10.17995 mm^2. The arm of bigger slot is 3.1906 mm.

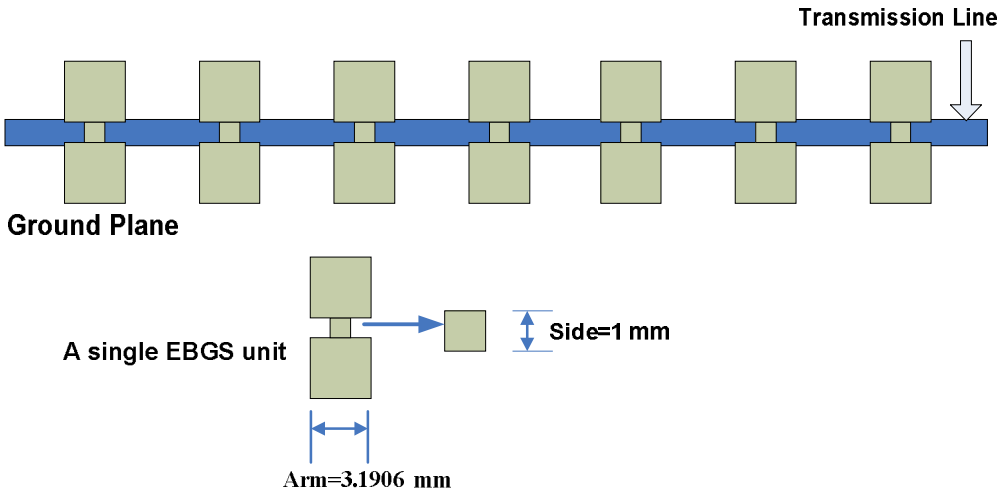

Figure 5.38: **Typical design of square patterned dumbbell shaped EBGS with two square shaped bigger slots (Arm = 3.1906 mm) and narrow slots of 1 mm* 1 mm (length*width).**

✧**Design 3**

The length and width of rectangular narrow slots are assumed 1.5 mm and 1 mm respectively thus the area of a narrow slot is 1.5 mm^2. Considering the area 21.3599 mm^2 the arm of the bigger slots is calculated. The remaining area for bigger slots is 19.8599 mm^2. A single slot has area of 9.92995 mm^2. The arm of bigger slot is 3.1512 mm.

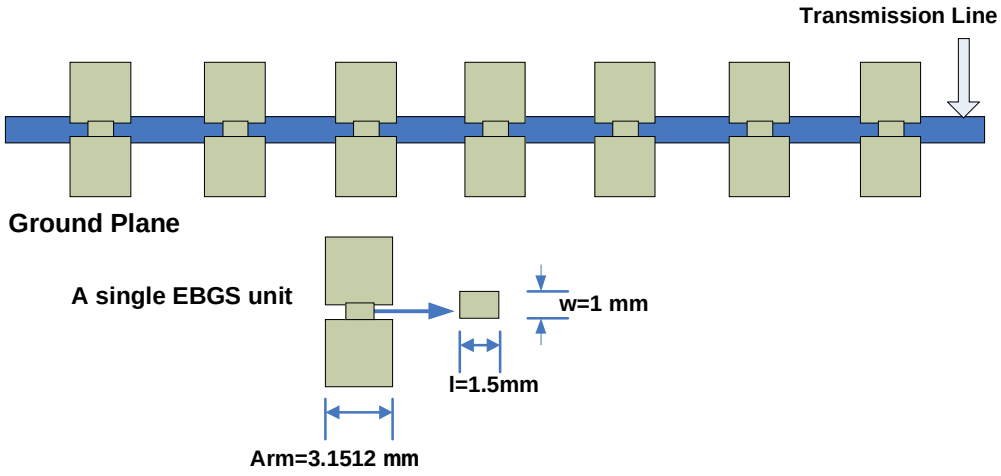

Figure 5.39: Typical design of square patterned dumbbell shaped EBGS with two square shaped bigger slots (Arm = 3.1512 mm) and narrow slots of 1.5 mm* 1 mm (length*width).

5.5.4 Square dumbbell shape results

The results of the designs made in section 5.5.3 are presented below:

✧**Design 1**

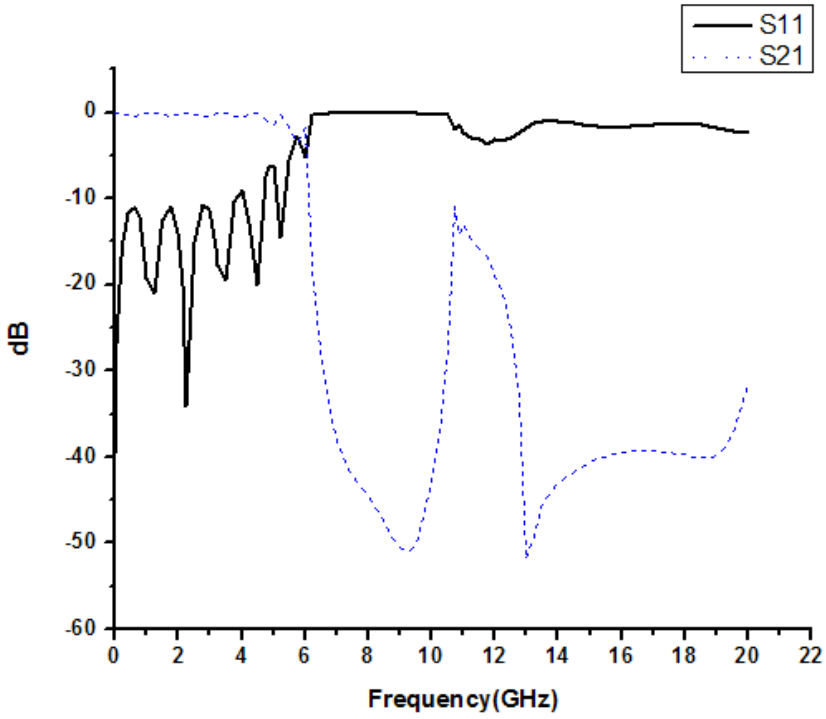

Figure 5.40: **S-parameter performance of square pattern dumbbell shaped EBGS with narrow slot's dimension of 1.5 mm*1.5 mm (length* width).**

S-parameter performance of square patterned dumbbell shaped EBGS has shown performance like stop band filter and here performance parameters are observed as follows - stopband starts from 6.3012 GHz and ends at 10.6089 GHz forming a narrow stopband of width 4.30768 GHz. 3dB cut off frequency = 6.019 GHz, passband width = 5.3763 GHz and ripple height is observed as -1.344 dB.

✧**Design 2**

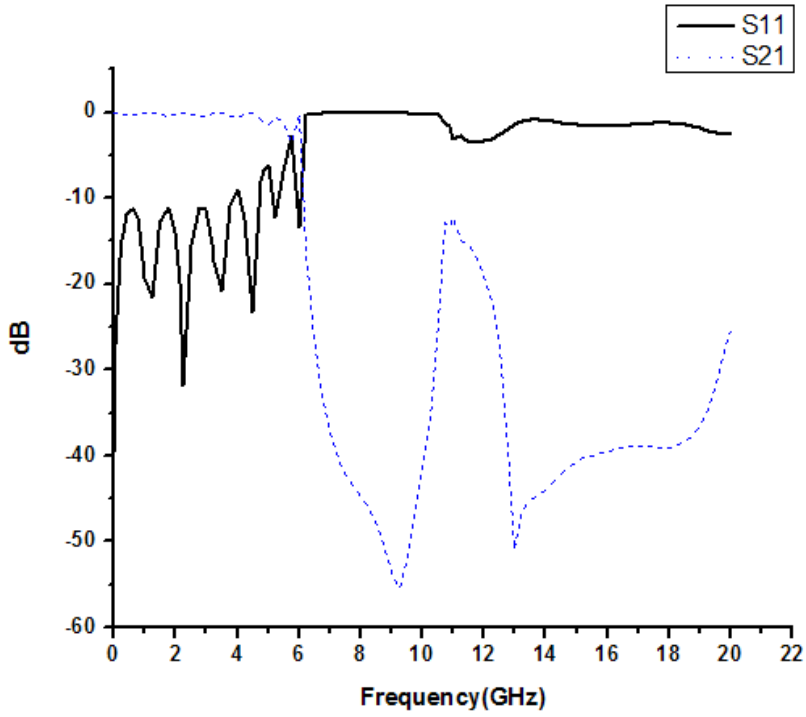

Figure 5.41: **S-parameter performance of square pattern dumbbell shaped EBGS with narrow slot's dimension of 1 mm*1 mm(length* width).**

The s-parameter performance is very much similar to the previous one. In this case stopband started at 6.3438 GHz and ended at 10.596 GHz; therefore, the stop band width became 4.252 GHz (nearly same compared to the above performance) and passband width is 6.0654 GHz as well as 3dB cut off frequency is observed at 6.0416 GHz. Therefore, smaller stopband and larger passband are found as well as cut off frequency is large and -3.426 dB ripple height is observed.

✧**Design 3:**

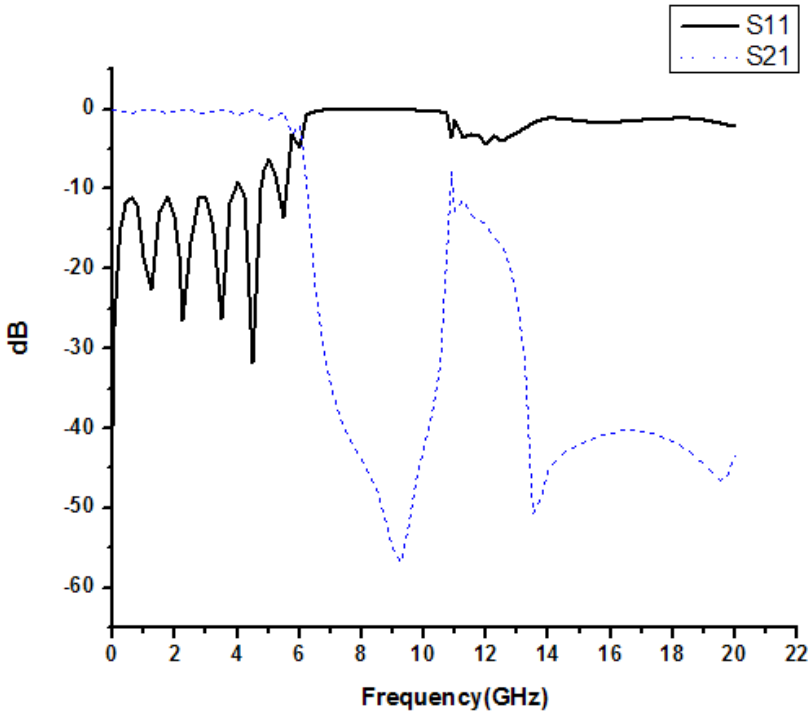

Figure 5.42: **S-parameter performance of square pattern dumbbell shaped EBGS with narrow slot's dimension of 1.5 mm*1 mm(length* width).**

This is also like the above performance. However, the stopband width is : 10.722- 6.4644= 4.25712 GHz and passband width is 5.5876 GHz. 3dB cut off frequency is 6.0347 GHz. However, though passband ripples are present; stopband ripple height is small which is -1.3502 dB.

Therefore analyzing all the above s-parameter performance of this section it can be said that for equal total area, change in dimension of narrow slot cause little difference in performance for square pattern dumbbell shape designs also.

5.6 Performance comparison for same area and same narrow slots having different shapes

In this section, dumbbell shape designs are made and simulated where the areas and dimensions of narrow slots kept constant. Three different shapes- circular, square and triangular pattern dumbbell EBGS are designed. Three different value of total area is used in the three sections- 5.6.1 Designs (a), 5.6.3 Designs (b) and 5.6.5 Designs (c). Standard 50Ω microstrip T-line and the substrate of 31 mils thick and dielectric constant of 2.45 are used for all the designs in this section.

5.6.1 Designs (a)

In this section total area is considered 45.0574 mm^2. For all shapes seven number of EBGS unit is used and inner element spacing is considered 10.43 mm.

✧Design a-1 : Square dumbbell shape

In this design, the side of square narrow slot is 1 mm. There are two same square shape bigger slot of arm 4.6935 mm. Thus the total area becomes 45.0574 mm^2.

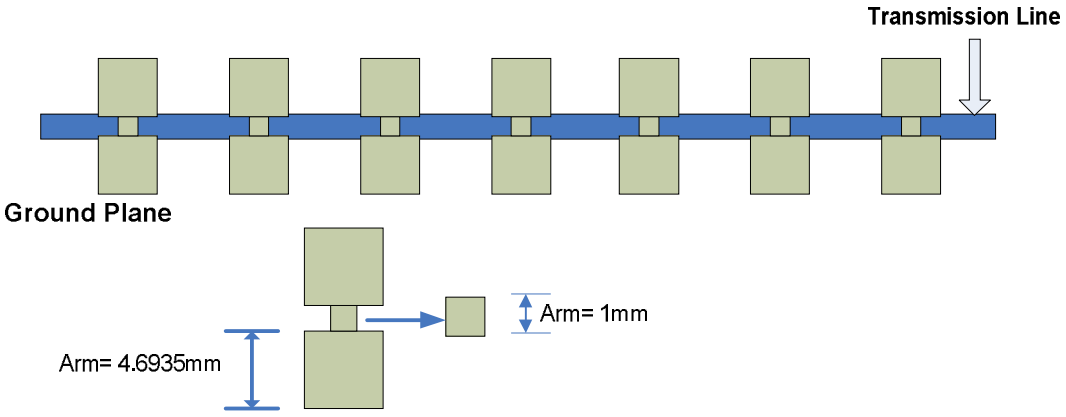

Figure 5.43: **Typical design of square patterned dumbbell shaped EBGS with two square shaped bigger slots (Arm = 4.6935 mm) and narrow slots of 1 mm* 1 mm (length*width).**

✧Design a-2 : Circular dumbbell shape

In this design, the side of square narrow slot is also 1 mm. There are two same circular shape bigger slots of 2.648 mm. Thus the total area becomes 45.0574 mm^2.

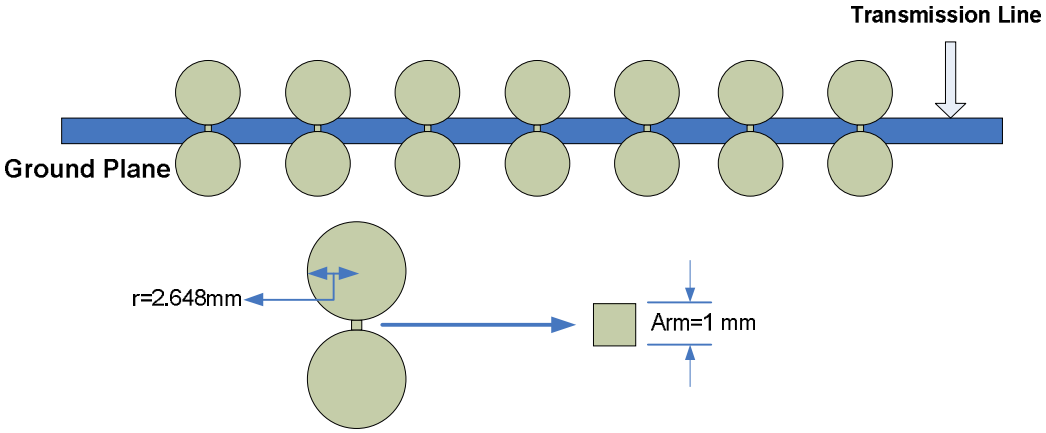

Figure 5.44: **Typical design of circular patterned dumbbell shaped EBGS with two circular shaped bigger slots (radius= 2.648 mm) and narrow slots of 1 mm* 1 mm (length*width).**

✧Design a-3: Triangular dumbbell shape

In this design, the side of square narrow slot is also 1 mm. There are two same triangular shape bigger slots of 7.13257 mm. In Zealand ie3d, triangle drawn by setting sides=3 of a circle. Therefore the radius of the circle is 4.118mm. Thus the total area becomes 45.0574 mm^2.

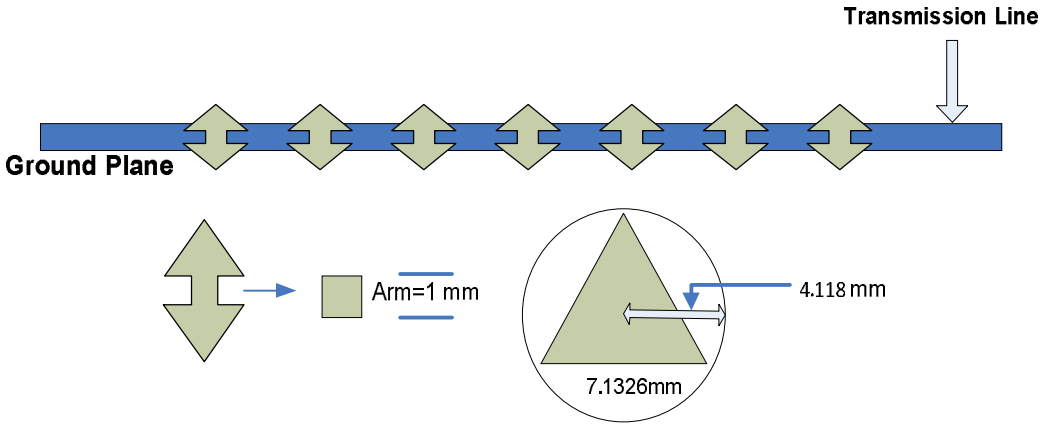

Figure 5.45: Typical design of triangular patterned dumbbell shaped EBGS with two equilateral triangular shaped bigger slots (Arm = 7.1326 mm) and narrow slots of 1 mm* 1 mm (length*width).

5.6.2 Results

✧Design a-1 : Square dumbbell shape

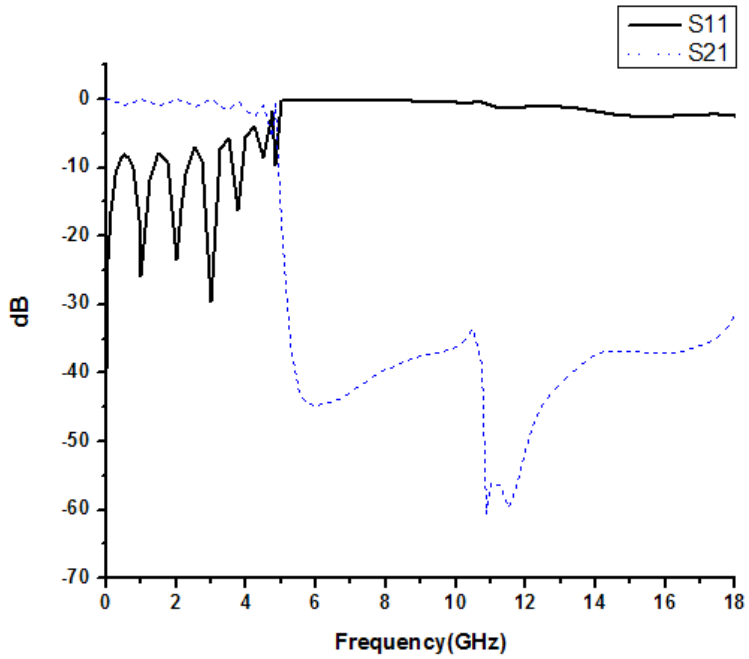

Figure 5.46: S-parameter performance of square pattern dumbbell shaped EBGS with total area of 45.0574 mm^2.

The s-parameter of the above graph shows performance of low pass filter(LPF). The insertion loss curve did not crossed 20 dB after the starting of the stop band up to our simulated range. Here the performance parameters are observed as follows - stopband starts from 5.0247 GHz, 3 dB cut off frequency = 4.7971 GHz, passband width = 3.896 GHz and ripple height = -2.8781 .

✧Design a-2 : Circular dumbbell shape

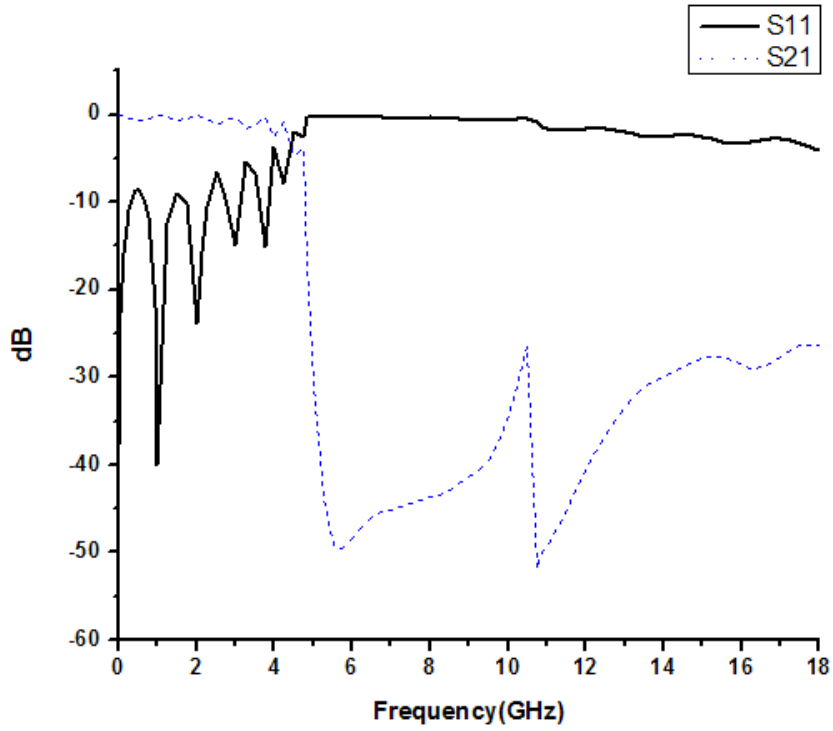

Figure 5.47: **S-parameter performance of circular pattern dumbbell shaped EBGS with total area of 45.0574 mm^2.**

This performance also shown similar kind performance like square patterned dumbbell shape EBGS. Stopband starts from 4.8728 GHz and 3dB cut off frequency is observed as 4.3882 GHz. Passband width of 3.8631 GHz is observed at 10 dB return loss line. The insertion loss curve did not crossed 20 dB after the starting of the stop band up to our simulated range. Therefore, the curve shows a good low pass performance. Though passband ripples are present; stopband ripple height is small which is - 2.5831 dB.

✧**Design a-3: Triangular dumbbell shape**

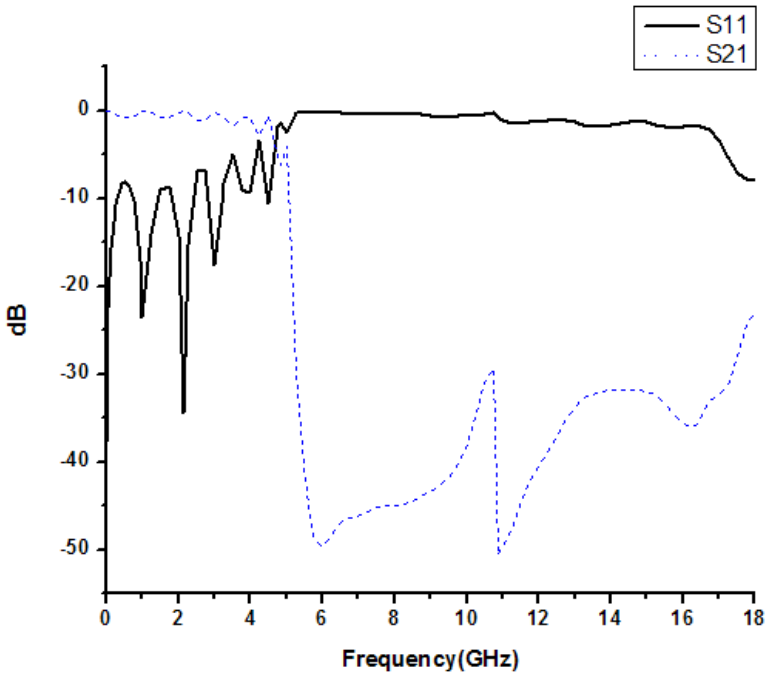

Figure 5.48: **S-parameter performance of triangular pattern dumbbell shaped EBGS with total area of 45.0574 mm^2.**

Again S-parameter performance of triangular patterned dumbbell shape EBGS has shown similar performance like square and circular patterned dumbbell shape EBGS of the same etching area and narrow slot. Here the performance parameters are observed as follows - stopband starts from 5.155 GHz, 3 dB cut off frequency = 4.628 GHz, passband width = 4.518 GHz and ripple height = -2.7582 dB (assume to be similar to the above performances).

Therefore from the study of same area and same narrow slot for square, circular and triangular pattern dumbbell shape designs, it is found that all shapes shows same performance.

5.6.3 Designs (b)

In this section total area is considered 21.3599 mm^2. For all shapes seven number of EBGS unit is used and inner element spacing is considered 10.43 mm.

✧**Design b-1 : Square dumbbell shape**

In this design, the side of square narrow slot is 1 mm. Remaining area for bigger slots is 20.3599 mm^2. A single bigger slot has area of 10.17995 mm^2 so the arm is 3.1906 mm.

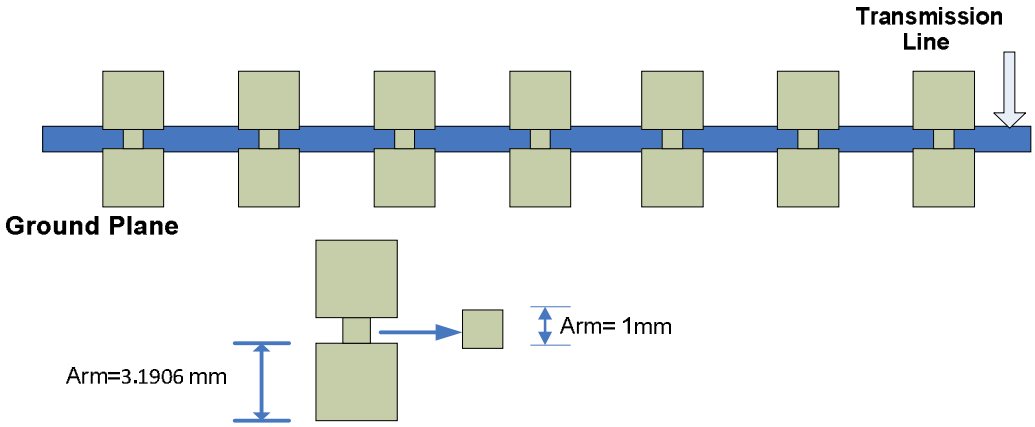

Figure 5.49: **Typical design of square patterned dumbbell shaped EBGS with two square shaped bigger slots (Arm = 3.1906 mm) and narrow slots of 1 mm* 1 mm (length*width).**

✧Design b-2 : Circular dumbbell shape

In this design, the side of square narrow slot is 1 mm. Remaining area for bigger slots is 20.3599 mm^2. A single bigger slot has area of 10.17995 mm^2 so the radius of bigger circular slot is 1.8mm.

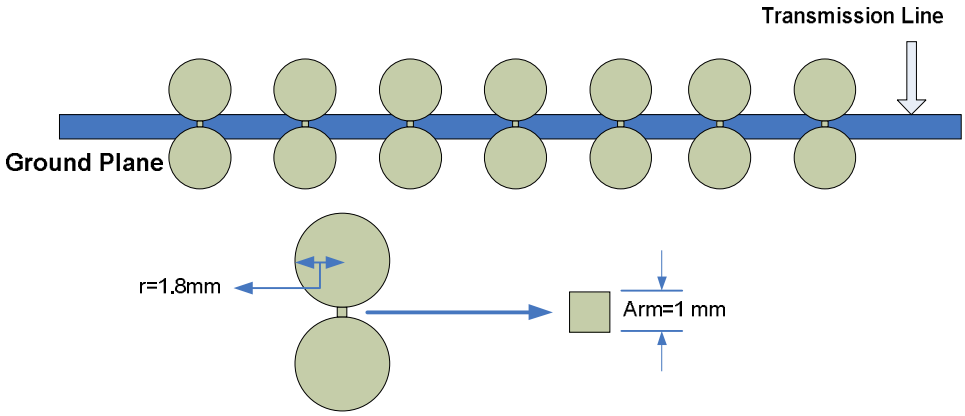

Figure 5.50: **Typical design of circular patterned dumbbell shaped EBGS with two circular shaped bigger slots (radius= 1.8 mm) and narrow slots of 1 mm* 1 mm (length*width).**

✧Design b-3: Triangular dumbbell shape

In this design, the side of square narrow slot is also 1 mm. There are two same triangular shape bigger slot of 4.8486 mm. In Zealand ie3d, triangle drawn by setting sides=3 of a circle. Therefore the radius of the circle is 2.7994 mm . Thus the total area becomes 21.3599 mm^2.

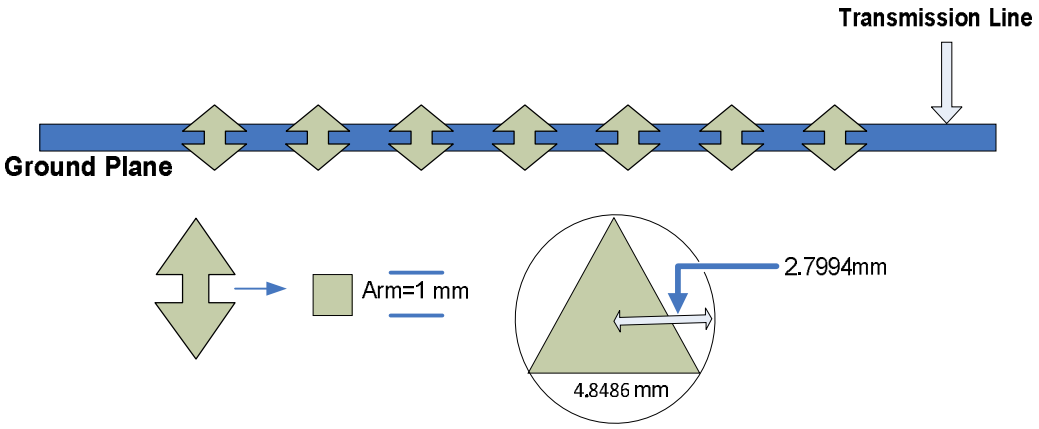

Figure 5.51: **Typical design of triangular patterned dumbbell shaped EBGS with two equilateral triangular shaped bigger slots (Arm = 4.8486 mm) and narrow slots of 1 mm* 1 mm (length*width).**

5.6.4 Results (b)

✧Design b-1 : Square dumbbell shape

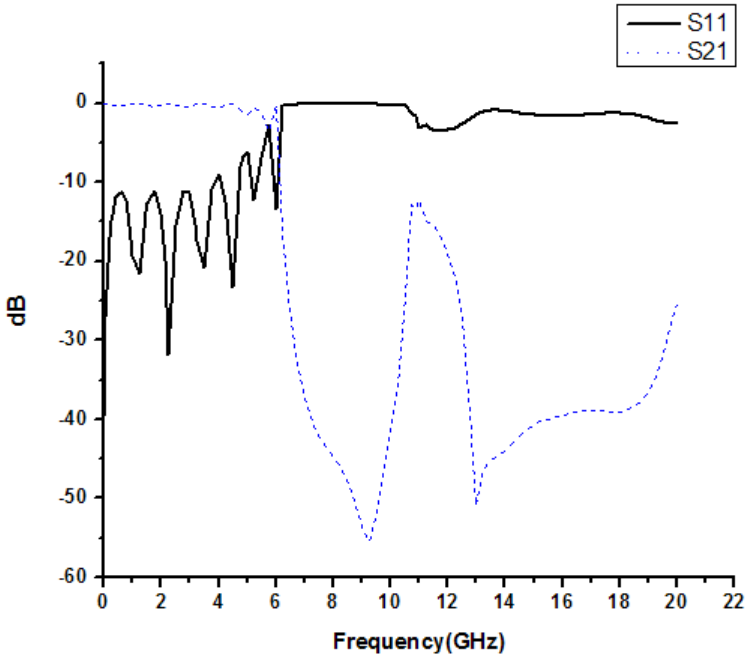

Figure 5.52: **S-parameter performance of square pattern dumbbell shaped EBGS with total area of 21.3599 mm^2.**

S-parameter performance of square patterned dumbbell shaped EBGS has shown performance like stop band filter. In this case stopband started at 6.3438 GHz and ended at 10.596 GHz; therefore, the stop band width became 4.252 GHz and passband width is 6.0654 GHz as well as 3dB cut off

frequency is observed at 6.0416 GHz. Therefore, smaller stopband and larger passband are found as well as cut off frequency is large and -3.426 dB ripple height is observed.

✧Design b-2 : Circular dumbbell shape

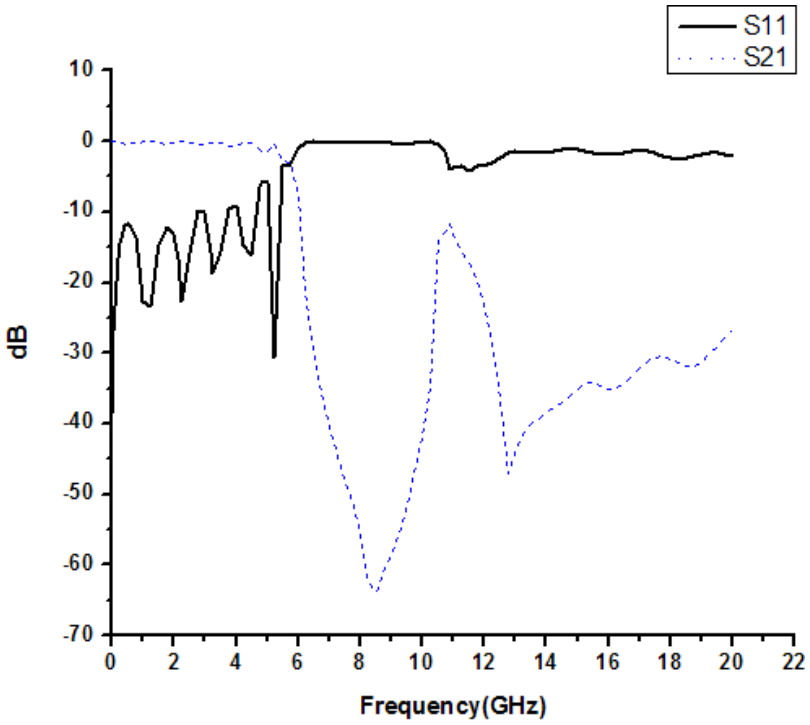

Figure 5.53: **S-parameter performance of circular pattern dumbbell shaped EBGS with total area of 21.3599 mm^2.**

The s-parameter performance is very much similar to the previous one. . In this case stopband started at 6.2277 GHz and ended at 10.4262 GHz; therefore, the stop band width became 4.198 GHz (nearly same compared to the above performance) and passband width is 5.4399 GHz as well as 3dB cut off frequency is observed at 5.7371 GHz. The maximum ripple height is observed -1.4701 dB.

✧**Design b-3: Triangular dumbbell shape**

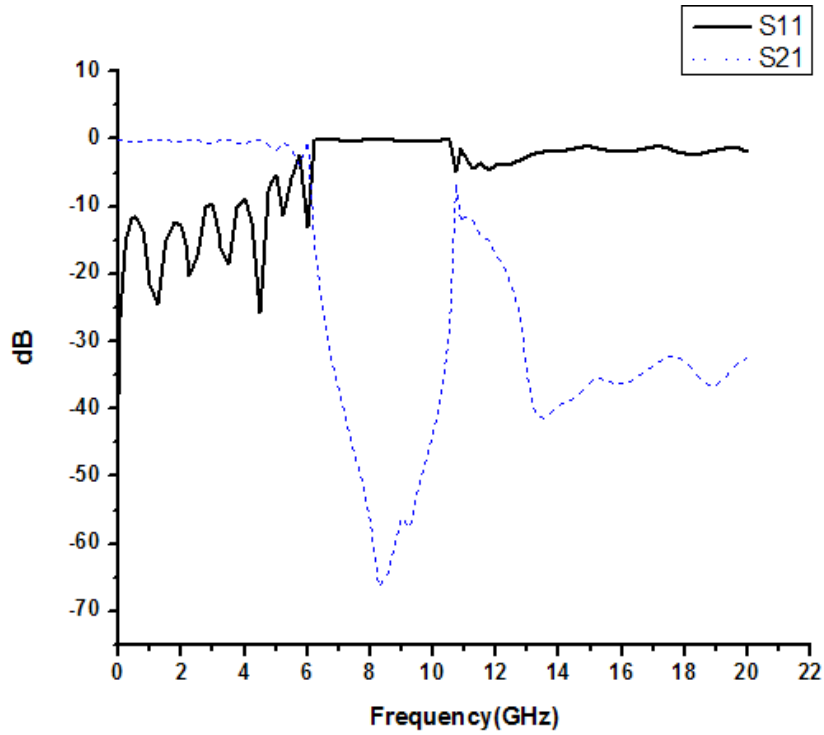

Figure 5.54: **S-parameter performance of triangular pattern dumbbell shaped EBGS with total area of 21.3599 mm^2.**

Again S-parameter performance of triangular patterned dumbbell shape EBGS has shown similar performance like square and circular patterned dumbbell shape EBGS of the same etching area and narrow slot. Here the performance parameters are observed as follows - stopband starts from 6.454 GHz and ends at 10.615 GHz forming a narrow stopband of width 4.1612 GHz (also nearly same compared to the above performances). 3 dB cut off frequency = 6.044 GHz, passband width = 5.5305 GHz and ripple height = - -3.4861 dB (assume to be similar to the above performance). From the study of same area and same narrow slot ,for the designs of this sections also the finding is the same that is all shapes shows same performance.

5.6.5 Designs (c)

In this section total area is also considered 21.3599 mm^2 but the dimension of narrow slot is different in this case. For all shapes seven number of EBGS unit is used and inner element spacing is considered 10.43 mm.

✧Design c-1 : Square dumbbell shape

In this design, the length and width of narrow slot is 1.5 mm and 1 mm respectively. Remaining area for bigger slots is 19.8599 mm^2. A single bigger slot has area of 9.92995 mm^2. so the arm is 3.1906 mm.

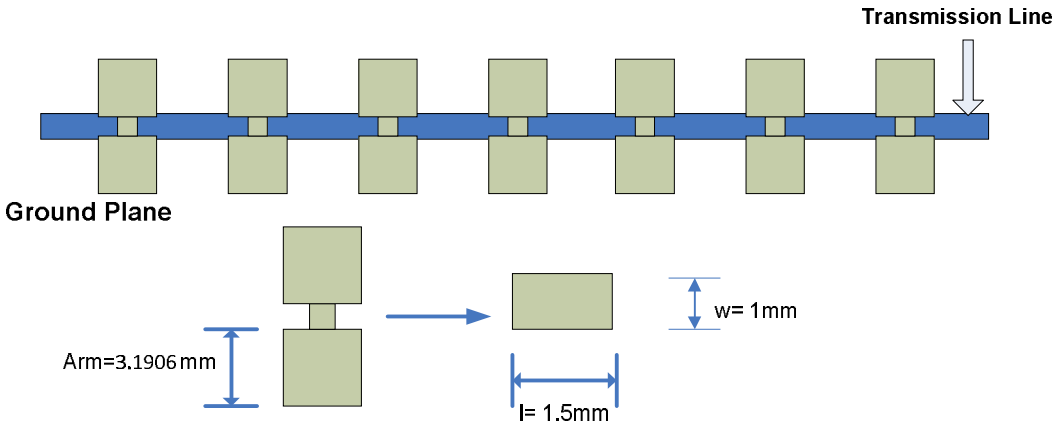

Figure 5.55: **Typical design of square patterned dumbbell shaped EBGS with two square shaped bigger slots (Arm = 3.1511 mm) and narrow slots of 1.5 mm* 1 mm (length*width).**

✧Design c-2 : Circular dumbbell shape

In this design, the length and width of narrow slot is 1.5 mm and 1 mm respectively. Remaining area for bigger slots is 19.8599 mm^2. A single bigger slot has area of 9.92995 mm^2. Thus the radius of the circular bigger slot is 1.7779 mm.

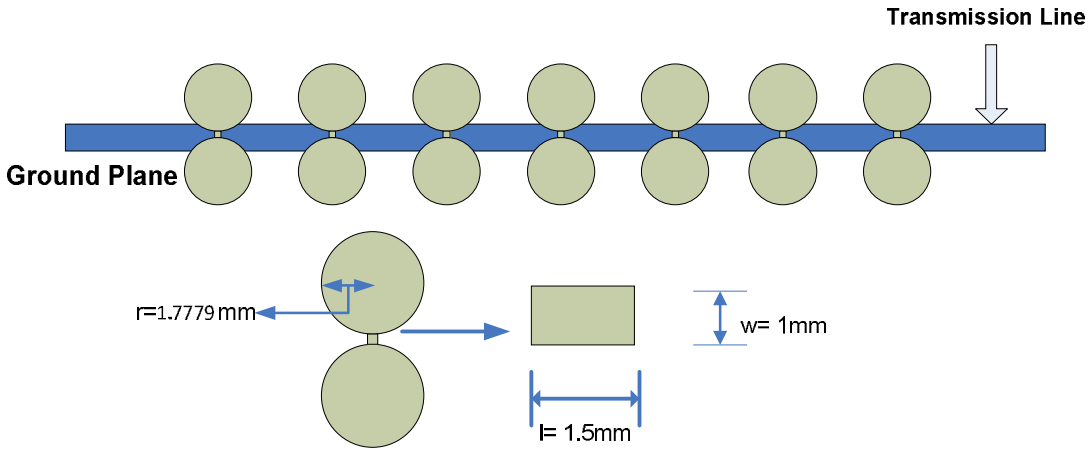

Figure 5.56: **Typical design of circular patterned dumbbell shaped EBGS with two circular shaped bigger slots (radius= 1.7779 mm) and narrow slots of 1.5 mm* 1 mm (length*width).**

✧**Design c-3: Triangular dumbbell shape**

In this design, the length and width of narrow slot is also 1.5 mm and 1 mm respectively. Remaining area for bigger slots is 19.8599 mm^2. A single bigger slot has area of 9.92995 mm^2. There are two same triangular shape bigger slot of arm 4.7887 mm. In Zealand ie3d, triangle drawn by setting sides=3 of a circle. Therefore the radius of the circle is 2.7648 mm. Thus the total area becomes 21.3599 mm^2.

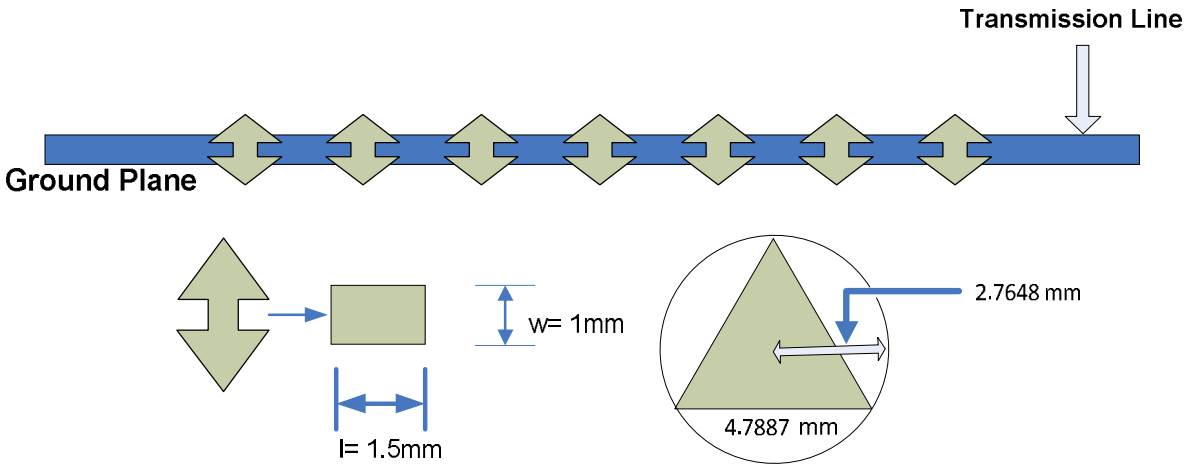

Figure 5.57: **Typical design of triangular patterned dumbbell shaped EBGS with two equilateral triangular shaped bigger slots (Arm = 4.7887 mm) and narrow slots of 1.5 mm* 1 mm (length*width).**

5.6.6 Results (c)

✧Design c-1 : Square dumbbell shape

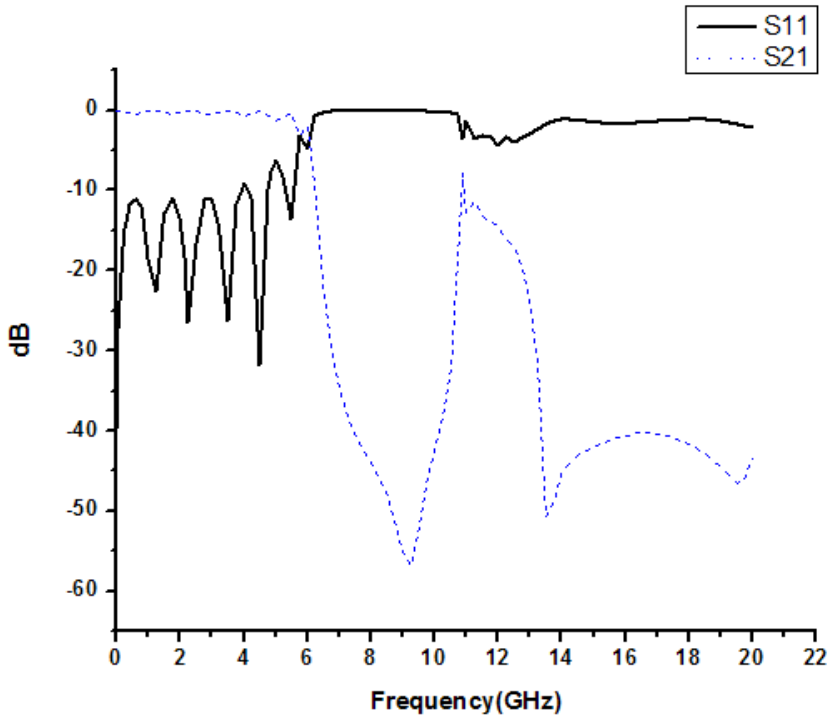

Figure 5.58: **S-parameter performance of square pattern dumbbell shaped EBGS with total area of 21.3599 mm2.**

The above S-parameter performance shows a narrow stopband performance.However, the stopband width is : 10.722- 6.4644= 4.25712 GHz and passband width is 5.5876 GHz. 3dB cut off frequency is 6.0347 GHz.Though passband ripples are present; stopband ripple height is small which is -1.3502 dB.

✧**Design c-2 : Circular dumbbell shape**

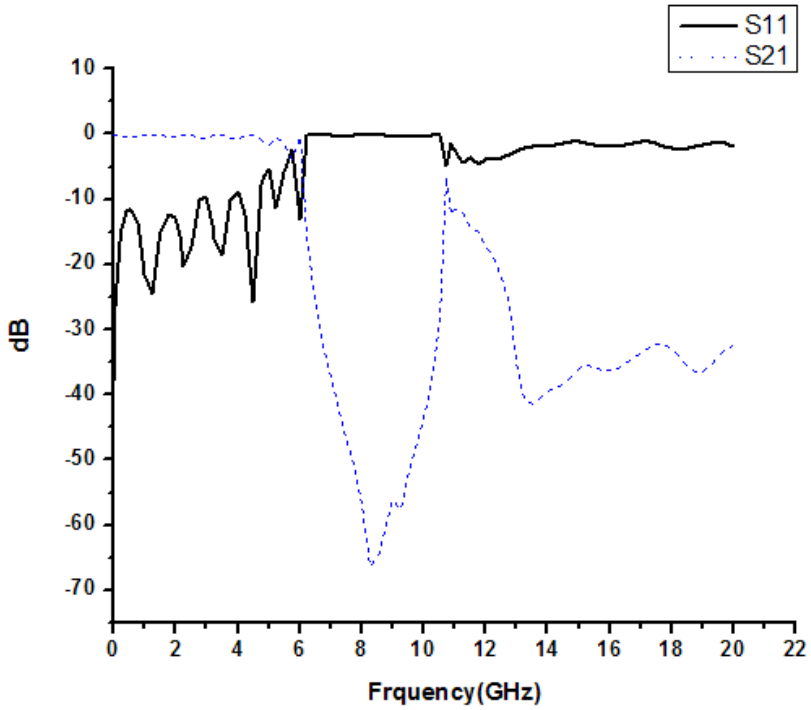

Figure 5.59: **S-parameter performance of circular pattern dumbbell shaped EBGS with total area of 21.3599 mm^2.**

The s-parameter performance is very much similar to the previous one. In this case stopband started at 6.366 GHz and ended at 10.598 GHz; therefore, the stop band width became 4.23167 GHz (nearly same compared to the above performance) and passband width is 6.0612 GHz as well as 3dB cut off frequency is observed at 6.043 GHz. Ripple height is observed as -3.6162 dB.

✧**Design c-3: Triangular dumbbell shape**

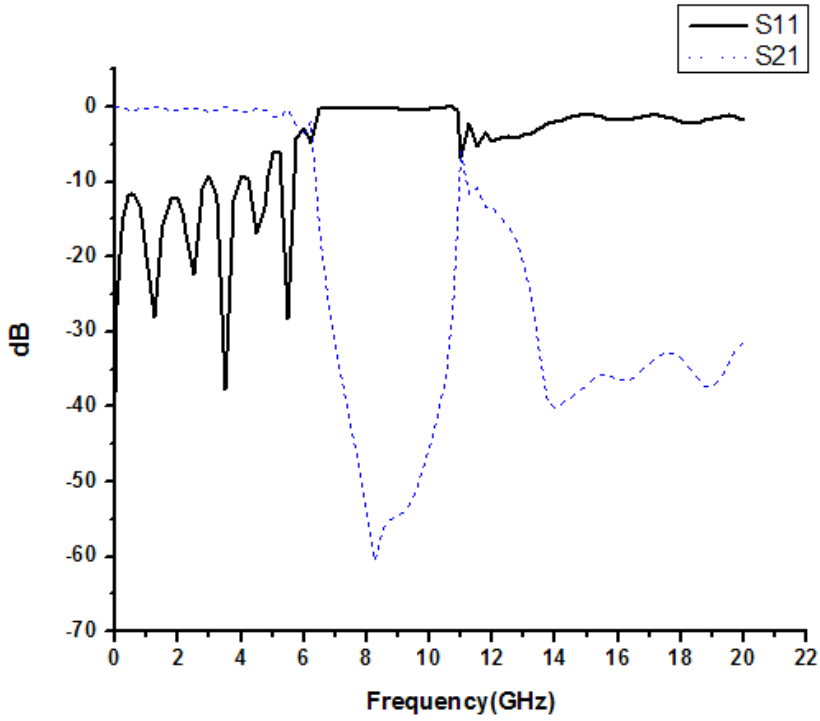

Figure 5.60: **S-parameter performance of triangular pattern dumbbell shaped EBGS with total area of 21.3599 mm^2.**

Once again S-parameter performance of triangular patterned dumbbell shape EBGS has shown similar performance like square and circular patterned dumbbell shape EBGS of the same etching area and narrow slot. Here the performance parameters are observed as follows - stopband starts from 6.603 GHz and ends at 10.8419 GHz forming a narrow stopband of width 4.239 GHz (also nearly same compared to the above performances). 3 dB cut off frequency = 5.896 GHz, passband width = 5.689 GHz and ripple height = -1.468 dB (assume to be similar to the above performance).

Also analyzing the performances of the designs of this section it can be said that same area and same dimension of narrow slots shows same performance for different shapes.

5.7 Binomially distributed non-uniform dumbbell shape designs

In chapter four it is seen that binomially distributed EBGS assisted transmission line gives relatively ripple free passband and wider stopband. Earlier in this chapter various dumbbell shape designs are studied and found that dumbbell shape designs gives better low pass filtering performance and many of them can be stated as perfect low pass filter. Almost all the above designs contain ripples. To achieve relatively ripple free passband binomially distributed dumbbell shape designs are made.

5.7.1 Circular dumbbell shape designs

Non- uniform binomially distributed circular pattern dumbbell shape designs are made in this section. The circular bigger slots are binomially distributed keeping the dimensions of narrow slots constants for all the designs made in this section. To calculate radius of circular bigger slots a method was followed which is stated in chapter four, section 4.4. Standard 50Ω microstrip T-line and the substrate of 31 mils thick and dielectric constant of 2.45 are used for all the designs in this section. The inner element spacing used is 10.43 mm.

✧Design 1

Circular pattern dumbbell shape nine EBGS elements are used in this design where total area of central element is made equal to the regular circular design having FF=0.50. Regular circular EBGS having FF=0.50 has area of 85.43966 mm^2. The length and width of rectangular narrow slots are 1 mm and .7 mm respectively which are constant for all EBGS elements. The bigger circular slots are binomially distributed where the coefficients of radius are calculated from binomial distribution. The coefficients for nine EBGS are 0.0143, 0.1143, 0.40, 0.80, 1.00, 0.80, 0.40, 0.1143 and 0.0143 respectively. The radius of bigger circular slot of central EBGS unit is calculated which is 3.6877 mm. Thus the radiuses of the bigger circular slots are 0.0472 mm, 0.4215 mm, 1.475 mm, 2.95 mm, 3.6877mm, 2.95mm, 1.475 mm 0.4215 mm and 0.0472 mm respectively. A typical geometry of design is shown bellow,

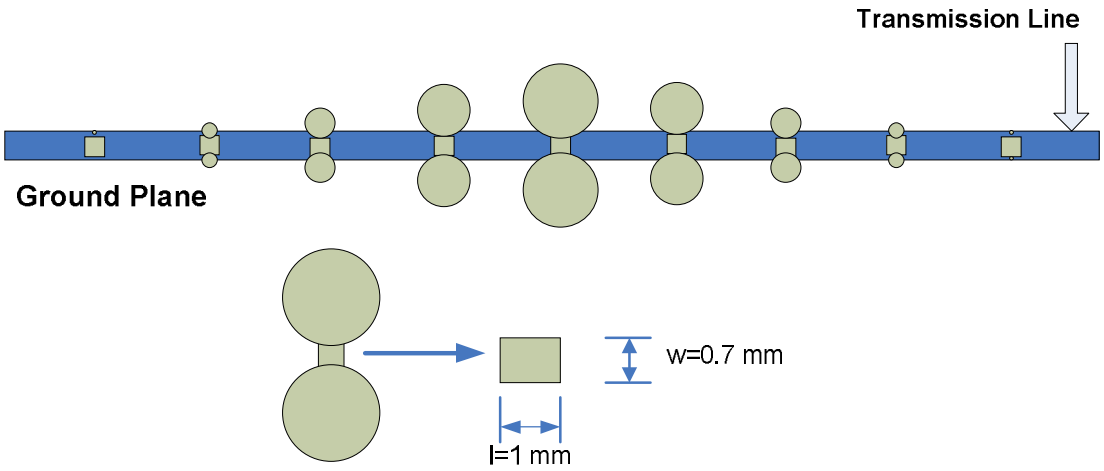

Figure 5.61: **Typical design of binomially distributed non-uniform circular patterned dumbbell shaped EBGS having nine EBGS unit with constant narrow slots of 1 mm* 0.7 mm (length*width).**

✧Design 2

In this design, circular pattern dumbbell shape ten EBGS elements are used where total area of central element is made equal to the regular circular design having FF=0.45. Regular circular EBGS having FF=0.45 has area of 69.20596 mm^2. The length and width of rectangular narrow slots are 1 mm and .7 mm respectively which are constant for all EBGS elements. The bigger circular slots are binomially distributed where the coefficients of radius are calculated from binomial distribution. The coefficients for ten EBGS are 0.00794, 0.07, 0.286, 0.67, 1.00, 1.00, 0.67, 0.286, 0.07 and 0.00794 respectively. The radius of bigger circular slot of central EBGS unit is calculated which is 3.3188 mm. Thus the radiuses of the bigger circular slots are 0.02635 mm, 0.23232 mm, 0.9492 mm, 2.2236 mm, 3.3188 mm, 3.3188 mm, 2.2236 mm, 0.9492 mm, 0.23232 mm and 0.02635 mm respectively. A typical geometry of design is shown bellow,

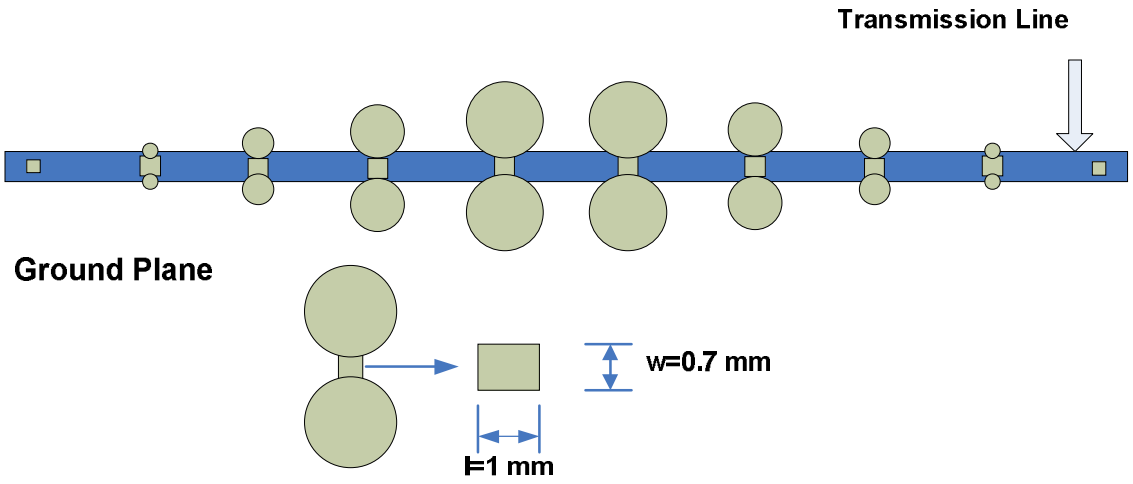

Figure 5.62: **Typical design of binomially distributed non-uniform circular patterned dumbbell shaped EBGS having ten EBGS unit with constant narrow slots of 1 mm* 0.7 mm (length*width).**

✧Design 3

Ten EBGS elements are used in this design where the total area of central element is made equal to the regular circular design having FF=0.50. Regular circular EBGS having FF=0.50 has area of 85.4397 mm^2. The length and width of rectangular narrow slots are 1 mm and .7 mm respectively which are constant for all EBGS elements. The bigger circular slots are binomially distributed where the coefficients of radius are calculated from binomial distribution. The coefficients for ten EBGS are 0.00794, 0.07, 0.286, 0.67, 1.00, 1.00, 0.67, 0.286, 0.07 and 0.00794 respectively. The radius of bigger circular slot of central EBGS unit is calculated which is 3.6876 mm. Thus the radiuses of the bigger circular slots are 0.02928 mm, 0.2581mm, 1.0546 mm, 2.4707 mm, 3.6876 mm, 3.6876 mm, 2.4707 mm, 1.0546 mm, 0.2581 mm and 0.02928 mm respectively. A typical geometry of design is shown bellow,

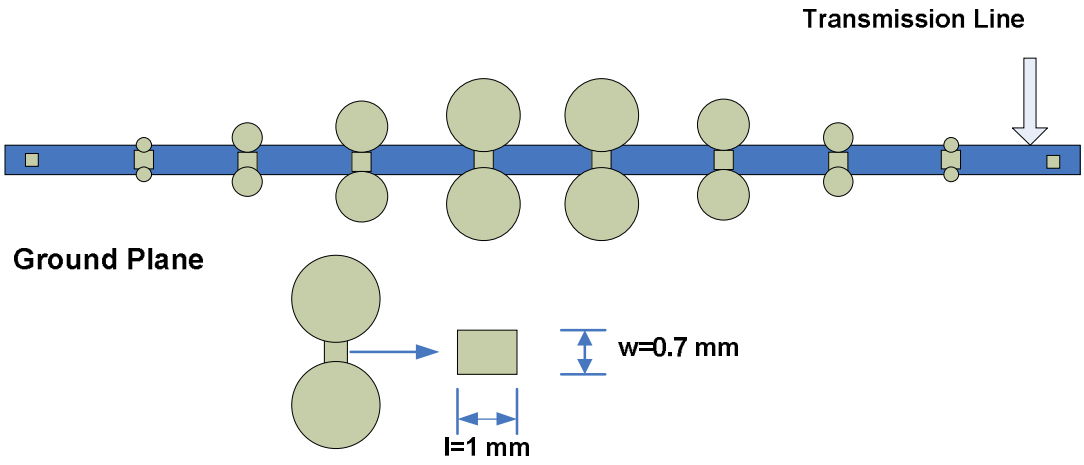

Figure 5.63: **Typical design of binomially distributed non-uniform circular patterned dumbbell shaped EBGS having ten EBGS unit with constant narrow slots of 1 mm* 0.7 mm (length*width).**

5.7.2 Circular dumbbell shape results:

S-parameter performance of the designs made in section 5.7.1 are shown and analyzed in this section.

✧Design 1

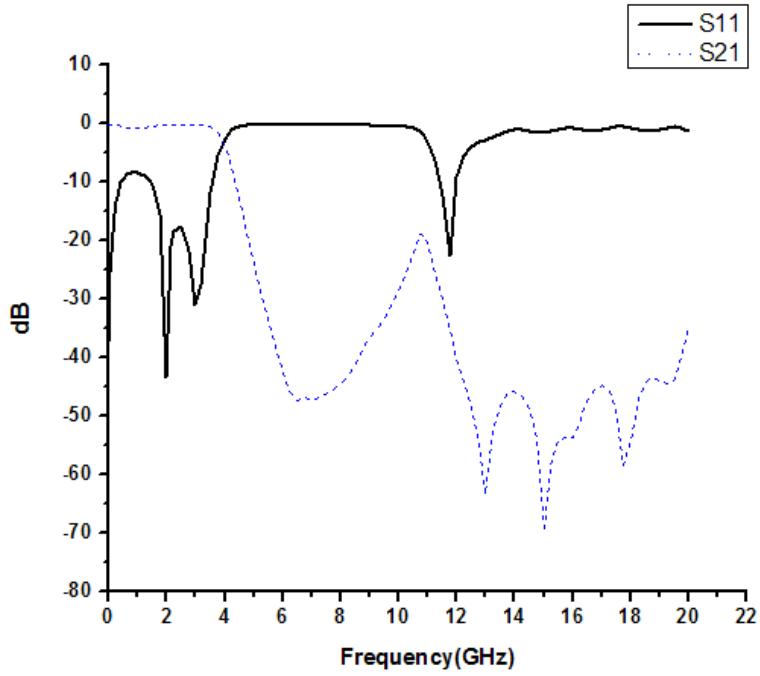

Figure 5.64: **S-parameter performance of binomially distributed circular pattern dumbbell shaped EBGS having nine EGBS unit containing constant narrow slots of dimensions 1mm * .7 mm (length * width) where the total area of the central EBGS is 85.43966 mm2.**

The s-parameter of the above graph shows performance of likely to be a low pass filter(LPF). At around 10.8 GHz the insertion loss curve just cross a little the 20 dB line and again it decreases.. Here the performance parameters are observed as follows - stopband starts from 4.81 GHz, 3 dB cut off frequency = 3.911 GHz, passband width = 3.573 GHz. There is only one ripple with negligible height is present in the passband and which is measured as -0.7733 dB.

✧Design 2

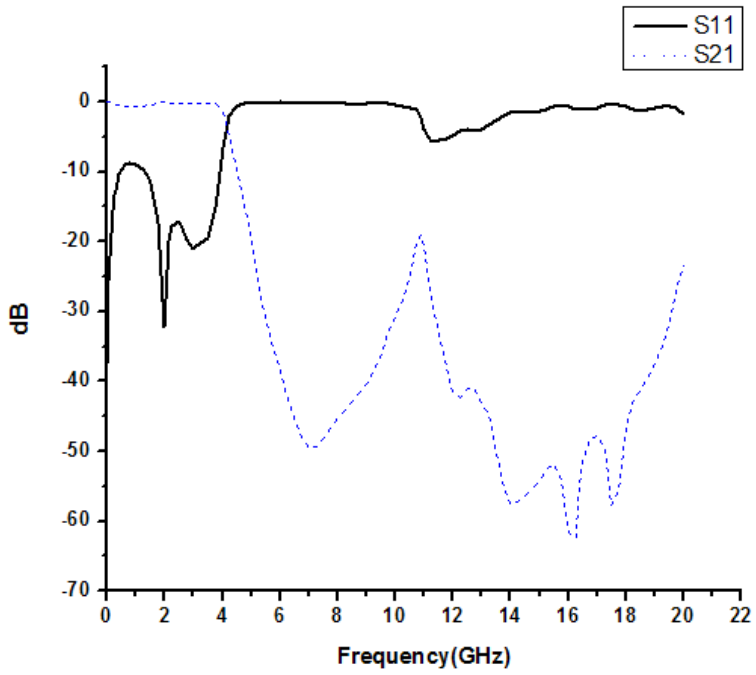

Figure 5.65: **S-parameter performance of binomially distributed circular pattern dumbbell shaped EBGS having ten EGBS unit containing constant narrow slots of dimensions 1mm * .7 mm (length * width) where the total area of the central EBGS is 69.20596 mm^2.**

In this figure, the performance looks like similar to the above performance. In this case also the number of ripple in the passband is only one; but in the stopband region Return Loss curve shows better performance. However, performance data are as follows - stopband starts from 4.994 GHz, 3dB cut off frequency = 4.1204 GHz, passband width = 3.898 GHz. The height of the ripple is negligible which is -0.5419 dB. Though insertion loss curve touches the 20dB line, it can be assumed as LPF.

✧**Design 3**

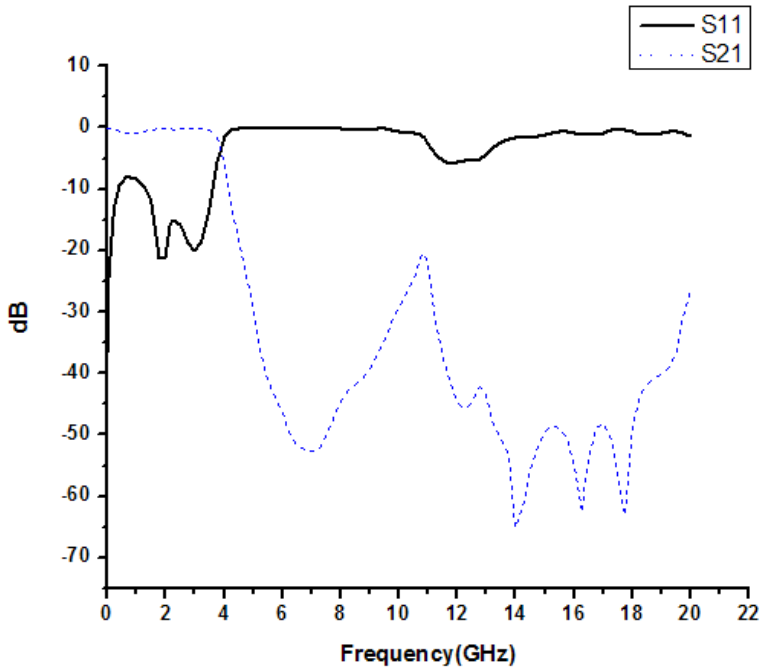

Figure 5.66: **S-parameter performance of binomially distributed circular pattern dumbbell shaped EBGS having ten EGBS unit containing constant narrow slots of dimensions 1mm * .7 mm (length * width) where the total area of the central EBGS is 85.43966 mm^2.**

S-parameter performance of the above graph has shown performance like low pass filter (LPF) and here performance parameters are observed as follows - stopband starts from 4.5793 GHz, 3dB cut off frequency = 3.8284 GHz, passband width = 3.6033 GHz. In this case also ripple height is very small and observed as -0.8167 dB. However, at the stopband region too much ups and downs of Insertion Loss curve are present; but it remains bellow 20dB. On the other hand Return Loss curve at that region shows quite good performance – remains above -5dB all the time.

Therefore studying the performances of binomially distributed circular pattern dumbbell shape designs it is found that the designs have considerably less ripples and good low pass filtering performance.

5.7.3 Square dumbbell shape designs

In this section, non- uniform binomially distributed square pattern dumbbell shape designs are made. The square bigger slots are binomially distributed keeping the dimensions of narrow slots constants for all the designs made in this section. To calculate arm of square bigger slots the arm of central square bigger slot is multiplied with the coefficient of binomial distribution which is

stated in chapter four, section 4.4. Standard 50Ω microstrip T-line and the substrate of 31 mils thick and dielectric constant of 2.45 are used for all the designs in this section. The inner element spacing used is 10.43 mm.

✧Design 1

Square pattern dumbbell shape nine EBGS elements are used in this design where total area of central element is made equal to the regular circular design having FF=0.50. Regular circular EBGS having FF=0.50 has area of 85.43966 mm^2. The side of square narrow slot is 1mm which is constant for all EBGS elements. The bigger square slots are binomially distributed where the coefficients of arm of squares are calculated from binomial distribution. The coefficients for nine EBGS are 0.0143, 0.1143, 0.40, 0.80, 1.00, 0.80, 0.40, 0.1143 and 0.0143 respectively. The arm of bigger circular slot of central EBGS unit is calculated which is 6.4976 mm. Thus the arm of the bigger circular slots are 0.08316 mm, 0.7426 mm, 2.599 mm, 5.198 mm, 6.4976, 5.198 mm, 2.599 mm 0.7426 mm and 0.08316 mm respectively. A typical geometry of design is shown bellow,

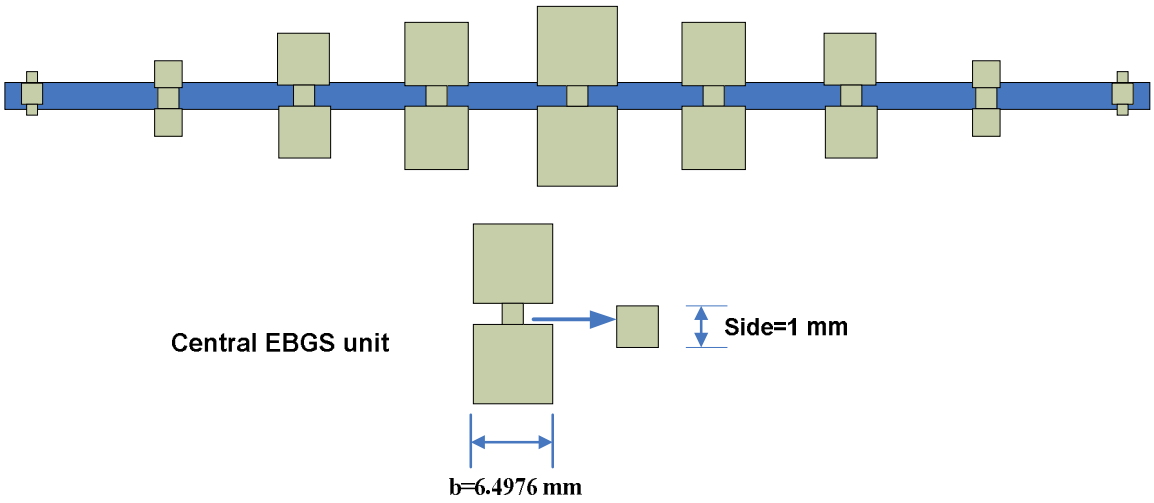

Figure 5.67: **Typical design of binomially distributed non-uniform square patterned dumbbell shaped EBGS having nine EBGS unit with Constant Square narrow slots of side 1 mm.**

✧Design 2

In this design, square pattern dumbbell shape ten EBGS elements are used where total area of central element is made equal to the regular circular design having FF=0.45. Regular circular EBGS having FF=0.45 has area of 69.20596 mm2. The side of square narrow slot is 1mm which is

constant for all EBGS elements. The bigger square slots are binomially distributed where the coefficients of arm of squares are calculated from binomial distribution. The coefficients for ten EBGS are 0.00794, 0.07, 0.286, 0.67, 1.00, 1.00, 0.67, 0.286, 0.07 and 0.00794 respectively. The arm of bigger square slot of central EBGS unit is calculated which is 5.8398 mm. Thus the arm of the bigger square slots are 0.0463 mm, 0.4087 mm, 1.6702 mm, 3.9126 mm, 5.8398 mm, 5.8398 mm, 3.9126 mm, 1.6702 mm, 0.4087 mm and 0.0463 mm respectively. A typical geometry of design is shown bellow,

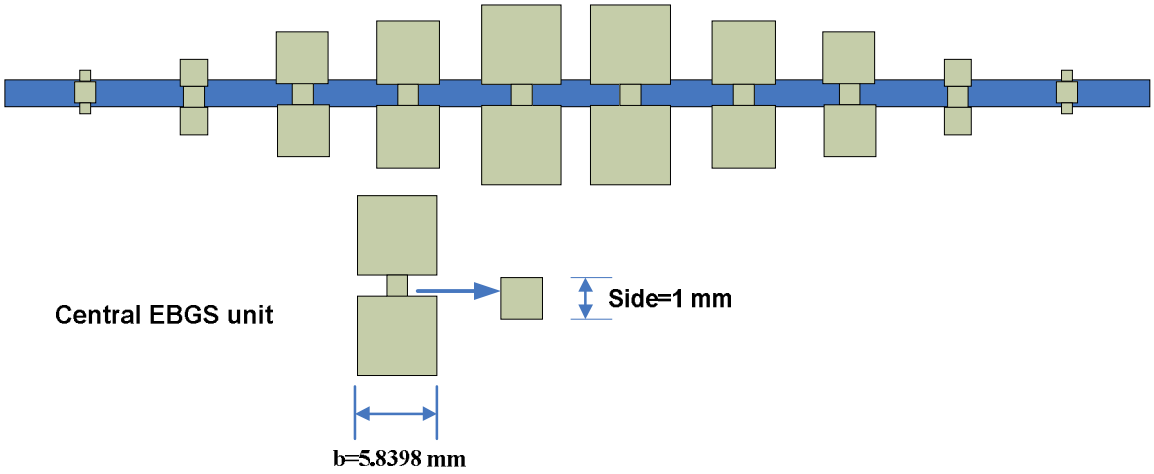

Figure 5.68: Typical design of binomially distributed non-uniform square patterned dumbbell shaped EBGS having ten EBGS unit with Constant Square narrow slots of side 1 mm.

✧Design 3

Ten EBGS elements are used in this design where the total area of central element is made equal to the regular circular design having FF=0.50. Regular circular EBGS having FF=0.50 has area of 85.4397 mm^2. The side of square narrow slot is 1mm which is constant for all EBGS elements. The bigger square slots are binomially distributed where the coefficients of arm of squares are calculated from binomial distribution. The coefficients for ten EBGS are 0.00794, 0.07, 0.286, 0.67, 1.00, 1.00, 0.67, 0.286, 0.07 and 0.00794 respectively. The arm of bigger square slot of central EBGS unit is calculated which is 6.4976 mm. Thus the arm of the bigger square slots are 0.05159 mm, 0.4548 mm, 1.8583 mm, 4.35339 mm, 6.4976 mm, 6.4976mm, 4.35339 mm, 1.8583 mm, 0.4548 mm and 0.05159 mm respectively. A typical geometry of design is shown bellow,

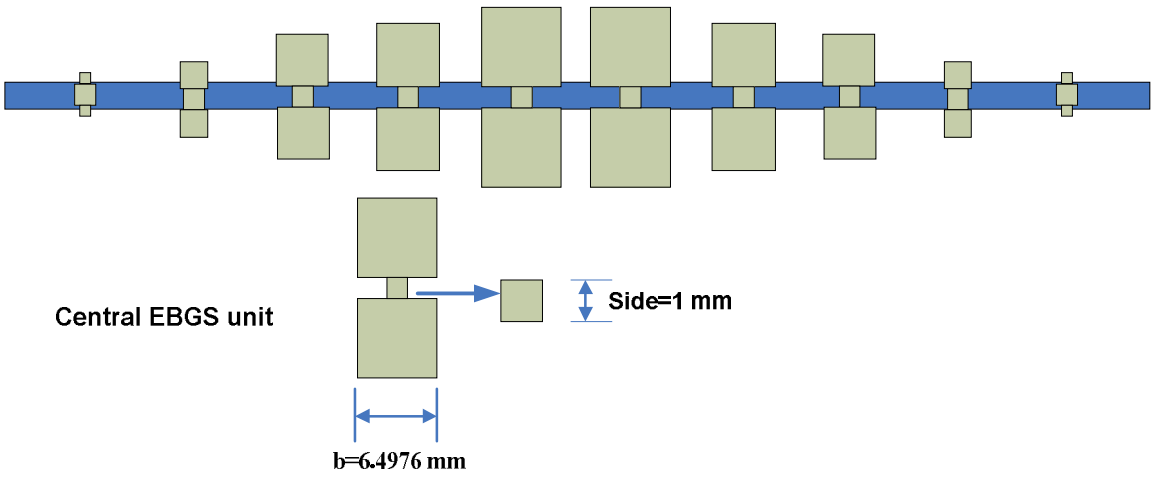

Figure 5.69: **Typical design of binomially distributed non-uniform square patterned dumbbell shaped EBGS having ten EBGS unit with constant square narrow slots of side 1 mm.**

5.7.4 Square dumbbell shape results:

S-parameter performance of the designs made in section 5.7.3 are shown and analyzed in this section.

✧Design 1

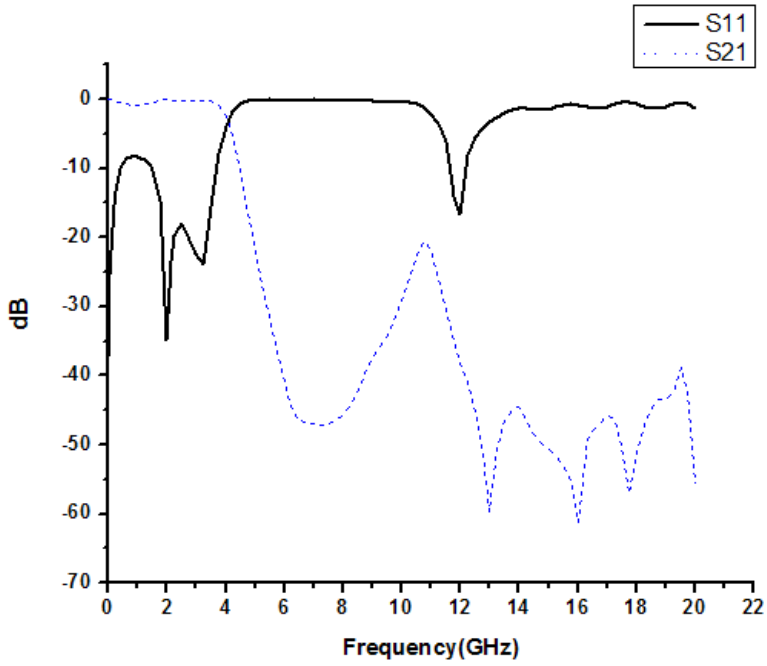

Figure 5.70: **S-parameter performance of binomially distributed square pattern dumbbell shaped EBGS having nine EGBS unit containing constant narrow slots of dimensions 1mm * 1 mm (length * width) where the total area of the central EBGS is 85.43966 mm^2.**

The s-parameter of the above graph shows performance of low pass filter(LPF). At around 11.5 GHz in the stopband region there is a considerable ripple of height -16.64 dB in return loss curve but the insertion loss curve remains bellow 20 dB. Here the performance parameters are observed as follows - stopband starts from 4.91 GHz, 3 dB cut off frequency = 4.046 GHz, passband width = 3.679 GHz. There is only one ripple with negligible height is present in the passband and which is measured as -0.791 dB.

✧Design 2

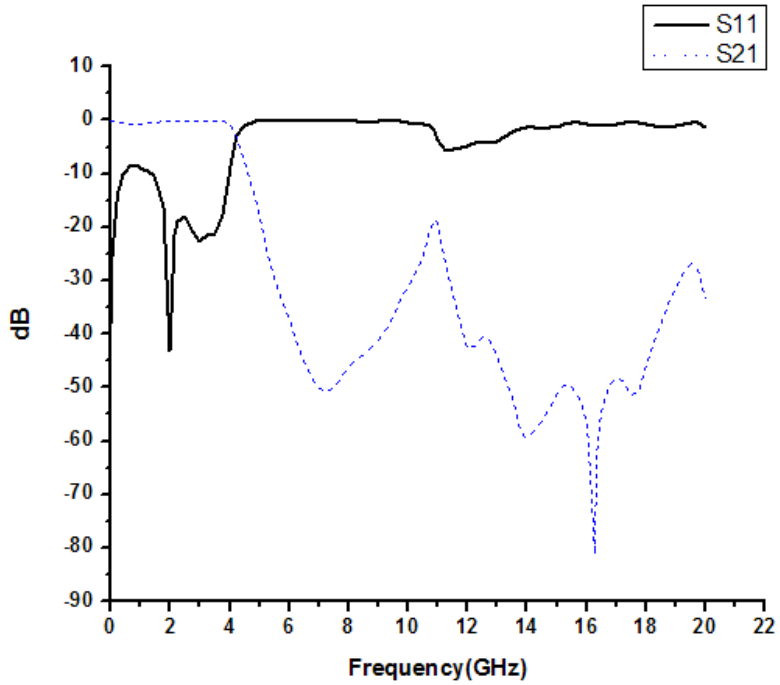

Figure 5.71: **S-parameter performance of binomially distributed square pattern dumbbell shaped EBGS having ten EGBS unit containing constant narrow slots of dimensions 1mm * 1 mm (length * width) where the total area of the central EBGS is 69.20596 mm^2.**

In this figure, the performance looks similar to the above performance. In this case also the number of ripple in the passband is only one; but in the stopband region Return Loss curve shows better performance. However, performance data are as follows - stopband starts from 5.076 GHz, 3dB cut off frequency = 4.207 GHz, passband width = 3.965 GHz. The height of the ripple is negligible which is -0.712 dB. Though insertion loss curve touches the 20dB line, it can be assumed as LPF.

✧**Design 3**

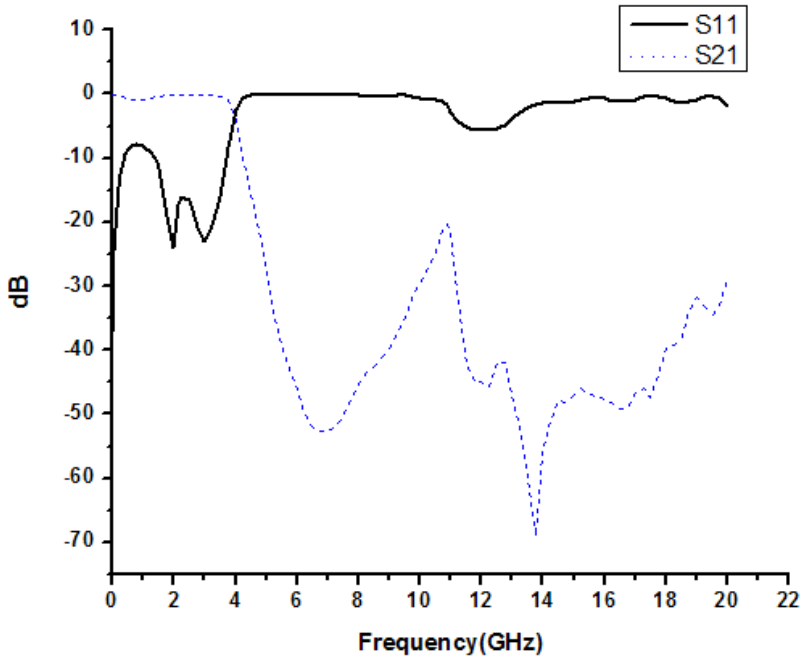

Figure 5.72: **S-parameter performance of binomially distributed square pattern dumbbell shaped EBGS having ten EGBS unit containing constant narrow slots of dimensions 1mm *1 mm (length * width) where the total area of the central EBGS is 85.43966 mm^2.**

S-parameter performance of the above graph also has shown performance like low pass filter (LPF) and here performance parameters are observed as follows - stopband starts from 4.6946 GHz, 3dB cut off frequency = 3.9177 GHz, passband width = 3.696 GHz. In this case also ripple height is very small and observed as -0.8634 dB. However, at the stopband region too much ups and downs of Insertion Loss curve are present; but it remains bellow 20dB. On the other hand Return Loss curve at that region shows quite good performance – remains well above -6dB all the time.

However, studying the performances of binomially distributed square pattern dumbbell shape designs it is found that the designs also have considerably less ripples and good low pass filtering performance. Therefore it can be said that the binomially distributed dumbbell shape designs gives better low pass filtering performance with negligible ripple effect.

5.8 Some Designs made to Achieve Low-pass Performance

Numerous irregular designs are made and simulated using Zealand ie3D EM simulation software and some of them showed good low pass performance with lower cutoff and less ripples. In this section three irregular designs and their performance will be described.

5.8.1 Designs

✧Design 1

This design is a uniform irregular design where rectangular shape seven EBGS elements are used. In this design the dimensions of rectangular slot is 4.6935 mm* 10.24 mm (length * width). The inner element spacing is 10.43 mm and the design is made on standard 50 ohm transmission line. Substrate thickness is 31 mils and dielectric constant is 2.45. A typical geometry of design is shown bellow,

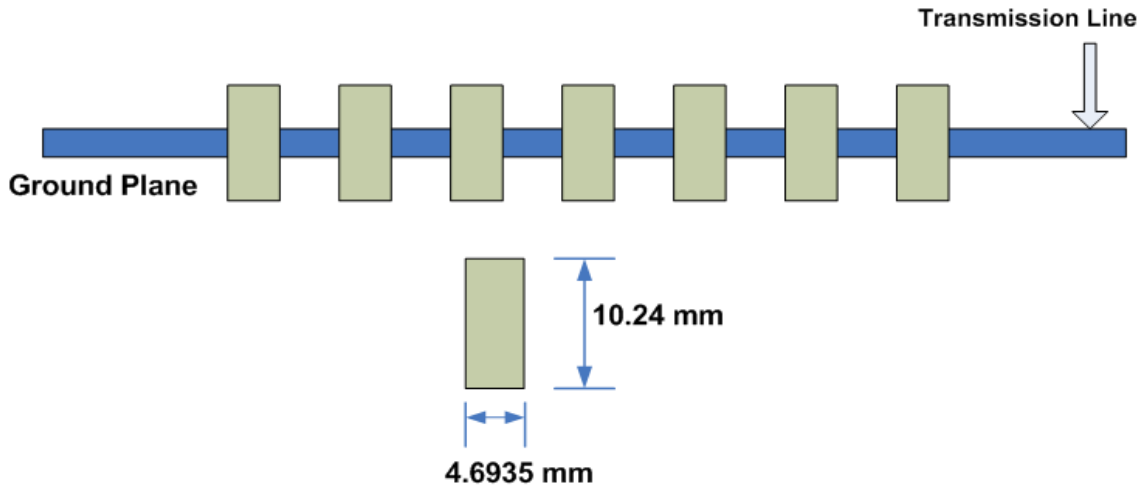

Figure 5.73: **Typical design of rectangular shaped uniform design.**

✧Design 2

This design is a non-uniform design where both the bigger slot and narrow slot is made non-uniform. Bigger slots are square shaped and narrow slots are rectangular shaped. Coefficients for bigger slots used are 0.25, 0.50, 0.75, 1.0, 0.75, 0.50 and 0.25 respectively and coefficients for narrow slots are 1.0, 0.75, 0.50, 0.25, 0.25, 0.50, 0.75 and 1.0 respectively. The reference arm for bigger slot is 5 mm and reference length of narrow slot is 5 mm. The inner element spacing is

10.43 mm and the design is made on standard 50 ohm transmission line. Substrate thickness is 31 mils and dielectric constant is 2.45. A typical geometry of design is shown bellow,

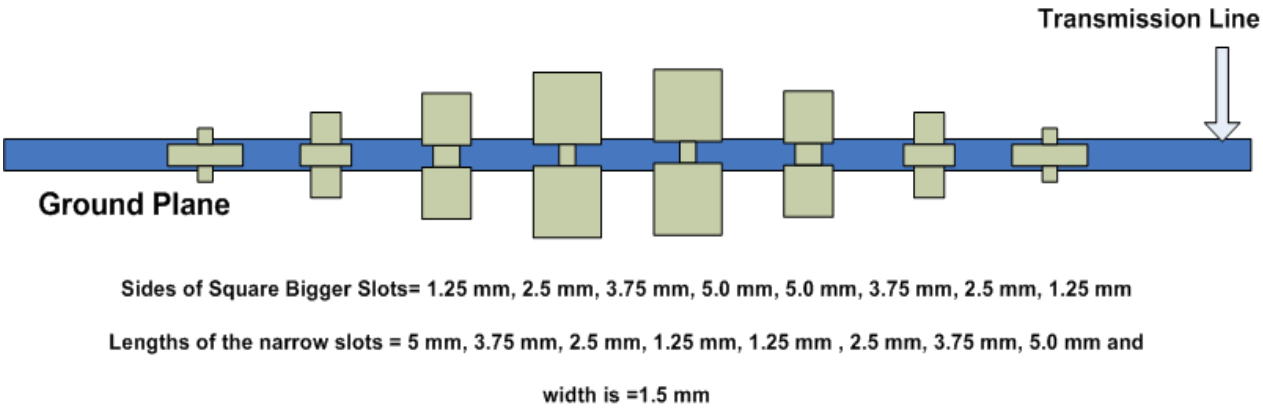

Figure 5.74: **Typical design of non-uniform irregular design having square shaped EBGS.**

✧Design 3

This design is also a non-uniform design where both the bigger slot and narrow slot is made non-uniform. Bigger slots are circular shaped and narrow slots are rectangular shaped. Coefficients for bigger slots used are 0.25, 0.50, 0.75, 1.0, 0.75, 0.50 and 0.25 respectively and coefficients for narrow slots are 1.0, 0.75, 0.50, 0.25, 0.25, 0.50, 0.75 and 1.0 respectively. The reference radius for bigger slot is 3.651 mm and reference length of narrow slot is 5 mm. The inner element spacing is 10.43 mm and the design is made on standard 50 ohm transmission line. Substrate thickness is 31 mils and dielectric constant is 2.45. A typical geometry of design is shown bellow,

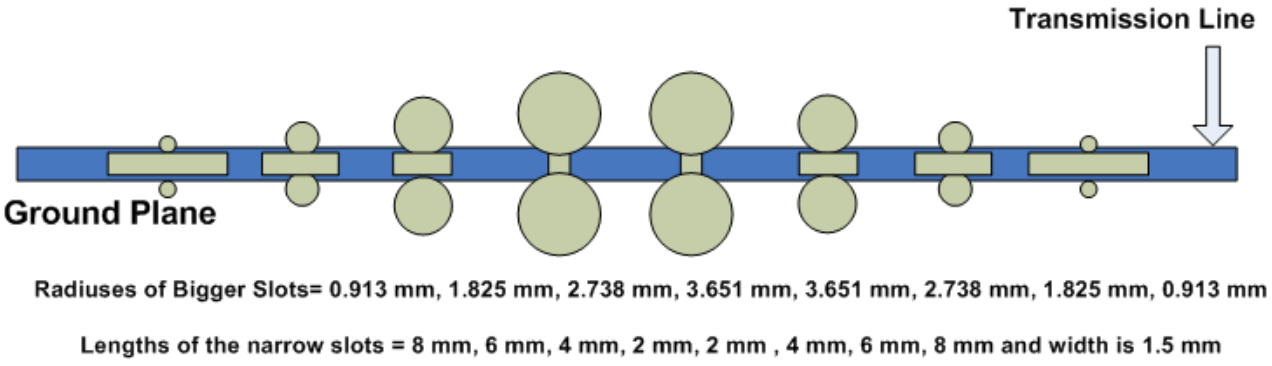

Figure 5.75: **Typical design of non-uniform irregular design having square shaped EBGS.**

5.8.2 Results

✧**Design 1**

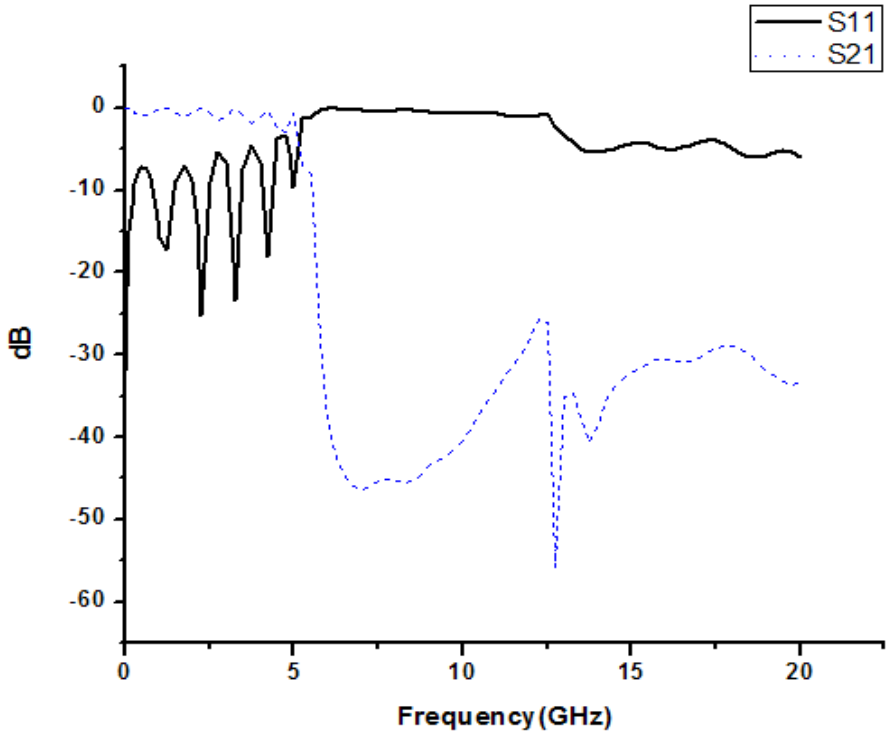

Figure 5.76: S-parameter performance of design 1.

The s-parameter of the above graph shows performance of low pass filter (LPF). Here the performance parameters are observed as follows - stopband starts from 5.6469 GHz, 3 dB cut off frequency = 5.091 GHz, passband width = 4.39 GHz. There is only one ripple with negligible height is present in the passband and which is measured as -2.9594 dB. Here, the insertion loss curve remains bellow 20 dB after the stopband starts.

✧**Design 2**

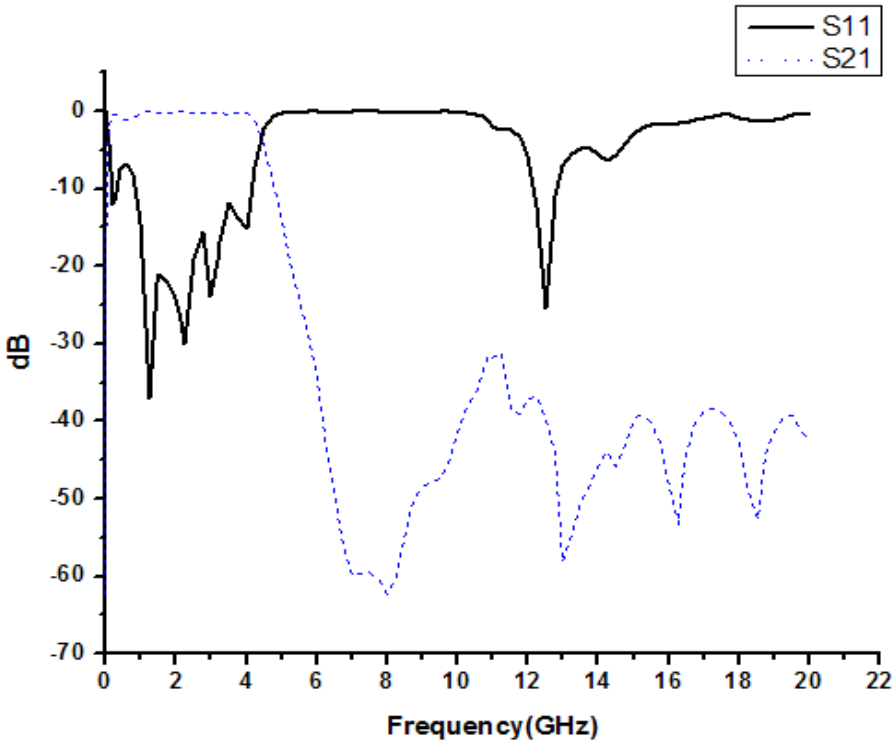

Figure 5.77: S-parameter performance of design 2.

The s-parameter of the above graph also shows performance of low pass filter (LPF). Here the performance parameters are observed as follows - stopband starts from 5.282 GHz, 3 dB cut off frequency = 4.402 GHz, passband width = 4.155 GHz. This design is more compact than the previous design. There is only one ripple with negligible height is present in the passband and which is measured as -0.598 dB. Here, the insertion loss curve remains bellow 20 dB after the stopband starts. There is only one disadvantage that is a ripple of return loss in the stopband region.

✧**Design 3**

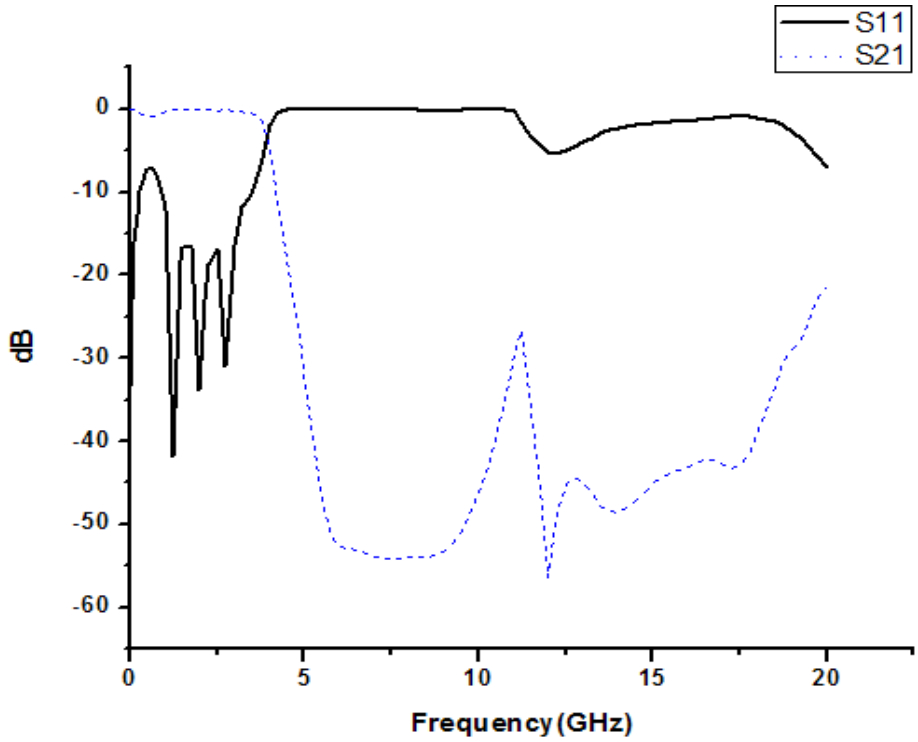

Figure 5.78: S-parameter performance of design 3.

The s-parameter of the above graph also shows performance of low pass filter (LPF) like previous two designs. Here the performance parameters are observed as follows - stopband starts from 4.569 GHz. 3 dB cut off frequency = 3.888 GHz which shows the most compact performance compared to previous designs. Passband width is observed = 4.155 GHz. There is only one ripple with negligible height is present in the passband and which is measured as -0.9565 dB. Here, the insertion loss curve remains bellow 20 dB after the stopband starts and also the return loss curve in the stopband region always remained under 5 dB. This can be stated as the best design of low pass filter.

5.9: Conclusion

In this chapter too many good designs are proposed with good performance on the basis of parametric studies. Some very simple designs are observed with great performance and some compound and complex designs are newly introduced in this chapter too. Narrow and wider stopband and low pass performances criterion analysis and effect of etching area on the performance of dumbbell shaped designs are closely inspected and a contradiction of same etching area is also shown here. A way of reducing passband ripples by binomially distributed non uniform designs is mentioned with example as well as S-parameter performance is observed through necessary designs.

Chapter 6 : Verification, Conclusions and Future Works

6.1 Verifications of simulated values

All the designs made and simulated in this thesis work using Zealand IE3D EM simulation software. We were unable to experiment investigations practically because of unavailability of required instruments. We designed an ideal transmission line and simulated it which showed us exactly the same performance that an ideal transmission line shows in practical experiments (section 3.2). It is proved that 1D and 2D designs produce the same performance and we also got identical performance from 1D and 2D designs simulation (section 3.6). Also we got optimum filling factor of 0.25 for circular shaped EBGS (section 3.5) which was previously reported by Prof. T. Itoh [1]. All other investigations we did were theoretically explained. From the study we can deduce that our simulated values were correct.

6.2 Conclusions

The work presented in this thesis was concerned with EBG assisted filters. At present EBG engineering is a special area in microwave engineering. EBGSs are periodic in nature and found to be very attractive in different microwave devices and components. EBG theories were reviewed to understand the passband and stopband phenomena of EBGSs. The depth and width of the stopband depends on few factors like FFs, number of elements, periods and substrate properties. Uniform circular, square, rectangular, triangular and hexagonal patterned EBGSs was investigated with variable number of EBG elements. The stopband-passband properties are reported by S-parameters performances. Different shapes of the EBG elements and different lattice structures were shown. Three rows of various uniform patterned EBGSs under the standard 50-ohm transmission line were simulated. Comparing with the result of one row uniform circular EBGSs it was found that three rows of uniform circular EBGSs and one row of uniform circular EBGSs yield very identical S-parameters performances. Therefore, to clarify and understand the fact a typical design with very narrow blank space at the beneath of T-line was simulated and found reduction of stopband completely. So, only 1-D uniform EBGSs were used onward. Effect of same

etching area for different patterned of uniform conventional EBGSs and some contradictory results to that effects were described. Binomial distribution and its application in designing non-uniform EBGSs is reported in chapter four. Using binomially distributed EBGS, relatively fewer ripples in the passband was achieved.

Lots of new shapes and designs of dumbbell shaped EBGSs are introduced in chapter five. They are described according to the fact of their S-parameter performances. Larger stopband and more compact performance than conventional EBGSs was achieved. Binomially distributed dumbbell shape designs were made and low pass performance having passband with relatively less ripple was achieved.

6.3 Recommendation for Future Work:

In the whole research work, attention was paid to simulate all the structures by commercial EM software **Zeland IE3D.** Investigations need to be justified experimentally by VNA and compared with simulated results. VNA measured the return loss performance of the T-lines. The future work can be mentioned in the following manner.

6.3.1 Results Validated By Theoretical Modeling

The EBGSs are actually complex geometries. Theoretical modeling is to be made for rectangular EBGS (as the results vary with the length and width of rectangle) and dumbbell shaped EBGS. Other complex designs like dual T-line designs need further research work to explain the behavior theoretically as well as multiple T-lines need to be considered.

6.3.2 Development of Algorithm

Researching proper algorithms for designing dumbbell shaped EBGS is left for further work as currently there is no such direct method of calculating correct parameters or correct size of dumbbell shaped EBGS for designing a filter for a particular pre defined performance (i.e. for a particular type of dual band performance how a dumbbell shaped EBGS can be chosen). All, in this paper, are just observation of performance of a pre-designed dumbbell shaped EBGS.

References

[1] V. Radisic, Y. Qian, R. Coccioli, and T. Itoh, "Novel 2-D photonic bandgap structures for microstrip lines," IEEE Microwave and guided wave lett., vol. 8 no. 2, pp. 69-71, Feb. 1998.

[2] T. Akaline, M. A. G. Laso, T. Lopetgi, and O. Vanbesien, "PBG-type microstrip filters with one-end and two-sided patterns," Microwave and Optical Tech. Lett., vol. 30, no. 1, July 5, 2001.

[3] D. Nesic and A. Nesic, "Bandstop microstrip PBG filter with sinusoidal variation of the characteristic impedance and without etching in the ground plane," Microwave and Optical Tech. Lett., vol. 29, no. 6, June 20, 2001.

[4] Q. Xue, K. M. Shum and C.H Chan, "Novel 1-D photonic bandgap microstrip transmission line," APS-International symposium, 2000, IEEE, vol. 1, page(s), 354-356.

[5] Nemai C Karm&ar and Mohammad N Mollah, "Investigation into non-uniform photonic bandgap micromipline lowpass filters." IEEE-Trans. Microwave Theory and Tech.. Feb-2003.

[6] Y. Qian er *a/*. " Simulation and experiment of photonic band-gap smctdres for microstrip circuits," I997 Asiapacifc microwave conference.pp.585-588.

[7] F-R Yang, K-P Ma, Y. Qian and T. Itoh "A uniplanar compact photonic-bandgap (UC-PBG) structure and its applications for microwave circuits," IEEE Trans.

[8] Chul-Soo Kim, Jun-Seok Park, Dal Ahn, and Jae-Bong Lim, "A Novel 1-D Periodic Defected Ground Structure for Planar Circuits," IEEE-MWCL, vol.10, no. 4, pp.131-133, April 2000.

[9] Dal Ahn, Jun-Seok Park, Chul-Soo Kim, Juno Kim, Y.Qian, and T. Itoh, "A design of the low-pass filter using novel microstrip defected ground structure," IEEE Trans. Microwave Theory and Tech., vol. 49, no. 1, pp. 86-93, Jan. 2001.

[10] **Leltxu Garde, Miguel Javier Yabar, and Carlos del Rio, "Simple modeling of DGS to design 1D-PBG low-pass filter," Microwave and Opt. Tech. Lett., vol. 37, no. 3, May 2003.**

[11] **Hai-Wen Liu, Xiao-Wei Sun, and Zheng-Fan Li, "A low-pass filter of wide stopband with a novel multilayer fractal photonic bandgap structure," Microwave and Opt. Tech. Lett., vol. 40, no. 5, March 2004.**

[12] **N.C. Karmakar and M. N. Mollah, "Investigations into nonuniform photonic-bandgap microstrip line filters," IEEE Trans. Microwave Theory Tech., vol. 51, no. 2, pp. 564-572, Feb. 2003.**

[13] **H. W. Liu, Z. F. Li, and X. W. Sun, "A novel fractal defected ground structure and its application to the low-pass filter," Microwave ant Opt. Tech. Lett. vol. 39, no. 6 December 20, 2003.**